THE INFLUENCE OF PARENT ROCKS ON THE NATURE OF SURFICIAL MATERIALS IN THE EDEN REGION

by

Donald John Hough

Thesis submitted for the degree of
Master of Science

Australian National University
Canberra

October 1983

The work in this thesis, except where acknowledged, is my own.

Don Hough

Don Hough

The Influence of Parent Rocks on the Nature of Surficial Materials in the Eden Region.

D.J. Hough

SUMMARY

In the Eden area, a study of the weathering of a granitoid (granite/adamellite composition), rhyolite, a sequence of metasediments of Ordovician age, sandstone and basalt showed that the particle-size, mineralogy and chemistry of the resultant surficial material strongly reflects its parent rock.

Where the surficial material is dominantly in situ three sorts of particle-size modes (Mode I, II and III) can be recognised. Mode I is 2 to 5 orders of magnitude larger than the parent rock framework grains and can be 1 to 3 orders of magnitude smaller than components in which variations in the landscape itself are involved. The existence of this mode is dependent on the aggregate properties of the parent rock. Mode II is coincident with the size distribution of the parent rock framework grains and its existence is dependent on the parent rock framework grains consisting of physiochemically resistant minerals. Mode III is <2μm in size and 2 to 5 orders of magnitude smaller than the parent rock framework grains. This mode is dependent on the physiochemical properties of the clay mineral group.

As a consequence of Mode II and to a lesser extent Modes I and III the soil particle-size distribution carries an image of its parent rock.

The order of persistance of the dominant minerals in the granitoid and rhyolite is plagioclase<<K-feldspar<quartz. The intensity of weathering is not sufficient to enable an equivocal determination of the relative persistance of the dominant minerals (quartz and illite) in the metasediment and sandstone.

The persistance of apatite is intermediate to that of plagioclase and K-feldspar, and zircon is more persistent than quartz. The variation in Zr concentration suggests the zircon is prone to dissolution.

The clay mineral assemblages of the clay size fraction is dominated by kaolinite, illite and dioctahedral vermiculite. Their relative proportion is dependent on the degree of weathering of the regolith and its parent rock. With increasing weathering the tendency is to form

kaolinite.

The size dependent distribution of the minerals inherited from the parent rock in the surficial material is dependent on their size distribution in the parent rock, their preemergent history, susceptibility to weathering and the degree of weathering they have undergone. Silt size (2-63μm) quartz is common in the surficial material of the area, being released from the parent rock through weathering. Its formation does not require exceptional forces as proposed by Pettijohn (1975). Differences in size dependent mineralogical trends for sands derived from granitoids of the area are due to differences in parent rock texture not climate as would be contended by Basu (1976).

None of the elements examined (including TiO_2, Al_2O_3, Fe_2O_3 and Zr) could be demonstrated to be immobile. The chemical mobility of an element is dependent on the reactivity of its host mineral(s) and the inherent solubility of the element on its release to the weathering environment.

Inorganic chemical fractionation occurs as a result of differences in element solubility and size dependent variation in chemistry. Physical processes are particularly important in causing changes in chemistry where the parent rock consists dominantly of chemically less reactive minerals, e.g., quartz and illite.

The variation in concentration of the less mobile trace elements can be used to distinguish surficial materials derived from different rock types.

ACKNOWLEDGEMENTS

This study was carried out at the Department of Geology, Australain National University. Facilities of the CSIRO Division of Soils, Canberra, were also used.

It is a pleasure to acknowledge the time and assistance given by the following people; K.A.W. Crook who supervised the thesis, P.H. Walker, A.J. Moss, B.W. Chappell, R. Freeman, Z. Wasik, J. Pennington and J. Hutka.

To those other people who also contributed to this study in many ways, thank you.

- CONTENTS -

LIST OF TABLES

LIST OF FIGURES

LIST OF PLATES

CHAPTER 1
INTRODUCTION

1.1 AIMS

In 1941 in his book 'Factors of Soil Formation' Jenny described the factorial approach to soils, using the five soil forming factors; climate, biota, topography, parent material and time.

The use of the factorial approach to soils has influenced research on many aspects of the science of surficial deposits, and has been a source of continuous discussion. The intensity of this argument is illustrated by the response (see Chesworth, 1976; Huggett, 1976; Yaalon, 1976) to Yaalon's (1975) proposition that it was only a matter of time before quantitative soil functions based on the five soil forming factors would be available.

Of the five factors, climate has received the most attention. Brewer (1976) has suggested that the preoccupation with the effect of climate is the reason for the comparative dearth of knowledge about the effect of the other factors, in particular parent rock. This dearth of knowledge about the effect of parent rock still remains. Clearly, if the effect of parent rock is to be determined, an extensive Empirical data base must be compiled.

The principal aim of this thesis is therefore to examine the influence of parent rock on weathering, by the assembly and analysis of a body of data on selected physical and chemical attributes of surficial materials and the landscapes in which they occur.

It is also intended to use this data to examine various paradigms used in the surficial sciences and to test the logic of the arguments used to support them. This may at times lead to what could be considered as a 'negative conclusion', viz., where the inadequacy of a particular paradigm can be shown, although an alternative is not immediately available.

The importance of 'negative conclusions' to the advancement of science is demonstrated by the Michelson-Morley experiment. With respect to this famous experiment, which set out to demonstrate

the existence of the ether, the Encyclopaedia Britannica (1982, Vol 12, p. 104) states "It was perhaps the most significant negative experiment in the history of science...To explain the result of the Michelson-Morley experiment, physics had to be recast on a new and more refined foundation."

1.2 THESIS FORMAT

This thesis is arranged as follows:

Chapter 1.3 defines the use of various terms and conventions.

Chapter 2 describes the study area and the choice of the rock types examined. Additionally, it provides information on the system used to label samples and reference to the various analytic and computational techniques used.

Chapters 3 to 7 describe the characteristics of each rock type and its surficial mantle.

Chapters 8 to 10 discuss the implications of these data (Chapters 3 to 7) with respect to particle-size distribution, mineralogy and chemistry of surficial materials.

Chapter 11 summarises the conclusions reached in this study.

1.3 TERMINOLOGY AND CONVENTIONS

The study of surficial materials and the landscapes in which they occur, involves many disciplines, e.g., physical geography, geochemistry, sedimentology, pedology. In any multidisciplinary study problems with conventions and terminology will arise.

These problems arise because terminology and conventions are often a result of historical circumstances which commonly vary from discipline to discipline. For example, the development of soil science and profile nomenclature in the temperate glaciated terrain of the northern hemisphere has been a source of frustration for workers in older, deeply weathered landscapes of the southern hemisphere.

The use of a particular word in a particular discipline often carries with it a specific meaning. Thus the meaning of a word can vary markedly: see Brewer's (1976, p.134) discussion of the term 'texture'.

Consequently, different workers may differ in their conception of what is implied by a particular term.

To avoid the confusion which could arise as a result of the multi-disciplinary nature of this thesis, the use of the following terms and conventions is clarified as follows.

Regolith

The term 'soil' has a variety of meanings (Hunt, 1972; Brewer, 1976). Consequently, if the term 'soil' were to be used extensively in this thesis, it could give rise to unintended, and therefore unanswered expectations. To avoid this, the term 'regolith' is used and is defined as 'the layer of fragmental and unconsolidated rock material', (Bates and Jackson, 1980, p.528).

Parent Rock

In this thesis rock types are classified according to geological rather than pedological criteria. It should be noted that criteria important in classifying a rock geologically, may have little or no pedological significance. Therefore, there should be no implicit expectation that materials with different parent rock names should develop profiles with differing characteristics. For instance, although marble and limestone (or silcrete and quartzite) have markedly different fabrics, it is quite possible because of their similarity in mineralogy and chemistry, that profiles developed on them could be indistinguishable.

Weathering/Soil Forming Processes

The definition of weathering used in this thesis is that of the Glossary of Geology (Bates and Jackson, 1980, p.697), which is 'The physical disintegration and chemical decomposition of rock that produces an in-situ mantle of waste.' Hence, differences in the degree of weathering between two samples can be recognised by the degree of comminution of its constituents or destruction of its primary minerals. As many of the effects of weathering are macroscopically visible, progressive differences in weathering can be generally recognised in the field.

The term, 'soil forming processes' is used in this thesis to describe those processes which give rise to the redistribution of constituents within the profile, and control the distribution of organic matter.

Clay/Clay Minerals

Classically the term clay is used both as a name for a specific group of minerals and as a textural term for particles <2μm. This has commonly led to the implicit assumption that most, if not all, clay minerals are in the clay fraction. In this thesis, 'clay' is used as a textural term and 'clay minerals' is used to refer to members of the phyllosilicate mineral group. The various clay minerals identified in this thesis are defined in Appendix A.

A semiquantitative estimate of the relative proportion of the different clay minerals in a carefully prepared sample can be readily determined by either X-ray or infrared spectroscopy. However, because of problems associated with variable composition, grain size etc., these techniques cannot be readily used to accurately determine the proportion of clay minerals, as a percentage of the whole sample. As H_2O+ occurs dominantly in the clay minerals, and is sufficiently uniform in concentration amongst those clay minerals found in the regolith samples examined, it is used as a surrogate measure of the total clay mineral content.

Size Measurements

The physical nature and size of attributes measured in this thesis varies markedly. These differences in attribute features- the materials vary from consolidated to unconsolidated and range in scale from 10^{-7} to 10^{1}m- require the use of different measurement techniques and size scales. For convenience it was decided: i) to retain the units in which the attributes were measured, rather than convert them to SI units, and ii) that textural terms used to describe unconsolidated material would be those defined by the International Scale, unless otherwise specified.

Profile Description

A sequence of samples within a regolith is commonly ordered from the surface downward (Northcote, 1979, p.3).

This has given rise to the tendency to describe the effects of processes in the down-profile direction. In some cases there are logical reasons for this. For example, organic matter is produced at the regolith surface. Through the effects of destruction and dilution, its concentration usually decreases with depth. Likewise, in a profile in which clay illuviation is an important process, the clay content is described as increasing with depth. This corresponds to the removal of clay from its source horizon and consequent deposition in the horizon beneath. This down-profile desciption of changes in attributes, is consistent with the direction of increasing effect of a specific process, the destruction and dilution of organic matter and illuviation. In a chronosequence, samples are usually described in the direction of increasing change. If changes in weathering are to be described, it would be logical to describe these changes in the sequence, least weathered to most weathered.

In this thesis, profiles were chosen such that an overall increase in the degree of weathering occurred up-profile. Given that weathering is the principal concern of this thesis, changes in sample attributes are, where appropriate, described up-profile. This approach has also been used by others; e.g., Brewer (1955), Eswarin and Bin (1978) and Ross et al. (1982).

Horizon Designation

The designation of conventional soil horizons (A, B, C horizons) relies principally on the recognition of vertical changes in regolith colour, particle-size, organic matter and fabric. There is no body of literature to which one can turn to demonstrate that a simple and persistent relationship exists between these horizons and the degree of weathering. Consequently, to discuss weathering, using samples which have been grouped into horizons according to criteria which may vary independently of weathering, adds nothing to a study of weathering.

Furthermore, there is an implication that same horizons from different profiles have more attributes in common, than do different horizons from the same profile. This implication need not be correct.

Thus, in this thesis weathering has generally been described from sample to sample, rather than from horizon to horizon. The use of an array of ungrouped samples to examine the effects of weathering is common (e.g., Gilkes and Little, 1972; Nesbitt et al., 1980)

The use of A, B, C horizon nomenclature in this thesis is restricted to the discussion of profile textural differentiation. Their use in this context is appropriate as the A and B horizons can be distinguished by particle-size criteria alone.

In this thesis the A, B, C and R horizons are defined as follows:

A Horizon	:	The A horizon has a lower clay content than the horizon below.
B Horizon	:	The B horizon has a clay content unlike the horizons above or below.
C Horizon	:	The C horizon retains the fabric of the parent rock.
R Horizon	:	The unweathered source of the C horizon.

Profile Nomenclature

Much thought was given as to whether regolith profiles should be classified according to one of the many existing soil classifications. Three factors discourage the extensive use of soil names in this thesis:

1) The use of any existing soil classification would tend to focus attention on the name of the profile rather than its attributes. This could lead one to have a preconceived (and therefore possibly erroneous) concept of the aggregate features of the profile.
2) Commonly, classifications tend to group profiles on the characteristics of their solum (A and B horizon). For example, Northcote (1979,p.25) states 'the solum is the object which the factual key is designed to classify.' Hence, the properties of the sub-solum, important in regolith studies, would find no expression in the profile name.

3) Soil classification tends to be arbitrary, in the sense that two profiles with only slight variations in their characteristics may have different names. The Factual Key (Northcote, 1979) is used as an example. If a textural differentiation greater than 1.5 texture groups occurs over a distance of less than 10cm, the profile is classified as duplex. If the distance exceeds 10cm, the profile is classified as gradational. Yet it is conceivable that a gradational and duplex profile may have more attributes in common when derived from the same rock type, than two duplex profiles derived from different rock types.

CHAPTER 2

PREAMBLE

2.1 THE FIELD AREA

The Eden region (Figure 2.1) was chosen for study as :

1) A variety of rock types occurred in the region.
2) The region has a comparatively uniform climate, topography and vegetation.
3) The regolith is dominantly insitu.
4) There are abundant exposures (road cuttings) of the regolith. This would reduce the chance of inadvertently sampling an atypical profile.
5) The information gained would contribute to other studies in the region, principally the environmental consequence of woodchipping.

2.2 THE PHYSICAL ENVIRONMENT

Geology : The generalised geology of the region is given in Figure 2.2.

Soils : Little is known of the characteristics or distribution of soils in the region. Stace et al. (1968) describe the soils of the region as soloths and red podzolics, whereas Northcote et al. (1975) describe them as yellow duplex. Leaching conditions are such that soil samples throughout the region have an acid pH (Appendix B).

Physiography : The area is generally hilly, with local relief in excess of 100m being common. Slopes are generally between 10° and 25°.

Vegetation : With the exception of small patches of rainforest occurring in sheltered gullies, and coastal heathlands, the dominant vegetation of the region consists of dry eucalypt forest dominated by Silvertop Ash and various stringy-bark species (Forestry Commission of NSW, undated). The length of time for which the current pattern of vegetation distribution in the region has persisted is not known.

Climate, Present and Past : The present climate of the study area is, according to the Koppen-Geiger system, warm temperate and subhumid (Strahler, 1969). Detailed climatic data are given in Reinson (1973). The average mid-summer temperature

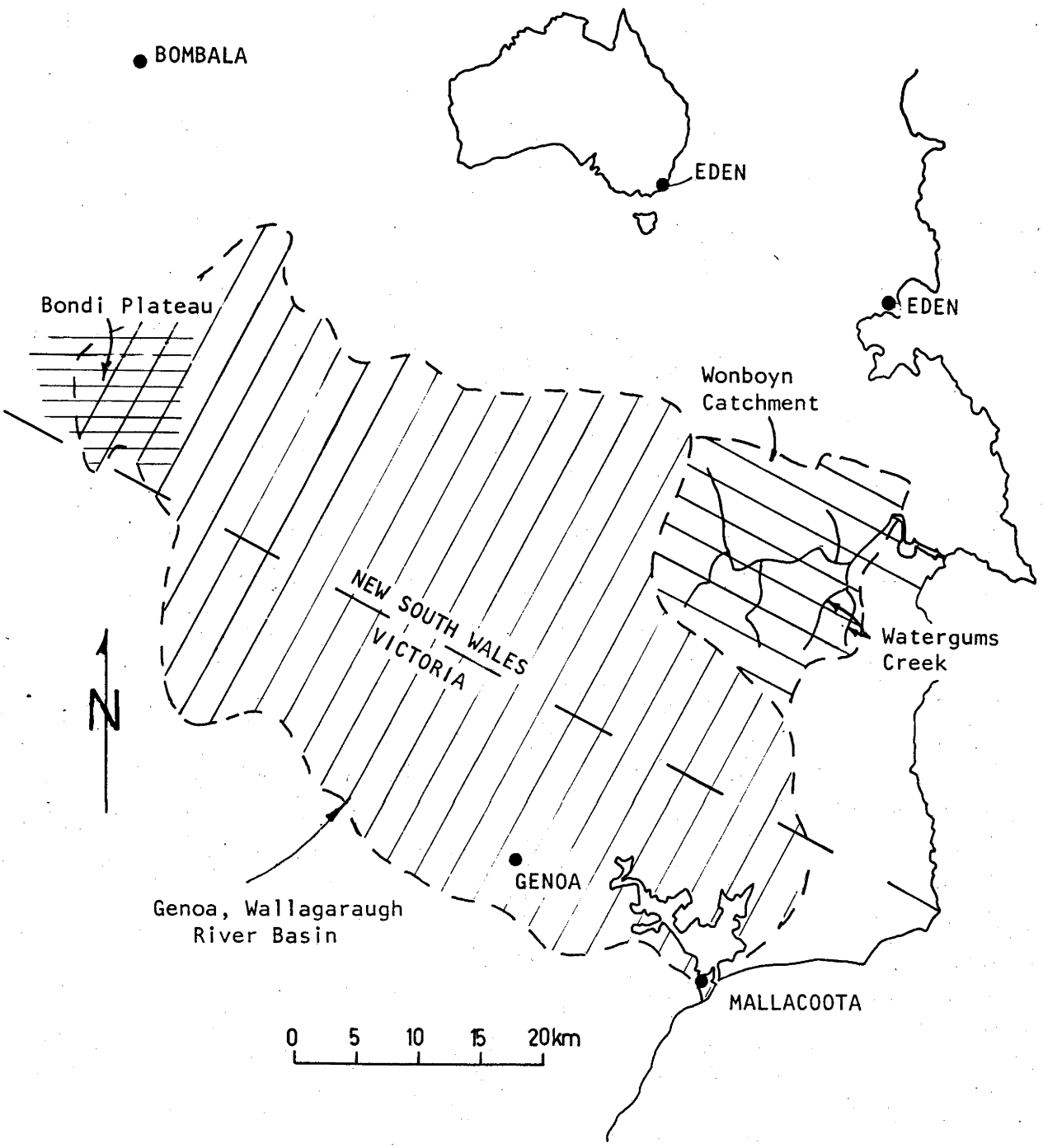

Figure 2.1 Location of the Eden study area.

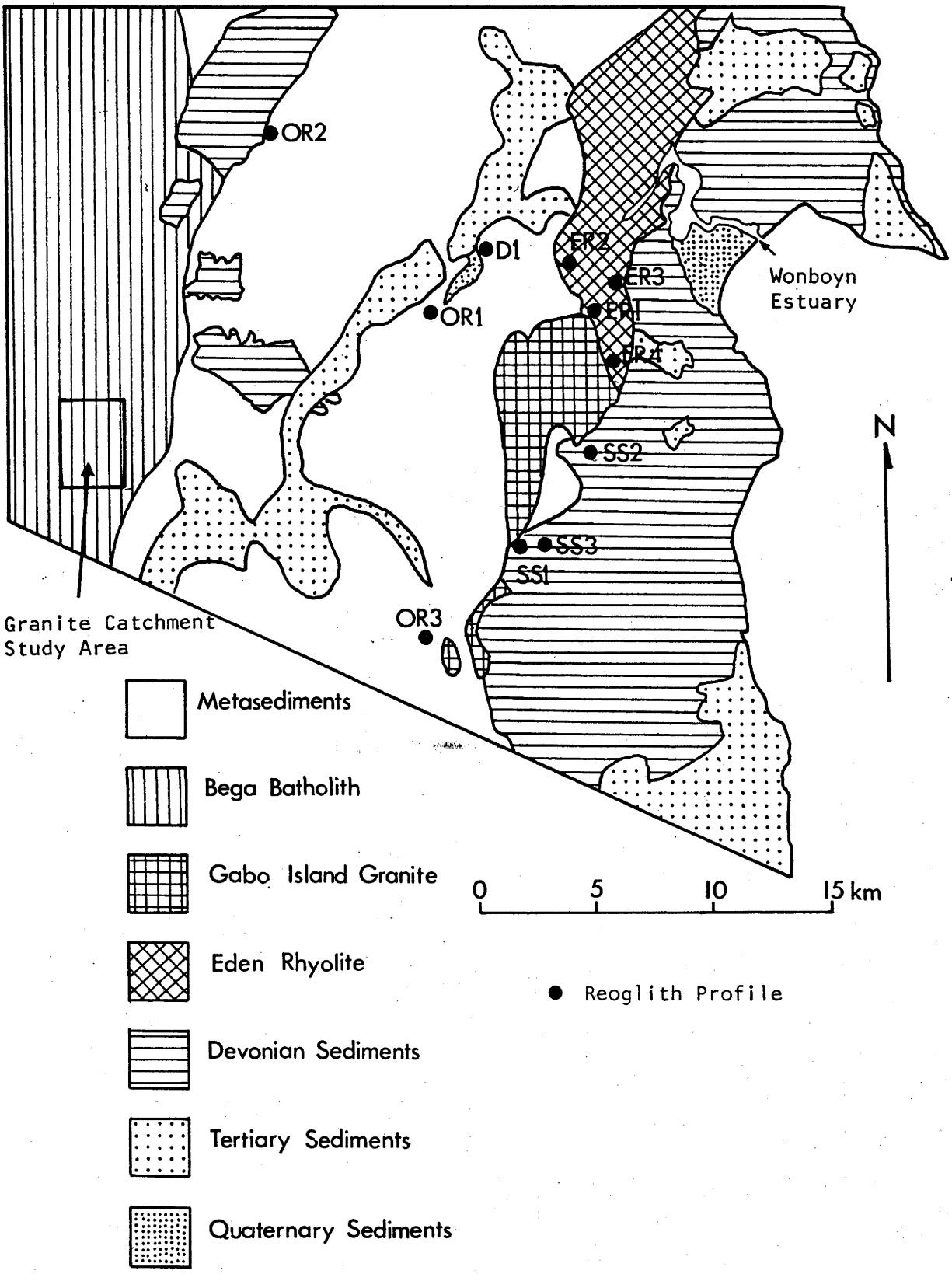

Figure 2.2 General geology of the Eden area (after Beams and Hough, 1977) showing location of the granite catchment study area and the profiles examined.

in the region varies from 26°C to 20°C (maximum) to 12°C to 9°C (minimum) whilst the average mid-winter temperature varies from 14°C to 9°C (maximum) to 9°C to -1°C (minimum). The extent of the temperature variation increases with relief and distance from the coast. Rainfall is evenly distributed throughout the year and currently varies within the study region from 1100mm to 800mm per annum. At higher altitudes part of the rainfall falls as snow.

Although current climatic data can be collected in considerable detail, their direct relevance to the formation of regolith which may have been interacting with the environment for considerable time (tens of thousands of years) is tenuous as climate is known to have varied in the past. A summary of Late Pleistocene and Holocene climates (McConnell, 1979) is given in Table 2.1. Walker and Coventry (1976) have suggested that, although changes in climate in the non-alpine areas may have altered the rate of soil weathering and leaching in the past 30,000 years, it has not altered the general direction of pedogenesis.

2.3 CHOICE OF REGOLITH PARENT ROCK

Five rock types were chosen, granite*, rhyolite, metasediment, sandstone and basalt.

Four of these, granite, rhyolite, metasediments and sandstone are examined in comparative detail. They can be considered to represent the comparatively quartzose end members of their respective suites; plutonic, volcanic, metasedimentary and sedimentary. The granite and rhyolite can be considered to be chemically and mineralogically similar, differing only in texture. Likewise, the metasediments and sandstone can be considered to be mineralogically and chemically similar, also differing in texture.

The examination of basalt is included for comparative purposes. Consequently it is considered in less detail. Basalt was chosen as

---

* Granite Nomenclature: Throughout this thesis the terms 'granite' and 'granitic' are used sensu lato unless specified as granite (s.s.) or granitic (s.s.) in which case they are used senso stricto.

Table 2.1 Summary of Holocene and Late Pleistocene climatic changes, from McConnell (1979).

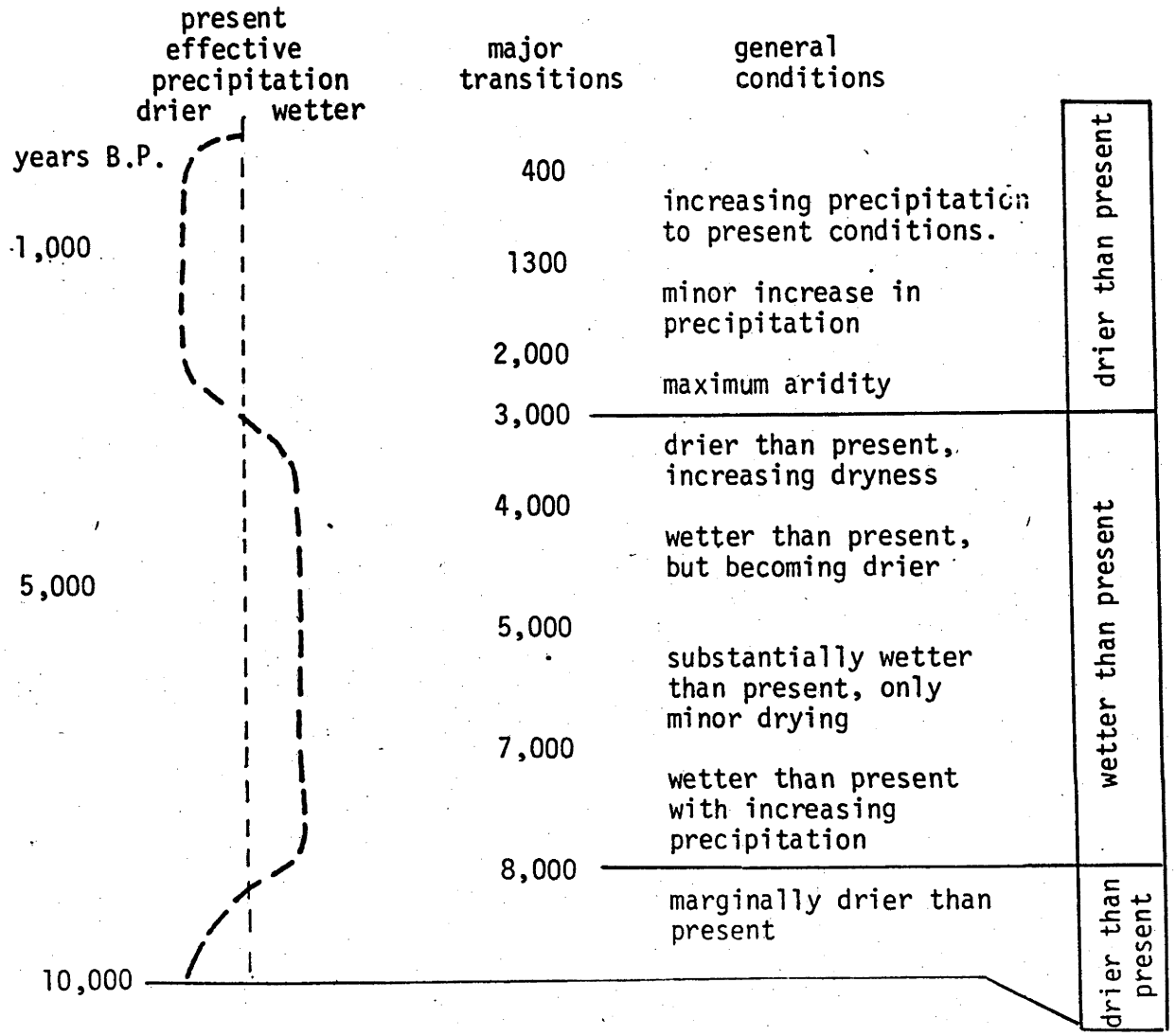

stage (year B.P.)	climatic conditions
10,000-22,000 24,000	lowest effective precipitation recorded - associated phase of major aridity
22,000-26,000 24,000	higher effective precipitation than at present
26,000-30,000	slightly lower effective precipitation than at present.
30,000-40,000	higher effective precipitation than at present, associated lake full period.
40,000-50,000	lower effective precipitation than at present.

compared with the other rock types it is quartz free and has very low concentrations of K_2O bearing minerals. Hence, it could provide, if necessary, a deductive basis for determining the role of quartz and K_2O bearing minerals on the resulting regolith. In addition, the profile chosen provides further evidence for the diversity of processes which give rise to texturally differentiated profiles.

Sampling the Parent Rock

In a landscape of varied rock types, it is common to attribute differences in physiographic prominence to variations in the susceptibility to weathering of the rocks present. In large drainage basins developed on relatively uniform rock , the drainage pattern is commonly controlled by variations in facture density.

Within a small area of 'uniform' rock type the question arises, are those rocks currently outcropping, exposed because those adjacent were predisposed to weathering (as a result of an initial physiochemical difference), or is exposure a result of chance and dependent only on landscape history. This problem is not readily resolved. In this thesis, the rocks outcropping in the proximity of the profiles examined were accepted (except where some features were obviously different) as being similar to and therefore representative of the profile parent rock.

2.4 SAMPLING THE REGOLITH

As it was impossible to choose profiles on the different rock types examined for which all factors, other than rock type, were identical, two sampling strategies could have been adopted.

For each rock type, choose a single profile and map the immediate landscape, so that differences in slope gradient and length, and regolith depth , texture, colour etc., between profiles can be isolated and described. As a result of the rapid lateral changes (at a scale of one to ten metres), and rocky nature of much of the regolith , the density of sampling required could only have been achieved by a network

of closely spaced trenches. This would have required more time than was available.

The second strategy was to choose several profiles from each rock type on the assumption that differences in site factors between profiles were either not appreciable, or not sufficient to invalidate conclusions drawn from the data. This strategy was chosen as the most expedient.

For each rock type, profiles were chosen such that they represented a range in the degree of weathering, and to a lesser extent, soil formation. As mentioned previously, profiles were chosen such that an overall increase in weathering occurred up-profile.

2.5 SAMPLE IDENTIFICATION

Rock and regolith samples are identified by an alphanumeric code, (Table 2.2). The letters identify the rock type. The number identifies the particular profile and sample within it. The use of alphanumeric codes is common, and is used extensively in 'A Handbook of Australian Soils', (Stace, et al ., 1968).

2.6 ANALYTICAL AND COMPUTATIONAL TECHNIQUES

The analytical techniques used to determine the physical and chemical characteristics of the materials examined are described in Appendix A. Chemical analyses are recorded using standard symbols (see Deer et al. 1963). The various computational techniques used, and references which provide detailed descriptions of these techniques, are given in Appendix A.

Table 2.2 Sample identification.

Regolith samples are identified as follows:

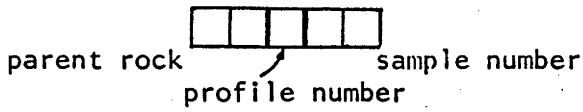

Parent rock code:

Granite: GR
Metasediment: OR
Rhyolite: ER
Sandstone: SS
Basalt dyke: D

Example: GR101 indicates sample 1, profile 1, developed on granite.

Rock samples: R replaces the profile number, e.g., GRR17 represents granite sample number 17.

Stream-bed sediment samples: S replaces the profile number, e.g., GRS5 indicates stream-bed sediments from granite catchment 5.

Average composition: This is referred to by using the suffix A, e.g., ERRA represents the average composition of the rhyolite rock samples.

CHAPTER 3

SURFICIAL MATERIALS DEVELOPED ON THE WALLAGARAUGH ADAMELLITE

3.1 INTRODUCTION

This chapter is arranged as follows. First, the characteristics of the landscape, parent rock and profiles examined are described (Section 3.2). This is followed by a description of particle-size distribution, mineralogy and chemistry (Section 3.3, 3.4 and 3.5 respectively). Finally, the chemistry of the landscape efflux is described in Section 3.6.

This chapter contributes to a mass balance study of five small catchments being carried out by the Forestry Commission of N.S.W. Their locations are given in Figures 2.2 and 3.1. Geologically the catchments lie on the eastern edge of the Bega Batholith; they are wholly within the Wallagaraugh Pluton and immediately north of the Croajingalong Pluton. Both plutons consist dominantly of adamellite. The Wallagaraugh Adamellite is distinguished from the Croajingalong Adamellite by its more felsic nature (Beams, 1980).

3.2 CATCHMENT CHARACTERISTICS

3.2.1. Physiography

The general topographic features of the area are shown in Figure 3.1. Valley cross sections are approximately V shaped, with slopes generally between 10° and 20°. The maximum relief in any catchment is approximately 200m.

Except during periods of extreme drought, the streams at the weir sites flow continuously. Under normal flow conditions, the streams are less than 1m in width and either floored by rock (a prerequisite for the construction of the weirs) or flood deposits.

Except for the general tendency of rock outcrops to occur along the ridges there is no simple pattern of regolith and rock outcrop occurrence.

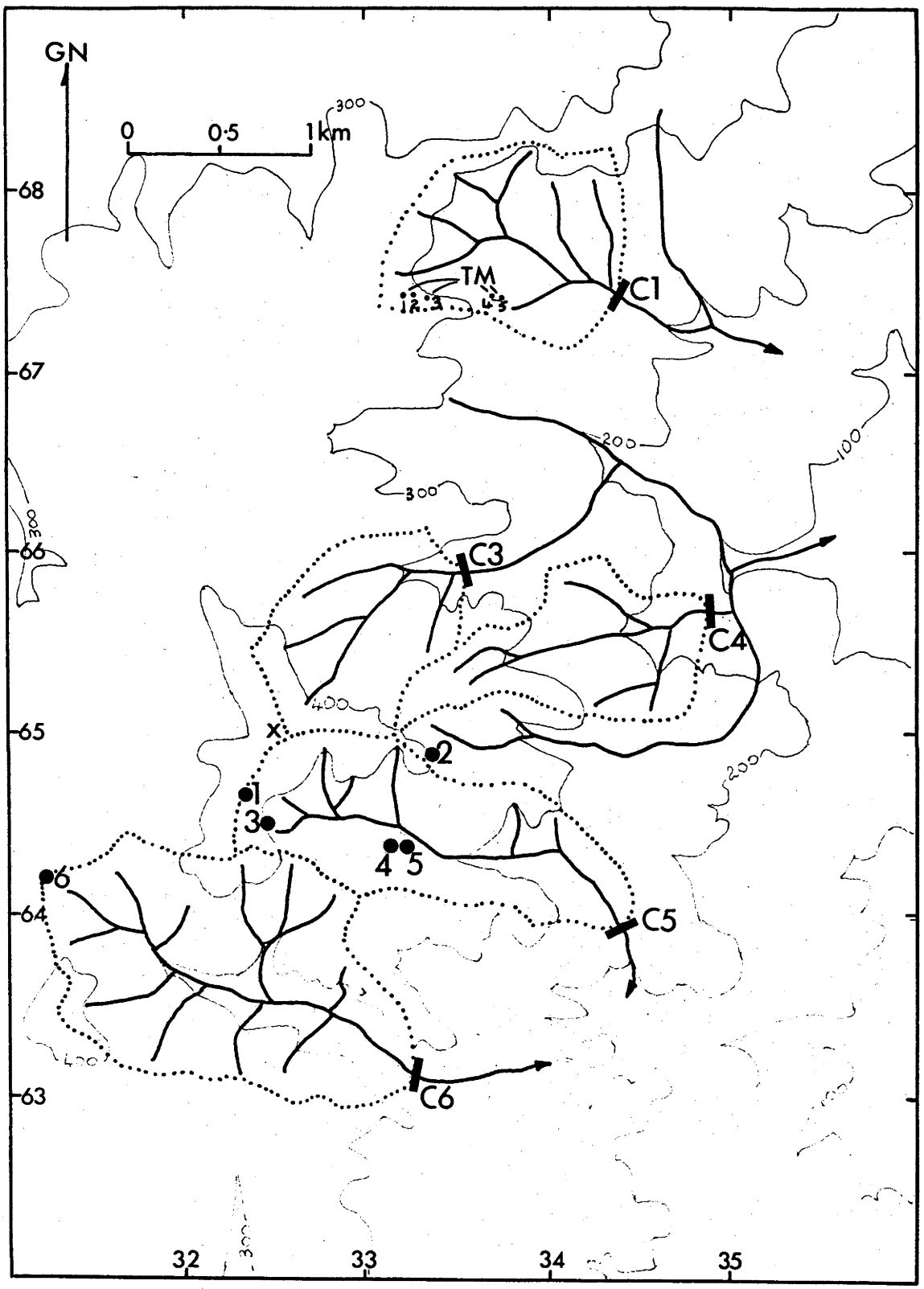

Figure 3.1 Catchment locality map: Catchment boundaries (dotted); weirs ▌; adjacent number indicates the catchment number; topography ~200~ in metres; regolith profiles (●); grus samples (×); termite mound samples (·TM). Coordinates are those of the Timbillica 1:25,000 sheet.

3.2.2. Vegetation

The vegetation has been described in Burgess et al. (1981, p.377) as follows:

> "The catchments were/are covered with what is best described as a mixed dry sclerophyll forest with silver top ash (Eucalyptus sieberi) being dominant. Other common upper story species include messmate (E. obliqua), yellow stringbark (E. muelleriana), yer[t]-chuk (E. conside[n]iana) and monkey gum (E. cypellocarpa). The understory is dominated by wattles (Acacia terminalis), Banksia serrata, Casuarina littoralis, Perso[o]nia luniaris, and P. levis. Occasional species associated with wet sclerophyll occur in gully corridors and in swampy areas. Ground cover includes leaf, branch and bark litter, grasses, sedges and some small shrubs. The study area has been subjected to a history of fire, and wildfire is not uncommon during the hot dry summers."

3.2.3. Bedrock Geology

On the basis of mineralogy and texture three distinct rock suites can be recognised within the catchments. These are:

1) granites with associated aplitic and pegmatitic phases
2) feldspar porphyry
3) basalt dykes

Granite and Associated Phases

Mineralogically the Wallagaraugh Adamellite varies from granite (s.s.) to adamellite, see Table 3.1 (locations of the rock samples examined are given in Figure 3.2). Burgess et al. (1981) have reported the occurrence of granodiorite in the catchment area. Although I have not examined every outcrop, closely spaced traverses (<300m apart) failed to find rocks of granodiorite composition. This, combined with the general uniformity of the Wallagaraugh Pluton, suggests that the occurrence of granodiorite is unlikely.

Table 3.1 Modal mineralogy of the Wallagaraugh Adamellite. Modes were determined from a count of 1,000 grains on stained slabs. The composition fields for the quartz-K-feldspar-plagioclase, shown below, are from Strekeisen (1973).

Sample Number	Sample Location*	Quartz %	K-feldspar %	Plagioclase %	Biotite %	Bulk Density g/cm^3
GRR1	343675	37	33	27	3	
GRR2	333681	32	40	27	1	2.62
GRR3	334666	33	36	29	2	
GRR4	332662	35	39	24	2	
GRR5	340658	32	39	25	4	
GRR6	349657	38	38	22	2	2.60
GRR7	313655	36	33	27	4	
GRR8	335659	36	34	25	5	2.62
GRR9	347651	37	40	21	2	
GRR10	326650	44	34	17	5	
GRR11	340652	33	31	22	4	
GRR12	332649	39	35	24	2	
GRR13	340648	34	39	24	3	
GRR14	323645	30	43	25	2	
GRR15	344640	36	38	23	3	
GRR16	333631	39	34	23	4	2.60
GRR17	325637	36	44	19	1	
GRR18	314631	32	32	31	5	
GRR19	333642	37	38	24	1	
GRR20	326629	34	38	25	3	

* Coordinates are those of the Timbillica 1:25,000 sheet.

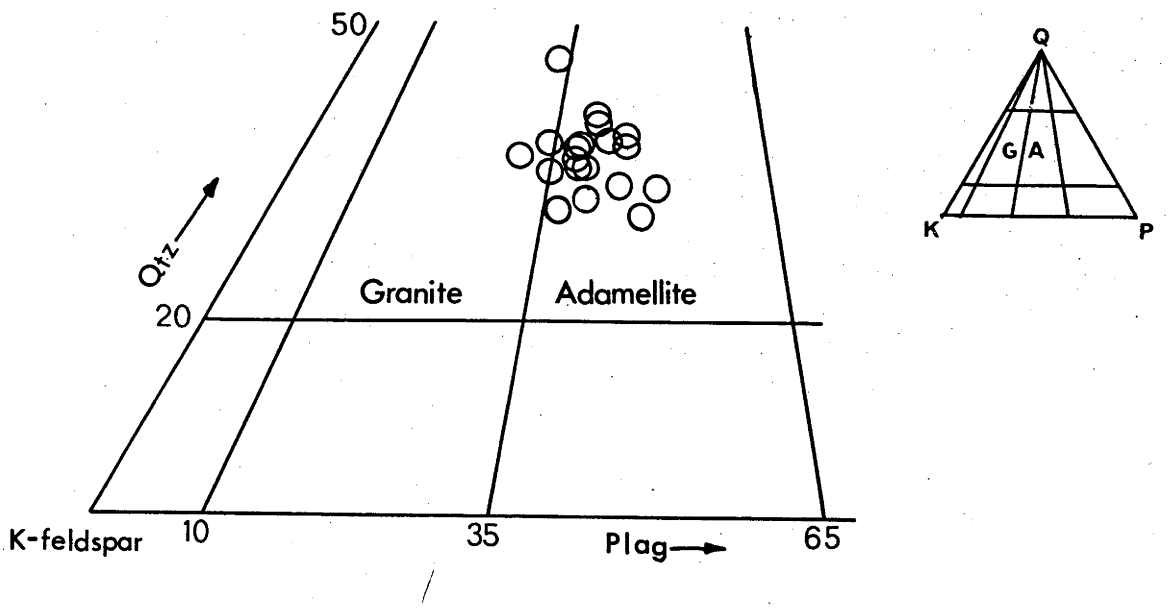

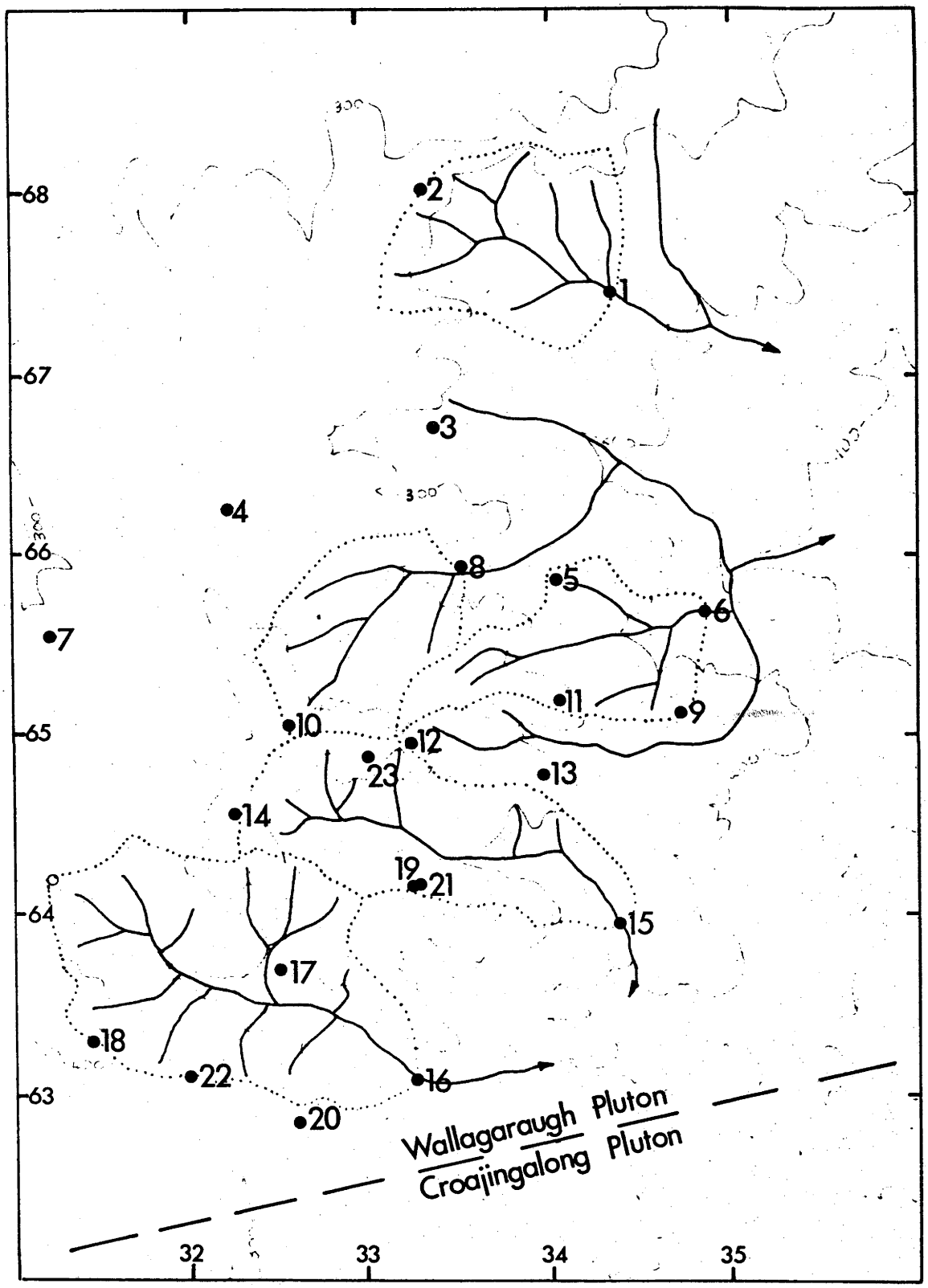

Figure 3.2 Rock sample locations (●) and the approximate boundary of the Wallagaraugh and Croajingalong Plutons.

The granite is usually salmon coloured. It is commonly even textured and coarse to very coarse grained, with most of the framework grains between 2 and 7mm in size (see Appendix C). A minor proportion of the granite is porphyritic with grains of quartz and feldspar to 1 cm set in a fine groundmass (1 to 2mm). The pegmatitic phase occurs as dykes up to 1m in width. The aplitic phase occurs either as thin dykes (<1m in width) or as pods up to several hectares in size.

The granite consists dominantly of quartz, K-feldspar, plagioclase and minor biotite.

Quartz usually occurs as anhedral equidimensional grains showing undulose extinction. K-feldspar is subhedral to euhedral, roughly equidimensional and occurs as dusty orthoclase microperthite. It is occasionally graphically intergrown with quartz. Plagioclase grains are subhedral to euhedral, usually equidimensional, rarely zoned, having carlsbad, albite and less commonly pericline twin development and are albite to oligioclase in composition. Biotite is often subhedral and occurs either as single crystals with ragged edges or as composite clots up to 2mm in size. Opaque minerals are commonly present within the biotite. Primary accessory minerals are allanite, zircon, apatite, fluorite and Fe/Ti oxide minerals (dominantly ilmenite).

Subsolidus alteration is common. It is expressed by the partial alteration of plagioclase to sericite and epidote, the dusty nature of the K-feldspar and the occurrence of chloritised biotite.

The aplitic phase (samples GRR22 and GRR23) consists of quartz, orthoclase microperthite, plagioclase (albite-oligioclase composition), minor biotite, and occasional muscovite and has a well developed granophyric texture.

Feldspar Porphyry

Two bodies of feldspar prophyry were located:

i) just north of the entrance to catchment 1 (location T331675).

ii) on the boundary of catchments 5 and 6 (GRR21, location T330642).

These bodies are circular in plan and each less than 2ha in area. They are characteristically porphyritic and contain subhedral laths of feldspar from 0.8mm to 8mm in length and anhedral phenocrysts of quartz from 0.5 to 2mm in size, set in a dark brown aphanitic groundmass. In thin section the feldspar phenocrysts consist of orthoclase microperthite and albite and are occasionally surrounded by a rosette-like,

quartzo-feldspathic reaction rim. The quartz phenocrysts are often embayed and are also surrounded by a quartzo-feldspathic reaction rim. The matrix consists either of a fine-grained granular intergrowth of quartz and feldspar or rosettes of intergrown quartz and feldspar. Subsolidus alteration products consists of sericite, carbonate and epidote.

Basalt Dykes

The basalt dykes are usually less than 2m in width and are discontinuous along strike. Their greatest traceable length is approximately 100m. They are estimated to constitute < 0.05% of the catchment bed rock.

3.2.4. Bedrock Chemistry

The variation in composition of rocks within the catchment area and of rocks belonging to the Wallagaraugh Adamellite but occurring outside the catchment area are given in Table 3.2. All samples, excepting GRR21, GRR22, GRR23 are of coarse, even grained adamellite. GRR21 is a feldspar porphyry, and GRR22 and GRR23 are both aplites.

The average, standard deviation, coefficient of variation, maximum and minimum concentration for various elements in adamellite samples occurring in the catchments are given in Table 3.3.

3.2.5 Bedrock Structure

The rocks within the catchment are relatively undeformed; foliation is absent and "blue grains of quartz" indicative of strain are rare. Joint density varies with rock type. Within the granite visible joints are commonly greater than 0.5m apart, whereas joint planes in the aplite tend to be less than 0.5m apart. Discontinuous stringers of vein quartz are occasionally present and are usually associated with 'shear zones'. The spacing between shear zones cannot be determined because of insufficient continuous outcrop.

Sample#	GRR12	GRR13	GRR17	GRR21	CRR22	GRR23
SiO_2	77.17	77.17	76.78	75.12	76.71	76.77
TiO_2	0.10	0.10	0.12	0.24	0.06	0.06
Al_2O_3	11.99	11.96	11.96	12.28	12.49	12.64
Fe_2O_3	0.58	0.71	0.41	0.85	0.30	0.32
FeO	0.43	0.25	0.58	0.88	0.39	0.33
MnO	0.06	0.03	0.03	0.03	0.02	0.03
MgO	0.61	0.62	0.72	0.83	0.60	0.57
CaO	0.38	0.22	0.61	0.58	0.35	0.32
Na_2O	3.35	3.37	2.97	2.90	3.69	3.52
K_2O	4.56	4.52	5.01	5.00	4.77	4.88
P_2O_5	0.02	0.02	0.03	0.04	0.01	0.02
S	<0.02	<0.02	0.05	<0.02	<0.02	0.03
loss	0.97	1.47	0.93	1.20	0.80	0.83
H_2O-	0.14	0.16	0.15	0.16	0.10	0.13
C	0.03	0.02	0.04	0.02	0.02	0.02
rest	0.06	0.07	0.05	0.08	0.06	0.05
	100.29	100.52	100.23	100.04	100.26	100.36
Trace elements						
P	70	65	100	185	25	40
Rb	252	263	184	201	241	273
Sr	36	33	79	74	16	14
Pb	29	31	30	9	35	31
Zr	96	89	106	228	84	72
Y	49	102	27	71	93	46
V	3	3	5	11	<1	<1
Cr	5	<1	4	2	2	4
Mn	409	225	179	195	169	165
Ni	<1	<1	<1	<1	<1	<1
Cu	4	<1	3	6	1	3
Zn	17	30	18	46	19	9

Sample#	GRR1	GRR8	GRR15	GRP16	AB202	AB203	AB204	AB205	AB206
SiO_2	75.54	75.14	76.81	74.75	75.41	77.53	75.96	74.92	76.53
TiO_2	0.15	0.20	0.12	0.21	0.20	0.08	0.15	0.21	0.06
Al_2O_3	12.41	12.23	12.16	12.63	12.61	12.45	12.42	12.79	12.39
Fe_2O_3	0.74	0.88	0.54	0.88	0.33	0.36	0.31	0.70	0.19
FeO	0.53	0.66	0.53	0.75	1.04	0.10	0.84	0.79	0.65
MnO	0.04	0.05	0.03	0.05	0.04	0.01	0.03	0.03	0.04
MgO	0.22	0.35	0.15	0.34	0.50	0.33	0.37	0.49	0.25
CaO	0.93	0.89	0.17	1.02	0.60	0.22	0.43	1.07	0.35
Na_2O	3.27	3.11	3.32	3.16	3.41	3.75	3.39	3.31	3.57
K_2O	4.64	4.51	4.72	4.76	4.58	4.41	4.62	4.63	4.67
P_2O_5	0.03	0.04	0.03	0.05	0.03	0.01	0.02	0.03	0.01
S	<0.02	<0.02	0.02	<0.02	<0.02	<0.02	0.10	<0.02	<0.02
H_2O+	0.74	0.83	0.80	0.95	0.80	0.47	0.75	0.45	0.60
H_2O-	0.31	0.37	0.31	0.37	0.15	0.17	0.14	0.14	0.13
CO_2	0.37	0.52	0.22	0.13	0.16	0.09	0.30	0.07	0.14
rest	0.11	0.13	0.10	0.15	0.12	0.09	0.11	0.13	0.08
			100.03				99.94		
O=S			0.01				0.05		
	100.03	99.91	100.02	100.20	99.98	100.07	99.89	99.76	99.66
Trace elements									
Ba	250	300	180	555	275	105	275	355	65
Rb	226	203	244	176	241	292	206	208	304
Sr	74	84	36.0	97	85	35.0	76	94	17.5
Pb	28.0	24.5	26.5	25.5	21.5	35.5	20.5	21.0	29.5
Th	37.6	30.8	25.8	31.8	26.6	20.4	26.2	27.6	23.4
U	3.6	3.6	6.6	2.6	8.0	10.4	5.8	5.0	9.4
Zr	118	154	100	158	126	69	108	122	64
Nb	9.5	8.5	11.5	8.5	12.5	14.5	9.0	9.0	13.0
Y	36	28	47	27	42	55	36	40	60
La	31	39	32	42	34	18	32	33	20
Ce	69	88	74	90	76	45	72	71	49
Nd	25	30	26	29	25	17	24	23	18
Sc	5	6	6	6	7	6	5	6	5
V	10	13	7	14	14	3	8	13	1
Cr	1	3	2	2	3	1	2	2	<1
Mn	345	380	260	410	330	70	260	200	345
Co	2	4	2	3	3	1	2	4	2
Ni	0.5	<0.5	<0.5	<0.5	1.0	<0.5	<0.5	1.0	<0.5
Cu	<0.5	<0.5	<0.5	1.0	3.0	2.5	15.5	<0.5	2.5
Zn	19	25	17	30	24	12	26	19	15
Ge	13.8	13.8	13.8	13.8	14.6	15.6	13.8	14.2	15.0
P (from Hough)	130	180	105	195					

Table 3.2 Chemistry of the Wallagaraugh Adamellite and associated phases. Samples GRR1,8,15,16 and AB202,204,205, 206 are from Chappell (unpublished data).

Table 3.3 Composition of the Wallagaraugh Adamellite; average concentration ($\bar{x}$), standard deviation (σ), coefficient of variation (C.V.), maximum and minimum concentration of elements in the catchment region.

wt%	$\bar{x}$	σ	C.V.	maximum	minimum
SiO_2	76.39	0.95	1	77.17	74.75
TiO_2	0.14	0.05	35	0.21	0.10
Al_2O_3	12.22	0.26	2	12.63	11.96
Fe_2O_3	0.68	0.17	25	0.88	0.41
FeO	0.53	0.16	30	0.75	0.25
MgO	0.43	0.22	52	0.72	0.15
CaO	0.60	0.35	58	1.02	0.17
Na_2O	3.23	0.15	5	3.37	3.11
K_2O	4.69	0.18	4	5.01	4.51
H_2O+ (2)	0.83	0.06	7	0.95	0.74
C (3)	0.03	0.01	30	0.04	0.02
ppm					
P	121	51	42	195	65
Rb	221	34	15	263	176
Sr	62	26	42	97	33
Pb	28	2	7	31	25
Zr	118	28	24	158	89
Y (1)	36	5	14	49	27
V	8	5	63	14	3
Cr	2	2	100	5	1
Mn	316	94	30	410	225
Ni	<1				
Cu	1	2	200	4	1
Zn	22	6	27	30	17
Bulk (4) Density	2.61	0.006	0.2	2.62	2.60 (g/cm^3)

1) excludes Y for sample GRR13 which is anomalously high
2) calculated from GRR1,8,15,16
3) calculated from GRR12,13,17
4) calculated from GRR2,6,8,16 Data is given in Table 3.1.

3.2.6. The Regolith

The regolith is heterogeneous. A reconnaissance investigation suggested that this heterogeneity can be represented by four profile types. The characteristics of these profiles are outlined below and summarised in Table 3.4. The soil names of these profiles are given in Table 3.4. With further investigation, it is probable that other profile types will be recognised.

The location of the regolith profiles sampled and sample depths are given in Figure 3.1 and Table 3.5 respectively. Profile descriptions are given in Appendix B. The distinguishing characteristics of the four profile types are as follows:

Type I

Except for the surface horizon this type varies in colour from yellowish brown to reddish brown (e.g., profile GR6); the surface horizon has a loamy to sandy loam texture and tends to be less gritty than types II and III; the depth of weathering is usually greater than 2m; rock outcrop in the vicinity of this type is uncommon; and the profiles are well drained.

Type II

Except for the surface horizon, this type is generally light grey in colour. It varies in texture from gritty sand to gritty clay, with the heavier textured horizons occasionally showing weakly developed mottling; and the depth of weathering is often greater than 2m. Although Type II often occurs on 5° to 15° slopes, it is poorly drained with the water table commonly at, or within 1m of the surface. Type II (e.g., profile GR2) usually occurs in discrete patches less than 1ha in size.

Type III

This type (e.g., profiles GR1, 3, 4 and 5) is the most common in the area and has the following characteristics: Except for the surface horizon, the soil is usually yellowish orange in colour; texturally

Table 3.4 Summary description of the types of regolith profile in the catchments.

TYPE	SOIL CLASSIFICATION		PARENT MATERIAL	DIAGNOSTIC FEATURES
	Great Soil Group classification [1]	Northcote classification [2]		
I	Red Earth	Gn	Adamellite	Yellowish brown/reddish brown colour; depth of weathering ≈ 2m.
II	Gleyed Podzolic	Dg	Adamellite	presence of hydrophillic vegetation; gleyed nature of profile.
III	Yellow Podzolic	Dy	Adamellite	yellowish orange colour; gritty texture; depth of weathering ≈ 2m.
IV	Red Earth/ Krasnozem	Gn	Basalt Dyke	brown/reddish brown colour; non-gritty, clay/medium clay texture.

1 Stace et al., 1968.

2 Northcote, 1979.

Table 3.5 Sample depths for profiles GR1, 2, 3, 4, 5, and 6.

Sample Number	Depth (cm)	Bulk Density (gcm^{-3})
PROFILE GR1		
1	0-2	0.92
2	3-8	1.53
3	15-20	1.78
4	30-35	1.72
5	50-55	1.61
6	65-70	1.62
7	115-120	1.68
8	190-200	2.18
PROFILE GR2		
1	0-3	1.53
2	27-33	1.76
3	39-44	1.80
4	48-53	1.52
5	80-85	1.72
6	125-130	1.77
7	155-160	1.64
PROFILE GR3		
1	0-2	1.75
2	10-15	1.72
3	20-25	1.43
4	30-35	1.66
5	53-58	1.52

Sample Number	Depth (cm)
PROFILE GR4	
1	0-5
2	15-20
3	25-30
4	35-40
5	50-70
PROFILE GR5	
1	0-5
2	25-30
3	55-60
PROFILE GR6	
1	0-5
2	10-15
3	20-25
4	50-55
5	100-105
6	150-155
7	195-200

it varies from gritty sand to gritty sandy loam at the surface and can grade to gritty sandy clay with depth; it is often less than 2m in depth; well drained; and rock outcrop is commonly associated with its occurrence.

Type IV

This type is uncommon within the catchment area (<0.05% of the area) and is formed from the weathering of basalt dykes. It is commonly brown to reddish brown in colour and has a clay to medium clay texture and often contains diagnostic core stones. Profile D1 (Appendix B), although not occurring in the area, is similar to those which do.

3.3 PARTICLE-SIZE SUITES IN THE CATCHMENTS

On the basis of their shape or size distribution, five suites of particles have been recognised in the area. These particle-size suites exclude those which are formed by the physical and chemical weathering of basalt dykes, porphyritic and pegmatitic phases of the granite and the chemical disintegration products of aplite.

The suites of particles can be grouped as follows:

1) those associated with granite outcrops
2) those associated with aplite outcrops
3) those resulting from the physiochemical weathering of granite
4) those due to termite activity
5) stream-bed sediments.

The size frequency distribution of suites 1, 3, 4 and 5 is shown in Figure 3.3.

3.3.1 Particles Associated with Granite Outcrops

The particles associated with granite outcrops vary from discrete blocks (tors), which are approximately 20cm to 200cm in size (Figure 3.3F), to exfoliation layers, to the products of granular disintegration (grus).

Figure 3.3 Particle-size suites in the catchment area and the size distribution of quartz and H_2O+ from selected samples of profile GR1.

Histogram Explanation

A: Average particle-size distribution of termite mounds, GRTA (Table 3.7).

B: Average particle-size distribution of stream-bed sediments, GRSA (Table 3.7).

C: Particle-size distribution of samples GR103 and GR104 (Table 3.6).

D: Particle-size distribution of sample GR108 (Table 3.6).

E: Particle-size distribution of grus (Table 3.7).

F: Size distribution of tors. (Their frequency distribution is unscaled and their size distribution is estimated from field observations).

G: Size dependent distribution of quartz and H_2O+, expressed as the percent of the whole sample contained within a specific 1ϕ fraction (Figure 3.6). The distribution of quartz and H_2O+ is the average of their respective distributions in samples GR103 and GR107.

The bar graph represents the common range in size of framework grains in the parent rock (see Appendix C).

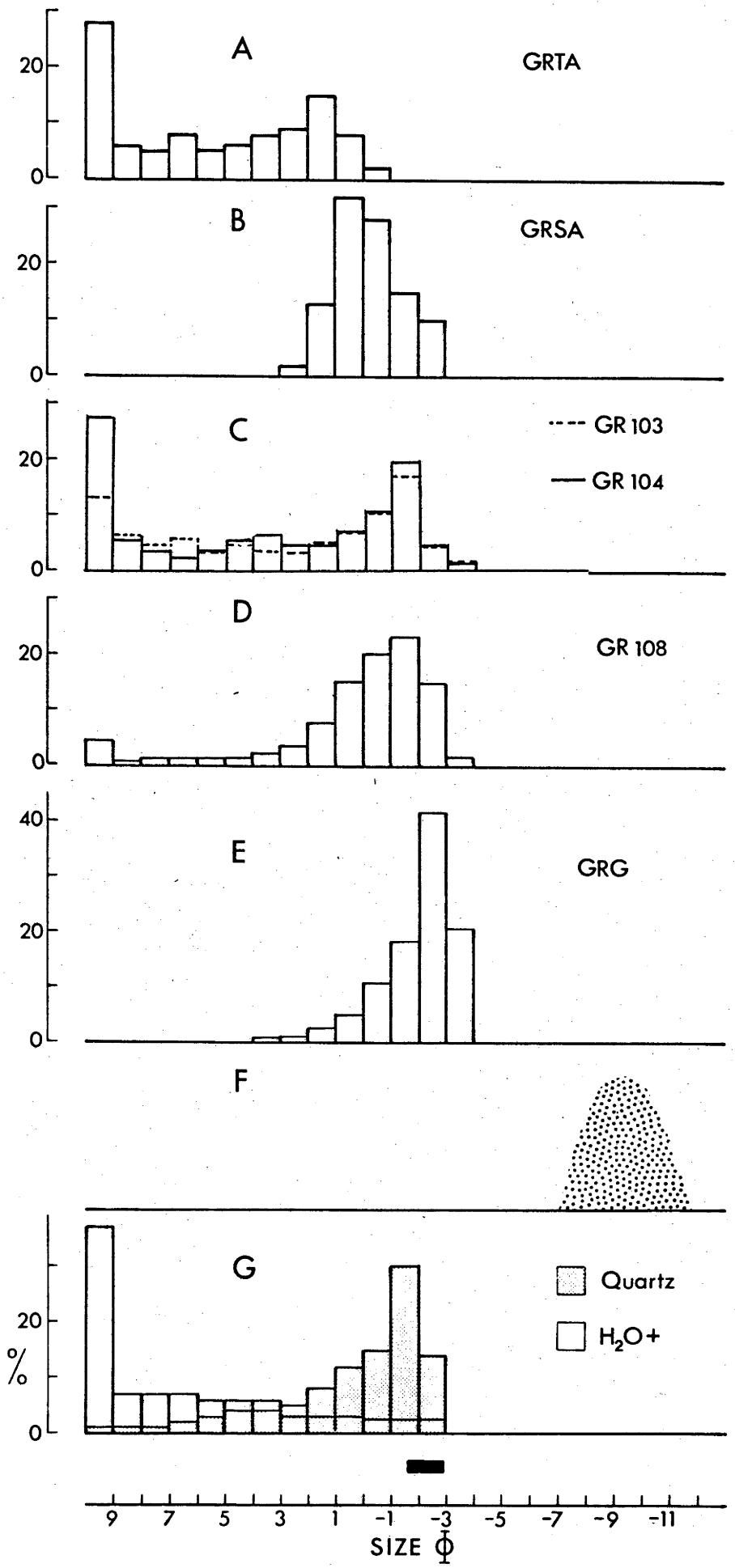
A
GRTA
B
GRSA
C
GR 103
GR 104
D
GR 108
E
GRG
F
G
Quartz
H2O+
%
20
0
40
9
7
5
3
1
-1
-3
-5
-7
-9
-11
SIZE Φ

SAMPLE NUMBER	SIZE ϕ <-9	8	7	6	5	4	3	2	1	0	-1	-2	-3	-4	>-4
GR101	3.8	1.5	1.5	2.8	3.2	3.3	2.4	3.3	7.4	16.8	25.9	19.4	2.0	7.2	0.0
GR102	12.3	4.5	5.3	5.9	5.2	6.5	5.0	5.9	8.8	12.2	16.0	8.6	2.5	1.2	0.0
GR103	13.7	6.7	3.3	5.6	5.6	6.2	4.8	5.6	8.4	11.3	11.0	14.4	3.3	0.1	0.0
GR104	28.0	5.5	4.5	6.1	3.0	4.5	3.8	3.4	4.7	7.0	10.7	15.1	3.5	0.3	0.0
GR105	24.9	4.8	4.2	3.7	2.9	5.5	5.9	4.6	4.6	7.4	11.1	15.7	4.6	1.1	0.0
GR106	28.2	1.6	3.8	3.0	3.9	5.5	5.9	4.6	4.6	7.4	11.1	19.1	4.1	0.3	0.0
GR107	11.0	2.0	1.3	1.9	3.8	5.1	5.8	4.9	6.2	8.4	11.0	25.5	13.0	0.1	0.0
GR108	4.5	0.8	1.1	1.4	1.4	1.6	2.2	3.7	7.9	15.3	20.1	23.3	15.0	1.7	0.0
GR201	10.6	4.1	5.7	6.8	6.9	7.6	4.2	8.6	20.2	20.4	4.9	0.0	0.0	0.0	0.0
GR202	10.2	3.7	5.7	7.4	6.9	7.5	4.6	8.5	19.0	20.6	5.9	0.0	0.0	0.0	0.0
GR203	11.6	2.5	4.1	4.5	5.8	6.0	3.6	6.0	13.2	16.5	19.9	6.3	0.0	0.0	0.0
GR204	38.6	2.4	3.3	4.3	5.5	4.7	3.0	4.4	7.8	9.5	11.5	5.0	0.0	0.0	0.0
GR205	50.7	1.7	2.3	3.0	3.9	4.8	3.3	4.9	8.3	8.6	8.6	2.1	0.4	0.0	0.0
GR206	26.2	2.5	2.7	3.8	4.7	6.2	4.8	7.6	12.3	12.3	13.7	3.2	0.0	0.0	0.0
GR207	11.9	2.6	2.6	3.4	3.4	4.4	5.5	7.2	12.0	20.5	21.0	5.5	0.0	0.0	0.0
GR301	8.5	3.3	4.7	5.5	6.8	5.7	5.5	5.2	9.2	10.3	9.3	20.6	6.2	0.2	0.0
GR303	26.0	3.5	3.0	3.5	3.0	4.8	4.4	4.0	5.2	7.6	13.6	15.6	5.6	0.2	0.0
GR304	25.8	3.2	2.3	3.9	3.9	5.2	5.2	4.0	4.0	6.0	11.2	17.2	8.0	0.1	0.0
GR305	18.7	2.9	2.6	3.5	3.9	5.6	5.6	4.4	5.2	6.8	10.6	20.0	9.6	0.6	0.0
GR401	4.1	2.1	3.4	4.2	4.6	4.8	4.9	6.4	9.8	14.3	20.5	17.9	1.4	1.0	0.5
GR402	5.0	3.0	3.8	4.3	4.4	4.8	4.5	5.7	9.0	12.8	22.7	16.9	1.3	1.0	0.8
GR404	9.0	3.9	4.7	5.0	5.3	6.3	5.9	7.4	10.9	14.8	13.6	11.8	1.0	0.4	0.0
GR404	19.7	4.0	4.4	4.5	4.5	4.9	5.2	6.5	9.4	11.9	15.4	6.8	2.2	0.5	0.0
GR405	30.2	2.8	3.5	3.2	2.8	2.2	4.4	6.7	11.7	14.6	9.5	8.1	0.3	0.0	0.0
GR501	4.3	2.5	2.7	2.8	3.3	3.3	3.0	4.3	7.3	10.1	12.6	21.6	12.7	8.2	1.1
GR502	3.8	2.6	3.1	3.5	3.8	4.2	3.3	4.9	7.7	10.1	18.7	22.9	9.2	2.1	0.0
GR503	4.8	2.2	3.4	4.3	4.7	4.7	3.9	5.8	9.5	12.3	16.7	10.9	5.4	7.8	3.8
GR601	16.7	3.7	5.7	8.5	11.7	12.2	4.7	6.8	11.3	9.6	4.5	2.7	0.8	1.2	0.0
GR602	16.6	3.5	4.6	6.7	11.3	11.6	4.6	6.1	10.5	8.0	3.0	2.1	6.7	4.4	0.4
GR603	26.5	3.0	4.3	6.8	10.9	11.4	4.7	6.2	10.4	7.6	4.0	2.1	1.1	1.0	0.0
GR604	39.9	2.3	3.5	5.9	7.3	9.0	3.1	4.4	7.9	5.9	5.1	5.0	0.4	0.3	0.0
GR605	46.7	2.2	3.3	4.8	7.0	7.5	2.8	3.9	7.4	6.2	4.8	2.8	0.6	0.0	0.0
GR606	48.9	1.8	3.3	4.5	6.8	6.4	2.3	3.7	7.1	6.0	4.8	2.8	0.9	0.7	0.0
GR607	44.9	2.7	3.5	5.1	6.8	6.5	2.8	3.9	7.9	6.7	4.7	4.1	0.4	0.0	0.0

Table 3.6 Particle-size distribution of profiles GR 1,2,3,4,5,6.

Table 3.7 Particle-size distribution (% under-size) of grus, termite mounds and stream-bed sediments.

Sample Number	Size ϕ														
Grus	4	3.5	3	2.5	2	1.5	1	0.5	0	-0.5	-1.0	-1.5	2.0	2.5	-3.0
GRG	0.1	0.2	0.4	0.7	1.0	1.7	2.2	2.8	4.7	6.2	7.9	10.2	21.1	20.3	20.3

Termite Mounds	Size ϕ												
	9	8	7	6	5	4	3	2	1	0	-1	-2	-3
GRTM1	36	5	5	4	5	9	8	8	10	9	1		
GRTM2	31	5	6	9	3	10	8	5	15	6	2		
GRTM3	29	11	3	6	7	6	8	6	15	7	2		
GRTM4	23	6	4	6	6	6	11	7	16	13	2		
GRTM5	23	6	3	9	4	7	8	12	18	4	6		

Stream-bed Sediment						
GRS1	1	10	30	25	20	14
GRS3	<1	4	29	39	25	2
GRS4	5	18	36	26	11	3
GRS5	3	20	33	18	6	19
GRS6	1	13	29	33	13	10

The tors are separated from each other by joint planes, with the tor representing the relatively unfractured core between joint intersections. The importance of jointing in determining the size and distribution of tors is described by Thomas (1974) and Twidale and Bourne (1975).

Often the tors have well developed exfoliation layers which are less than 20cm thick. Usually the thicker the layer, the greater its lateral extent. Exfoliation layers rarely cover an entire rock surface as they are truncated either by joint planes or by changes in curvature of the rock surface. The mode of formation of exfoliation layers has been reviewed by Ollier (1971).

After the wildfire during the summer of 1978/79, smooth surfaced, wafer-like exfoliation layers 3 to 5mm thick and up to 400cm^2 in size, (Plate 1B) were common on exposed surfaces of unweathered rock. The occurrence of such thin layers (often less than, or equal to the size of a single grain in thickness) and their relative smoothness, suggests that parting of exfoliation layers is preferentially intragranular.

Grus is dominantly between 0.5 and 30mm in size (Figure 3.3E). Where particles greater than 30mm occur they are usually sufficiently fragile to be crushed between a boot and a hard object. Grus need not form consequent to exfoliation, but can form by the in situ granular disintegration of the rock mass (Plate 2A).

The conformity between the size distribution of grus and that predicted by the Rosin Ramler distribution ('Rosin's Law') or its variants has been noted by many workers (Krumbein and Tisdell, 1940; Kittleman, 1964; Russel, 1976). This conformity is also shared by the grus sample analysed (Figure 3.4; Table 3.7) although deviation does occur at the distribution extremities.

Although 'Rosin's Law' has been empirically shown to describe the distribution of crushed coal, the relevance of this crushing analogy to the origin of grus is questionable. For instance, the maximum size of crushed coal is dependent on the mechanical features of the crushing device, and the force leading to its comminution is unconfined compression. Neither of these features have any apparent analogies in the environment in which grus is formed.

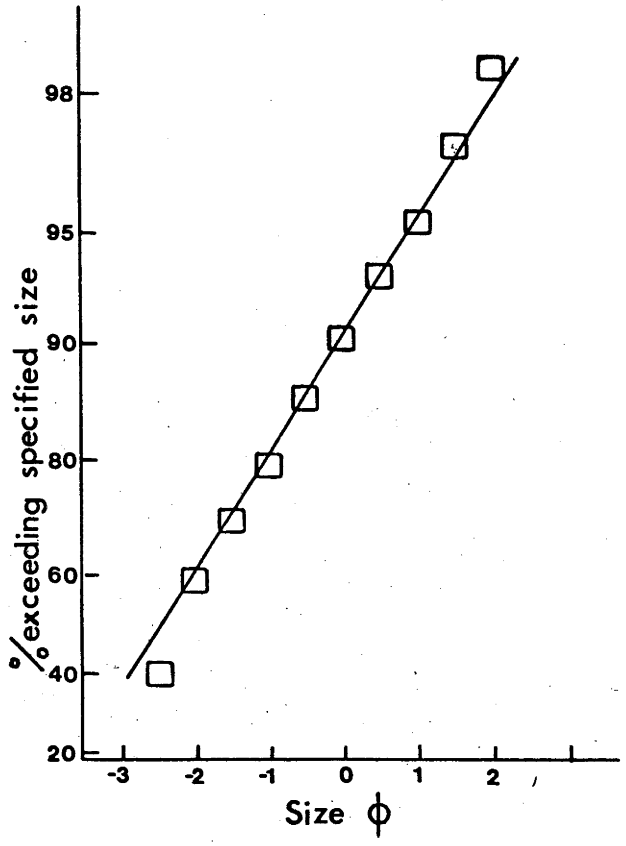

Figure 3.4 Size cumulative frequency (Rosin's Probability Scale) distribution of grus sample GRG. See Kittleman (1964) for an explanation of the Rosin' Probability Scale. The solid line is that predicted by Rosin's Law.

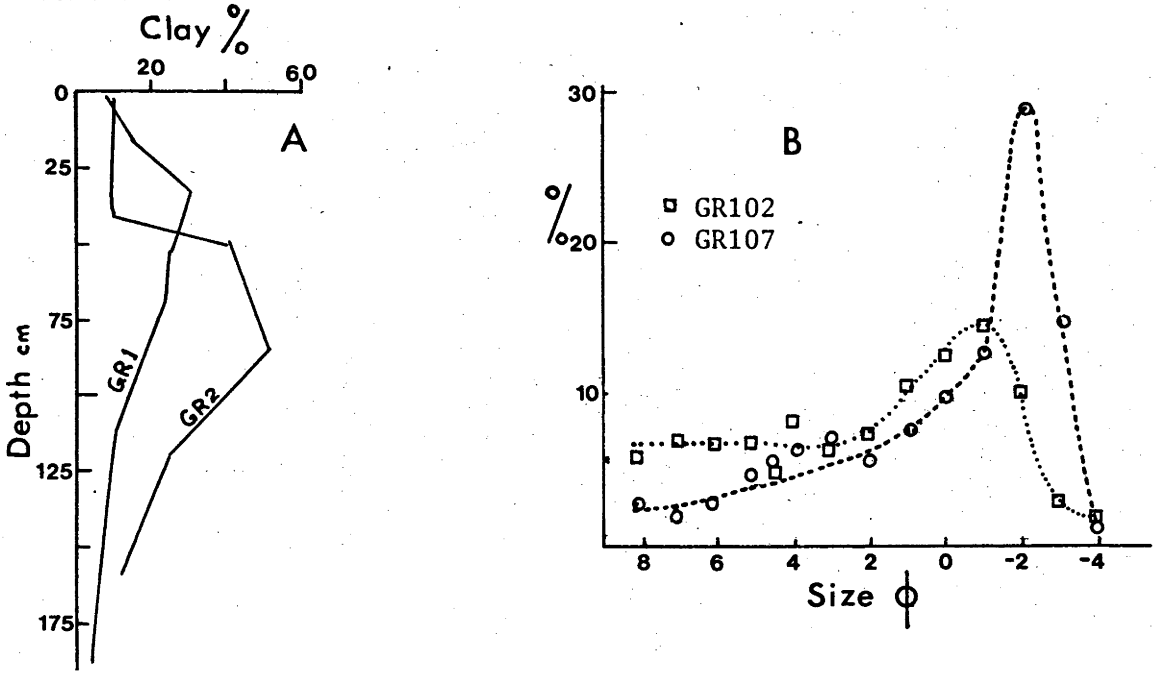

Figure 3.5 Particle -size distribution of weathering profiles.

A: Depth dependent variation in clay content for profiles GR1 and GR2. Profiles GR1 and GR2 were chosen as illustrative examples.

B: Variation in the particle-size distribution of the non-clay fraction with weathering.

Bustin and Mathews (1979), Isherwood and Street (1976) and Tassel and Grant (1980) have attributed the formation of grus to the incipient weathering of biotite, and its consequent expansion. This leads to microcrack development and physical weakening of the rock. Unfortunately, these studies do not supply data on the nature of the disintegration products and the extent to which their size distribution conforms to the Rosin function.

Although the incipient weathering of biotite provides a simple explanation of the cause of fragmentation, it is probable that this explanation is incomplete, as:

1) concomitant with the alteration of biotite, the rock mass is undergoing changes due to incipient hydration which is likely to affect all minerals present; and
2) the susceptibility of a rock to granular disintegration appears to be unaffected by the proportion of biotite. For example, the Wallagaraugh Adamellite commonly contains <3% biotite which is low compared with the biotite content of rocks examined in the studies cited above.

At present no explanation for the processes controlling grus formation can be offered.

3.3.2. Particles Associated with Aplite Outcrops

Aplite in the area is, in comparison to the granite, strongly jointed. The spacing between joint planes is usually less than 50cm.

Aplite outcrops are often characterised by the occurrence of polygonal particles 5cm to 40cm in size (Plate 1A). These particles usually have conchoidal to subconchoidal fracture surfaces and fragile serrated edges.

Fire is probably a significant process in the formation of these particles. Those particles shown in Plate 1A (and many like them throughout the catchments) appeared to have formed immediately after 1978/79 fire. They are also similar to descriptions of particles formed by the effect of fire given by Blackwelder (1927).

3.3.3. Particle-size Distribution of Regolith Profiles

The particle-size distribution for samples from profiles GR1, 2, 3, 4, 5 and 6 is given in Table 3.6.

The data (Figure 3.3C and D) show the existence of a clay size mode and a coarse sand/gravel size mode. These modes are described separately as the clay fraction and the non-clay fraction.

Clay Fraction

Generally the clay content increases up profile until it reaches a subsurface maximum, and then decreases (Figure 3.5A). The depth of the near surface maxima varies, but is usually less than 50cm.

Non-Clay Fraction

With increasing weathering, reflected by the decrease in modal size (e.g., between samples GR107 and 102, Figure 3.5B) particles in the non-clay fraction tend to become more uniformly distributed throughout.

The particle-size distribution of this fraction can be shown (Section 3.4) to be controlled dominantly by the distribution of quartz in the regolith and its antecedent distribution in the parent rock.

3.3.4. Particle-Size Distribution Due to Termite Activity

Termite mounds are scattered throughout the area. The particle-size distributions of samples from five mounds are given in Table 3.7. The average particle-size distribution for these samples (GRTA) is shown in Figure 3.3A.

Field texturing of the termite mound source material (both surface and subsurface) showed that it was always more gritty, and depleted in the silt/fine sand fraction, than the termite mound material.

This size sorting effect of termite activity has also been described by others (Watson, 1975; Lee *et at.*, 1981).

3.3.5 Particle-Size Distribution of Stream-Bed Sediments

The particle-size distribution of stream-bed sediment grab samples collected from the stilling ponds at weirs C1, C3, C4, C5 and C6 is given in Table 3.7. The average particle-size distribution of the 5 samples (GRSA) is plotted in Figure 3.3B. This average provides only an indication of the particle-size distribution of the stream-bed sediments as: i) the grab samples are not statistically representative of the sediment in the stilling pond; and ii) the sediment in the stilling pond is not representative of the bed load sediment, as some of it is lost over the weir during storm discharge. However, the stream-bed sediment size distribution reflects:

1) the particles available for transport and which can be readily moved in the stream/slope environment (Friedman, 1979).
2) breakage of particles within the stream environment (Moss, 1972a,b).
3) the high energy fluvial environment which (a) separates particles <100μm from the stream-bed environment, removing them in suspension, and (b) determines the size distribution of the resulting lag deposit.

3.4 REGOLITH MINERALOGY

As quantitative changes in mineralogy with depth in a profile can result from the removal of a particular particle-size fraction, the variation in mineralogy with particle-size needs to be known. This variation is described for selected samples (Section 3.4.1) and the relationship between mineralogy and particle-size modes discussed (Section 3.4.2). This is followed by a description of the depth dependent variation in mineralogy (Section 3.4.3).

3.4.1 Size Dependent Variation in Mineralogy

Because of the time involved in isolating size separates, particularly those requiring separation by repeated decanting, only two samples were chosen for size factionation. Samples GR107 and GR103 which have similar clay contents (11.0% and 13.7% respectively), were chosen because they differed in their degree of weathering. This difference is expressed by the decrease in their respective K-feldspar concentrations from 25% to 10% (Table 3.9).

The mineralogy of the size separates and the size dependent distributions of quartz, K-feldspar and clay minerals is given in Table 3.8 and Figures 3.6 and 3.7 respectively.

Quartz

In sample GR107, $<10\%$ of the quartz is finer than 1ø. Thin section observations of the parent rock showed quartz grains of this size occurring only in aplitic and porphyritic varieties. The single well defined mode (-1.5ϕ) (Figure 3.6B) is not consistent with either an aplite or a porphyry being the source of sample GR107. Consequently, it is reasonable to argue that the parent rock was even textured and that during the formation of GR107, quartz comminution has occurred. The similar modal quartz sizes of samples GR107 and GR103 supports the contention that their source rocks were similar in texture. Consequently, the higher proportion of quartz ($\sim 40\%$) in the finer than 1ø fraction of GR103, compared with the less-weathered GR107, suggests continued quartz comminution with increasing weathering.

Table 3.8 Mineralogy and $\%H_2O+$ of size separates from samples GR103 and GR107. Plagioclase was detected only in the sand fraction of sample GR107. (nd - not detected, ndet - not determined.)

	Size Separate SIZE ϕ													
	<9	8	7	6	5	4	3	2	1	0	-1	-2	-3	Total Sample
Horizon GR103														
% of whole sample	13.7	6.7	3.3	5.6	5.6	6.2	4.8	5.6	8.4	11.3	11.0	14.4	3.3	100
% quartz	8	12	23	38	51	63	61	72	82	88	88	93	90	62
% K-feldspar	10		25			30		20		5		5		10
% H_2O+	10.5		6.0			1.6		0.9		0.4		0.2		2.47
% clay minerals 7Å	40		50			100		nd						ndet
10Å	25		40			tr		nd						ndet
14Å	35		10			nd		nd						ndet
Horizon GR107														
% of whole sample	11.0	2.0	1.3	1.9	3.8	5.1	5.8	4.9	6.2	8.4	11.0	25.5	13.0	100
% quartz	1.5	6	7	6	6	12	13	20	24	34	46	54	59	40
% K-feldspar	tr		10			30		35		45		25		25
% H_2O+	12.0	11.7	10.3	11.3	11.0	8.7	9.2	6.3	4.2	2.8	2.2	1.9	1.9	3.17
% clay minerals 7Å	40	70	60	60	60	85	85	100	50	nd				ndet
10Å	55	30	40	40	40	15	15	tr	50	nd				ndet
14Å	5	tr	tr	tr	tr	nd	nd	nd	nd	nd				ndet

Figure 3.6 Size dependent variation in mineralogy for samples GR103 and GR107. The size dependent variation is expressed as:

1) Concentration % (Figure A only).
2) %Sf/T. This represents the percent of the whole (or total; T) sample concentration of a particular mineral in a specific size fraction (Sf) and applies to figures B,C,D,E. See Brewer (1955) as an example.

The percent of the whole sample in each size fraction was calculated from measurements at 1ϕ intervals (Table 3.8). For any 1ϕ interval for which data were not available, the data were calculated by interpolation.

Concentration %

A: Quartz

Percent of whole sample in each size interval

B: Quartz 1ϕ intervals

C: Quartz

D: K-feldspar

E: H_2O+

Size intervals are those of the International Scale (Cl, clay; Si, silt; FS, fine sand; CS, coarse sand; Gr, gravel).

Size distribution of quartz in the Wallagaraugh Adamellite.

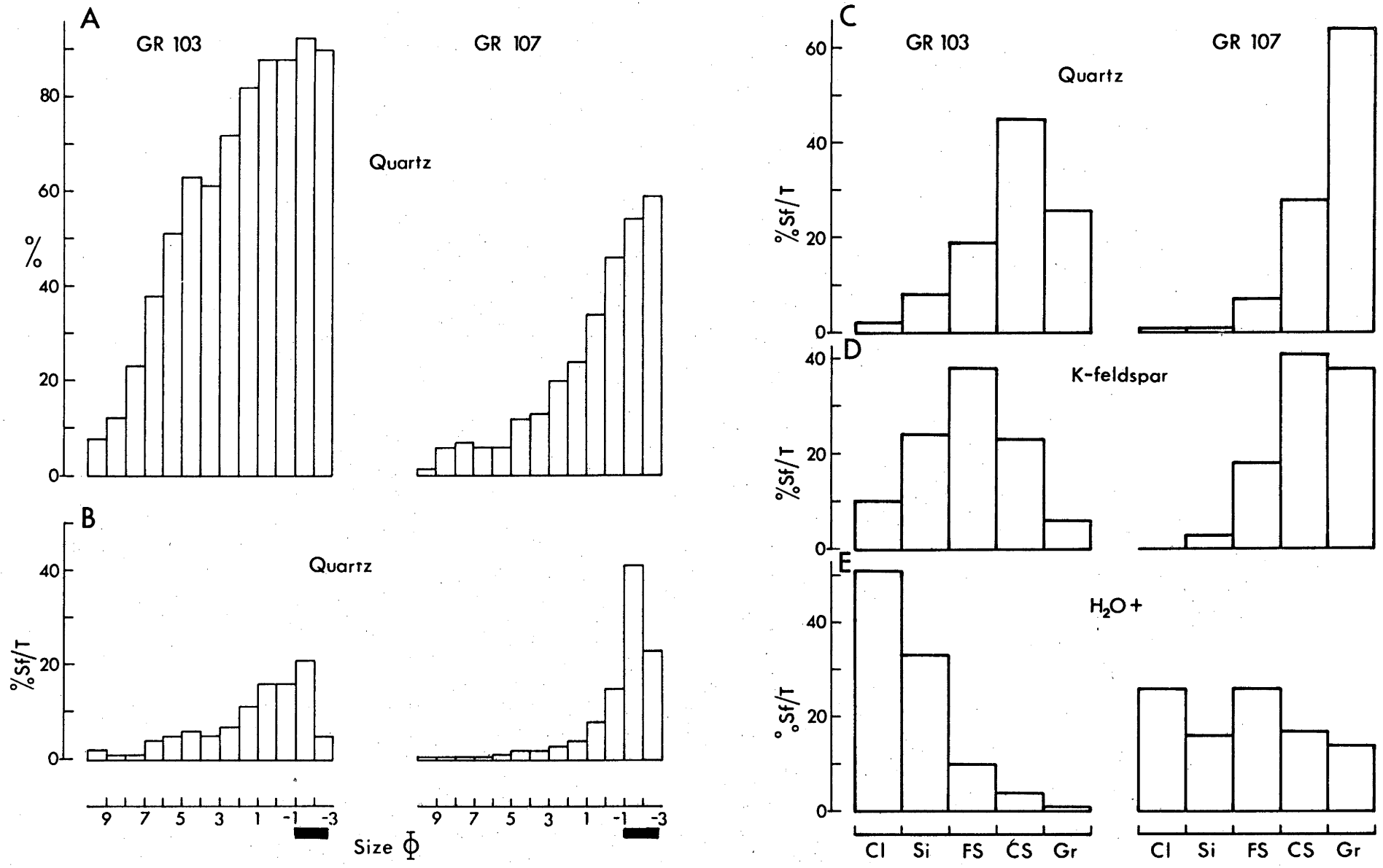
A
GR 103
GR 107
Quartz
%
80
60
40
20
0
B
Quartz
%Sf/T
40
20
0
9 7 5 3 1 -1 -3
Size Φ
C
GR 103
GR 107
Quartz
%Sf/T
60
40
20
0
D
K-feldspar
%Sf/T
40
20
0
E
H2O+
°Sf/T
40
20
0
Cl Si FS CS Gr
Cl Si FS CS Gr

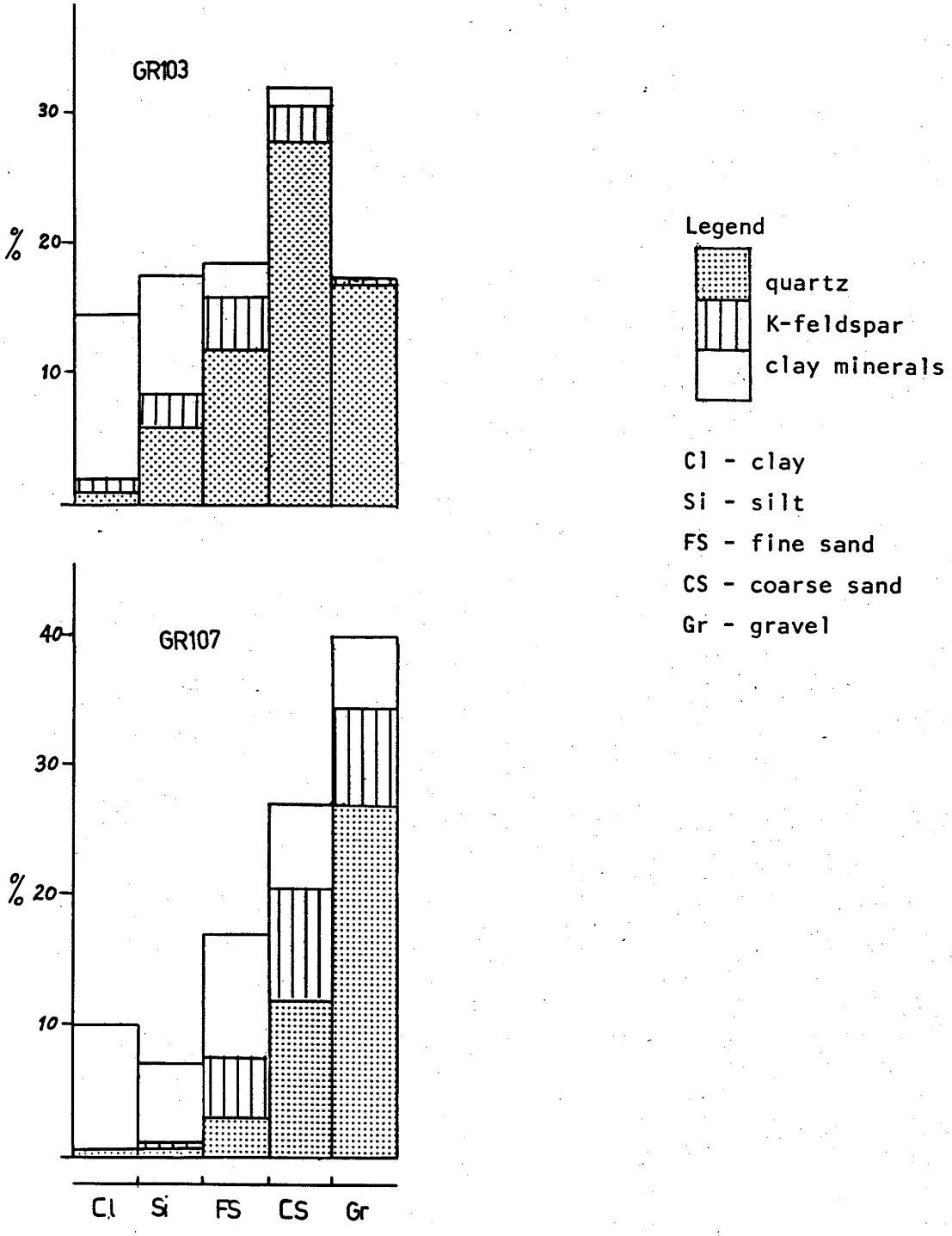

Figure 3.7 Particle-size as a function of mineralogy.

K-feldspar

In even textured rock samples, K-feldspar and quartz have a similar size distribution. In comparison to quartz, K-feldspar is finer grained in sample GR107 and undergoes greater reduction in size between samples GR107 and 103.

This is consistent with the susceptibility of feldspar to breakage along twin/cleavage planes (Pittman, 1969) and to chemical weathering.

Clay Minerals

As noted in Chapter 2, H_2O+ is used as a surrogate measure of the total clay mineral concentration. The occurrence of clay minerals in the non-clay fraction (Figure 3.6E) is attributed to their retention in partially weathered but still physically coherent feldspar and biotite grains. Scanning electron microscopy and visual observations showed that the clay minerals did not occur as, silt, sand and gravel size aggregates a result of incomplete dispersion.

Although samples GR107 and 103 have similar clay contents, 11.0% and 13.7% respectively, the proportion of the total clay mineral content in the clay fraction increased from approximately 25% to 50% (Figure 3.6E). This indicates that, i) the generation of clay lags the generation of clay minerals, and ii) there is a tendency of clay minerals with increased weathering to concentrate in the clay fraction.

The clay mineralogy of size separates given in Table 3.8 shows that considerable variation can occur in the relative proportion of a clay mineral with size. For example, in sample GR107, the relative proportion of kaolinite (7Å peak) varies from 40% in the <9ø separate to 100% in the 3-2ø separate.

The size dependent distribution of quartz, feldspar and clay minerals described here, is consistent with the results of other studies of granite weathering (Brewer, 1955; Rice, 1973; Eswarin and Bin, 1978).

3.4.2 The Relationship Between Mineralogy and the Particle-Size Modes of Samples GR103 and GR107

The relationship between mineralogy and particle-size modes is most readily demonstrated when the particle-size distribution of a sample is plotted as a function of the size distribution of its mineral components, viz., the magnitude of a particle-size class is equivalent to the sum of the concentration of its individual mineral components. The proportion of a mineral in a size fraction is the product of the percent of the mineral in that size fraction and the percent of the whole sample in that size fraction.

The relationship between mineralogy and particle-size is plotted in Figure 3.7. It shows that the: i) clay size mode is dominated by clay minerals, and ii) the non-clay mode is dominated by quartz. Hence, this mode reflects the size distribution of quartz in the parent rock (section 3.4.1), and its comparative resistance to physiochemical weathering.

3.4.3 Depth Dependent Variation in Mineralogy

The mineralogy of the various profiles is given in Table 3.9 and plotted in Figure 3.8. With respect to whole sample mineralogy, Figure 3.8 shows that generally:

1) the relative proportion of quartz increases up profile.
2) the relative proportion of feldspar decreases up profile.
3) the relative proportion of neoformed minerals (dominantly clay minerals) increases up profile to a near surface maxima and then decreases.

Based on the rate of depletion within the profile of the three dominant minerals in the granite, their relative persistence is quartz> K-feldspar >> plagioclase.

Clay Mineralogy (clay fraction)

The dominant minerals in the clay fraction are kaolinite, illite and vermiculite. Quartz, K-feldspar and iron oxides are present in trace to minor proportions.

Table 3.9 Mineralogy of the whole sample and the clay fraction, as determined by XRD* and IR+ spectroscopy. Mineralogical proportion: tr, trace; nd, not detected.

	Mineralogy % Whole Sample				Clay Mineralogy % Clay Fraction*			
					---------- Å ----------			
Horizon	Quartz+	K-feldspar*	Plagioclase*	Illite*	14	12	10	7
GR101	80	5	nd	nd	50	tr	15	35
GR102	57	13	nd	nd	30	tr	25	45
GR103	62	10	nd	nd	35	tr	25	40
GR104	58	10	nd	nd	30	tr	25	45
GR105	46	15	nd	nd	20	tr	30	50
GR106	42	20	tr	nd	20	tr	35	45
GR107	40	25	tr	nd	5	tr	55	40
GR108	42	40	5	nd	10	tr	60	30
GR201	76	15	tr	nd	40	nd	tr	60
GR202	78	15	tr	nd	45	nd	tr	55
GR203	79	15	tr	nd	30	nd	10	60
GR204	64	15	nd	nd	30	nd	10	60
GR205	41	10	nd	nd	20	tr	10	70
GR206	56	20	tr	nd	30	tr	10	60
GR207	50	30	5	nd	nd	tr	30	70
GR301	70	30	nd	nd	65	nd	tr	35
GR302	72	25	nd	nd	55	nd	nd	45
GR303	52	25	nd	nd	20	nd	20	60
GR304	42	30	nd	nd	20	nd	25	55
GR305	44	30	nd	nd	10	tr	40	50
GR401					10	25	5	60
GR402					20	5	15	60
GR403					20	5	15	60
GR404					15	5	15	70
GR405					10	5	20	70
GR501					75	nd	nd	25
GR502					75	nd	nd	25
GR503					40	nd	20	40
GR601					70	nd	nd	30
GR602					75	nd	nd	25
GR603					75	nd	nd	25
GR604					60	nd	nd	40
GR605					60	nd	nd	40
GR606					60	nd	nd	40
GR607					50	nd	nd	50

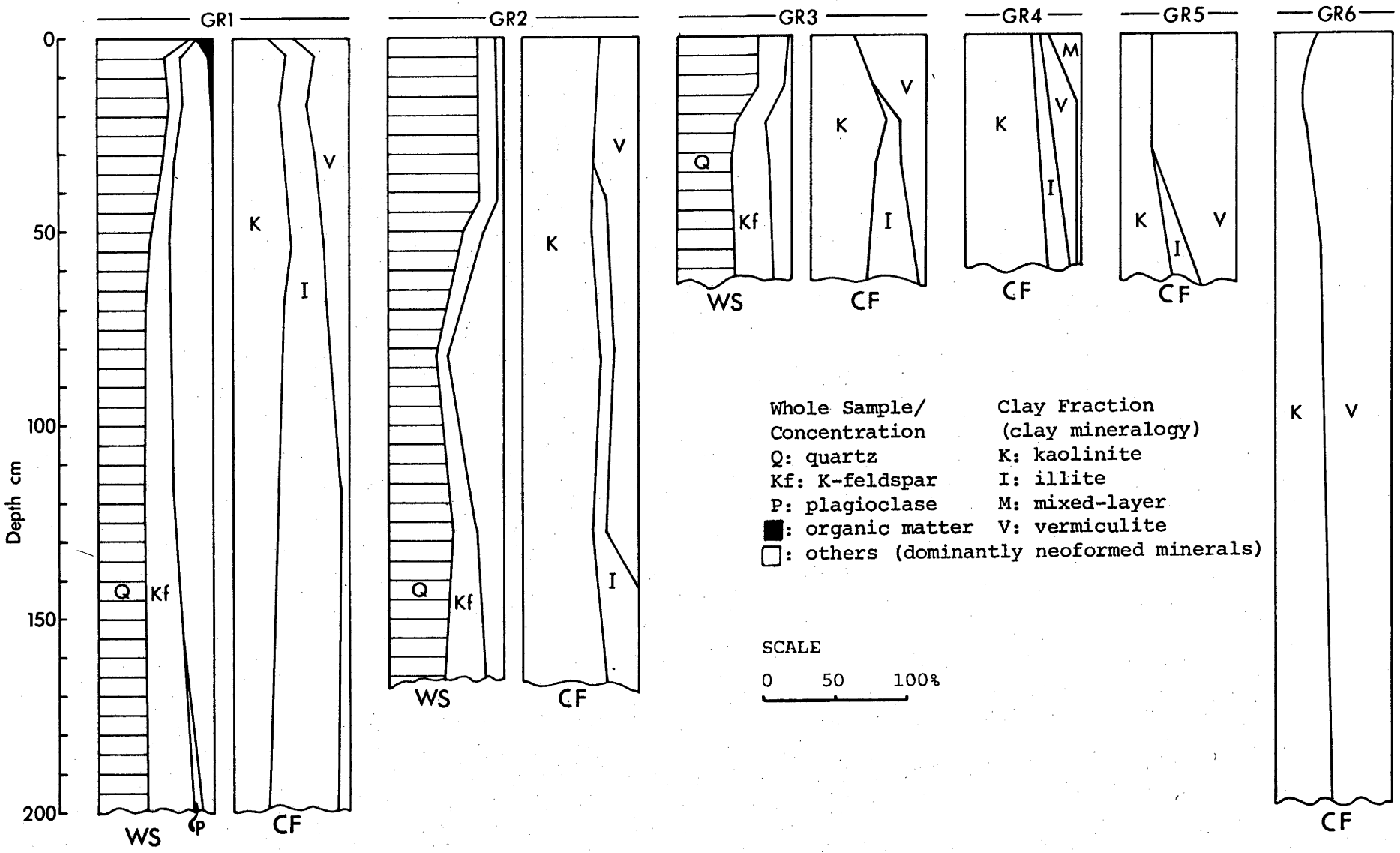

Figure 3.8 Depth dependent variation in mineralogy for profiles GR1, 2, 3, 4, 5, 6. Mineralogy is described for the whole sample (WS) and the clay fraction (CF, clay mineralogy).

The relative proportions of clay minerals vary with depth within a single profile, and from profile to profile. Kaolinite and vermiculite are usually codominant with the proportion of illite decreasing up profile (Figure 3.8).

As other workers have used depth dependent changes in (clay fraction) clay mineralogy as a basis to argue for specific mineral transformations, it could have been expected that I would do likewise. I have not done so, because predictions based on this approach are likely to be in error for the following reasons:

1) The clay fraction on which the primary to neoform mineral transformations are conventionally based does not include all clay minerals present in the sample (Figure 3.6E).
2) A change in the relative proportion of a clay mineral can occur through either:
   i) the transformation of one clay mineral to another.
   ii) the release of pre-existing clay minerals from the non-clay fraction through the effects of continued physical or chemical weathering of primary minerals. For example, it is possible that much of the illite present in the less weathered samples (e.g., GR108, 107) is due to the release of illite present in the rock and which was formed by the subsolidus alteration of plagioclase.
3) The XRD techniques used to estimate mineral proportions are only approximate. Crystallinity, particle-size, and sample preparation all affect peak shape (Mills and Zwarich, 1972; Stoke and Larsen, 1973).

Direct observation of the mineral transformations, (e.g., TEM studies of ultra-thin sections, e.g., Kitagawa and Kakitani, 1977; Eggleton and Busek, 1980) which would resolve this problem were outside the scope of this thesis.

The clay mineralogy data presented here, will form the basis for comparing the dependence of clay mineralogy on parent rock.

3.5 REGOLITH CHEMISTRY

The chemistry of the parent rock has been given in Table 3.3. As primary minerals can form a major part of the regolith, consideration of their chemistry and partitioning of elements between them is important: this is described first.

As changes in profile chemistry can occur through the selective removal of particular particle-sizes, the variation in chemistry with particle-size is described next. This is followed by a description of the depth dependent variation in chemistry.

The chemical constraints on the origin of the texture contrast developed in profile GR1 are then described.

3.5.1 Parent Rock : Element Partitioning

The partitioning of elements between different minerals in granite has been described in detail by Chappell (1966), Rhodes (1969) and Joyce (1970). Chappell (1966) has shown that mineral analysis should not be accepted at face value, an issue commonly ignored by workers in the field of rock weathering. For example:

1) Lelong et al. (1976) in a review of element partitioning as an aid to understanding weathering, give the CaO content of biotite as 0.X%. Chappell (1966) has shown that the CaO content of biotite is always <0.01% and that high CaO values (e.g., Lelong et al., 1976) are due to apatite inclusions.
2) Nesbitt et al. (1980) (in a paper on the behaviour of alkali and alkali earth elements during weathering), discuss the partitioning of Sr in granite. They assume that Sr occurs dominantly in plagioclase, citing Turekin and Kulp (1965) as the authority. This citation is made despite:
   i) that in 1956 the complexities of trace elements partitioning were poorly understood;
   ii) comments by Wedepohl (1978, p.38-G-1) that plagioclase and K-feldspar are almost as equally important as Sr host minerals; and
   iii) the considerable amount of data in Smith (1974) which shows that K-feldspar and plagioclase are both important Sr host minerals.

The calculation of element partitioning is illustrated by the following example: Consider Sr partitioning between K-feldspar and plagioclase, i) if the Sr concentration in plagioclase is approximately twice that of K-feldspar, and ii) if the K-feldspar abundance is approximately twice that of plagioclase, then approximately equal proportions of Sr will occur in plagioclase and K-feldspar.

Major element partitioning amongst the dominant minerals (quartz, feldspar and biotite) have been calculated from mineral probe analysis (Table 3.10) and is given in Table 3.11. A summary of element partitioning based on Table 3.11 and data in Chappell (1966), Rhodes (1969), Joyce (1970) and Lambert and Holland (1974) is given in Table 3.12.

3.5.2 Chemistry of Size Separates from Samples GR103 and GR107

The chemistry of size separates which represent 50% and 65% of samples GR103 and 107 respectively is given in Table 3.13 and plotted in Figure 3.9. For the size separates analysed: CaO, Na_2O, P, Sr and Mn are depleted compared with the parent rock in both samples; whereas K_2O is depleted only in sample GR103. All other elements are enriched in specific size fractions and by necessity depeleted in others.

The results of factor analysis, the correlation matrix and rotated factor matrix, are given in Table 3.14 and 3.15 respectively. Because of Cu and Zn contamination during the preparation of separates coarser than 5ø, Cu and Zn have been excluded from the statistical analysis. These results suggest that the chemistry of the size separates can be readily described in terms of the variations in the proportion of the primary rock forming and neoformed minerals.

Neoformed Minerals

H_2O+ is present in only minor proportions in the primary minerals, is only a minor component of the parent rock and is concentrated in the neoformed minerals. Consequently elements whose size dependent variation has a strong positive correlation with H_2O+ are likely to be concentrated in the neoformed minerals. The composition of the neoformed minerals is indicated by the high loadings of Al_2O_3, Fe_2O_3, MgO, H_2O+, P, Rb, V, Mn, Ni and moderate loadings on Cr and Pb on Factor 1 (Table 3.15). This is consistent with the neoformed minerals consisting of kaolinite, illite,

Table 3.10 Electron microprobe mineral analysis of GRR8. Analyst, D. Walker (accelerating voltage, 15kv; beam current, 3nA; beam diameter <2μm). Details of analytical procedures and accuracy are given in Reed and Ware (1975). Abundance less than the detection limit is indicated as '-'.

%									
SiO_2	TiO_2	Al_2O_3	FeO	MnO	MgO	CaO	K_2O	Na_2O	Σ
K-feldspar									
65.75	-	19.01	-	-	-	0.11	10.82	4.37	100.06
65.05	-	18.30	-	-	-	-	15.31	1.24	99.89
66.95	-	19.10	-	-	-	-	7.03	6.67	99.75
65.35	-	18.61	-	-	-	-	13.21	2.61	99.79
65.12	-	18.74	-	-	-	-	13.77	2.46	100.09
65.13	-	18.79	-	-	-	-	11.88	3.49	99.29
65.23	-	18.59	-	-	-	-	13.56	2.43	99.80
64.80	-	18.70	-	-	-	-	14.52	1.76	99.79
65.14	-	18.40	-	-	-	-	14.76	1.62	99.92
Plagioclase									
66.98	-	20.77	-	-	0.12	0.82	0.36	10.86	100.03
65.50	-	21.67	-	-	-	2.25	0.69	9.77	99.89
66.79	-	20.87	-	-	0.09	1.14	0.43	10.65	99.97
67.26	-	20.89	-	-	-	0.88	0.31	10.69	100.04
65.61	-	21.83	-	-	-	2.41	0.64	9.82	100.31
65.34	-	22.05	-	-	-	2.70	0.79	9.25	100.13
Biotite									
34.76	3.48	14.22	24.24	0.46	6.28	-	9.04	-	92.49
35.22	2.79	15.32	26.04	0.72	6.65	-	8.35	0.26	95.35
35.37	3.96	14.79	25.14	0.52	6.52	-	9.27	-	95.58
35.37	3.73	14.67	24.58	0.54	6.27	-	9.47	-	94.64

Table 3.11 Major element partitioning amongst quartz, K-feldspar, plagioclase and biotite. This example is calculated for GRR8 using the modal mineralogy, whole rock chemistry and electron microprobe analyses given in Tables 3.1, 3.2 and 3.10 respectively. Columns list the concentration of the particular oxide in the mineral (%) and the proportion of the whole rock oxide concentration present in the mineral (%T).

	Quartz		K-feldspar		Plagioclase		Biotite		Recovery
	%	%T	%	%T	%	%T	%	%T	%
SiO_2	100	48	65	26	66	22	35	2	98
TiO_2	0	0	0	0	0	0	3.8	38	38
Al_2O_3	0	0	18.5	52	21.2	44	14.8	6	102
FeO	0	0	0	0	0	0	25	86	86
MnO	0	0	0	0	0	0	0.6	60	60
MgO	0	0	0	0	0	0	6.4	92	92
* CaO	0	0	0	0	0	100	0	0	100
* Na_2O	0	0	2.7	30	10.2	80	0	0	110
* K_2O	0	0	13.3	100	0.5	3	9.0	10	113

* As a result of alteration, intergrowth and zoning the concentration of CaO, Na_2O, K_2O in feldspar is highly variable. The adequate recovery of SiO_2 and Al_2O_3 indicates that the high Na_2O and K_2O recovery is a result of sampling problems (i.e. the small number of grains analysed) rather than errors in the determination of the mineral proportions or chemical analysis. As plagioclase is the only major Ca bearing phase it has been assumed to contain all CaO.

Table 3.12 Element partitioning between minerals of the Wallagaraugh Adamellite. The minor phases formed during subsolidus alteration, e.g., epidote, sericite and the alteration products of biotite have not been included.

	Quartz	K-feldspar	Plagioclase	Biotite	Apatite	Zircon	Opaques
SiO_2	+++	+++	+++	+	-	-	-
*TiO_2	-	-	-	+++	-	-	+++
Al_2O_3	-	++++	+++	+	-	-	-
*Fe_2O_3	-	-	-	++++	-	-	+++
*FeO	-	-	-	++++	-	-	+++
MgO	-	-	-	++++	-	-	-
CaO	-	-	++++	-	-	-	-
Na_2O	-	++	++++	-	-	-	-
K_2O	-	++++	+	+	-	-	-
ɤH_2O+	-	-	-	++++	-	-	-
P	-	-	-	-	++++	-	-
Rb	-	++++	+	+	-	-	-
Sr	-	+++	+++	-	-	-	-
Pb	-	++++	+	+	-	-	-
Zr	-	-	-	-	-	++++	-
†Y	-	-	-	-	+++	+++	-
*V	-	-	-	++++	-	-	+++
§Cr							
*Mn	-	-	-	++++	-	-	+++
§Ni							
§Cu							
Zn	-	-	-	++++	-	-	-

Symbols	% of total
++++	100-60
+++	60-30
++	30-5
+	5-2
-	<2

§Cr, Ni, Cu have average concentrations 2ppm, contamination from the WC mill is likely to be an important source of Cr and Ni at these low concentrations.

*Opaque minerals principally magnetite and ilmenite could contain varying amount of these elements, further detailed study is required to accurately determine the exact partitioning.

†Allanite is present in trace quantities and will contain Y.

ɤH_2O+ will also be present in the subsolidus alteration products.

Sample#	GR103 <9φ	GR103 8,7φ	GR103 5,4φ	GR103 3,2φ	GR103 1,0φ	GR103 -1,-2φ	GR107 <9φ	GR107 8,7φ	GR107 5,4φ	GR107 3,2φ	GR107 1,0φ	GR107 -1,-2φ	GRS5 4,3φ	GRS5 2,1φ	GRS5 0,-1φ
SiO_2	44.36	58.42	79.73	88.05	95.44	97.19	39.25	45.46	50.53	60.35	72.63	84.04	84.11	93.68	92.64
TiO_2	0.56	1.57	1.04	0.51	0.11	0.08	0.35	0.82	0.90	0.48	0.16	0.04	0.27	0.05	0.04
Al_2O_3	31.19	24.18	9.15	5.27	1.80	1.32	32.25	30.68	27.07	21.00	14.06	8.35	6.62	3.19	3.65
Fe_2O_3	4.09	2.44	1.25	0.97	0.40	0.57	6.97	5.88	5.45	3.50	1.45	0.67	0.46	0.11	0.14
FeO	0.06	0.05	<0.01	<0.01	<0.01	<0.01	0.07	0.06	0.04	0.07	<0.01	<0.01	<0.01	<0.01	<0.01
MnO	0.01	0.01	<0.01	<0.01	<0.01	<0.01	0.01	0.02	0.02	0.01	<0.01	<0.01	0.01	<0.01	<0.01
MgO	0.80	0.43	0.14	0.20	0.11	0.09	0.84	0.33	0.43	0.35	0.15	0.06	0.05	0.06	0.06
CaO	0.02	0.04	0.09	0.03	0.01	0.01	0.01	0.03	0.06	0.06	0.03	0.02	0.04	0.05	0.07
Na_2O	0.08	0.17	0.26	0.11	0.02	0.02	0.27	0.26	0.66	0.53	0.42	0.24	0.56	0.48	0.53
K_2O	2.82	4.71	4.62	2.73	0.87	0.36	3.03	3.25	3.99	6.12	7.14	3.70	4.14	2.02	2.06
P_2O_5	0.01	0.01	0.03	0.01	<0.01	<0.01	0.01	<0.01	0.03	<0.01	<0.01	<0.01	0.01	<0.01	<0.01
S	<0.02	<0.02	<0.02	<0.02	<0.02	<0.02	<0.02	<0.02	<0.02	<0.02	<0.02	<0.02	<0.01	<0.01	<0.01
loss	16.47	8.36	3.15	2.26	0.94	0.64	17.21	13.30	10.85	7.93	3.57	2.40	4.11	0.67	0.55
H_2O-	4.90	1.01	0.38	0.27	0.06	0.13	5.36	2.45	1.58	1.54	0.70	0.48	2.45	0.09	0.06
C	0.61	0.78	0.67	0.63	0.31	0.16	0.31	0.44	0.15	0.10	0.06	0.04	0.37	0.13	0.11
rest	0.08	0.07	0.25	0.04	0.01	0.01	0.08	0.09	0.34	0.08	0.05	0.03	0.13	0.02	0.02
	100.56	100.46	99.71	100.18	99.71	100.29	100.35	100.18	100.37	100.48	99.66	99.55	100.51	100.33	99.76
Trace elements															
P	85	35	50	20	10	5	70	55	60	40	30	15	70	20	20
Rb	365	257	146	90	31	21	285	248	197	259	256	127	124	73	73
Sr	24	31	41	20	5	2	15	17	34	40	41	26	33	16	20
Pb	17	21	24	12	3	3	38	60	55	50	37	19	18	8	8
Zr	69	151	1530	122	36	45	111	159	1980	132	59	40	695	20	31
Y	12	19	53	10	4	4	12	18	72	12	7	4	22	5	6
V	67	46	26	18	4	6	89	62	56	34	11	4	5	<1	<1
Cr	32	21	19	16	8	8	40	10	8	8	7	5	7	7	6
Mn	78	70	34	18	7	7	63	125	152	114	42	16	71	13	21
Ni	8	6	<1	<1	<1	<1	11	8	5	4	<1	<1	<1	<1	<1
Cu	3	14	54	12	6	11	3	35	39	17	9	11	49	2	<1
Zn	29	28	30	7	3	1	45	112	109	60	19	6	15	<1	1

Table 3.13 Chemistry of size separates from samples GR103 and GR107 and stream-bed sediments from catchment 5.

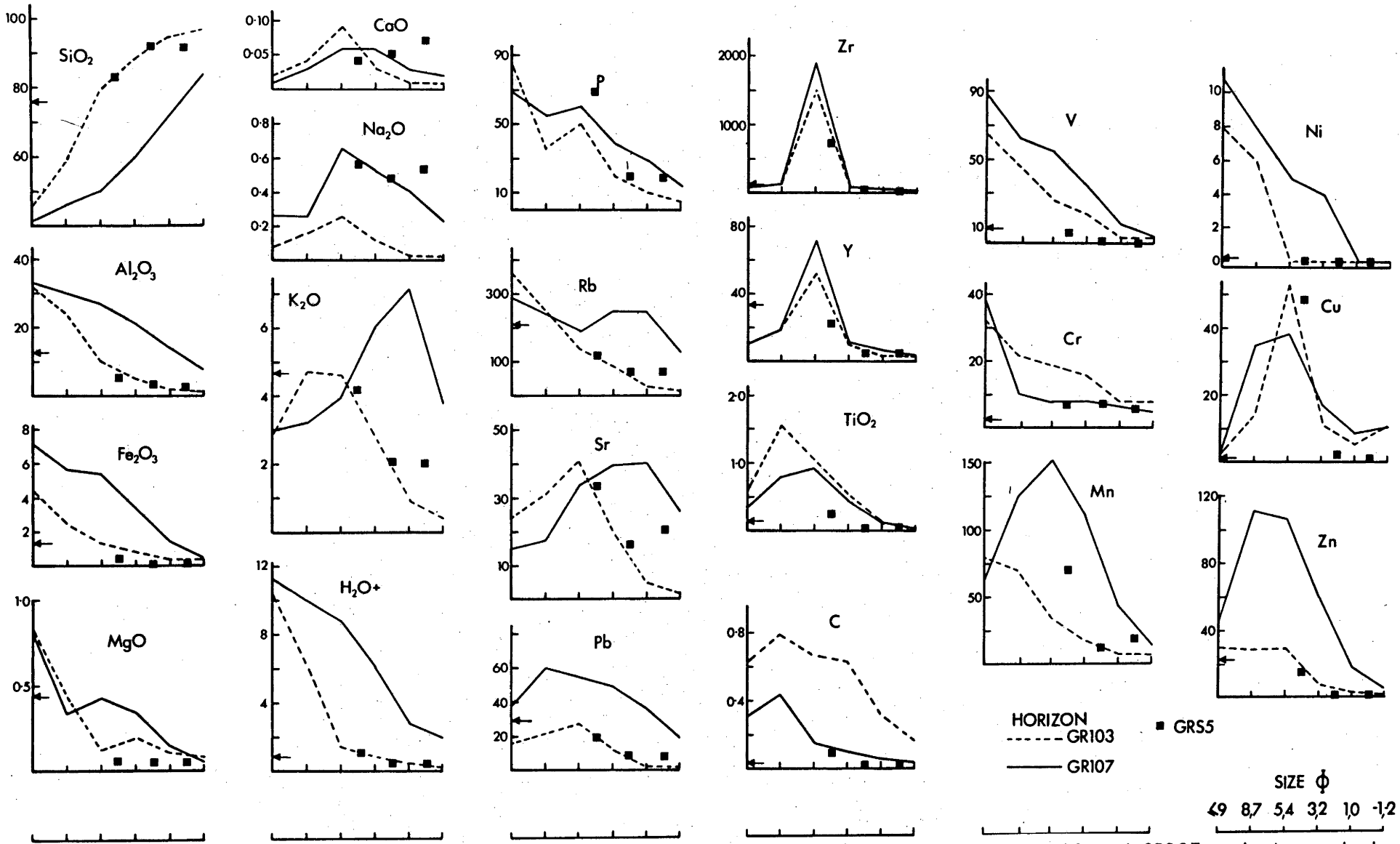

Figure 3.9 Size dependent variation in chemistry for size separates from samples GR103 and GR107 and stream-bed sediment samples from catchment 5 (GRS5). See Table 3.14 for data. Where the parent rock concentration occurs on scale it is indicated by an arrow.

	TiO2	Al2O3	Fe2O3	MgO	CaO	Na2O	K2O	H2O+	C	P	Rb	Sr	Pb	Zr	Y	V	Cr	Mn	Ni	Qtz	K-spar
SiO2	-0.47	-0.99	-0.93	-0.85	-0.14	-0.50	-0.37	-0.98	-0.18	-0.89	-0.89	-0.31	-0.73	-0.16	-0.31	-0.93	-0.55	-0.82	-0.92	0.97	0.10
TiO2	-	0.46	0.29	0.27	0.60	0.19	0.30	0.36	0.70	0.41	0.37	0.42	0.30	0.45	0.58	0.44	0.25	0.50	0.37	-0.42	0.16
Al2O3		-	0.92	0.86	0.08	0.42	0.32	0.98	0.19	0.89	0.90	0.27	0.70	0.11	0.27	0.94	0.57	0.81	0.93	-0.97	-0.14
Fe2O3			-	0.82	0.02	0.43	0.14	0.96	0.05	0.83	0.71	0.07	0.74	0.18	0.30	0.95	0.55	0.78	0.93	-0.87	-0.34
MgO				-	-0.13	0.11	0.05	0.88	0.30	0.87	0.79	0.03	0.32	-0.02	0.10	0.92	0.85	0.51	0.92	-0.76	-0.39
CaO					-	0.57	0.56	0.00	0.21	0.23	0.12	0.77	0.40	0.75	0.75	0.03	-0.15	0.39	-0.13	-0.16	-0.59
Na2O						-	0.71	0.37	-0.45	0.33	0.37	0.70	0.08	0.56	0.59	0.25	-0.22	0.72	0.18	-0.56	0.53
K2O							-	0.19	-0.12	0.25	0.56	0.93	0.58	0.17	0.22	0.10	-0.08	0.39	0.05	-0.53	0.87
H2O+								-	0.14	0.89	0.84	0.14	0.67	0.10	0.25	0.95	0.59	0.79	0.96	-0.93	-0.28
C									-	0.32	0.20	0.01	-0.24	0.05	0.14	0.32	0.53	-0.03	0.26	-0.07	-0.18
P										-	0.84	0.32	0.54	0.30	0.41	0.90	0.70	0.67	0.82	-0.82	-0.16
Rb											-	0.49	0.57	-0.04	0.09	0.77	0.57	0.64	0.77	-0.93	0.15
Sr												-	0.49	0.44	0.47	0.07	-0.07	0.40	-0.03	-0.44	0.86
Pb													-	0.35	0.44	0.56	-0.03	0.87	0.53	-0.78	0.25
Zr														-	0.98	0.15	-0.09	0.42	-0.04	-0.12	0.18
Y															-	0.29	-0.01	0.54	0.11	-0.27	0.16
V																-	0.75	0.68	0.97	-0.84	-0.38
Cr																	-	0.07	0.71	-0.45	-0.42
Mn																		-	0.65	-0.82	0.07
Ni																			-	-0.85	-0.43
Quartz																				-	-0.07
K-feldspar																					-

$^{*}P_{99.9}$ = 0.82 n=12
$^{*}P_{99.9}$ = 0.71
$^{*}P_{99}$ = 0.57
$^{*}P_{95}$ = 0.50
$^{*}P_{90}$

*confidence limits cited ignore the constant sum effect in chemical analysis

Table 3.14 Correlation matrix for size separates from samples GR103 and GR107.

Table 3.15 Rotated factor matrix for size separates from samples GR101 and GR107.

	Factor				
Variable	I	II	III	IV	Communality
SiO2	-0.97	-0.17	-0.14	-0.02	0.99
TiO2	0.31	0.26	0.55	0.56	0.79
Al2O3	0.97	0.13	0.10	0.04	0.96
Fe2O3	0.95	-0.10	0.18	-0.13	0.96
MgO	0.91	-0.11	-0.08	0.25	0.91
CaO	-0.06	0.59	0.76	0.16	0.91
Na2O	0.34	0.55	0.49	-0.54	0.96
K2O	0.21	0.96	0.08	-0.10	0.98
H2O+	0.99	-0.02	0.09	-0.09	0.99
C	0.14	-0.06	0.14	0.94	0.92
P	0.88	0.09	0.23	0.23	0.88
Rb	0.86	0.44	-0.12	0.15	0.97
Sr	0.13	0.92	0.34	0.04	0.97
Pb	0.65	0.37	0.37	-0.45	0.90
Zr	0.02	0.08	0.95	-0.02	0.93
Y	0.17	0.11	0.96	0.03	0.96
V	0.96	-0.11	0.14	0.18	0.99
Cr	0.64	-0.18	-0.17	0.59	0.82
Mn	0.74	0.22	0.47	-0.27	0.83
Ni	0.97	-0.15	-0.02	0.12	0.98
Quartz	-0.93	-0.33	-0.08	0.06	0.98
K-feldspar	-0.28	0.95	0.10	-0.10	0.99
Percent of variance explained					
	48.4	16.2	16.7	10.6	
cumulative percent of variance					
	48.4	66.6	83.3	93.9	

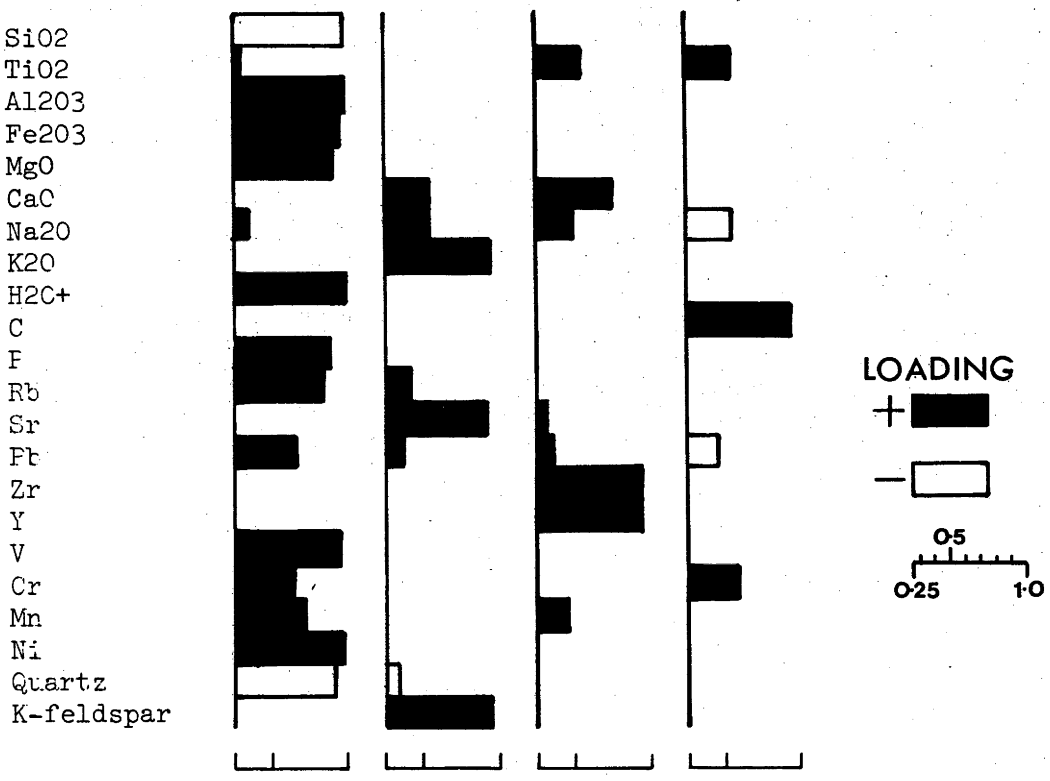

vermiculite, iron oxides and associated ab/adsorbed trace elements.

Quartz

As expected, quartz shows a significant positive correlation only with SiO_2 (Table 3.14). The inverse loading (Factor 1, Table 3.15) of quartz and those elements concentrated in the neoformed minerals, reflects their codominance. The decrease in SiO_2 concentration with size (Figure 3.9) is consistent with the variation in quartz concentration shown in Figure 3.6A.

Feldspar

Plagioclase could only be detected (trace proportions) in separates from sample GR107 (Table 3.8). The low concentration of CaO, Na_2O and Sr in the clay fraction indicate that they are not retained to any extent in the neoformed minerals. Strontium, unlike CaO and Na_2O is an important component of K-feldspar (Table 3.12). Consequently, the distribution of Sr in the size separates is controlled dominantly by K-feldspar. This is indicated by the high positive loadings of Sr, K_2O and K-feldspar on Factor II (Table 3.15).

The dominant elements likely to reflect the distribution of K-feldspar are K_2O, Rb, Pb (Table 3.12). Of these, K_2O shows the strongest correlation with K-feldspar. The variation in K_2O concentration with size (Figure 3.9) is consistent with the size dependent variation in K-feldspar concentration given in Table 3.8. In comparison to K_2O, Rb is retained in the neoformed minerals (high loading on Factor I, Table 3.15), thus its distribution is determined by both the distribution of the neoformed minerals and K-feldspar. The behaviour of Pb is enigmatic; no explanation for its distribution can be offered at this stage.

Biotite

The MgO submaxima developed in the 5ø to 4ø and 3ø to 2ø fractions for samples GR107 and GR103 (Figure 3.9) is consistent with the expected distribution of biotite and is supported by similar submaxima for Fe_2O_3, V, Mn, Zn in the same size intervals.

Accessory Minerals

Those elements (P, Y, Zr, Ti) concentrated in the accessory minerals of the parent rock all show well developed maxima or submaxima in the 8ø to 4ø range. This is consistent with the fine grained nature of their primary host minerals (apatite, zircon and ilmenite).

Summary

The size separates are usually depleted in mobile elements occurring in those parent rock minerals which are susceptible to weathering, e.g., CaO and Na_2O in plagioclase.

Factor analyses shows that the variation in chemistry is consistent with the samples consisting of varying proportions of primary and neoformed minerals consisting dominantly of kaolinite, illite and vermiculite.

There is a marked and generally systematic change in element concentration with size. Although the absolute concentration for an individual element may vary, this size dependence is approximately the same for both samples. This size dependent variation in chemistry reflects the varying physiochemical properties of their host minerals (Section 3.4) and the differences between the two samples and the degree of weathering.

3.5.3 Chemistry of Profiles GR1, 2 and 3

The chemistry of profiles GR1, 2 and 3 is given in Table 3.16 and illustrated in Figure 3.10.

Profile GR2 differs from profiles GR1 and 3. The principal difference is reflected in the distribution of Fe_2O_3 and Y. In profile GR2 Fe_2O_3 varies from ~0.7% at its base, to a maximum of ~5.2%, whereas in profiles GR1 and 3 it varies from ~2.7% at the base to a maximum of ~3.2%. With the data available, the difference in Fe_2O_3 concentration is attributed to differences in site drainage between the three profiles. Profiles GR1 and 3 are well drained, whereas profile GR2 is frequently waterlogged. The variation in the degree

Table 3.16 Chemistry of profiles GR1, 2 and 3.

Sample#	GR101	GR102	GR103	GR104	GR105	GR106	GR107	GR108	GR201	GR202
SiO_2	85.06	78.13	82.67	73.12	72.92	65.36	68.20	73.27	88.30	90.49
TiO_2	0.17	0.60	0.52	0.55	0.41	0.34	0.28	0.26	0.41	0.38
Al_2O_3	1.09	9.05	8.84	14.45	15.14	19.08	19.08	14.60	3.94	3.72
Fe_2O_3	0.08	1.28	1.25	2.25	2.19	2.81	2.71	2.01	0.34	0.50
FeO	<0.01	<0.01	0.05	0.07	0.06	0.05	0.04	0.09	<0.01	<0.01
MnO	<0.01	0.01	<0.01	<0.01	0.01	0.01	0.01	0.01	0.01	<0.01
MgO	0.52	0.68	0.49	0.73	0.68	0.81	0.74	0.71	0.53	0.54
CaO	0.10	0.06	0.06	0.04	0.04	0.04	0.04	0.14	0.05	0.05
Na_2O	0.04	0.09	0.08	0.08	0.14	0.18	0.31	1.06	0.19	0.23
K_2O	0.46	2.16	1.99	2.48	3.14	3.73	4.62	4.96	1.36	1.41
P_2O_5	<0.01	0.01	0.01	0.02	0.01	0.02	0.01	0.01	0.01	0.01
S	<0.02	<0.02	<0.02	<0.02	<0.02	<0.02	0.02	<0.02	<0.02	<0.02
loss	12.29	8.07	4.67	6.55	5.56	7.60	4.37	3.02	5.28	3.01
H_2O-	1.31	1.33	0.65	1.03	1.17	1.33	1.03	0.57	0.60	0.42
C	7.45	2.65	0.90	0.53	0.40	0.40	0.10	0.70	2.23	0.97
rest	0.03	0.07	0.06	0.07	0.06	0.07	0.07	0.06	0.05	0.05
	99.84	100.22	100.70	100.42	100.37	100.11	100.49	100.21	100.48	100.40
Trace elements										
P	65	55	35	50	45	55	45	50	85	45
Rb	21	120	109	160	163	195	204	184	73	75
Sr	21	24	18	20	24	27	30	43	15	13
Pb	5	13	11	14	16	21	38	65	11	12
Zr	126	318	280	266	210	181	183	182	237	238
Y	10	16	15	15	12	11	12	12	27	26
V	5	24	22	35	29	39	28	19	10	11
Cr	7	15	16	21	17	20	11	<1	13	14
Mn	25	40	29	36	36	42	52	87	39	27
Ni	<1	1	2	2	<1	3	2	1	<1	<1
Cu	<1	1	1	1	1	1	1	<1	2	1
Zn	1	8	8	12	12	17	19	20	4	2

Sample#	GR203	GR204	GR205	GR206	GR207	GR301	GR302	GR303	GR304	GR305
SiO_2	90.62	80.60	64.82	79.11	74.69	84.05	85.78	72.92	66.46	68.14
TiO_2	0.32	0.37	0.42	0.38	0.15	0.44	0.42	0.38	0.35	0.26
Al_2O_3	4.33	8.07	17.69	12.04	14.17	6.69	6.79	14.16	17.78	17.15
Fe_2O_3	0.62	3.45	5.00	0.79	0.63	0.84	0.83	2.50	3.16	2.79
FeO	0.05	0.07	0.15	0.05	0.06	<0.01	0.05	0.04	0.07	0.04
MnO	<0.01	<0.01	0.01	<0.01	<0.01	0.01	0.01	0.01	0.01	0.01
MgO	0.60	0.61	0.72	0.68	0.62	0.53	0.57	0.66	0.69	0.65
CaO	0.04	0.04	0.04	0.03	0.07	0.07	0.04	0.06	0.08	0.07
Na_2O	0.19	0.21	0.18	0.28	1.07	0.17	0.12	0.16	0.22	0.23
K_2O	1.39	1.54	1.36	2.46	4.22	2.81	2.81	3.11	3.71	4.15
P_2O_5	0.01	0.01	0.01	<0.01	0.01	0.01	0.01	0.01	0.01	0.01
S	<0.02	0.02	0.03	0.02	<0.02	<0.02	<0.02	0.02	<0.02	0.02
loss	1.99	5.13	9.78	4.00	4.48	4.61	2.33	6.30	7.70	6.71
H_2O-	0.30	0.67	2.11	1.02	0.85	0.65	0.34	1.21	1.47	1.23
C	0.27	0.65	0.77	0.09	0.11	1.49	0.10	0.37	0.30	0.05
rest	0.04	0.06	0.06	0.06	0.06	0.07	0.06	0.06	0.06	0.06
	100.21	100.17	100.26	99.89	100.24	100.31	99.83	100.38	100.31	100.28
Trace elements										
P	30	45	60	25	30	45	35	60	70	60
Rb	79	95	108	154	249	104	106	137	162	171
Sr	11	13	15	15	28	28	26	29	31	31
Pb	11	17	27	32	33	18	16	25	29	32
Zr	177	177	171	192	99	337	287	190	166	178
Y	25	27	31	39	48	17	15	17	17	18
V	21	69	58	17	9	14	15	34	42	32
Cr	13	17	40	21	11	14	13	21	21	12
Mn	19	20	25	23	29	68	38	53	74	60
Ni	<1	2	7	3	1	1	2	4	5	2
Cu	1	2	2	23	22	2	1	3	4	5
Zn	2	6	12	8	12	6	5	13	17	13

Figure 3.10 Depth dependent variation in chemistry for profiles GR1,2,3. Except for C and H_2O+ element concentrations have been normalised (% loss or gain) with respect to the average parent rock concentration.

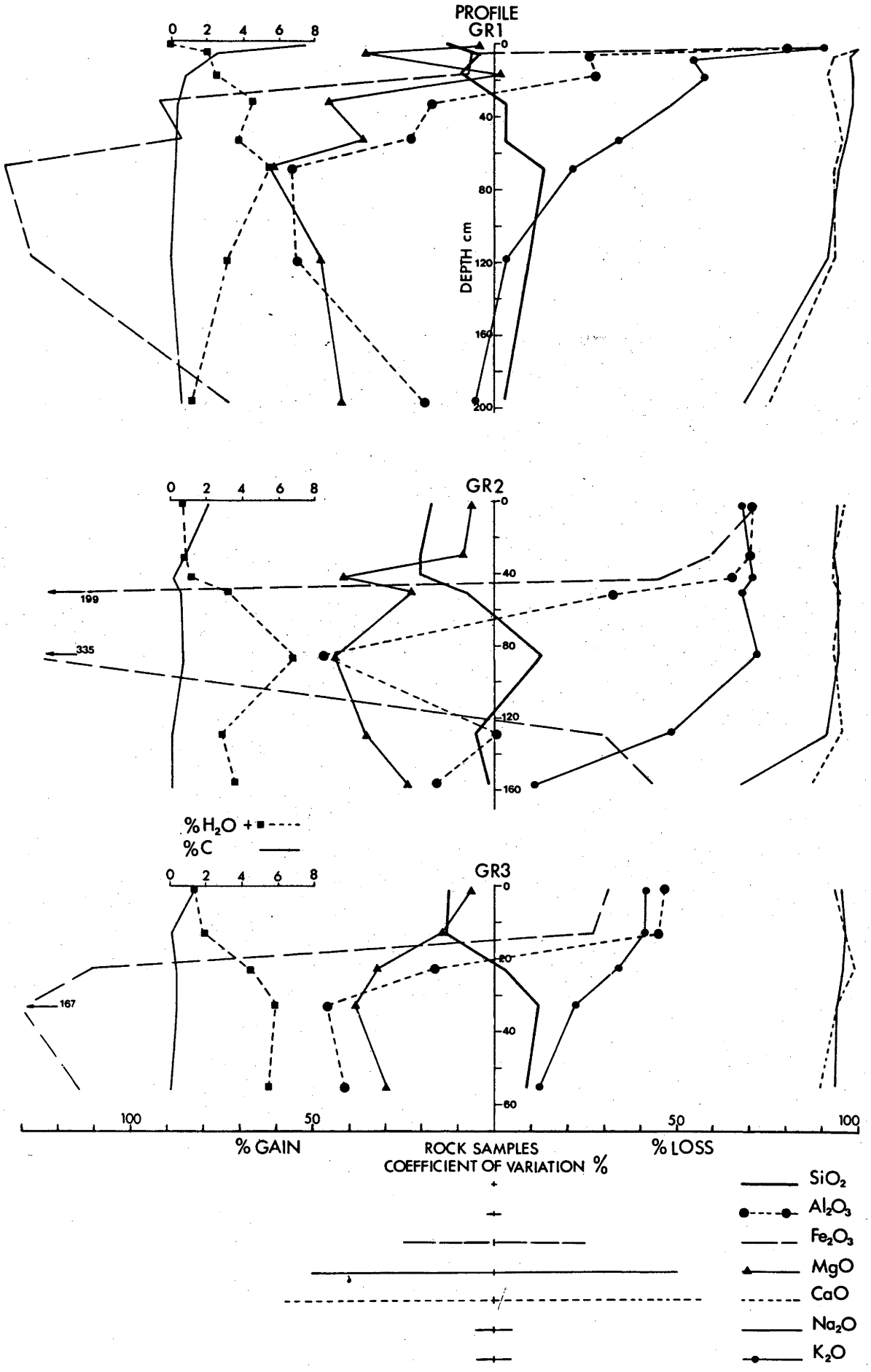

Figure 3.10 continued.

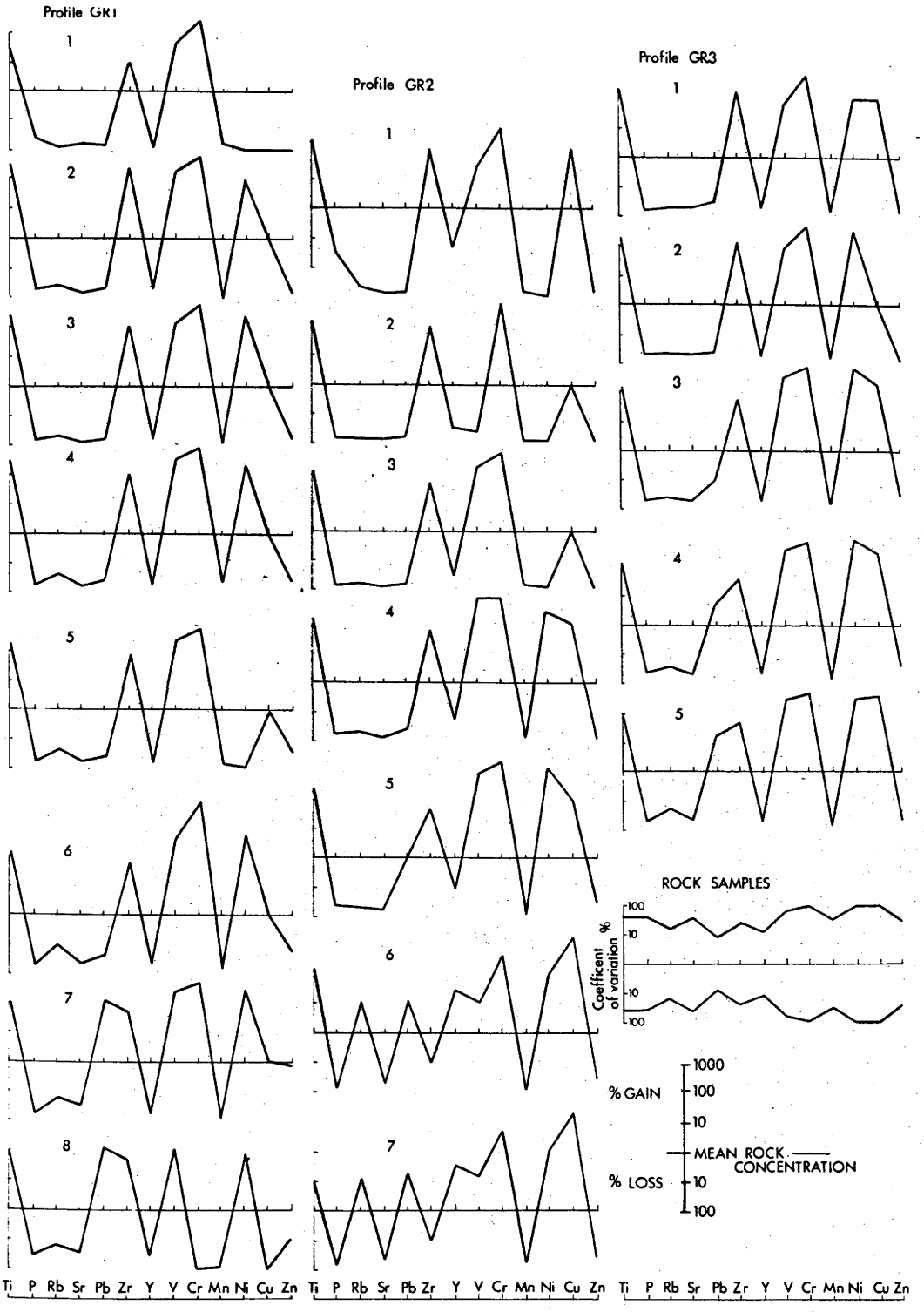

of waterlogging with fluctuations in rainfall, would provide conditions of varying Eh. This would be favourable to the episodic mobilisation of Fe and its consequent redistribution within profile GR2. The effect of drainage could be verified by the examination of the distribution of Fe_2O_3 at other sites prone to waterlogging.

In the absence of data suggesting that Y is retained in the neoformed phase it is probable that the anomalously high Y concentration in profile GR2 reflects anomalously high Y concentrations in the parent rock, presumably with the Y being present in a resistant accessory mineral.

The variation in chemistry with weathering and soil formation can be examined in two ways:

1) Relative changes: These are calculated by comparing the composition of the weathered material with that of the parent rock. This method has the disadvantage in that a relative increase in element abundance can occur through either the selective removal of other elements or the addition of that element.
2) Absolute changes: These can be calculated when a unit volume of rock produces an equivalent volume of weathered material. Weathering at constant volume is indicated by the retention of the parent rock texture (Gardner, et al., 1978). Alternatively, absolute changes can be calculated by comparing variations in chemistry with a phase which is chemically and physically immobile.

Relative changes in Chemistry

Only persistent changes common to the three profiles are discussed. The relative changes are plotted in Figure 3.10. The relative changes in chemistry are examined in conjunction with mineralogical and textural changes, by factor analysis. The correlation matrix and rotated factor matrix are given in Table 3.17 and 3.18 respectively.

The data set used in the factor analysis consists of chemical, mineralogical and textural data from profiles GR1, 2 and 3 (the H_2O+ value for sample GR101 was set at $H_2O+ = 0$) and for parent rock samples

	TiO2	Al2O3	Fe2O3	FeO	MgO	CaO	Na2O	K2O	H2O+	C	P	Rb	Sr	Pb	Zr	Y	V	Cr	Mn	Zn	Qtz	Kspar	Plag	Clay
SiO2	0.14	-0.96	-0.64	-0.19	-0.31	-0.13	-0.14	-0.54	-0.64	0.38	-0.17	-0.55	-0.28	-0.52	0.28	0.00	-0.39	-0.18	-0.16	-0.53	0.79	-0.28	-0.13	-0.31
TiO2	-	-0.10	0.43	-0.59	0.31	-0.59	-0.82	-0.64	0.47	0.16	-0.29	-0.65	-0.38	-0.43	0.90	-0.60	0.57	0.71	-0.62	-0.42	0.54	-0.73	-0.77	0.63
Al2O3		-	0.61	0.14	0.34	0.07	0.12	0.59	0.66	-0.60	0.06	0.65	0.20	0.58	-0.25	0.03	0.36	0.20	0.12	0.49	-0.78	0.32	0.10	0.31
Fe2O3			-	-0.32	0.44	-0.35	-0.48	-0.16	0.87	-0.16	-0.16	-0.13	-0.20	0.17	0.17	-0.37	0.93	0.71	-0.36	0.00	-0.17	-0.31	-0.47	0.84
FeO				-	-0.40	0.88	0.86	0.64	-0.43	-0.34	0.83	0.53	0.81	0.10	-0.43	0.48	-0.39	-0.59	0.84	0.77	-0.62	0.65	0.89	-0.56
MgO					-	-0.47	-0.42	-0.08	0.49	-0.03	-0.38	-0.08	-0.31	0.07	0.22	-0.08	0.38	0.43	-0.55	0.06	-0.04	-0.19	-0.43	0.46
CaO						-	0.76	0.56	-0.45	-0.23	0.83	0.41	0.89	0.13	-0.38	0.28	-0.40	-0.60	0.84	0.62	-0.47	0.55	0.81	-0.57
Na2O							-	0.74	-0.56	-0.36	0.54	0.74	0.59	0.31	-0.67	0.70	-0.60	-0.74	0.86	0.63	-0.67	0.79	0.99	-0.70
K2O								-	-0.16	-0.60	0.40	0.89	0.61	0.64	-0.50	0.41	-0.38	-0.63	0.65	0.74	-0.88	0.91	0.71	-0.52
H2O+									-	-0.21	-0.28	-0.06	-0.29	0.07	0.20	-0.34	0.81	0.78	-0.47	-0.08	-0.12	-0.35	-0.56	0.85
C										-	-0.10	-0.62	-0.23	-0.42	0.17	-0.30	-0.07	0.06	-0.30	-0.43	0.55	-0.53	-0.33	-0.02
P											-	0.21	0.88	-0.07	-0.15	0.13	-0.20	-0.43	0.73	0.70	-0.39	0.39	0.61	-0.40
Rb												-	0.35	0.58	-0.61	0.58	-0.35	-0.49	0.59	0.63	-0.86	0.76	0.71	-0.39
Sr													-	0.19	-0.21	0.08	-0.27	-0.53	0.75	0.72	-0.50	0.58	0.63	-0.49
Pb														-	-0.46	0.16	-0.07	-0.26	0.23	0.31	-0.61	0.61	0.24	-0.12
Zr															-	-0.53	0.31	0.44	-0.49	-0.30	0.56	-0.56	-0.62	0.32
Y																-	-0.45	-0.44	0.41	0.50	-0.44	0.52	0.68	-0.39
V																	-	0.75	-0.46	-0.17	0.08	-0.49	-0.58	0.90
Cr																		-	-0.65	-0.46	0.30	-0.70	-0.74	0.92
Mn																			-	0.62	-0.58	0.65	0.89	-0.63
Zn																				-	-0.76	0.64	0.67	-0.35
Quartz																					-	-0.70	-0.65	0.20
K-feldspar																						-	0.75	-0.62
Plagioclase																							-	-0.70
Clay																								-

*P_{99} = 0.46 *confidence limits cited ignore the constant
*P_{95} = 0.36 sum effect in chemical analysis

Table 3.17 Correlation matrix for samples from profiles GR1, 2, 3 and rocks GRR1, 8, 12, 13, 15, 16, 17, 21, 22, 23.

Table 3.18 Rotated factor matrix for samples from profiles GR1, 2 and 3 and rocks GRR1, 8, 12, 13, 15, 16, 17, 21, 22, 23.
Graphic representation of the factor loadings is shown below.

	Factor					
Variable	I	II	III	IV	V	Communality
SiO2	-0.20	-0.70	-0.60	0.12	0.01	0.92
TiO2	-0.23	-0.37	0.43	0.69	-0.20	0.90
Al2O3	0.10	0.79	0.55	-0.04	0.02	0.96
Fe2O3	-0.11	0.19	0.92	0.08	-0.13	0.93
FeO	0.84	0.23	-0.24	-0.19	0.31	0.95
MgO	-0.41	0.27	0.37	0.46	0.24	0.65
CaO	0.87	0.15	-0.27	-0.22	0.02	0.91
Na2O	0.55	0.36	-0.44	-0.45	0.38	0.97
K2O	0.40	0.85	-0.26	-0.13	0.10	0.98
H2O+	-0.24	0.21	0.89	0.14	-0.06	0.93
C	-0.15	-0.64	-0.10	-0.11	-0.30	0.55
P	0.96	0.01	-0.06	0.00	0.01	0.94
Rb	0.21	0.79	-0.16	-0.31	0.33	0.90
Sr	0.89	0.28	-0.18	0.02	-0.14	0.93
Pb	-0.10	0.83	-0.05	-0.27	-0.23	0.83
Zr	-0.11	-0.34	0.12	0.85	-0.21	0.92
Y	0.08	0.22	-0.30	-0.30	0.82	0.93
V	-0.12	-0.07	0.90	0.15	-0.13	0.92
Cr	-0.37	-0.26	0.79	0.22	-0.03	0.88
Mn	0.76	0.25	-0.31	-0.36	0.11	0.89
Zn	0.66	0.54	-0.01	0.08	0.37	0.88
Quartz	-0.40	-0.79	-0.14	0.27	-0.24	0.94
K-feldspar	0.35	0.71	-0.43	-0.19	0.14	0.88
Plagioclase	0.62	0.31	-0.42	-0.40	0.39	0.97
Clay	-0.35	-0.15	0.88	0.13	-0.03	0.95
Percent of variance explained	24.4	24.0	23.8	10.1	7.0	
Cumulative percent of variance	24.4	48.4	72.2	82.3	89.3	

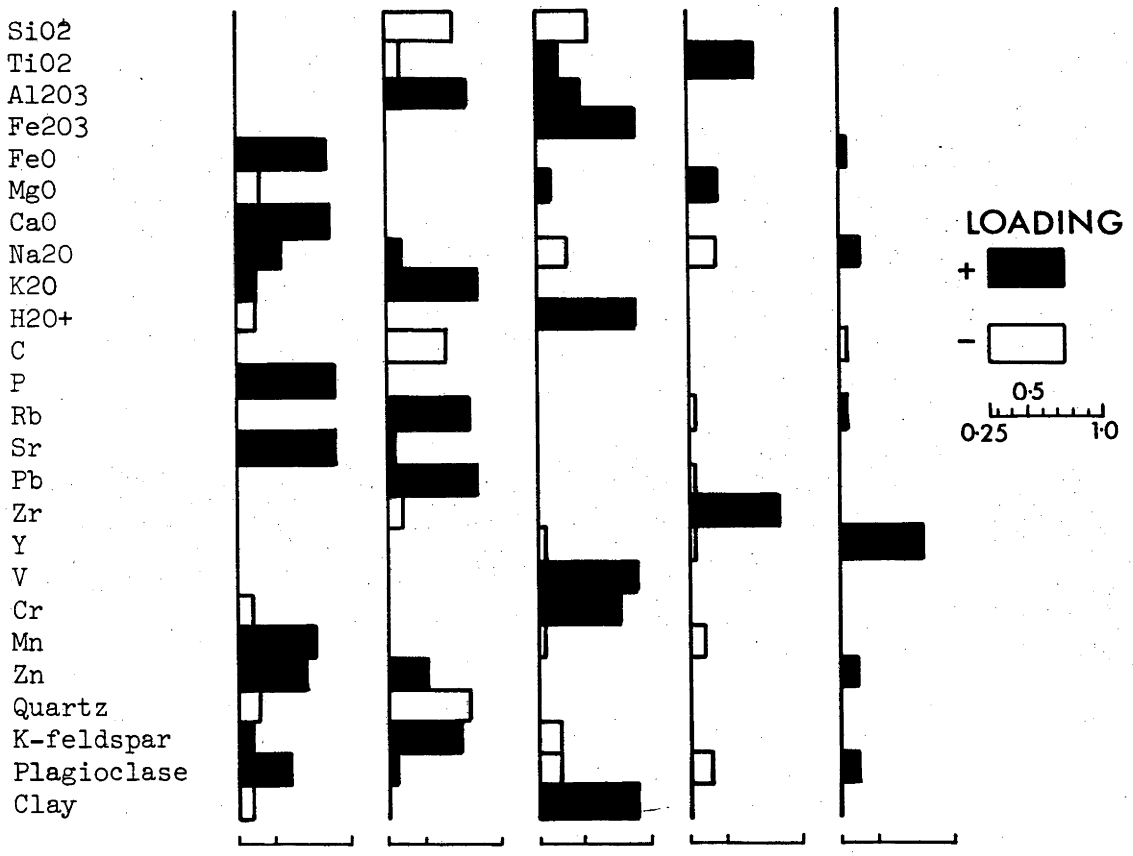

(GR1, 8, 12, 13, 15, 16, 17, 21, 22 and 23), the clay content was defined as zero. Nickel and Cu were excluded because of the effect of their low and variable concentration on the factor analysis.

Five factors explain 89% of the variation in the data set. Except for MgO and C, which have communalities of 0.65 and 0.55 respectively, the communality for all other variables usually exceeds 0.90.

The features controlling the variation in the data set are interpreted from the factor loadings as follows:

Factor I. This reflects changes which occur with incipient weathering: i.e. 1) the oxidation of FeO; and 2) the weathering of labile minerals and the consequent leaching of the mobile elements present in them. The labile minerals are plagioclase (loss of Ca, Na, Sr), apatite (loss of P) and biotite (oxidation of FeO and loss of Mn and Zn). The loss of these elements from the base of the profiles is illustrated in Figure 3.10.

Factor II. This reflects the distribution of K-feldspar (loading on K-feldspar, K_2O, Rb, Pb) and quartz (loading on quartz and SiO_2).

Factor III. This reflects the distribution of clay, loading on elements present in the clay minerals and associated oxides (clay content, Al_2O_3, Fe_2O_3, H_2O+, V, Cr).

Factor IV. This reflects the distribution of the resistate accessory minerals zircon (Zr) and ilmenite (Ti) which, because of their small size and resistance to chemical weathering, differ in their behaviour from other minerals.

Factor V. This is essentially a single element factor, loading principally on Y and reflects the absence of a high correlation between Y and the other chemical, mineral and textural phases examined.

When the factor analytic results of the two data sets, size separates and profile/rock samples (Tables 3.15 and 3.18 respectively) are compared, the mineralogical features controlling the distribution of some elements (e.g., Y and Sr) appear to differ. These differences

are outlined in Table 3.19. The reasons for these differences and their internal consistency are as follows:

Yttrium: In the parent rock Y occurs in both apatite and zircon (Table 3.12). With incipient weathering, much of the apatite is destroyed and Y and P are leached from the immediate weathering environment. The corresponding shift in Y/P concentration that occurs is shown in Figure 3.11B.
Once incipient weathering has occurred, zircon (because of its comparative inertness), becomes the dominant Y host mineral, and a positive correlation would be expected between Y and Zr. This correlation occurs for the size separates and profile samples shown in Figure 3.11A.

Strontium: In the parent rock Sr occurs in both plagioclase and K-feldspar (Table 3.12). Plagioclase compared with K-feldspar is readily destroyed with weathering.
The progressive decline in Sr concentration with the destruction of plagioclase is shown in Figure 3.11C. In this figure, Na_2O is used as a surrogate for plagioclase. This is justified by the dominant occurrence of Na_2O in plagioclase, and its removal through leaching when it is released with weathering. The non zero concentration of Sr at zero Na_2O concentration (Figure 3.11C) reflects the occurrence of Sr in K-feldspar. The loss of Sr through the destruction of plagioclase corresponds with the shift in Sr/K_2O concentration from X to X^1 in Figure 3.11D. Because of the dominant occurrence of K_2O in K-feldspar, it is used as its surrogate.
Inspection of Table 3.9 shows that plagioclase can be destroyed without a marked change in K-feldspar concentration. Once plagioclase is removed (as is the case in most of the size separates and profile samples), K-feldspar becomes the dominant Sr host mineral and a systematic variation between Sr and K-feldspar develops (Figure 3.11D).

Table 3.19 The data set dependent variation in the factors controlling the distribution of yttrium and strontium.

DATA SET	
Size Separates	Profile and Rock Samples
(See Tables 3.14 and 3.15 for results).	(See Table 3.17 and 3.18 for results).
YTTRIUM	
At the 99% confidence limit Y is only correlated with Zr (r=0.98). The covariance of Y and Zr is interpreted as reflecting the variation in their host mineral, zircon. This is consistent with the high positive loading of Y and Zr on Factor 3 (Table 3.15).	Table 3.18 shows that Factor IV is dominated by Y, suggesting that it is behaving independently of all other elements.
STRONTIUM	
The high positive loading of Sr, K_2O and K-feldspar on Factor II (Table 3.15) is consistent with the distribution of Sr being controlled by K-feldspar.	The high positive loadings on CaO, Na_2O, Sr and plagioclase on Factor I (Table 3.18), suggests that for this data set the distribution of Sr is controlled by plagioclase. The loadings on the other elements in Factor I is attributed to the oxidation and leaching of biotite.

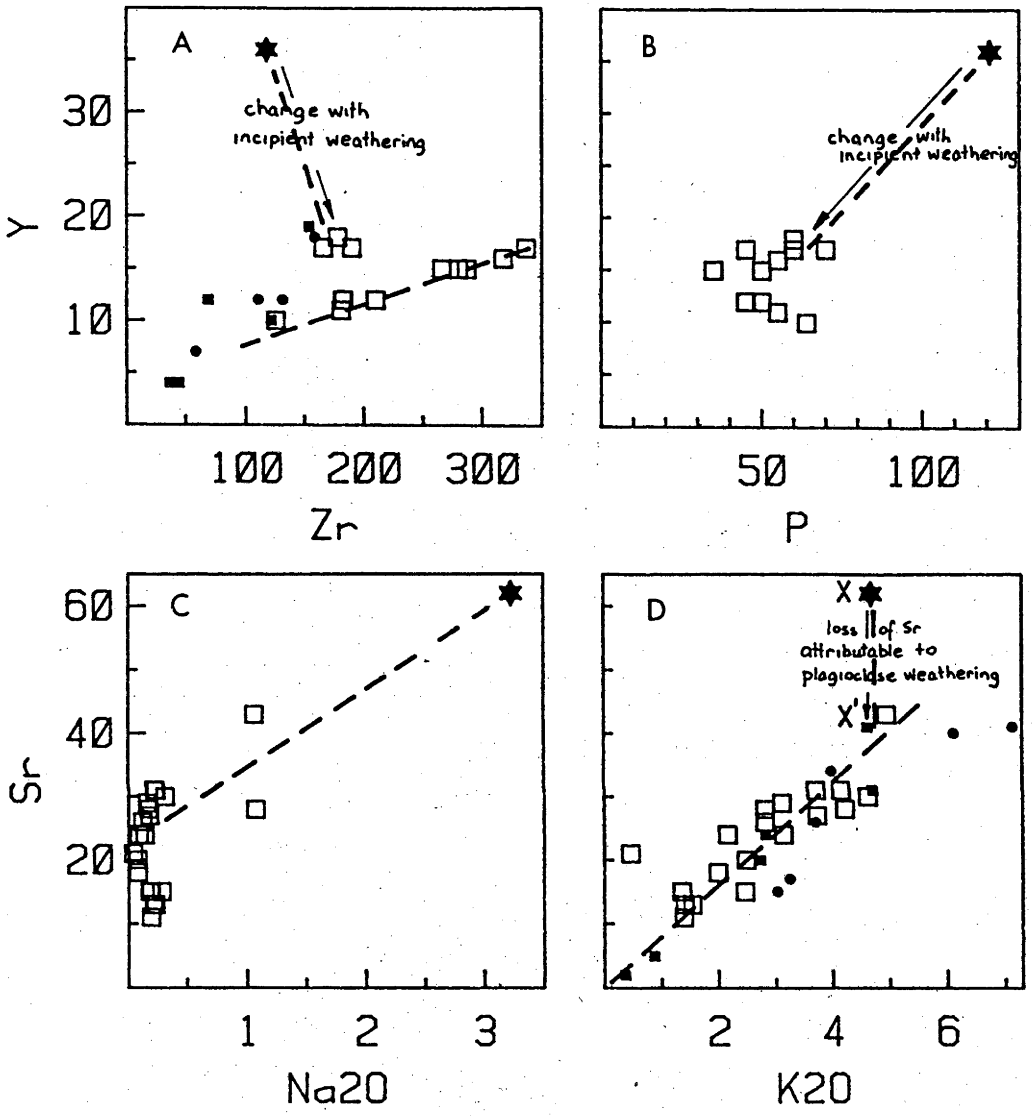

Figure 3.11 Variation in Y-Zr-P and Sr-Na_2O-K_2O concentration for size separates (from samples GR103 and 107), profiles and rock samples. Samples from profile GR2 have been excluded from the Y-Zr-P plot because of their anomalously high Y concentration.

Symbols

★ : Average rock concentration (GRA).
□ : Samples from profiles GR1, 2, 3.
■ ● : Size separates from samples GR103 and 107 respectively.
--- : Concentration trend lines.

This discussion of the factors controlling the distribution of Y and Sr demonstrates the importance of determining the extent to which conclusions drawn from multivariate statistical analyses are data set specific. It also demonstrates that a knowledge of element partitioning is integral to the understanding of the processes controlling weathering chemistry.

Volumetric Changes

The concentration (as mass per unit volume of Al_2O_3, SiO_2, Fe_2O_3, MgO, TiO_2, and Zr are plotted in Figure 3.12. (Bulk density measurements for the various samples are given in Table 3.5). The only samples in which parent rock fabric was retained (as determined under a binocular microscope), and hence the unit volume relationship between the rock and its weathered equivalent maintained, were samples GR106, 107, 108 and GR305.

Figure 3.12 shows that when regolith chemistry is compared with the parent rock on a mass per unit volume basis: 1) Al_2O_3 remains constant or decreases; 2) SiO_2 decreases and 3) Fe_2O_3, MgO, TiO_2 and Zr all show variable behavior, being either lost or gained.

The interpretation of the losses and gains remains equivocal even if changes in chemistry are compared with the basal sample of each profile rather than GRRA.

The near surface increase in TiO_2 and Zr (Figure 3.12) is attributed to the following. There is a limit in the extent to which weathering can continue while maintaining the volumetric relation between the parent rock and weathered residue. With weathering and leaching, the strength of the weathered material will be reduced to a point where it will collapse, being no longer able to support the weight of the overburden. A unit volume of rock will now occupy a lesser volume of regolith. This results in an increase in the volumetric concentration of the less soluble species, e.g., TiO_2 and Zr. The decrease in TiO_2 and Zr in sample GR101 compared with GR102 is attributed to the combined effects of: dilution with vein quartz, removal of

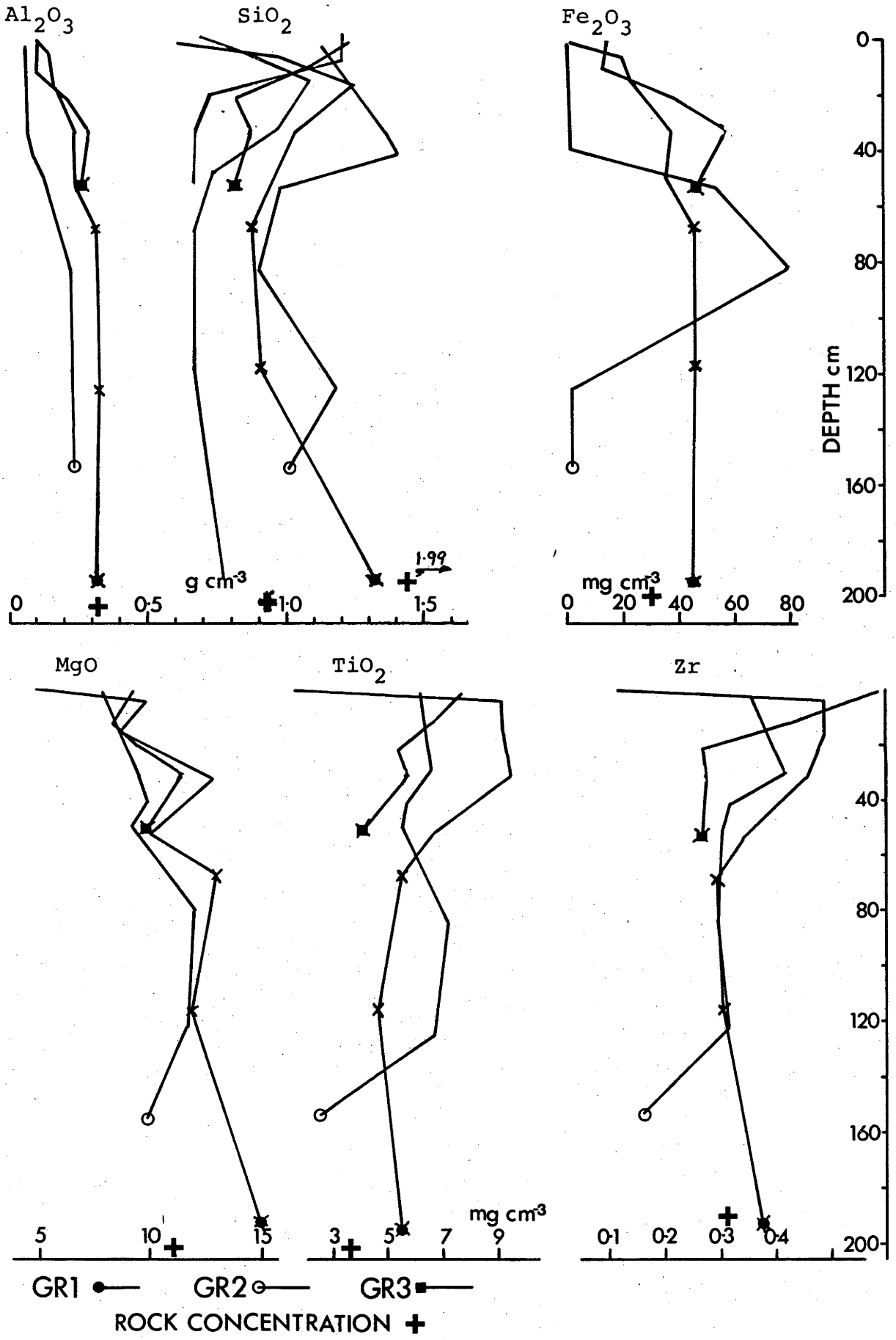

Figure 3.12 Depth dependent variation in the concentration (mass per unit volume basis) of selected elements and quartz (red) for profiles GR1, 2 and 3. Samples in which changes with weathering have been at constant volume are indicated 'x'.

silt size material containing TiO_2 and Zr and a decrease in bulk density of sample GR101 as a result of biological activity.

The near surface decrease in Al_2O_3, Fe_2O_3, and MgO concentration (Figure 3.12) is consistent with the decrease in the clay fraction relative to the non-clay fraction, the clay fraction being enriched in these elements compared with the remaining framework grains (Figure 3.9).

Two minerals with which absolute changes in chemistry could potentially be determined are zircon and quartz. Zircon is known for its comparative resistance to weathering. For the granite Zr is likely to occur almost exclusively in zircon (Table 3.12). Figure 3.12 shows that Zr can not be demonstrated to be immobile. Consequently, the use of zircon as an immobile phase is precluded. Quartz in comparison to zircon is abundant. If quartz is only slightly mobile then because of its relative high concentration in the parent rock, errors incurred when calculating the degree of absolute change may not be that great. The concentration of quartz (Figure 3.12) shows that for profiles GR1 and GR3, quartz undergoes sufficient loss to preclude its use as an immobile phase.

As neither quartz or zircon or any of the elements examined in Figure 3.12 could be unequivocally demonstrated to be immobile throughout the three profiles, the calculation of absolute changes based on an immobile phase is precluded.

3.5.4 Chemical Constraints on the Origin of the Textural Differentiation in Profile GR1

Profile GR1 was chosen for discussion as it is the profile about which the most is known (Figure 3.13).

As textural differentiation is one of the key characteristics on which horizons described in Chapter 1 (p.6) are recognised, the A, B, C, R horizon designation is appropriate and is used.

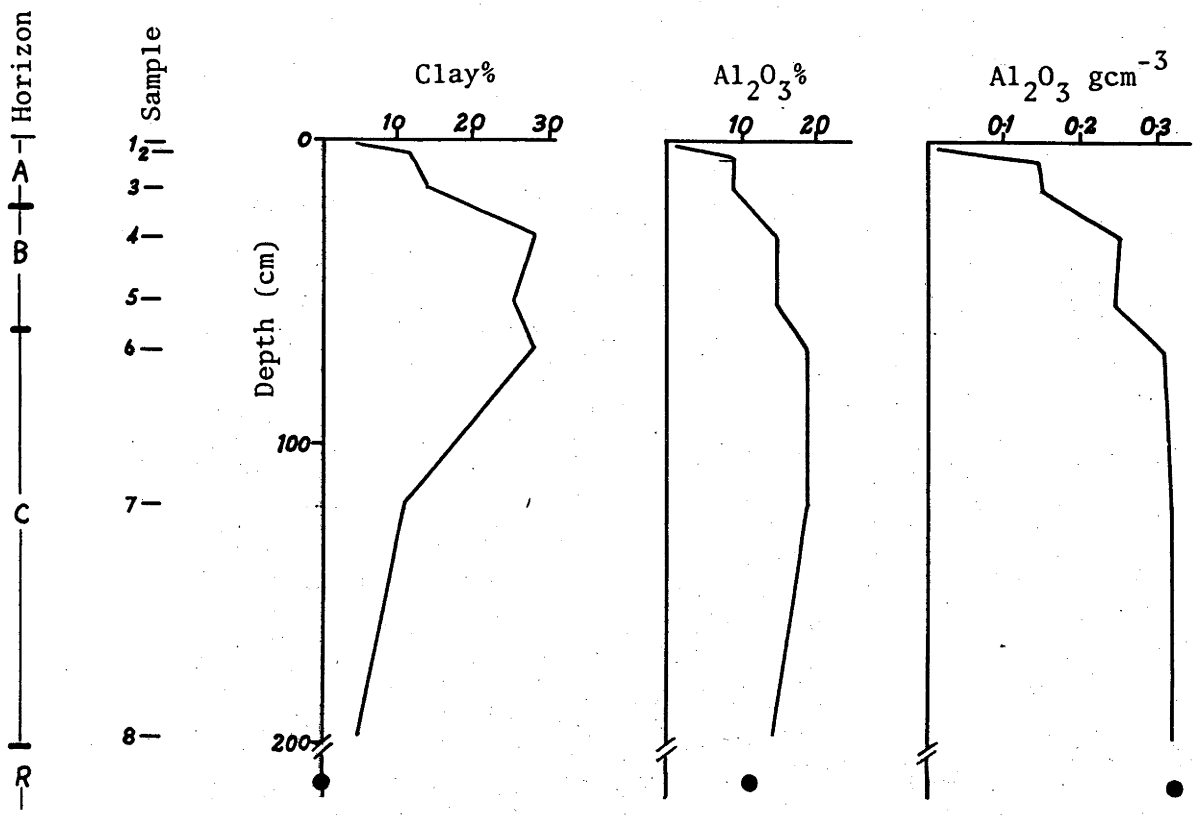

Figure 3.13 Depth dependent variation in clay and Al_2O_3 content of profile GR1. Rock concentration is indicated as '● '.

Profile GR1 can be divided into two sections, depending on whether the clay content is increasing or decreasing. In a profile free of genetic breaks, contiguous horizons will have the closest genetic relationship. The absence of genetic breaks in profile GR1 is demonstrated by the near constant modal particle-size (Table 3.6). Consequently the profile is divided into the R and C horizon and the B and A horizon.

Increase in Clay Content from the R Horizon to the C/B Horizon Interface

The range of processes leading to the increase in clay content can be readily constrained. The generation of the clay fraction is dependent on two processes.

Firstly, it was shown in Section 3.4.2 that the clay fraction consists dominantly of neoformed clay minerals rather than comminuted primary minerals. The mass balance of Al_2O_3 shows that it is essentially retained during the transformation of the R horizon to C horizon (Figure 3.13C). Given that feldspar is the dominant Al_2O_3 primary host mineral, it must be the principal source of clay minerals. Thus the formation of clay minerals is dependent on the weathering of feldspar.

Secondly, once weathering has occurred, comminution of the weathered and partly weathered feldspar must occur to generate clay. It has been shown (Figure 3.7) that the proportion of clay minerals in the clay fraction varies and that the formation of clay lags the formation of clay minerals.

Thus the up-profile increase in clay content within the C horizon reflects the progressive increase in the chemical destruction of the primary minerals and the comminution of their weathered products.

In contrast to those processes which lead to an increase in clay content within the C horizon, delineation of those processes which lead to a decrease in the clay content in the near surface horizons is less simple.

Decrease in Clay Content from the C/B Horizon Interface to the Surface

Two potential hypothesis emerge to explain this textural differentiation. These are:

Hypothesis 1. There is no net loss of clay from the profile. The textural differentiation is a result of the vertical redistribution of clay, viz., its removal from the A horizon and deposition in the B horizon.

If there has been an addition of clay to the B horizon, the clay content of the B horizon should then exceed the clay content of the most weathered C horizon sample, GR106. It does not.

Clay minerals are the most aluminous phase present in the profile. If clay has been added to the B horizon then the percentage concentration of Al_2O_3 in the B horizon should exceed that of sample GR106, the most weathered C horizon sample. Figure 3.13B shows that the concentration of Al_2O_3 in the B horizon is less than GR106.

On the above two criteria, the vertical redistribution of clay can be precluded.

Hypothesis 2. There is a net loss of clay from the profile. The rate of loss is greatest at the surface and decreases with depth. The variation in clay and Al_2O_3 concentration is such that I can find no criteria to preclude the operation of this process.

The decrease in the concentration of Al_2O_3 in the B horizon relative to sample GR106 (C horizon) suggests that clay loss has also occurred from the B horizon. The approximate constant clay content (25 to 28%) of the B and top of the C horizon (samples GR104,105 106) does not preclude this loss. As stated previously, a considerable portion of the total clay mineral content can occur in the non-clay fraction and the generation of clay lags the formation of clay minerals. Thus it is possible, even with a net loss of clay, that the clay content of the B horizon can be maintained, simply through the comminution and further weathering of pre-existing partially weathered feldspar.

It is not possible, from the data available, to determine unequivocally how the loss of clay occurred.

There is growing evidence to suggest that aluminous compounds may be more soluble than previously thought, and that substantial clay loss from a profile by solution may occur (Koppi and Williams, 1980). Given the common occurrence of clay minerals throughout the granite landscape, it would be injudicious, on the evidence to date, to propose that solution processes are important in textural differentiation.

The ability of moving water to cause size fractionation is well established (Moss and Walker, 1978). It is reasonable to propose that within a regolith the clay fraction could be selectively separated from the inherently less mobile framework grains. The decrease in the rate of clay loss with depth would then correspond to an associated decrease in the water flux with depth.

3.6 CHEMISTRY OF THE CATCHMENT EFFLUX

Conditions prevailing within the regolith represent only one part of the total chemical environment of a landscape. For example, although considerable P is lost through leaching during incipient weathering, it is probable that during the movement of dissovled P through the landscape, it will interact with surface active phases and coprecipitating ions and be removed from solution. Consequently, dissolved P will form only a small proportion of the total catchment efflux. Thus it is important not to assume that the behaviour of an element in a selected portion of a landscape will be indicative of its behaviour throughout the entire landscape.

The stream environment is a point in a landscape at which the dissolved and particulate efflux budgets can be conveniently measured and compared with losses from the regolith. Many processes affect the composition of the particulate and dissolved load. Dissolved load sampling should be stratified according to time and discharge, and particulate load (organic and inorganic) sampling should be stratified to account for differences in the size, shape and density of the material. For example, the concentration of P, Ti and Zr are likely,

because of the small dense nature of some of their host minerals (apatite, ilmenite and zircon), to show considerable point to point variation within in the stream-bed.

The rate at which dissolved and particulate loads are removed from the catchment is variable.

1) Dissolved load loss occurs at all discharges and generally the concentration decreases with increasing discharge.

2) Suspended load concentration is determined by both the existence of a source of suspendable material and discharge. Commonly it is the rate of supply rather than stream water velocity which limits the suspended efflux.

3) The rate of bed load removal increases with stream velocity, but a threshold velocity exists below which bed load movement will not occur.

As a result of the variation in processes controlling the removal of dissolved and particulate (suspended and bed load) material from the catchment, it is not possible to predict the time span required, such that a steady state relation could be assumed to exist (if ever it does) between the dissolved and particulate load. The existence of steady state conditions is required if the relative rates (on a whole catchment basis) of weathering and solutional and particulate denudation are to be calculated.

There was insufficient time available to allow the collection of suspended sediment samples. Thus the detail in which it was initially intended to describe the catchment efflux was reduced.

3.6.1 Particulate Load

The chemistry of size separates collected from catchment 5 are given in Tables 3.13 and plotted in Figure 3.9. $SiO_2 + Al_2O_3 + K_2O + H_2O+$ form approximately 99% of the size separates, with SiO_2 forming approximately 85%. This simple chemistry reflects the relatively simple mineralogy of the size separates. They consist dominantly of quartz and minor K-feldspar and its weathered products. The relatively low trace element abundances are consistent with this mineralogy (Table 3.20).

Table 3.20 Modal mineralogy of stream-bed sediments from the catchments. Size, refers to the oversize fraction. The mineral modes were defined according to the criteria of Basu (1976).

	% Quartz						% Feldspar						% Rock Fragments					
	Size ϕ						Size ϕ						Size ϕ					
Catchment No.	3	2	1	0	-1	-2	3	2	1	0	-1	-2	3	2	1	0	-1	-2
1	78	85	90	87	82	60	24	15	8	7	4	0	0	0	2	6	16	40
3	61	69	73	65	56	30	38	29	22	17	12	7	0	2	5	16	32	63
4	69	75	76	74	62	36	31	24	21	16	9	4	0	1	3	10	29	60
5	66	76	78	79	70	43	34	24	20	14	12	6	0	0	2	7	18	51
6	75	80	70	72	68	54	25	20	25	19	13	3	0	0	5	9	21	43

3.6.2 Dissolved Load

Analyses of stream waters from catchments 1, 3, 4, 5, 6 5, 6 are plotted in Figures 3.14 and 3.15. Analyses of Mg, Ca, K, Na, Cl, HCO_3 and pH were supplied by the Forestry Commission of NSW, and SiO_2 was analysed on subsamples provided by them (Table 3.21). The samples represent base flow and rising and falling discharge.

Figure 3.14 shows that the dominant cation/anion pair is Na and Cl. This is consistent with the composition of stream water found by Reinson (1973) for the same area (Figure 3.14 field B.). The dominance of Na and Cl is due to the proximity of the catchments to the coast and consequent marine aerosol fallout (Reinson, 1973).

The relation of water chemistry to a portion of the system $K/Na\text{-}Al_2O_3 - SiO_2 - H_2O$ at 25°C and 1 atmosphere pressure is given in Figure 3.15. Although the boundaries of the various stability fields have been determined for pure mineral species in a closed system at particular pressure temperature conditions, these diagrams are relevant as they give an indication of the general tendencies of weathering and neoformation (Fernandes-Marcos et al., 1979; Sarazin et al., 1976).

Conventionally these results would indicate that on a catchment basis the waters are chemically buffered with respect to kaolinite; saturated with respect to quartz and gibbsite; and undersaturated with respect to K-feldspar, mica, plagioclase, montmorillonite and amorphous silica.

In gross terms this suggests that the dominant chemical reactions controlling stream water chemistry are the transformation of feldspar/biotite to kaolinite and the subsequent release of K, Na, Ca and SiO_2. This is consistent with mineralogical evidence which shows that the proportion of K-feldspar and plagioclase decreases with weathering, with the dominant product of neoformation being kaolinite. (Tardy (1971) considers that on the basis of its chemical composition dioctahedral vermiculite can be considered analogous to kaolinite).

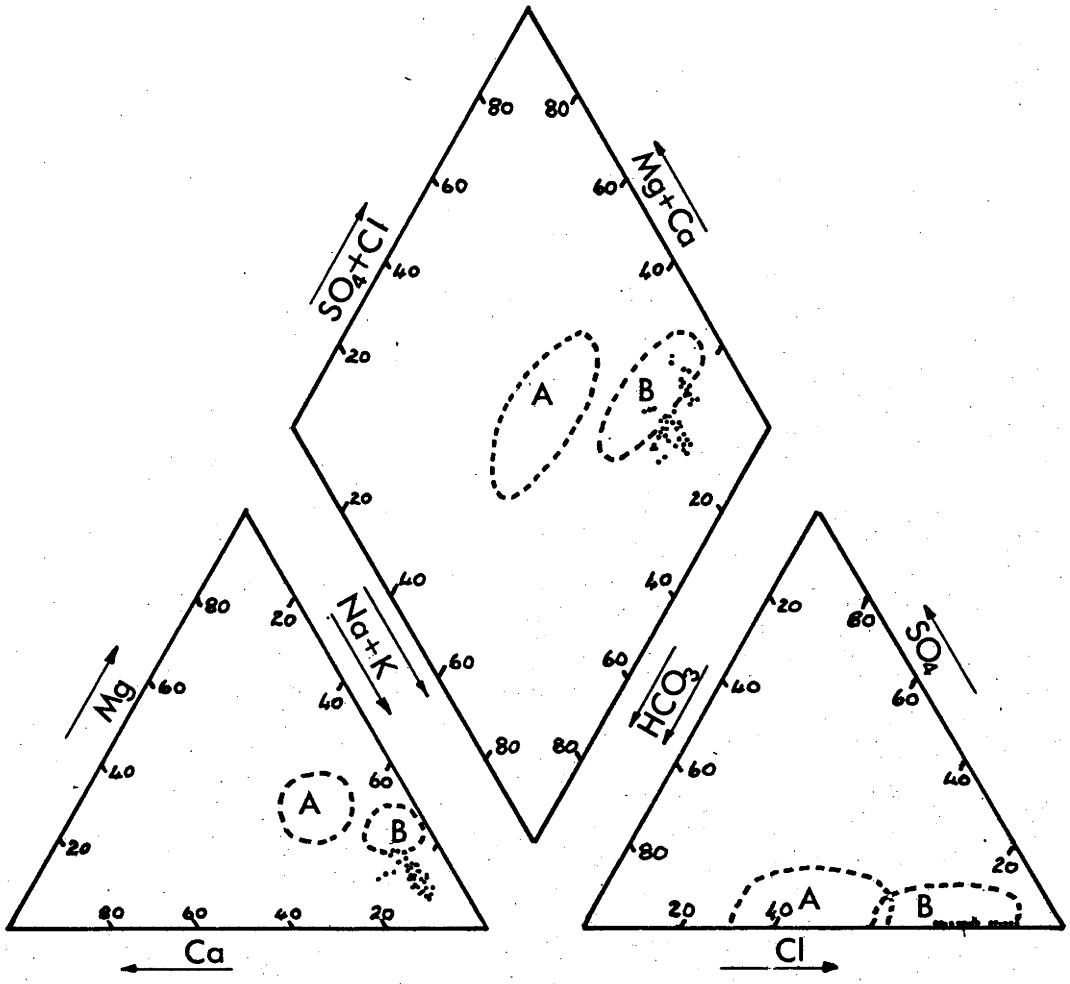

Figure 3.14 Catchment stream water chemistry (diagram after Piper, 1944). Cation and anion analysis are in me%. Sulphate analyses were not available. Reinson (1973) has shown that compared with the sum of the bicarbonate and chloride concentrations the sulphate concentration is <10%. Consequently, for illustrative purposes the sulphate concentration has been assumed to be zero. Fields labelled 'A' and 'B' are from Reinson (1973): fields 'A' and 'B' represent the composition of stream waters from the western and eastern portions of the Genoa-Wallagaraugh River Basin.

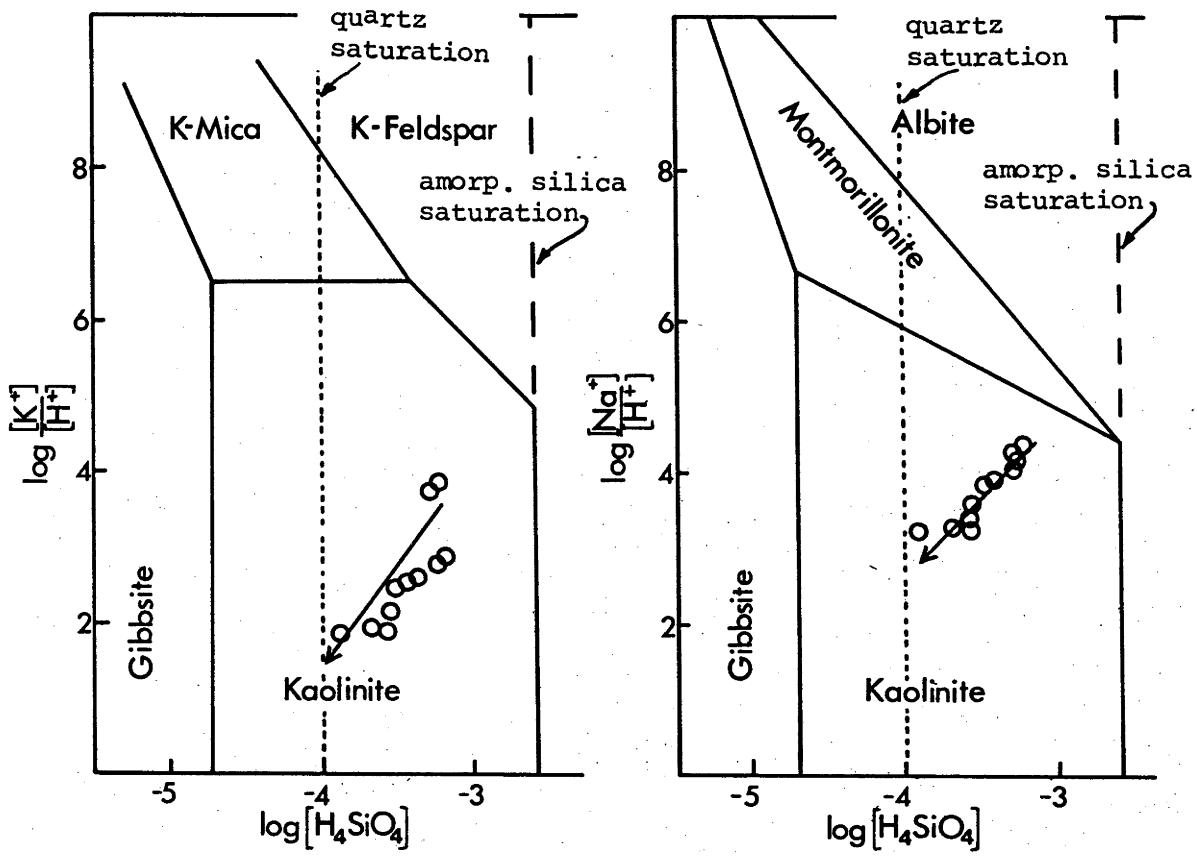

Figure 3.15 Variation in catchment stream water chemistry for a portion of the system K/Na-Al_2O_3-SiO_2-H_2O at 25°C and 1 atmosphere pressure (after Garrels, 1967). The arrow indicates the direction of change in water composition with increasing discharge. It was assumed that the molality of the dissolved constituents equals their activity.

Table 3.21 Dissolved SiO_2 concentration of stream-water samples from catchments 1, 3, 4, 5, and 6.

STREAM WATER ANALYSIS CATCHMENT STUDY AREA

SAMPLE NUMBER			ppm SiO2
110	EC1	1/7	16
120	EC1	8/7	30
130		15/7	8
140	EC3	1/7	16
150		8/7	31
160		15/7	12
170	EC3	1/7	25
180		2	23
190		4	22
200		6	19
210		9	18
220		12	18
230		15	12
240	EC3	16/7	12
250		2	16
260		4	12
270		6	11
280		10	12
290		15	13
300		21	13
310	EC3	24	13
320	EC3	177]	14
330		3	14
340		4	12
350		6	16
360	EC3	2/81	30
370		3	28
380		6	25
390	EC4	1/7	19
400		8/7	20
410	EC4	15/7	17
420		2	16
430		4	16
440		5	16
450		8	16
460	EC4	16/7	16
470		6	17
480		12	17
490		16	16
500		20	16
510	EC4	17/7	16
520		6	
530		12	17
540		18	18
550		23	17
560	EC4	18/7	18
570		6	17
580		12	12
590		18	
600		23	18
610	EC4	19/7	18
620		7	18
630		15	18
640		21	18
650	EC5	1/7	
660		8/7	32
670		15/7	18
680	EC5	11/7	17
690		7	17
700		12	18
110	EC5	17/7	18
120		24	18
130	EC5	18/7	23
140		6	23
150		12	23
160		18	23
170		24	23
180	EC6	1/7	27
190		8/7	35
200	EC6	15/7	31
210		3	32
220		4	29
230		5	26
240		6	23
250		9	
260		11	
270	EC6	16/7	21
280		6	20
290		12	16
300		19	18

Samples were provided by the NSW Forestry Commission. Sample numbers are those of the Commission.

Analyses were done by staff of the Water Laboratories, CSIRO Land Use Research, Canberra.

The degree of SiO_2 saturation with respect to quartz of the stream waters varies with discharge (Figure 3.15), being a maximum at base flow and decreasing to a mimimum at peak discharge. The variation in SiO_2 concentration is attributed to differences in the dominant source area of the stream waters: 1) at base flow, stream waters have had a maximum interaction with the regolith and consequently have a high SiO_2 concentration as a result of the weathering of feldspar, whereas 2) with increasing discharge much of the water leaving the catchment has not interacted with regolith as it has either fallen directly into the main drainage system or its ephemeral extensions.

Brewer (1973) and Tardy et al. (1973) have shown that conventional generalisations with respect to stream water chemistry/ weathering reactions are prone to exceptions and that the average catchment condition may give little indication of the actual point to point variation in catchment conditions. For example, when considering the degree of SiO_2 saturation of stream waters with respect to quartz (Figure 3.19), quartz would be predicted to be insoluble. Figure 3.13 however, suggests that quartz is soluble. This difference reflects the point to point variation in conditions affecting mineral solubility within the catchment.

3.6.3 Partitioning Between Dissolved and Particulate Load

In the absence of suitable empirical data, the potential importance of partitioning of the major elements between the dissolved and particulate load has been calculated using the following assumptions:

1) Quartz does not dissolve or undergo comminution.
2) All aluminous minerals are converted to clay size kaolinite.
3) Titanium and Fe species are assumed to be insoluble and retained in the clay and silt size fractions.
4) Acid leaching conditions prevail, with Mg, Ca, K and Na being leached from the system as bicarbonate.

These assumptions require the addition of 130kg of H_2O and CO_2 to weather one tonne of rock of composition GRRA.

These results (Table 3.22) provide an indication of the potential importance of both the dissolved and particulate load in small catchment budgets. The dissolved and particulate load each form approximately 50% of the total load.

Table 3.22 Major element partitioning with the weathering of 1,000kg (cube 73cm on edge) of granite, composition GRRA.

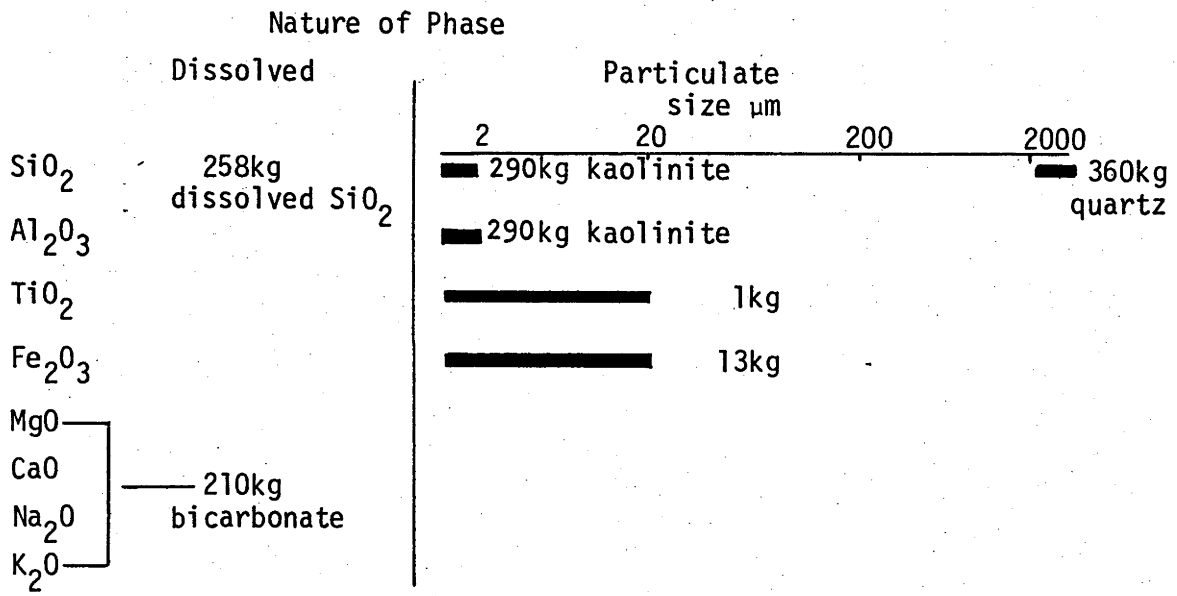

PLATE 1
A) Fire induced fragmentation of aplite in the catchment area.
B) Fire induced fragmentation of a coarse grained adamellite outcrop in the catchment area.

PLATE 2

A) A coarse grained adamellite undergoing granular disintegration.

B) Weathering profile developed on coarse grained adamellite.

CHAPTER 4

SURFICIAL MATERIALS DEVELOPED ON RHYOLITE

4.1 INTRODUCTION

The rhyolite parent rock forms part of the Eden Rhyolite which has been described in detail by Steiner (1966) and Beams (1980).

4.1.1 Parent Rock

Petrology

In the area in which the regolith profiles occur (Figure 2.2) the bed rock is a densely welded rhyolite tuff. The rhyolite is commonly porphyritic, consisting of euhedral to subhedral quartz phenocrysts which are occasionally embayed; minor prismatic albitic plagioclase; rare sanidine phenocrysts and accessory zircon and apatite (Beams, 1980) set in a grey aphanitic groundmass. The size and proportion of phenocrysts vary from flow to flow. They generally range in size* from 0.5mm to 4mm, (Table 4.1) and generally constitute <10% of the rock.

The groundmass originally contained considerable glass which has since recrystallised. It now consists of interlocking quartz, K-feldspar and albite crystals and unidentified clay minerals (Beams, 1980). The crystals in the groundmass vary in size from 5μm to 20μm.

Chemistry

Analyses of the Eden Rhyolite samples from south of Eden are given in Table 4.2. The variation in minor element concentration is probably a result of post-depositional alteration (devitrification and hydration) and the variation between flows. As rocks ERR6, 7 and 8 occur closest to the profiles examined, their average composition (ERRA) is used to calculate the change in chemistry which occurs

---

* The size distribution of quartz phenocrysts given in Table 4.1, is not intended to be used as a statistical basis for estimating the mean size and variance of the source population. The size of phenocrysts can vary markedly between samples. Phenocryst size was originally recorded at 0.25Ø intervals, with the aim of examining the size distribution of phenocrysts in individual rock specimens. Due to problems in the interpretation of the size distributions obtained, this line of research was abandoned. The measurements have now been reduced to 1Ø intervals and should only be used to provide a general indication of the range in size of the phenocrysts.

Table 4.1 Size distribution of 621 quartz phenocrysts from the Eden Rhyolite. The distribution was based on thin section measurements of the maximum phenocryst diameter, which were subsequently adjusted according to criteria given in Friedman (1958). The measurements were made on all (11) thin sections of the Eden Rhyolite held by the Dept of Geology, ANU.

Size	ϕ	3	2	1	0	-1	-2
	mm	0.063	0.25	0.50	1.0	2.0	4.0
% less than specified size		1	9	31	64	95	100

Table 4.2 Rhyolite chemistry (B.W. Chappell, unpublished analyses).

Sample#	ERR1	ERR2	ERR3	ERR4	ERR5	ERR6	ERR7	ERR8
SiO_2	77.64	81.33	75.22	75.07	74.59	75.10	75.73	76.01
TiO_2	0.13	0.10	0.20	0.28	0.24	0.24	0.25	0.28
Al_2O_3	11.65	11.29	11.92	11.57	12.23	12.20	12.24	11.85
Fe_2O_3	1.09	0.30	0.84	1.10	0.92	0.83	0.86	0.75
FeO	0.23	0.23	1.30	1.42	1.02	1.14	0.98	1.46
MnO	<0.01	0.01	0.15	0.04	0.03	0.04	0.03	0.04
MgO	0.22	0.23	0.37	0.68	0.50	0.43	0.51	0.64
CaO	0.01	0.01	0.09	0.14	0.55	0.66	0.16	0.47
Na_2O	3.37	0.08	2.77	2.63	3.63	3.04	2.63	2.46
K_2O	3.48	3.42	4.60	4.33	4.11	4.53	4.49	4.06
P_2O_5	0.01	0.02	0.05	0.07	0.06	0.06	0.06	0.07
S	0.02	<0.02	0.02	<0.02	0.03	<0.02	0.04	<0.02
H_2O+	0.84	1.77	1.60	1.30	0.95	0.78	0.96	1.18
H_2O-	0.30	0.41	0.29	0.31	0.30	0.18	0.38	0.30
CO_2	0.13	0.15	0.62	0.31	0.32	0.22	0.09	0.17
rest	0.18	0.07	0.17	0.20	0.17	0.18	0.18	0.18
	99.30		100.21		99.65		99.59	
O=S	0.01		0.01		0.01		0.02	
	99.29	99.42	100.20	99.45	99.64	99.63	99.57	99.92
Trace elements								
Ba	775	80	645	810	585	715	760	695
Rb	127	163	168	139	154	179	165	152
Sr	59	9.2	26.0	55	60	63	34.0	69
Pb	20.5	54	65	5.5	13.5	20.5	4.0	19.5
Th	19.6	13.2	18.4	20.4	21.6	20.2	21.4	19.6
U	5.2	5.4	4.8	4.2	4.8	4.8	4.8	4.4
Zr	192	79	171	224	206	210	209	208
Nb	12.0	9.0	10.5	11.0	11.0	11.0	11.0	10.5
Y	37	52	52	53	59	61	52	50
La	41	20	28	39	38	38	40	35
Ce	97	56	71	96	94	95	101	86
Nd	41	19	30	38	39	39	42	35
Sc	5	7	7	11	9	10	10	10
V	2	2	9	20	13	12	13	22
Cr	<1	<1	<1	5	2	1	2	12
Mn	15	45	1200	340	240	290	195	290
Co	2	<1	<1	3	4	3	2	6
Ni	<0.5	<0.5	2.0	3.0	2.0	1.0	<0.5	8.0
Cu	4.5	<0.5	8.0	2.5	10.5	6.0	2.5	6.5
Zn	43	7	87	137	65	38	42	87
Ga	16.6	18.8	17.0	16.8	18.6	18.8	19.0	17.6
P (Hough Data)	55	95	260	335	330	315	300	310

with weathering. The average, standard deviation, coefficient of variation, maximum and mimimum concentration of elements in these three rocks are given in Table 4.3.

Unlike the granite there is less confidence about the extent to which those rocks analysed represent the parent rock of the profiles examined. The rhyolite immediately after deposition would have been extremely reactive due to its high temperature, glassy nature and finely divided state. Consequently, local variations in mineralogy and chemistry are likely to occur with the movement of water through the consolidating pile. This variation would lead to some areas being predisposed to weathering.

Rock Structure

The dominant structural features present are:

1) Joints developed as a result of the cooling and compaction of the rhyolite (Collins, 1977).
2) Fracture cleavage. This is not uniformly developed throughout the area, but where it is strongly developed it is recognised by the presence of macroscopically visible planes which are between 0.5cm and 30cm apart.

4.1.2 Regolith

The regolith is often gravel rich and is usually <1m deep. Areas greater than 1ha in size, in which the regolith is <40cm deep or consists of a gravelly veneer overlying a more or less continuous rock surface, are common. The profiles examined are described in Appendix B. The depths of the various samples taken are given in Table 4.4. Typical profiles are illustrated in Plate 3.

4.2 REGOLITH PARTICLE-SIZE

The regolith developed on the rhyolite can be divided, on the basis of the dominant size of particles present, into (1) rubble fields, in which gravel size material is common and clay is either absent or minor, and (2) weathering profiles, in which clay is comparatively abundant.

Table 4.3 Average composition of the rhyolite: $\bar{x}$ average concentration; σ, standard deviation; C.V., coefficient of variation; and maximum and minimum for rocks ERR6, 7, 8.

wt%	$\bar{x}$	σ	C.V.	Maximum	Minimum
SiO_2	75.61	0.47	0.6	76.01	75.10
TiO_2	0.26	0.02	8	0.28	0.24
Al_2O_3	12.10	0.21	2	12.24	11.85
Fe_2O_3	0.81	0.04	5	0.86	0.75
FeO	1.19	0.24	20	1.46	0.98
MgO	0.53	0.11	21	0.64	0.43
CaO	0.43	0.25	58	0.66	0.16
Na_2O	2.72	0.29	11	3.03	2.46
K_2O	4.36	0.26	6	4.53	4.06
H_2O+	0.97	0.14	14	1.18	0.78
C	0.04	0.02	50	0.06	0.02
ppm					
P	308	7	2	315	300
Rb	165	14	8	179	152
Sr	55	19	35	69	34
Pb	15	9	60	20	4
Zr	209	1	1	210	208
Y	54	6	11	61	50
V	16	6	38	22	12
Cr	5	6	120	12	1
Mn	258	55	21	290	195
Ni	3	4	133	8	<1
Cu	5	2	40	7	3
Zn	56	27	48	87	38

Table 4.4 Sample depths for profiles ER1, 2, 3, 4.

Sample	Depth (cm)	Sample	Depth (cm)
Profile ER1		Profile ER3	
1	5-10	1	0-8
2	12-17	2	20-30
3	55-65	3	33-40
4	90-100	4	60-65
		5	110-120
		6	170-180
Profile ER2		Profile ER4	
1	0-10	1	0-10
2	25-30	2	22-29
3	57-62	3	32-38
4	80-85	4	62-70
5	95-105	5	94-100

Rubble Fields

These areas are associated with extensive rock outcrops. The particles present are commonly between 1cm and 40cm in size (Plate 3). The larger particles commonly have planar bounding faces, and are probably formed by the preferential separation of the rock mass along pre-existing fracture and joint planes. Particles of this size are not restricted to rubble fields; they also occur in the weathering profiles (Plate 3).

Weathering Profiles

The particle-size distributions of samples from the profiles are given in Table 4.5.

Non-Clay Fraction: With weathering, there is a decrease in gravel content and a concomitant increase in the silt content. A schematic illustration of this change is given in Figure 4.1A. The schematic illustration is based on the change with weathering in the sequence of samples ER405 to 404 to 204 (Figure 4.2).

Clay-Fraction: The clay content increases from the base of the profile to a maximum and then decreases in the near surface samples (Figure 4.1B).

Particle-Size Modes

Within the rhyolite landscape, four particle-size modes can be identified. An individual mode can be masked by an adjacent mode, and need not be obvious or present in all samples. The distribution of these modes is shown in Figure 4.2 and described as follows:

1) -9 to -2ø Mode: The statistical definition of this mode is logistically difficult because of the number and size of the samples which would be required. Many of the particles of this mode have planar surfaces which are interpreted as being formed by the rock mass separating along pre-existing cleavage/joint planes.

   Continued breakage of particles of this mode will result in particles free of low cohesion cleavage/joint planes. At this stage, further comminution probably occurs as a consequence

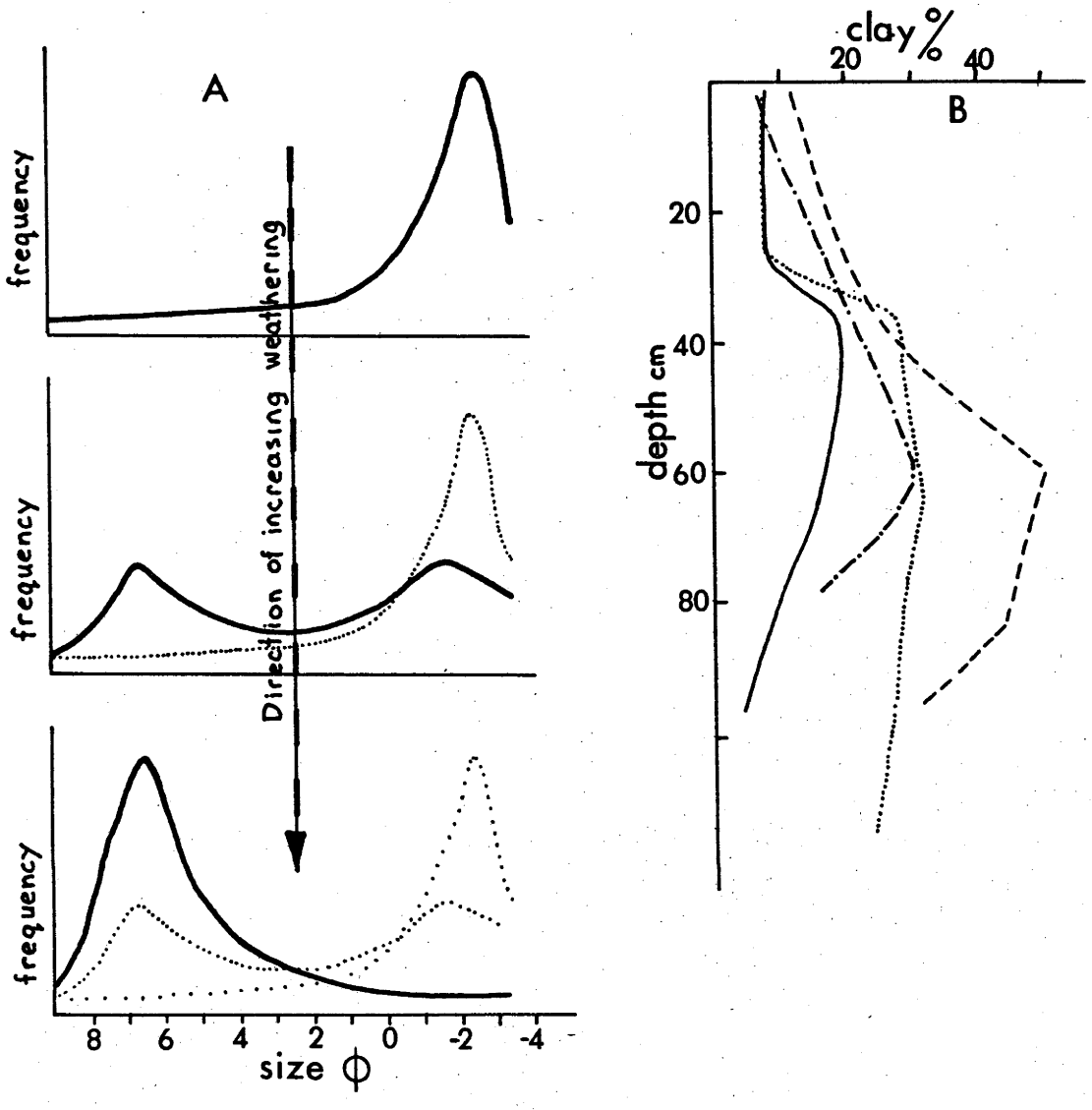

Figure 4.1 Particle size distribution of profiles ER1, 2, 3, 4.

A : Schematic variation in the particle size distribution of the non-clay fraction with increasing weathering (the distributions are unscaled). Antecedent states of weathering are shown ghosted. For ease of presentation the mode due to quartz phenocrysts has been removed.

B : Depth dependent variation in clay content.

Legend Profile

ER1 -·-·-·
ER2 - - - -
ER3 ·····
ER4 ——

SAMPLE NUMBER	SIZE ϕ														
	<9	8	7	6	5	4	3	2	1	0	-1	-2	-3	-4	>-4
ER101	7.6	5.4	14.4	18.1	9.3	8.5	4.9	3.2	4.9	10.1	11.4	1.6	0.6	0.0	0.0
ER102	13.1	8.5	16.1	19.1	6.3	8.1	3.4	2.4	4.0	7.2	8.5	2.8	0.0	0.0	0.0
ER103	30.3	7.2	15.7	21.8	5.9	4.5	2.0	0.8	1.2	3.3	6.1	1.2	0.0	0.0	0.0
ER201	12.3	5.6	13.7	18.8	9.1	6.6	4.2	3.4	4.6	6.2	6.1	4.4	5.0	0.0	0.0
ER202	17.9	3.9	10.1	14.3	6.6	6.3	2.5	2.0	2.9	3.8	6.7	15.5	6.6	0.9	0.0
ER203	51.2	3.6	8.0	10.6	3.1	1.8	1.1	1.0	1.1	1.7	6.8	10.0	0.0	0.0	0.0
ER204	43.8	4.2	10.0	17.0	4.1	2.4	1.2	0.8	1.2	2.4	5.2	2.0	5.7	0.0	0.0
ER301	8.0	2.3	12.2	13.9	8.4	8.1	7.5	8.4	10.6	8.9	6.8	1.3	0.8	0.0	2.8
ER302	8.3	2.9	11.2	9.2	6.7	6.2	5.4	6.1	7.8	9.5	11.9	2.4	2.1	1.5	8.8
ER303	20.2	5.7	14.8	11.0	7.1	6.5	5.4	5.4	6.9	7.5	6.3	1.4	0.3	0.0	1.5
ER304	32.5	8.4	19.0	12.7	5.2	5.2	3.6	3.1	3.4	3.1	2.7	1.0	0.1	0.0	0.0
ER305	25.2	9.9	20.3	14.0	7.9	5.6	4.5	3.3	3.3	3.3	2.2	0.5	0.0	0.0	0.0
ER306	23.6	9.7	18.8	14.0	8.2	5.6	5.1	5.1	5.4	3.5	0.8	0.2	0.0	0.0	0.0
ER401	7.0	1.7	8.9	9.9	5.3	5.9	4.8	5.6	8.6	10.1	6.2	13.2	11.0	1.8	0.0
ER402	7.7	2.0	14.0	11.2	5.6	5.5	4.5	5.4	8.4	10.3	8.0	10.6	6.1	0.7	0.0
ER403	17.3	2.8	6.3	5.3	2.7	2.9	3.0	4.2	7.3	10.1	7.4	17.7	7.8	2.3	2.9
ER404	14.9	2.6	4.2	3.8	1.8	1.6	2.5	4.0	9.3	15.8	10.6	20.8	6.9	1.2	0.0
ER405	4.2	1.0	1.1	0.7	0.7	0.7	1.4	1.9	5.9	7.6	6.1	23.4	22.4	15.0	7.9

Table 4.5 Particle-size distribution of profiles ER1,2,3,4.

Figure 4.2 Distribution of particle-size modes in the rhyolite landscape.

Explanation

A, B, C, D: Particle-size distribution of samples ER101, 204, 404 and 405 respectively. The degree of weathering increases from histogram D through to histogram A.

E: This represents an estimate based on field observation of the size distribution of particles occurring in rubble fields.

F: Quartz phenocrysts; size distribution of quartz phenocrysts, see Table 4.1.

Quartz and H_2O+ histogram represents for sample ER204 the percentage of total quartz and H_2O+ present in the individual size fractions. See Section 4.3 for an explanation.

Bar graph: size distribution of quartz and feldspar crystals in the groundmass.

G: Schematic representation of the size distribution of the various particle-size modes.

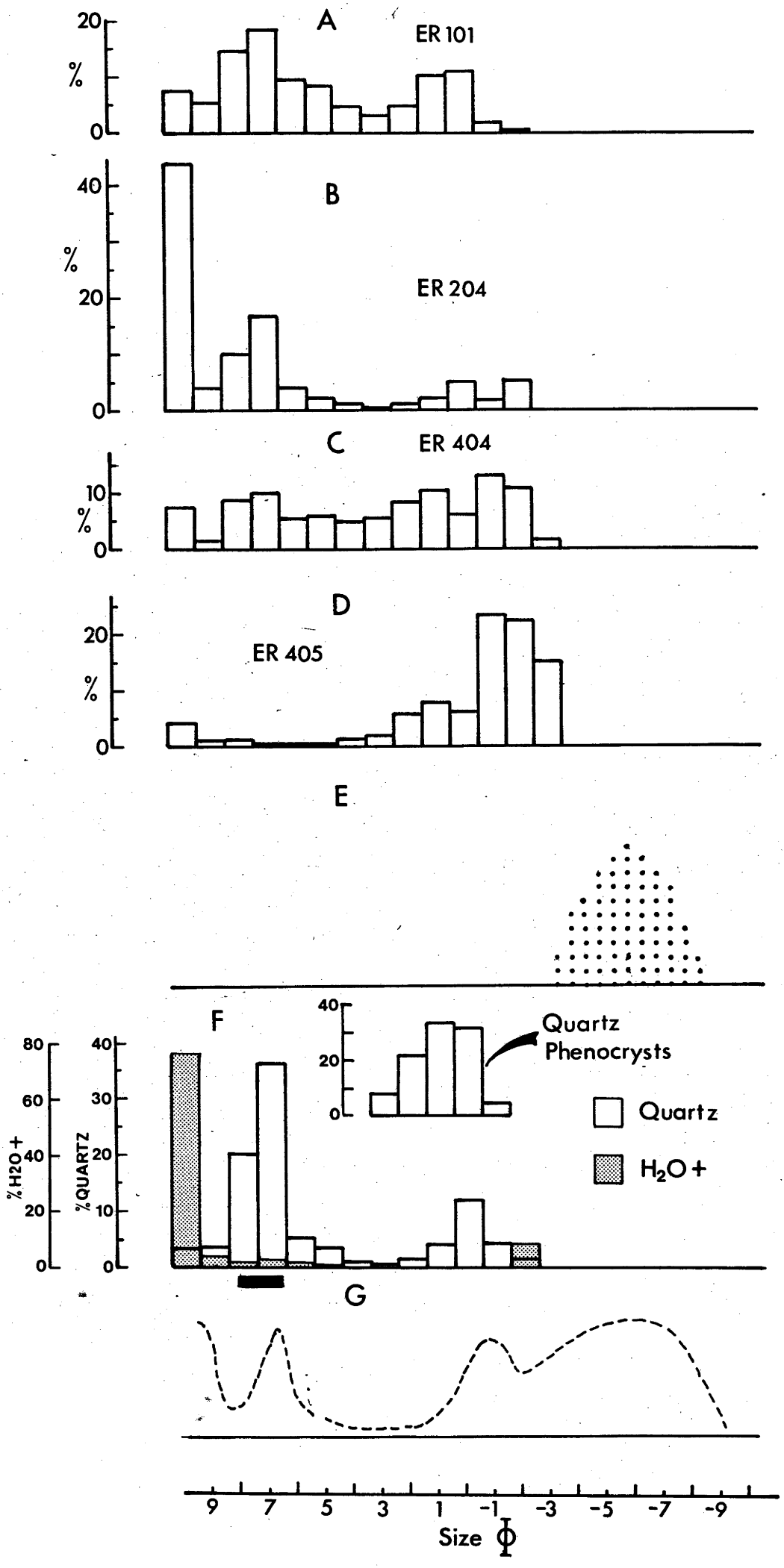
A
ER 101
20
%
0
B
ER 204
40
%
20
0
C
ER 404
10
%
0
D
ER 405
20
%
0
E
F
40
20
0
Quartz
Phenocrysts
Quartz
H2O+
80
60
40
20
0
%H2O+
40
30
20
10
0
%QUARTZ
G
9
7
5
3
1
-1
-3
-5
-7
-9
Size Φ

of fatigue and chemical weathering. Once chemical weathering becomes an important process leading to particle comminution, modes related to the physiochemical properties of the primary minerals rather than the aggregate properties of the parent rock are possible. For instance, particles formed by failure along fracture/joint planes are 10^3 to 10^5 times larger than the size of minerals in the groundmass.

2) -1 to 1ø Mode: This mode is present in sample ER101 and ER204 (Figure 2.4). The common occurrence of bipyramidal quartz crystals in this mode and the correspondence of the size of the mode with the size distribution of quartz phenocrysts in the parent rock (Figure 4.2F) suggests that this mode is due to the release of quartz phenocrysts.

3) 6 to 8ø Mode: This mode is shown in Figure 4.2A, B, C. This mode is attributed to the release of quartz grains from the groundmass consequent to chemical weathering. This is supported by the correspondence of the size of the mode with; i) the modal distribution of quartz in sample ER204; and ii) the size distribution of quartz in the groundmass of the parent rock (Figure 4.2F).

4) Finer than 9ø Mode: The occurrence of this mode (see Figure 4.2B) is attributed to the accumulation of clay minerals in this size range. This is illustrated by the distribution of H_2O+ in horizon ER204 (Figure 4.2F).

4.3 REGOLITH MINERALOGY

4.3.1 Size Dependent Variation in Mineralogy of Sample ER204

Sample ER204 was chosen for size fractionation because of the high degree of weathering it has undergone. Most of the labile minerals have been destroyed, with the sample consisting essentially of quartz and clay minerals (Tables 4.6 and 4.7). Consequently the mineralogy of the size separates from sample ER204 should be indicative of the maximum mineralogical and chemical size dependent fractionation, that presently occurs within the rhyolite landscape.

The mineralogy of the size separates is given in Table 4.6.

Table 4.6 Mineralogy and $\%H_2O+$ for size separates of sample ER204.

	Size Separate Φ													Whole sample
	<9	8	7	6	5	4	3	2	1	0	-1	-2	-3	
% of whole sample	43.8	4.2	10.0	17.0	4.1	2.4	1.2	0.8	1.2	2.4	5.2	2.0	5.7	100
% quartz	3	35	77	81	52	61	43	43	60	72	93	83	12	40
% K-feldspar	tr	tr	tr	nd	tr	tr	tr	tr	tr	nd	nd	nd	nd	2
% Plagioclase	nd	nd	nd	nd	nd	tr	tr	nd	nd	nd	nd	nd	nd	tr
% H_2O+	13.1	7.2	1.6	1.2	3.9	4.3	6.4	7.3	4.0	1.2	1.1	1.1	11.6	7.2
% clay mineral 7Å	45	80	80	100	90	100	70	70	100	100	nd	nd	nd	45
10Å	tr	20	20	nd	10	tr	30	30	nd	nd	nd	nd	nd	tr
14Å	55	tr	nd	nd	nd	nd	nd	nd	nd	nd	nd	nd	nd	55

Table 4.7 Mineralogy of the whole sample and the clay fraction, determined by XRD* and IR+ spectroscopy. Mineral proportion: tr, trace; nd, not detected.

	Mineralogy % (Whole Sample)				*Clay Mineralogy % (Clay Fraction)			
					Å			
Sample Number	Quartz+	K-feldspar*	Plagioclase*	Illite*	14	12	10	7
ER101	66	7	tr	nd	80	nd	nd	20
ER102	71	7	nd	nd	70	nd	nd	30
ER103	51	10	tr	nd	40	nd	10	50
ER104	46	14	2	nd				
ER201	55	5	tr	nd	30	nd	nd	70
ER202	53	5	nd	nd	10	nd	5	80
ER203	33	2	nd	nd	10	nd	20	70
ER204	40	2	tr	nd	55	nd	tr	45
ER205	45	12	tr	nd				
ER301					nd	70	20	10
ER302					nd	60	25	10
ER303					nd	70	15	20
ER304					nd	40	30	25
ER305					nd	30	30	40
ER306					nd	40	30	30
ER401	71	nd	nd	nd	nd	nd	90	10
ER402	70	nd	nd	nd	5	5	80	10
ER403	59	nd	nd	nd	nd	nd	90	10
ER404	61	tr	nd	nd	70	5	20	10
ER405	64	tr	nd	nd	nd	75	25	10

The distribution of quartz and H_2O+ is plotted in Figure 4.3. The data indicates the following:

1) The quartz - H_2O+ plot (Figure 4.3D) is consistent with the size separates consisting essentially of two components, quartz and clay minerals. As previously explained, H_2O+ is used as a surrogate measure of clay mineral concentration, the H_2O+ concentration of 13.5% representing approximately 100% clay mineral.
2) Most of the clay minerals are concentrated in the finer than 9ø fraction (Figure 4.3B). The H_2O+ sub-mode in the -2 to -3ø fraction is due to the presence of sesquioxide nodules. Table 4.6 shows that considerable variation in clay mineralogy occurs with size. For instance illite (10Å) is present only in trace amounts in the clay fraction, and yet can constitute up to 30% of the other size fractions.
3) Quartz forms two modes; they are 7 to 6ø and 0 to -1ø in size (Figure 4.3A). The quartz grains of the coarse mode consist dominantly of bipyramidal crystals. This, and the correspondence of this mode with the general size distribution of quartz phenocrysts (Figure 4.3C) is consistent with the mode being formed through the release of quartz phenocrysts with weathering of the parent rock. The difference between the 0 to -1ø mode and the size distribution of the quartz phenocrysts is attributed to sample variation. The phenocrysts in the parent rock of sample ER204 are coarser than the modal size of phenocrysts in the rock samples (Table 4.1).

The 7 to 6ø mode corresponds to the size distribution of quartz in the groundmass (Figure 4.3C). The formation of this mode is, like the 0 to 1ø mode, attributed to the release of quartz from the parent rock with weathering. It should be noted that the origin of quartz in the two modes differs. The phenocrysts were formed at elevated temperatures, whereas the quartz in the groundmass formed with devitrification of the original glass. Devitrification would have occurred below the α to β transition temperature of quartz. Consequently, it is unlikely that many of the deformational features described in quartz from phaneritic plutonic rock (Moss and Green, 1975) would occur in quartz of the rhyolite groundmass.

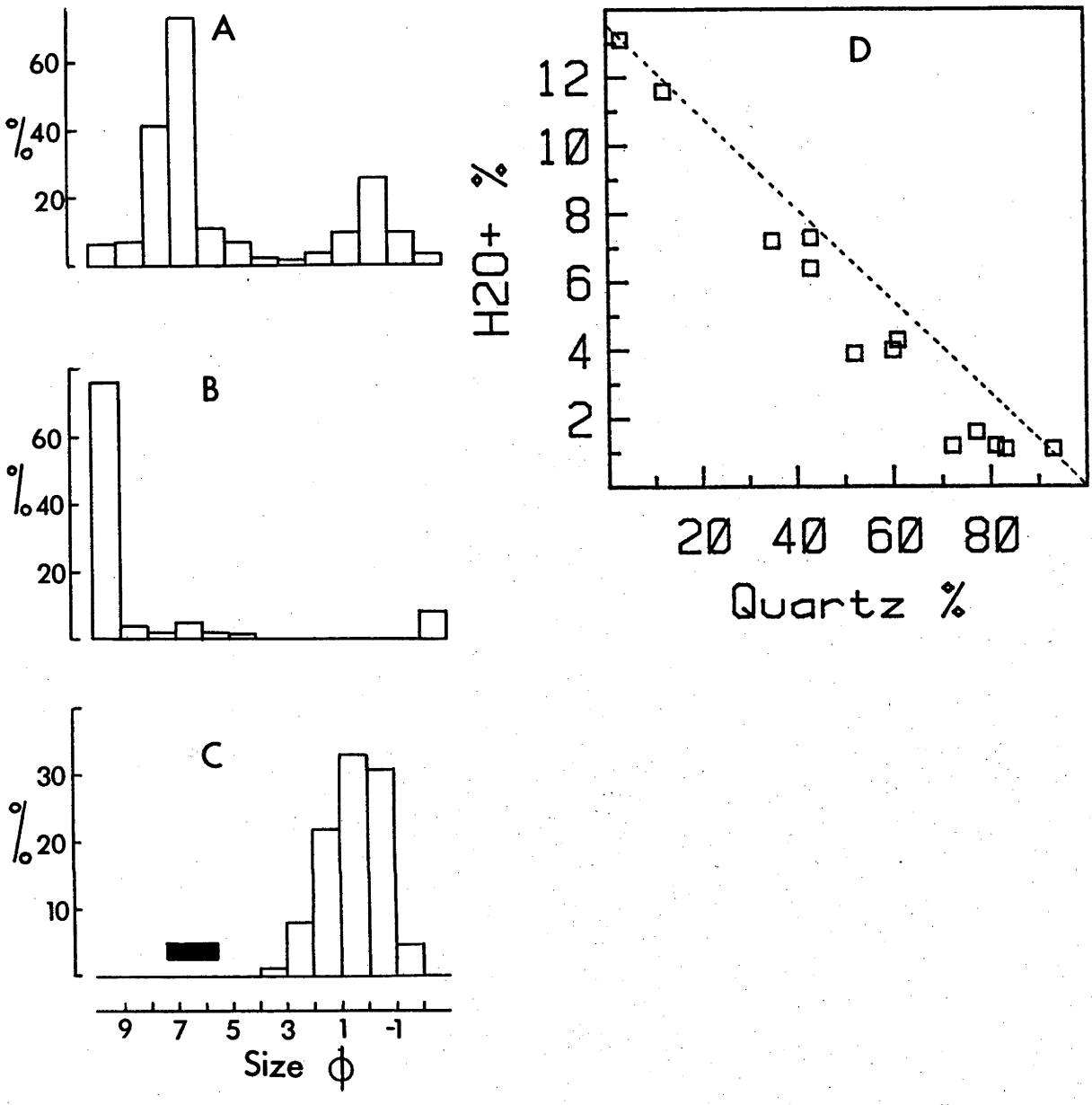

Figure 4.3 Size dependent variation in quartz and H_2O+ content of sample ER204.

A: Percent of total quartz in each 1ϕ size fraction.

B: Percent of total H_2O+ in each 1ϕ size fraction.

C: The histogram represents the size distribution of quartz phenocrysts in the parent rock (Table 4.1). The bar graph is vertically unscaled and represents the range in size of grains in the groundmass of the parent rock.

D: Quartz-H_2O+ plot of 1ϕ size separates.

There is a tendency in Australia to attribute the occurrence of silt size quartz in a regolith to aeolian accession (McConnell, 1979). Aeolian accession as a source of silt in the rhyolite profiles can be precluded by circumstantial evidence: Aeolian accession would require dust deposition only on areas underlain by rhyolite, as silt size modes are not present in regolith derived from other rock types of the area (Chapter 8).

4.3.2 Depth Dependent Variation in Mineralogy

The mineralogy of the various samples is given in Table 4.7 and illustrated in Figure 4.4. The distribution of quartz, K-feldspar, plagioclase and the total proportion of clay minerals is similar to that described for the granite regolith (Section 3.4.2). Based on their persistence in the profile, the order of increasing susceptibility to weathering of the dominant primary minerals is quartz < K-feldspar << plagioclase.

Clay Mineralogy (Clay Fraction)

The clay minerals consist dominantly of kaolinite, illite, vermiculite and a 12Å mixed layer clay. In contrast to the granite regolith, there is a greater variation in clay mineralogy within and between profiles. For example, within the granite regolith the proportion of illite, where present, decreased up profile. In contrast, illite in the rhyolite regolith shows no consistent pattern of variation. At this stage no unequivocal explanation can be provided to account for the variability.

4.4 REGOLITH CHEMISTRY

The partitioning of major elements in the rhyolite is likely to be similar to that of the granite. However, trace element partitioning of the rhyolite is likely to be more complex and not as readily determined. This occurs for the following reasons. With the crystallisation of the glass, some elements are likely to become segregated as discrete phases along crystal interfaces. The fine grainsize of the rhyolite groundmass inhibits the identification, determination of chemistry and modal abundance of many of these phases.

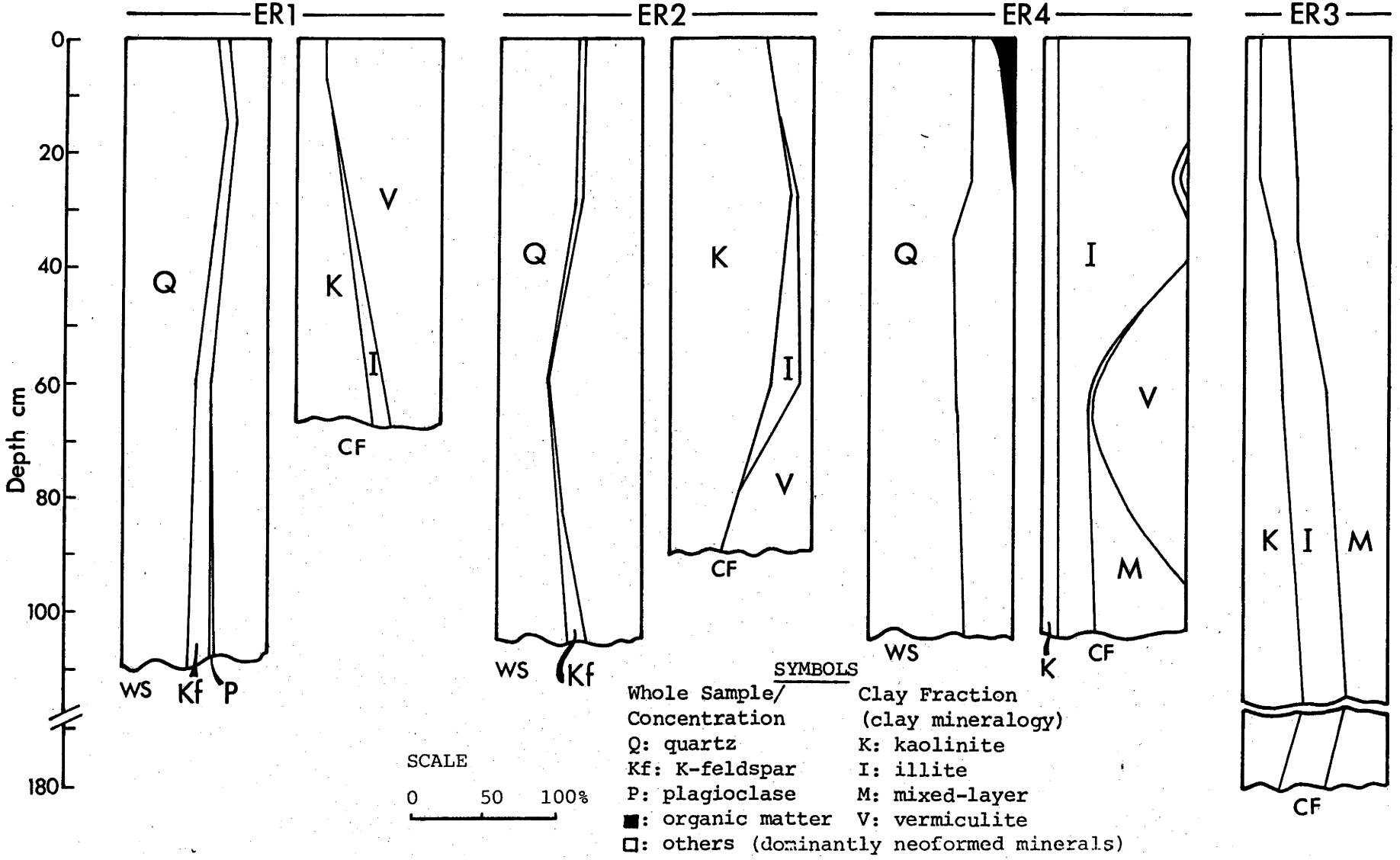

Figure 4.4 Depth dependent variation in mineralogy for profiles ER1, 2, 3, 4. Mineralogy is described for the whole sample (WS) and the clay fraction (CF, clay mineralogy).

Chemistry of Size Separates from Sample ER204

The analysis of the finer than 9ø, 8ø to 7ø, 7ø to 6ø and 0ø to -1ø fractions, which represent 76% of sample ER204 are given in Table 4.8 and illustrated in Figure 4.5.

$SiO_2+Al_2O_3+Fe_2O_3+H_2O+$ exceeds 98% in each of the size separates analysed. This is consistent with size separates consisting dominantly of quartz, clay minerals and minor iron oxide minerals. The enrichment of the clay fraction in all elements examined (except SiO_2 and C) is consistent with the concentration of clay minerals and iron oxide minerals in this fraction (Figure 4.3B). The concentration of SiO_2 in the other fractions is consistent with quartz being the dominant mineral in these fractions (Table 4.6).

Chemistry of Profiles ER1, 2 and 4

The chemistry of profiles ER1, 2 and 4 is given in Table 4.8 and the variation in relative concentration is plotted in Figure 4.6.

Compared with profiles ER1 and ER4, profile ER2 is enriched in Ti, Fe, Cr and Mn. The processes that have led to this enrichment are not understood. The possible occurrence of an extra-profile source of clay enriched in these elements, such as may be expected from the weathering of a basalt, is not supported by field observations.

The chemistry of profiles ER1, 2 and 4 is discussed with the aid of factor analysis. The correlation matrix and rotated factor matrix are given in Tables 4.9 and 4.10 respectively.

Factor I reflects: 1) the weathering of 'biotite' with the oxidation of FeO and the leaching of Mn and Zn; 2) the weathering of plagioclase and K-feldspar and the consequent loss through leaching of CaO, Na_2O, Sr and K_2O; and 3) the loss of P through the weathering of apatite.

Table 4.8 Chemistry of profiles ER1, 2, 4 and size separates from sample ER204.

Sample#	ER101	ER102	ER103	ER104	ER201	ER202	ER203	ER204	ER205
SiO_2	82.37	81.16	72.92	71.16	71.69	69.52	55.99	63.21	68.19
TiO_2	0.72	0.71	0.46	0.28	2.14	2.32	1.03	0.55	0.35
Al_2O_3	7.50	9.71	15.81	16.29	7.82	11.50	21.68	20.20	17.44
Fe_2O_3	1.33	1.48	1.46	2.19	5.18	8.16	7.74	4.99	3.59
FeO	<0.01	<0.01	0.09	0.06	<0.01	0.16	0.17	0.04	0.04
MnO	0.01	0.01	<0.01	<0.01	0.09	0.03	0.01	0.01	<0.01
MgO	0.64	0.65	0.73	0.70	0.80	0.73	0.94	0.80	0.71
CaO	0.06	0.05	0.02	0.04	0.30	0.11	0.09	0.05	0.03
Na_2O	0.19	0.19	0.18	0.30	0.12	0.14	0.06	0.06	0.22
K_2O	1.08	1.32	2.10	3.53	0.80	0.87	0.66	0.90	2.08
P_2O_5	0.02	0.02	0.02	0.02	0.03	0.03	0.02	0.02	0.01
S	<0.02	<0.02	<0.02	<0.02	<0.02	0.02	0.02	0.02	0.02
loss	6.32	5.17	6.45	5.71	11.55	7.00	12.00	9.07	7.75
H_2O-	0.90	0.95	1.17	0.82	4.17	1.17	2.25	1.65	1.31
C	1.78	0.71	0.33	0.69	1.81	0.67	0.45	0.21	0.01
rest	0.07	0.07	0.08	0.07	0.11	0.13	0.10	0.08	0.07
	100.32	100.55	100.33	100.36	100.64	100.71	100.50	99.99	100.49
Trace elements									
P	75	80	80	65	180	140	135	115	95
Rb	45	61	111	145	43	49	59	68	97
Sr	18	14	16	20	42	21	25	24	24
Pb	16	17	19	23	22	24	21	18	14
Zr	335	344	323	250	435	432	254	271	261
Y	38	43	48	47	33	29	31	45	46
V	28	32	33	22	121	180	159	92	42
Cr	10	11	12	8	78	110	92	44	19
Mn	61	53	27	12	655	135	42	27	17
Ni	<1	<1	2	<1	2	4	6	4	2
Cu	2	2	1	5	6	9	8	4	2
Zn	14	15	12	8	28	39	47	35	19

Sample#	ER401	ER402	ER403	ER404	ER405	ER204 <9ϕ	ER204 7,6ϕ	ER204 8,7ϕ	ER204 0,-1ϕ
SiO_2	77.08	80.60	73.82	77.77	78.33	39.60	90.76	90.50	95.40
TiO_2	0.37	0.36	0.29	0.25	0.26	0.59	0.46	0.39	0.14
Al_2O_3	6.80	8.56	14.75	13.56	13.06	32.81	5.22	5.29	2.28
Fe_2O_3	0.50	0.73	1.55	1.02	0.81	9.74	0.90	0.81	1.09
FeO	<0.01	<0.01	0.09	0.05	0.07	<0.01	<0.01	<0.01	<0.01
MnO	<0.01	<0.01	<0.01	<0.01	<0.01	0.01	<0.01	<0.01	<0.01
MgO	0.30	0.31	0.55	0.43	0.47	0.40	0.23	0.14	0.18
CaO	0.05	0.02	0.01	<0.01	0.01	0.06	0.02	0.01	0.02
Na_2O	0.07	0.06	0.06	0.06	0.05	0.06	0.06	0.05	0.04
K_2O	1.76	2.02	2.90	3.26	3.38	0.70	0.63	0.67	0.15
P_2O_5	0.02	0.03	0.03	0.03	0.02	0.04	<0.01	<0.01	0.01
S	<0.02	<0.02	<0.02	<0.02	<0.02	0.02	<0.01	<0.01	<0.01
loss	13.45	6.95	6.19	4.04	3.40	16.11	1.50	2.15	1.27
H_2O-	1.80	0.98	1.11	0.55	0.43	3.03	0.22	0.21	0.13
C	7.08	2.31	0.47	0.11	0.04	0.19	0.06	0.22	0.05
rest	0.06	0.07	0.07	0.06	0.07	0.11	0.03	0.02	0.01
	100.46	99.72	100.31	100.53	99.93	100.24	99.81	100.03	100.59
Trace elements									
P	105	110	140	105	80	190	30	15	20
Rb	98	121	163	161	170	84	31	32	8
Sr	31	23	29	22	22	37	8	8	2
Pb	18	28	54	48	19	29	4	3	5
Zr	262	288	230	200	221	205	70	59	67
Y	35	41	44	47	50	56	18	16	6
V	12	14	23	16	14	174	21	17	<1
Cr	11	8	12	10	10	82	15	12	<1
Mn	20	18	19	15	17	38	18	13	<1
Ni	<1	1	3	1	2	15	2	2	<1
Cu	2	3	<1	1	2	17	8	5	10
Zn	7	9	11	11	11	57	15	14	6

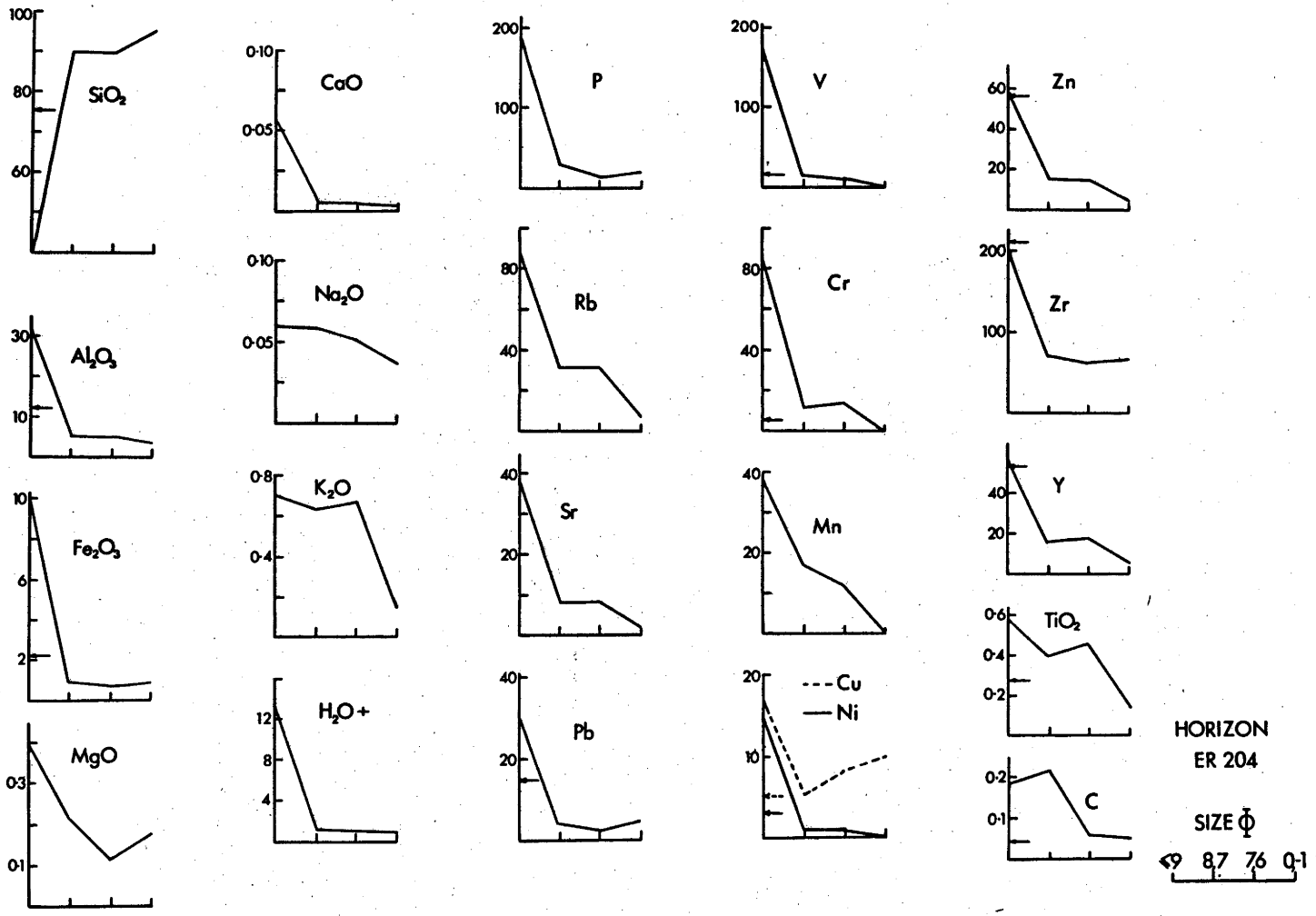

Figure 4.5 Size dependent variation in chemistry of size separates from sample ER204. Where the parent rock concentration occurs on scale it is indicated by an arrow.

Figure 4.6 Depth dependent variation in chemistry for profiles ER1,2,4. Except for C and H_2O+ element concentrations have been normalised (% loss or gain) with respect to the average parent rock concentration.

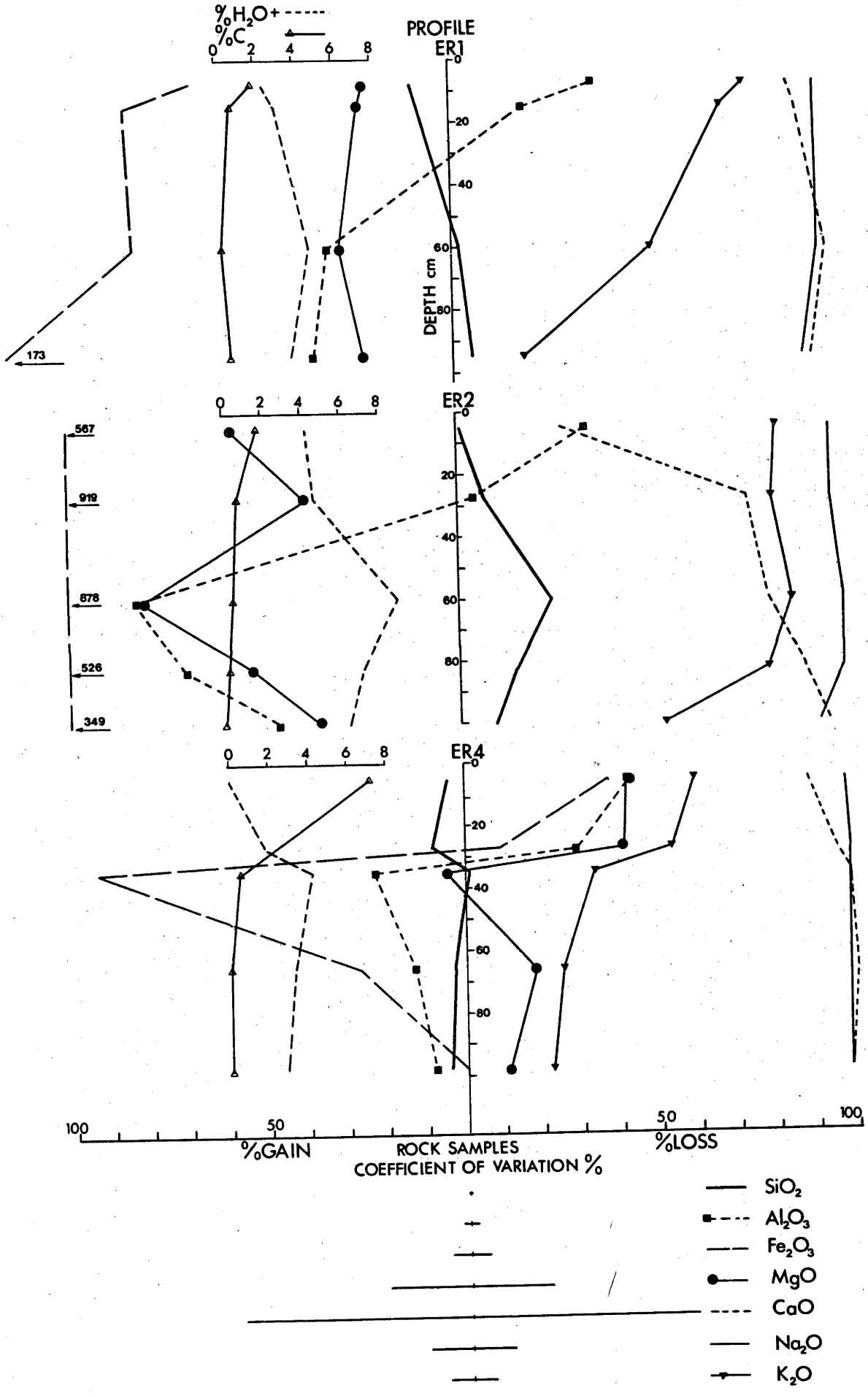

Figure 4.6 continued.

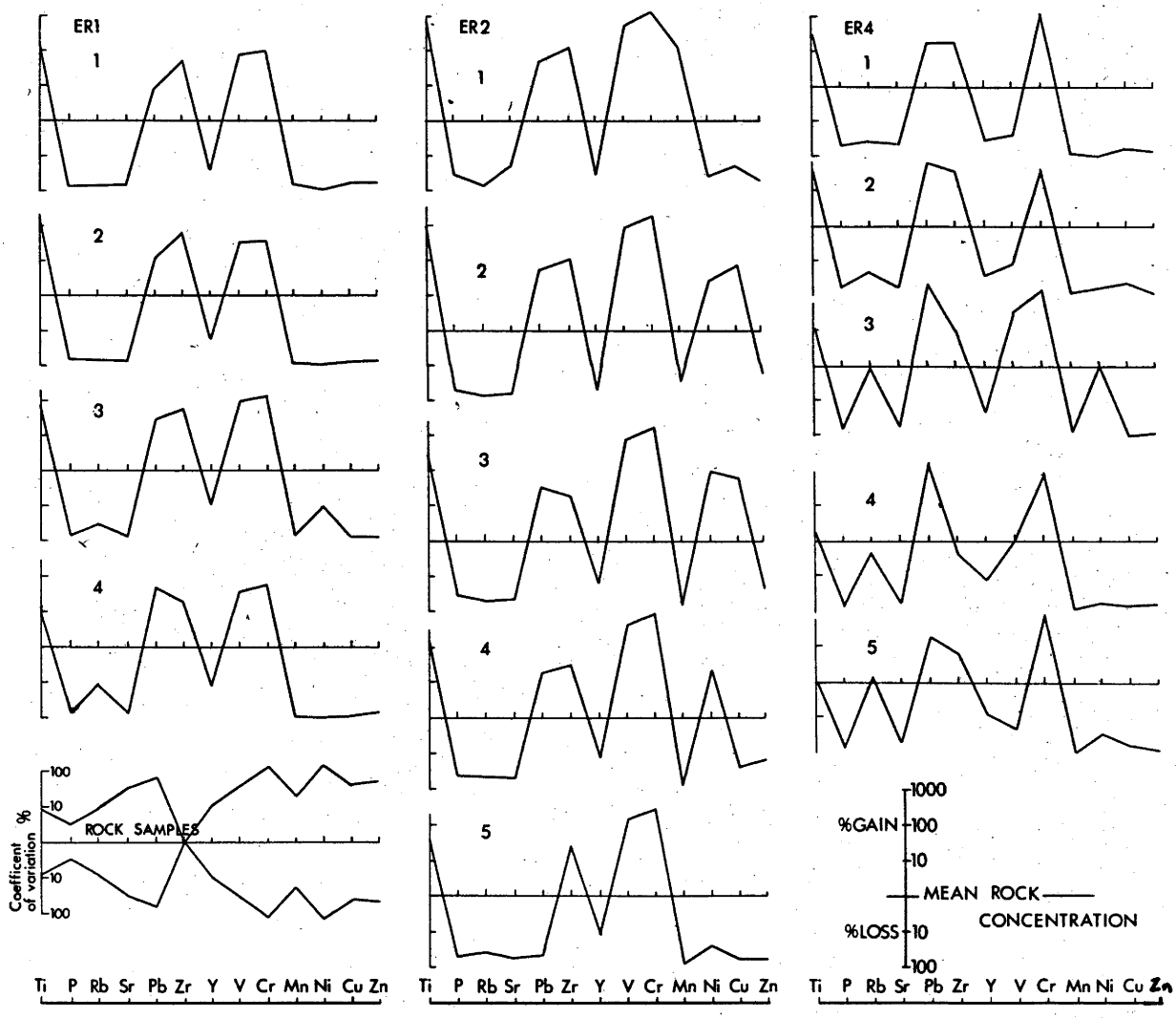

	TiO2	Al2O3	Fe2O3	FeO	MgO	CaO	Na2O	K2O	H2O+	C	P	Rb	Sr	Pb	Zr	Y	V	Cr	Mn	Zn	Qtz	Kspar	Plag	Clay
SiO2	-0.24	-0.85	-0.76	0.02	-0.70	0.01	0.10	0.28	-0.83	0.28	-0.03	0.24	0.01	0.06	0.01	0.22	-0.67	-0.62	0.04	-0.36	0.76	0.05	0.06	-0.67
TiO2	-	-0.17	0.77	-0.24	0.52	0.08	-0.28	-0.64	0.33	0.06	-0.02	-0.71	-0.06	-0.05	0.87	-0.72	0.85	0.88	0.53	0.18	0.00	-0.27	-0.28	0.27
Al2O3		-	0.44	-0.04	0.57	-0.18	-0.11	-0.03	0.79	-0.55	-0.11	0.06	-0.16	0.06	-0.32	0.13	0.31	0.23	-0.35	0.18	-0.69	-0.03	-0.07	0.60
Fe2O3			-	-0.25	0.76	-0.06	-0.33	-0.65	0.76	-0.16	-0.11	-0.66	-0.16	-0.05	0.55	-0.65	0.98	0.96	0.19	0.28	-0.41	-0.29	-0.30	0.61
FeO				-	-0.14	0.80	0.96	0.69	-0.41	-0.30	0.92	0.50	0.83	-0.25	-0.45	0.56	-0.21	-0.22	0.38	0.78	-0.55	0.93	0.97	-0.35
MgO					-	-0.02	-0.22	-0.52	0.81	-0.41	-0.11	-0.60	-0.13	-0.20	0.44	-0.37	0.72	0.66	0.21	0.34	-0.54	-0.08	-0.18	0.58
CaO						-	0.80	0.40	-0.33	-0.15	0.85	0.22	0.91	-0.19	-0.09	0.39	0.00	0.00	0.70	0.66	-0.45	0.75	0.78	-0.30
Na2O							-	0.72	-0.49	-0.27	0.91	0.51	0.77	-0.36	-0.43	0.64	-0.30	-0.32	0.40	0.63	-0.51	0.97	0.99	-0.44
K2O								-	-0.56	-0.30	0.55	0.93	0.49	0.05	-0.75	0.84	-0.68	-0.66	0.02	0.17	-0.24	0.69	0.71	-0.62
H2O+									-	-0.43	-0.36	-0.45	-0.38	0.10	0.23	-0.36	0.68	0.61	-0.15	0.06	-0.44	-0.41	-0.46	0.75
C										-	-0.21	-0.25	-0.06	-0.07	0.20	-0.46	-0.10	-0.03	-0.03	-0.33	0.54	-0.34	-0.28	-0.11
P											-	0.38	0.87	-0.19	-0.27	0.41	-0.04	-0.03	0.60	0.76	-0.54	0.85	0.92	-0.28
Rb												-	0.36	0.27	-0.81	0.78	-0.69	-0.66	-0.14	0.00	-0.12	0.44	0.50	-0.47
Sr													-	-0.07	-0.28	0.38	-0.11	-0.08	0.65	0.71	-0.43	0.72	0.78	-0.34
Pb														-	-0.14	-0.07	-0.05	0.00	-0.16	-0.28	0.27	-0.43	-0.35	0.14
Zr															-	-0.68	0.62	0.64	0.40	-0.11	0.26	-0.38	-0.45	0.20
Y																-	-0.71	-0.74	-0.03	0.07	-0.27	0.65	0.61	-0.42
V																	-	0.99	0.28	0.33	-0.34	-0.28	-0.28	0.61
Cr																		-	0.32	0.31	-0.28	-0.31	-0.29	0.56
Mn																			-	0.46	-0.22	0.38	0.38	-0.21
Zn																				-	-0.68	0.64	0.69	0.08
Quartz																					-	-0.58	-0.55	-0.27
K-feldspar																						-	0.97	-0.45
Plagioclase																							-	-0.40
Clay																								-

*P99.9= 0.72
*P99 = 0.61
*P95 = 0.48

*confidence limits cited ignore the constant sum effect in chemical analysis
N = 17

Table 4.9 Correlation matrix for samples from profiles ER1, 2, 4 and rocks ERR6, 7 and 8.

Table 4.10 Rotated factor matrix for samples from profiles ER1, 2, 4 and rocks ERR6, 7, and 8.
Graphic representation of the factor loadings is shown below.

	Factor					
Variable	I	II	III	IV	V	Communality
SiO2	-0.08	-0.21	-0.94	0.04	0.01	0.94
TiO2	0.03	0.98	0.02	0.04	0.07	0.96
Al2O3	-0.01	-0.21	0.94	0.23	0.02	0.99
Fe2O3	-0.04	0.75	0.63	0.00	0.02	0.94
FeO	0.93	-0.28	0.00	0.06	-0.09	0.96
MgO	-0.02	0.55	0.64	0.32	-0.22	0.89
CaO	0.91	0.08	-0.13	0.07	0.03	0.87
Na2O	0.90	-0.32	-0.11	0.11	-0.19	0.97
K2O	0.51	-0.73	-0.21	0.25	0.13	0.93
H2O+	-0.33	0.34	0.82	0.25	0.05	0.96
C	-0.20	0.13	-0.41	-0.83	-0.06	0.92
P	0.97	-0.07	-0.03	0.01	0.03	0.95
Rb	0.32	-0.81	-0.14	0.17	0.34	0.92
Sr	0.92	-0.05	-0.10	-0.09	0.16	0.91
Pb	-0.23	-0.10	0.00	0.03	0.93	0.94
Zr	-0.23	0.91	-0.20	0.09	-0.13	0.95
Y	0.37	-0.76	-0.11	0.43	-0.06	0.91
V	0.02	0.82	0.52	-0.04	0.05	0.96
Cr	0.03	0.84	0.46	-0.09	0.12	0.95
Mn	0.64	0.56	-0.26	0.18	0.08	0.83
Zn	0.82	0.17	0.34	-0.02	-0.11	0.83
Quartz	-0.59	0.04	-0.73	-0.22	0.16	0.95
K-feldspar	0.85	-0.30	-0.05	0.22	-0.32	0.97
Plagioclase	0.90	-0.32	-0.06	0.09	-0.20	0.97
Clay	-0.28	0.29	0.74	-0.17	0.08	0.75
Percent of variance explained	32.5	27.4	21.3	5.7	5.3	
Cumulative percent of variance	32.5	59.9	81.2	86.9	92.2	

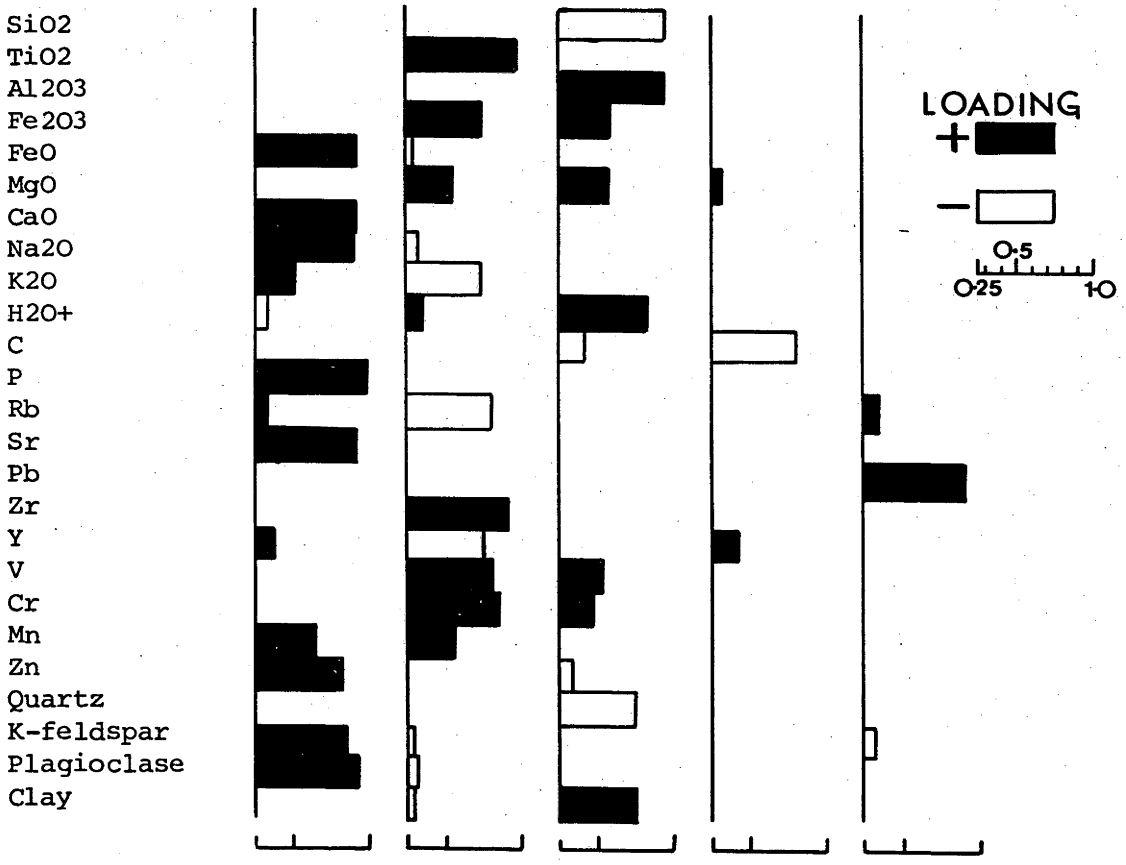

Factor II reflects: 1) the covariance of TiO_2 and Zr presumably as both TiO_2 and Zr are present in resistant accessory minerals which accumulate within the weathered residue; 2) variation in Fe_2O_3, MgO, H_2O+, V, Cr and to a lesser extent Mn. The association of this group of elements reflects their high concentration in profile ER2; 3) the distribution of K_2O and Rb. The high loading and correlation (0.93) is due to their concentration in K-feldspar; 4) at this stage no explanation can be offered to account for the behaviour of Y.

Factor III reflects: the contrasting behaviour of quartz (loading on quartz and SiO_2) and the neoformed minerals (loading on Al_2O_3, Fe_2O_3, MgO, H_2O+, V, Cr and clay). With particle size dependent fractionation in the surface horizon, these two mineral groups (quartz and neoformed minerals) are separated.

Factor IV and V are single element factors, loading on C and Pb respectively, reflecting their low correlation with other variables in the data set.

Thus much of the variation in chemistry is consistent with:
1) the weathering of susceptible minerals and consequent leaching of soluble salts and
2) the removal of the neoformed clay minerals from the surface horizon.

Much of the discussion developed from Figure 3.12 is based on those samples in which weathering has been isovolumetric. Isovolumetric changes in the rhyolite profiles can not be readily demonstrated. Consequently, there is no discussion of the mass per unit volume changes in chemistry for the rhyolite profiles.

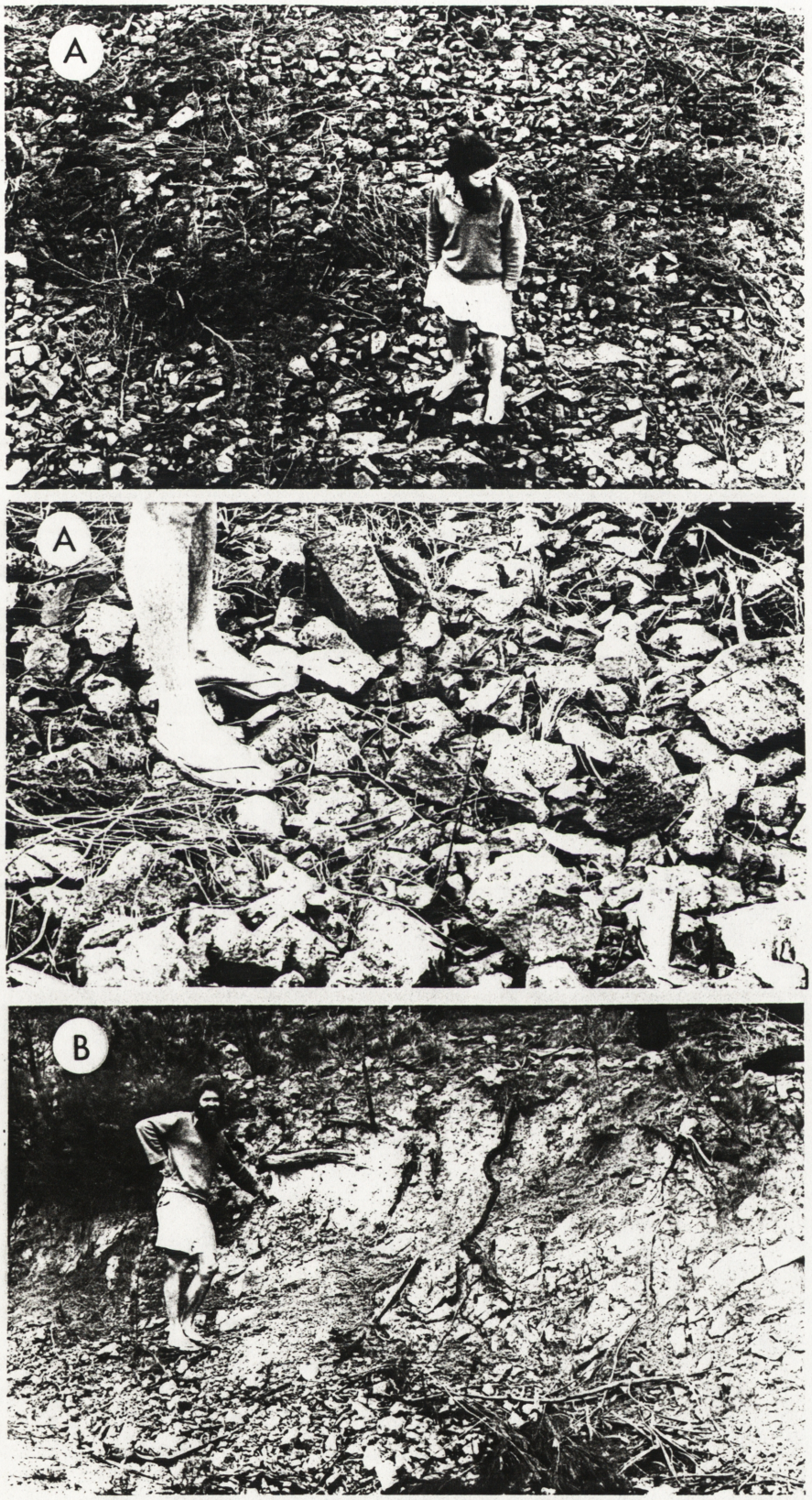

PLATE 3

A) Rubble field developed on the Eden Rhyolite.
Location: Round Hill Lookout (Kiah 8823-I-S 574794).

B) An example of the characteristically skeletal and stoney nature of weathering profiles developed on the Eden Rhyolite.
Location: Kiah 8823-I-S 572795.

CHAPTER 5

SURFICIAL MATERIALS DEVELOPED ON METASEDIMENTS

5.1 INTRODUCTION

The metasediments consist of a steeply dipping isoclinally folded sequence of interbedded sandstone, siltstone, phyllite (cleaved mudstone) and minor cherts. They form part of a flysch sequence of Ordovician age, which is considered to be relatively uniform in composition over much of southeastern Australia (Cas et al., 1980).

Individual beds may be up to several metres in thickness, but are often less than 1.5m thick.

The following discussion of the parent rock and its weathering, excludes cherts and associated silicified shales and those areas which have undergone contact metamorphism.

Due to incipient weathering of the sediments to depths exceeding 10m to 20m, exposures of unweathered metasediments do not occur in the area. The weathered rocks have a pale brown colour, and although still coherent, can be readily ground between hard surfaces. The depth of incipient weathering is probably due to the near vertical bedding and the strongly jointed and cleaved nature of the rock which facilitates the deep seepage of water.

Parent Rock

Mineralogy: X-ray diffraction analysis indicates that the incipiently weathered sediments consist dominantly of quartz and illite and trace proportions of kaolinite and feldspar. The proportion of quartz and illite varies with grain size; the coarser textured sandstones are enriched in quartz and depleted in illite compared with the finer textured mudstones.

Structure: Collins (1977) has recorded three phases of folding in the metasediments of the Eden area. The intensity of deformation was such that it produced tight, dominantly isoclinal folding

and resulted in some bedding transposition and the development of fracture and slaty cleavage. The cleavage is best developed in the finer grained rocks.

Regolith

Three profiles OR1, 2 and 3 are examined, (see Figure 2.2 for their locations). The profiles are described in Appendix B and the depths of the various samples are given in Table 5.1. A typical profile is illustrated in Plate 4.

Within each of the profiles sampled the lithology of the gravel-size particles is constant. This suggests that the composition of the source material from which the individual profiles were formed is relatively invariant. The gravel-size particles of profile OR1 consist of phyllite whereas those of profiles OR2 and OR3 consist of fine grained sandstone.

5.2 REGOLITH PARTICLE-SIZE

The particle-size distribution of profiles OR1, 2 and 3 is given in Table 5.2 and Figure 5.1. An examination of the data (Table 5.2) showed that there is no systematic variation in particle-size distribution between the profiles which could be attributed to differences in parent rock texture.

For convenience, the particle-size distributions are divided into two fractions, the clay and non-clay fractions.

Non-Clay Fraction

Although not recorded in the profiles examined, the upper size limit of particles in the non-clay fraction is 20cm to 30cm. Field observations suggest that particles intermediate in size between those sampled and those 20cm to 30cm in size form a continuum as represented in Figure 5.1C. The maximum particle-size is restricted by the ubiquitous presence of planes of low cohesion (e.g., fracture, cleavage, bedding planes) along which the rock mass readily separates.

Table 5.1 Sample depths for profiles OR1, 2, 3.

Sample	Depth (cm)
Profile OR1	
Parent Rock: phyllite	
1	0-2
2	3-5
3	7-10
4	25-30
5	100-110
Profile OR2	
Parent Rock: fine grained sandstone	
1	0-10
2	10-20
3	20-30

Sample	Depth (cm)
Profile OR3	
Parent Rock: fine grained sandstone	
1	0-7
2	7-12
3	12-18
4	22-30
5	80-90

SAMPLE NUMBER	SIZE (ϕ) <9	8	7	6	5	4	3	2	1	0	-1	-2	-3	-4	>-4
OR101	14.9	4.3	5.3	4.2	6.9	7.0	6.5	6.5	5.1	3.9	3.7	5.8	8.5	8.5	8.9
OR102	12.5	2.9	4.2	4.4	4.0	4.6	4.4	4.4	3.2	2.7	2.8	7.8	10.7	11.7	19.7
OR103	17.1	5.4	5.6	3.7	3.2	4.6	3.9	3.5	2.1	1.8	4.1	8.0	9.8	13.3	13.9
OR104	7.3	2.0	2.6	2.0	3.2	3.6	3.2	3.1	2.5	2.5	2.4	10.3	13.0	17.7	24.6
OR201	16.0	5.2	5.5	6.1	5.5	6.1	5.1	4.2	3.8	3.2	4.0	7.5	9.1	8.6	10.1
OR202	14.0	5.4	5.1	4.9	4.7	4.4	3.9	3.3	6.0	2.8	3.8	15.6	7.4	7.1	11.6
OR203	20.4	6.0	6.3	5.8	5.5	5.3	4.4	3.5	3.9	3.9	3.6	7.8	10.1	6.8	6.7
OR301	10.2	7.1	3.2	7.2	6.3	7.5	7.3	6.5	4.5	2.3	1.9	5.4	6.2	13.9	10.5
OR302	11.8	3.8	7.3	7.3	6.3	7.4	7.0	6.1	4.2	1.8	1.0	9.5	8.1	9.2	9.2
OR303	14.1	4.7	7.1	6.7	5.8	6.7	6.1	5.4	3.6	1.9	2.9	5.1	6.2	13.9	9.8
OR304	22.4	4.8	7.0	5.7	4.3	4.8	4.6	3.8	2.5	1.3	1.8	8.7	10.4	10.4	7.5
OR305	9.1	2.6	3.3	3.0	2.5	2.9	3.0	2.0	1.2	0.8	0.6	1.8	7.7	15.7	43.8

Table 5.2 Particle-size distribution of profiles OR1,2,3.

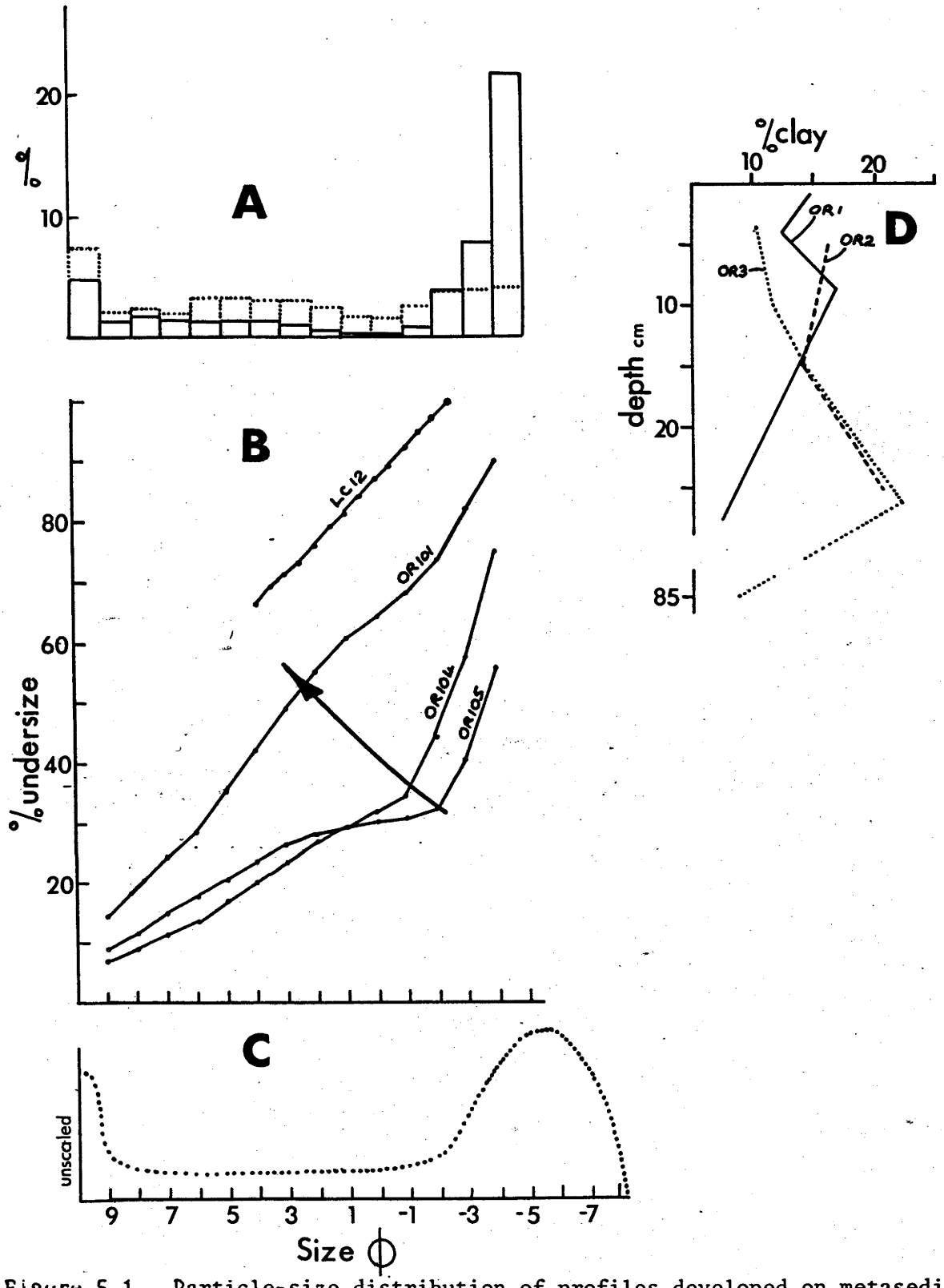

Figure 5.1 Particle-size distribution of profiles developed on metasediments.

A) Frequency distribution of samples OR305 (solid) and OR101 (dotted).

B) Cumulative frequency distribution of samples LC12, OR101, 104, and 105. The arrow indicates the direction of the progressive change in particle-size distribution with increasing weathering. LC12 is a partial analysis of a highly weathered sample from a profile developed on parent rock similar to that of profiles OR1, 2 and 3 (data from Hough, 1981).

C) Schematic distribution of the dominant particle-size modes developed in a metasediment landscape.

D) Depth dependent variation in clay content for profiles OR1 (solid), OR2 (dashed) and OR3 (dotted).

Figure 5.1C shows that a gravel-size (2-300mm) mode can be recognised. This mode is dominant in the less weathered samples examined (e.g., OR104 and OR105, Figure 5.1B). The tablet shape of the particles in this mode (Plate 4) suggests that its size distribution is controlled by the nature of the cleavage/bedding planes of the parent rock.

With weathering, as expressed by the decrease in mean particle-size, the magnitude of the gravel-size mode decreases and the non-clay fraction tends to become relatively uniform throughout the 2μm to 20/30cm range. This is illustrated by the change in histogram shape (Figure 5.1A*) and the decrease in the inflexion at 2mm as shown in Figure 5.1B.

Due to the presence of silt/sand size quartz in the parent rock it could have been expected that with the comminution of the gravel, a well defined silt or sand size mode would develop. For the samples examined, this does not appear to have happened. The absence of the silt/sand size mode could be a result of the following processes:

1) Weathering has not been of sufficient intensity to produce a well defined mode. This presumes that with further weathering the destruction of the gravel-size mode would result in the production of monomineralic particles whose size distribution would reflect the grain-size distribution of the parent rock.

2) A well defined mode may not in fact develop, but may remain spread over several size fractions. This could occur as a result of two processes:

i) In contrast to rhyolite and granite, where a considerable difference in the chemical stability exists between quartz and the dominant coexisting mineral (feldspar), the difference in stability between quartz and illite (the codominant minerals in metasediments)

---

* As described earlier, there is no discernable systematic variation between the profiles which could be attributed to differences in parent rock. Therefore, any supposition that sample OR305 should *per se* have a sand content greater than sample OR101 as a result of their respective parent rocks being sandstone and phyllite is not warranted. Further, this supposition would rest on the assumption that the geological classification of parent material is always relevant.

may be considerably less. Consequently the combined physical properties of both quartz and illite would determine the distribution of the particle-size mode.

ii) As the metasediments have undergone severe deformation, quartz, instead of consisting dominantly of relatively unstrained single grains, will consist, depending on the degree of deformation and recrystallisation, of strained or strain free mono- or poly-crystalline grains. Consequently with weathering, these quartz grains are unlikely to behave as coherent entities. Hence their fragmentation is likely to result in a diffuse particle-size mode not directly related to the grain size of the parent rock.

Clay Fraction

The high proportion and irregular distribution of gravel within the profiles makes the delineation of a persistent variation in clay content with depth difficult. The general tendency (Figure 5.1D) is for the clay content to increase up profile, and then to decrease in the near surface samples.

5.3 REGOLITH MINERALOGY

The mineralogy of the samples examined is given in Table 5.3 and is illustrated in Figure 5.2

Changes in profile mineralogy are buffered with respect to the parent rock concentration by the high proportion of gravel-size rock fragments within the profile. Thus the profiles consist dominantly of quartz and illite.

The up profile increase in quartz content (Figure 5.2) is attributed to the selective removal of clay which is, compared with the non-clay fraction, enriched in clay minerals and depleted in quartz.

The clay mineralogy (clay fraction, Figure 5.2) consists dominantly of illite (inherited from the parent rock) and lesser proportions of kaolinite, vermiculite and a 12Å mixed-layer clay mineral. There is a tendency with weathering for the 10Å illite peak to broaden, indicating the gradual loss of lattice K_2O (Reinson, 1973).

Table 5.3 Mineralogy of the whole sample and the clay fraction, determined by XRD[+] and IR[*] spectroscopy. Mineral proportions: ++, 20-40%; tr, trace; nd, not detected.

Sample Number	Mineralogy % Whole Sample				Clay Mineralogy %[+] Clay Fraction			
	Quartz[*]	K-feldspar[+]	Plagioclase[+]	Illite[+]	Å 14	12	10	7
OR101	55	nd	nd	++	10	tr	75	15
OR102	53	nd	nd	++	25	tr	70	5
OR103	48	nd	nd	++	10	10	75	10
OR104	36	nd	nd	++	10	5	75	10
OR105	35	nd	nd	++				
OR201					20	10	60	10
OR202					30	10	50	15
OR203					20	20	50	10
OR301	66	nd	nd	++	tr	tr	80	20
OR302	63	nd	nd	++	10	10	60	20
OR303	63	nd	nd	++	5	5	60	30
OR304	53	nd	nd	++	10	10	60	25
OR305	58	nd	nd	++	5	10	45	40

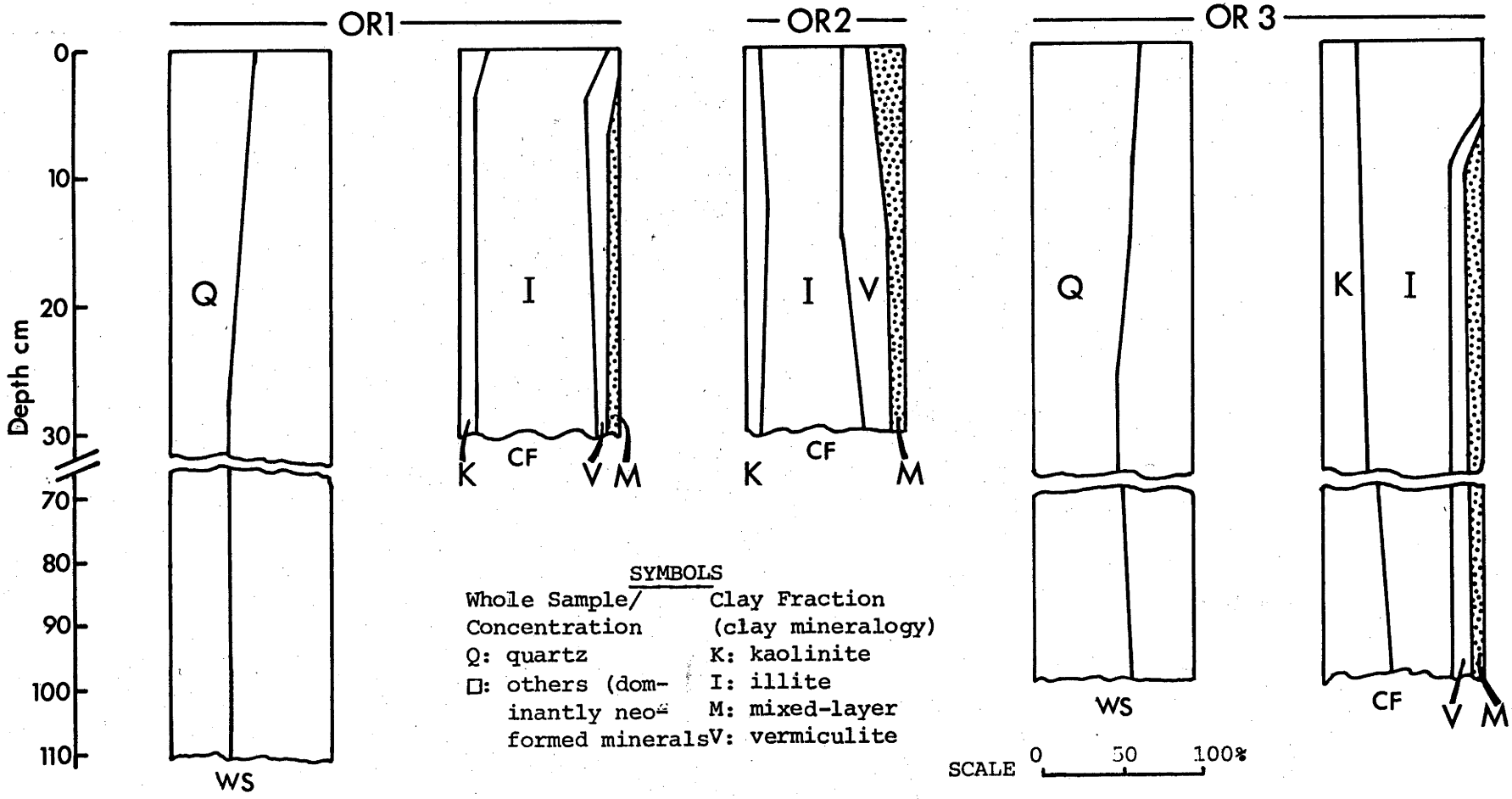

figure 5.2 Depth dependent variation in mineralogy for profiles OR1, 2, 3. Mineralogy is described for the whole sample (WS) and the clay fraction (CF, clay mineralogy).

5.4 REGOLITH CHEMISTRY

Parent Rock Chemistry

As stated in the introduction (Section 5.1) unweathered rock samples do not occur in the study area. Because of the relative uniformity of the Ordovician flysch sequence over much of southeastern Australia (Cas et al., 1980) analysis of typical Ordovician flysch given by Wyborn and Chappell (1983) (Table 5.4) can be considered to be indicative of the composition of the rocks in the study area prior to weathering.

Wyborn and Chappell (1983) found that the chemistry of the flysch was consistent with original detrital mineralogy consisting dominantly of illite and quartz.

In order to compare the least weathered samples from profiles OR1 and OR3 (OR105 and 305 respectively) (Table 5.5) with analyses of Wyborn and Chappell (1983), those elements which are codominant (Al_2O_3 and SiO_2) and those which are concentrated in illite (Al_2O_3, K_2O and Rb) are used (Figure 5.3). Figure 5.3 shows that relative to the unweathered equivalents, OR105 and 305 are depleted in K_2O and Rb and have similar SiO_2/Al_2O_3 concentrations. This is consistent with OR105 and 305 representing the leached equivalents of the rocks analysed by Wyborn and Chappell (1983). Relative to Al_2O_3, K_2O and Rb are lost with the leaching of illite. Leaching however, would cause little change in the relative concentration of SiO_2 and Al_2O_3.

Table 5.4 Chemistry of Ordovician flysch of the Snowy Mountains Region (from Wyborn and Chappell, 1983).

Sample	LW103	LW101	LW 99	LW104	LW 96	LW 98	LW105	LW 95	LW100	LW102	LW113
SiO_2 (%)	61.17	64.26	64.31	67.70	69.28	71.32	72.73	74.13	74.46	74.60	74.64
TiO_2	0.89	0.74	0.89	0.81	0.74	0.58	0.70	0.76	0.73	0.61	0.68
Al_2O_3	19.43	17.45	17.26	16.60	14.39	12.48	13.19	12.28	12.26	12.06	12.10
Fe_2O_3	1.77	1.59	2.47	1.25	2.06	1.57	0.53	1.94	2.02	1.33	1.03
FeO	4.16	3.90	3.05	3.03	3.11	3.77	3.57	1.96	1.60	2.52	2.52
MnO	0.05	0.05	0.06	0.03	0.05	0.11	0.05	0.03	0.03	0.04	0.06
MgO	2.64	2.44	2.30	1.83	2.57	2.56	1.76	1.72	1.55	1.49	1.82
CaO	0.17	0.33	0.04	0.19	0.09	0.66	0.78	0.19	0.07	0.75	0.17
Na_2O	0.58	0.50	0.19	0.40	0.11	1.26	1.33	0.14	0.52	1.85	0.21
K_2O	5.37	5.51	5.61	4.94	3.84	2.53	3.26	3.91	2.97	2.80	3.80
P_2O_5	0.17	0.16	0.13	0.16	0.13	0.13	0.12	0.17	0.38	0.15	0.16
S	<0.02	<0.02	<0.02	<0.02	<0.02	0.13	0.05	<0.02	<0.02	<0.02	<0.02
H_2O+	3.19	2.64	2.93	2.73	3.01	2.46	1.56	2.19	2.63	1.46	2.29
H_2O-	0.28	0.19	0.50	0.25	0.32	0.19	0.12	0.35	0.61	0.15	0.31
CO_2	0.10	0.02	0.06	0.01	0.06	0.32	0.20	0.07	0.01	0.01	0.01
rest	0.23	0.22	0.26	0.30	0.18	0.13	0.17	0.19	0.20	0.17	0.13
O = S						100.25 0.06	100.04 0.01				
Total	100.20	100.00	100.05	100.23	99.94	100.19	100.03	100.03	100.04	99.99	99.98
Ba(ppm)	740	630	1075	1440	585	475	435	580	580	370	570
Rb	253	271	272	229	169	109	172	199	115	164	177
Sr	28.0	44.0	37.0	38.0	32.0	145	107	19.0	33.0	107	53
Pb	14	17	13	8	16	11	27	9	15	23	11
Th	25.4	23.0	24.6	29.4	20.0	17.0	23.2	23.2	22.2	24.4	20.4
U	4.4	3.6	3.0	4.6	2.8	2.0	3.2	3.4	3.6	3.4	3.0
Zr	184	170	200	252	177	129	238	288	293	264	209
Nb	18.0	15.0	18.0	16.0	15.0	10.0	15.0	15.0	14.0	12.0	14.0
Y	33	26	27	33	28	21	30	30	50	39	33
La	38	25	28	43	24	32	33	20	37	40	38
Ce	87	84	59	101	20	74	77	43	85	84	87
Nd	31	30	22	34	26	26	26	21	39	32	32
Sc	22	18	19	17	15	14	10	12	12	11	11
V	114	98	108	90	82	80	54	63	62	55	61
Cr	99	79	128	74	96	84	46	90	86	47	70
Co	17	17	8	13	11	17	12	7	10	12	4
Ni	39	40	41	26	34	38	21	23	29	22	14
Cu	9	53	11	1	22	104	10	10	12	19	24
Zn	106	108	82	77	104	86	75	66	70	76	53
Ga	26.0	24.0	24.0	21.0	19.0	16.0	16.0	14.0	15.0	15.0	15.0

Figure 5.3 Comparison of OR105 and OR305 with analyses of unweathered Ordovician rocks (●) from Wyborn and Chappell (1983) (Table 5.4).

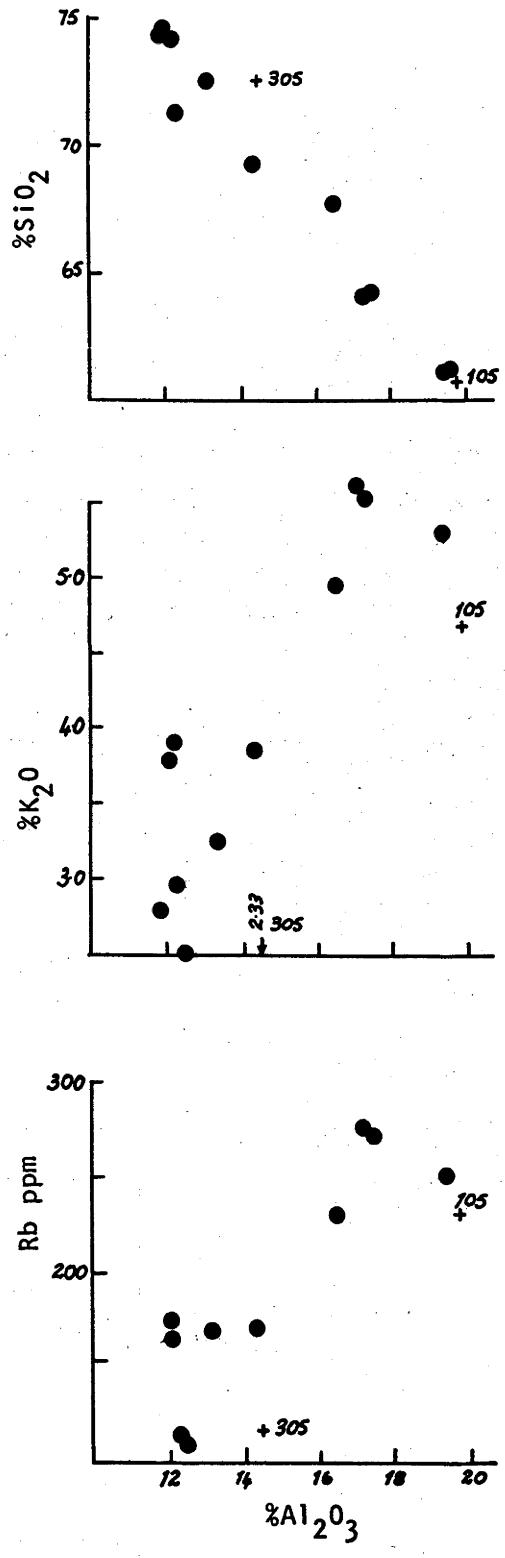

A Summary of Various Chemical Features of the Profiles

1) The combined concentration of SiO_2+, Al_2O_3 + K_2O + H_2O+ exceeds 95% (Table 5.5). In general, the depth dependent trends of the various elements for the two profiles (OR1 and OR3) parallel each other (Figure 5.4).

2) Although the profiles are qualitatively similar, the quantitative chemical differences are sufficient (Figure 5.5) to warrant the calculation of a separate correlation matrix for each profile (Table 5.6). The high correlation which exists between quartz-Al_2O_3, K_2O-Al_2O_3 and K_2O-Rb (Figure 5, 6A, B, C) indicates that the gross variation in chemistry is determined by the varying proportions of two end members: a SiO_2 end member (quartz) and a Al_2O_3- K_2O -Rb end member (illite). The codominance of quartz and illite is consistent with the profile and parent rock mineralogy.

3) The variation in profile chemistry (i.e., the relative proportion of quartz and illite) is attributed dominantly to physical processes. Illite, because of its '001' cleavage is, compared with quartz, concentrated in the clay fraction. As a consequence of this size differentiation, when clay loss occurs, the residium is enriched in quartz. This gives rise to the correlations described in Figure 5.5A, B, C.

The variation in the clay/H_2O+ plot (Figure 5.5D) is consistent with physical processes being the major determinant of changes in profile chemistry. If the generation of the clay mineral rich clay fraction were dependent on chemical weathering then a positive correlation between clay content and H_2O+ would be expected. From Figure 5.5D it is clear that this does not occur. If, as proposed above, the generation of the clay fraction is a physical process, then it would be expected that the clay content would increase independently of H_2O+ with weathering. This is shown by the change in clay content between samples OR105, 104 and OR305, 304 (Figure 5.5D).

Thus the variation in clay/H_2O+ content for samples OR104 to 101 and OR304 to 301 is consistent with the following two processes occurring contemporaneously:

Sample#	OR101	OR102	OR103	OR104	OR105	OR301	OR302	OR303	OR304	OR305
SiO_2	68.94	69.51	66.49	59.63	60.51	75.64	77.08	78.87	68.79	71.33
TiO_2	0.67	0.82	0.84	0.80	0.76	0.73	0.77	0.78	0.69	0.59
Al_2O_3	10.09	12.32	14.26	19.13	19.99	8.73	9.10	9.76	15.39	14.40
Fe_2O_3	4.72	5.98	7.75	7.27	6.21	3.57	3.65	2.62	4.50	3.99
FeO	<0.01	0.18	0.15	0.25	0.27	<0.01	<0.01	0.07	0.08	0.12
MnO	0.04	0.01	0.01	0.01	0.01	0.03	0.02	0.01	0.01	0.01
MgO	0.91	1.05	1.14	1.35	1.37	0.62	0.44	0.51	0.65	0.46
CaO	0.22	0.07	0.05	0.04	0.02	0.10	0.08	0.06	0.05	0.05
Na_2O	0.11	0.11	0.12	0.22	0.20	0.20	0.18	0.20	0.21	0.45
K_2O	2.04	2.60	3.04	4.30	4.66	1.83	1.83	2.12	2.59	2.33
P_2O_5	0.07	0.07	0.09	0.05	0.09	0.02	0.02	0.02	0.01	0.02
S	0.02	<0.02	<0.02	0.02	0.02	<0.02	<0.02	<0.02	<0.02	<0.02
loss	12.20	7.73	6.44	7.11	5.96	8.01	6.38	5.18	7.01	6.40
H_2O-	1.16	1.02	0.82	0.73	0.43	1.51	0.97	0.80	1.11	1.50
C	4.95	1.95	1.36	0.77	0.10	2.55	1.50	0.89	0.46	0.15
rest	0.09	0.10	0.10	0.11	0.11	0.08	0.08	0.08	0.09	0.08
	100.11	100.56	100.49	100.28	100.17	99.57	99.64	100.28	100.07	100.23
Trace elements										
P	430	350	345	445	465	115	105	85	85	80
Rb	114	151	172	201	229	106	107	117	155	117
Sr	53	36	40	46	30	28	25	24	25	24
Pb	23	27	31	36	31	30	33	27	31	36
Zr	294	288	265	202	167	267	266	278	220	227
Y	32	37	40	34	38	34	36	37	32	30
V	61	78	88	109	110	56	58	57	84	70
Cr	62	75	85	107	110	54	55	54	78	68
Mn	283	132	46	42	31	220	137	57	37	50
Ni	7	8	8	12	16	4	3	4	9	9
Cu	<1	2	15	18	25	9	10	11	15	23
Zn	34	33	43	57	73	19	16	14	23	34

Table 5.5 Chemistry of profiles OR1 and OR3.

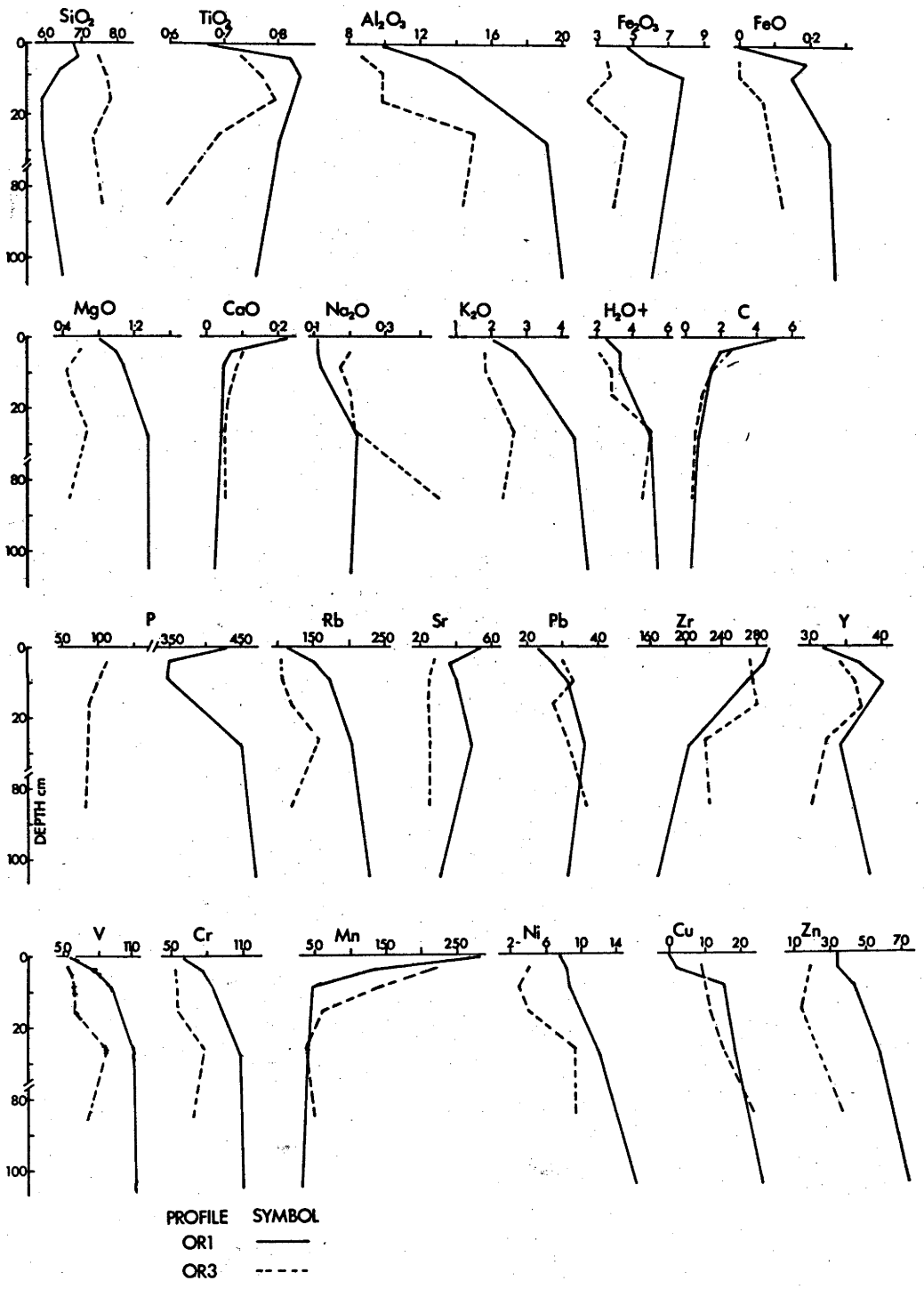

Figure 5.4 Depth dependent variation in chemistry for profiles OR1 and 3.

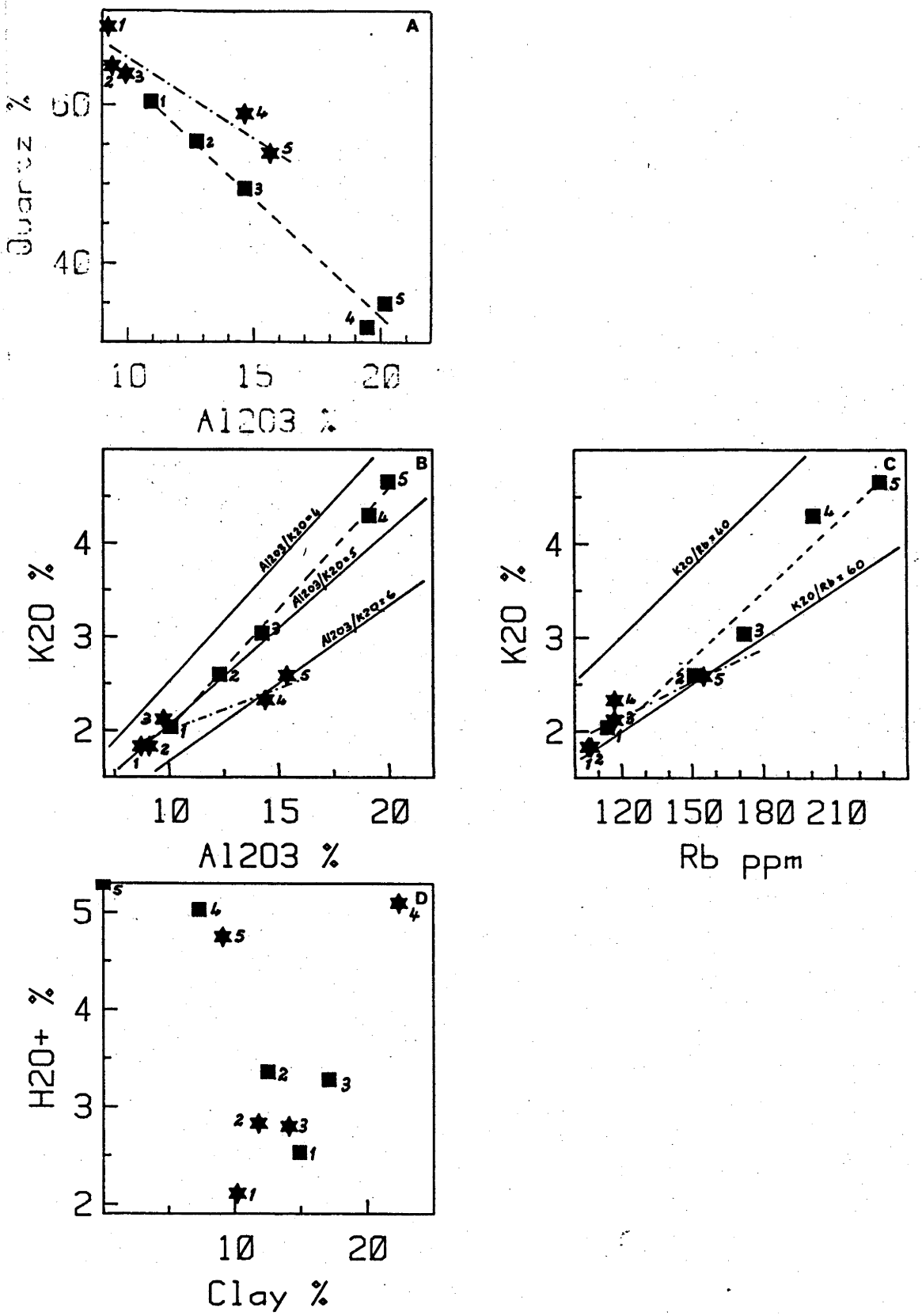

Figure 5.5 Scatterplots of chemical and mineralogical features of profiles OR1 (■) and OR3 (✱). Lines of best fit are shown dashed. The K_2O/Rb ratio is calculated for K_2O (%) and Rb (ppm).

	TiO2	Al2O3	Fe2O3	FeO	MgO	CaO	Na2O	K2O	H2O+	C	P	Rb	Sr	Pb	Zr	Y	V	Cr	Mn	Ni	Cu	Zn	Qtz	Clay
SiO2		-0.96 -0.92	-0.91						-0.94 -0.88			-0.89			0.95 0.98	0.88	-0.93 -0.93	-0.95 -0.96		-0.88 -0.93	-0.89	-0.92	0.99 0.88	
TiO2							-0.91									0.97					-0.93	-0.99		
Al2O3				0.90	0.99		0.94	0.99 0.95	0.98 0.99	-0.88		0.98			-0.98 -0.96		0.99 0.95	0.99 0.97		0.92 0.98	0.94		-0.96	
Fe2O3										-0.97	0.93				-0.88									
FeO					0.93	-0.95 -0.91		0.91	-0.97	0.93 -0.91	-0.95						0.94	0.91	-0.91		0.88			
MgO							0.92	0.99	0.97	-0.91		0.98		0.89	-0.95		0.99	0.99	-0.88	0.89	0.94	0.91	-0.98	
CaO								-0.88		0.99 0.99	0.98	-0.88							0.98 0.99					
Na2O								0.94	0.95						-0.93		0.90	0.92			0.94	0.88 0.92	-0.97	
K2O									0.99 0.94			0.98 0.90			-0.98		0.98 0.92	0.99 0.92		0.94 0.91	0.94	0.96	-0.99 -0.95	
H2O+												0.95			-0.97 -0.94		0.96 0.94	0.98 0.96		0.95 0.94		0.92	-0.97 -0.97	-0.90
C											0.97	-0.94	0.88				-0.93	-0.90 0.97	0.98					
P																			0.97					
Rb															-0.95		0.97 0.92	0.98 0.88	-0.90	0.92	0.96	0.93	-0.95 -0.91	0.91
Sr																			0.89					
Pb																	0.91		-0.88					
Zr																0.90	-0.93 -0.93	-0.96 -0.96		-0.98	-0.93	-0.99	0.98 0.90	0.92
Y																				-0.89		-0.96		
V																		0.99 0.99	-0.90	0.87 0.89	0.93	0.89	-0.97 -0.97	
Cr																			-0.87	0.90 0.93	0.94	0.93	-0.99 -0.97	
Mn																								
Ni																						0.98	-0.92 -0.88	-0.97
Cu																						0.94 0.94	-0.93	
Zn																							-0.95	-0.91
Quartz																								
Clay																								

Table 5.6 Correlation matrix for samples from profiles OR1 (upper figure) and OR3 (lower Figure). P_{99}=0.95, P_{95}=0.88 (confidence limits cited ignore the constant sum effect in chemical analyses).

i) further physical weathering, which results in the clay content increasing independently of H_2O+; and
ii) clay loss, which results in a concomitant decrease in H_2O+ and clay.

4) The effect of chemical processes on chemistry, although subsidiary to physical processes, is evident. This is shown by the decrease in the K_2O/Al_2O_3, and K_2O/Rb ratios with decreasing K_2O concentration (Figure 5.6B, C). These changes in element ratios, with decreasing K_2O concentration are consistent with the leaching of illite and its subsequent transformation to kaolinite (Wedepohl, 1978).

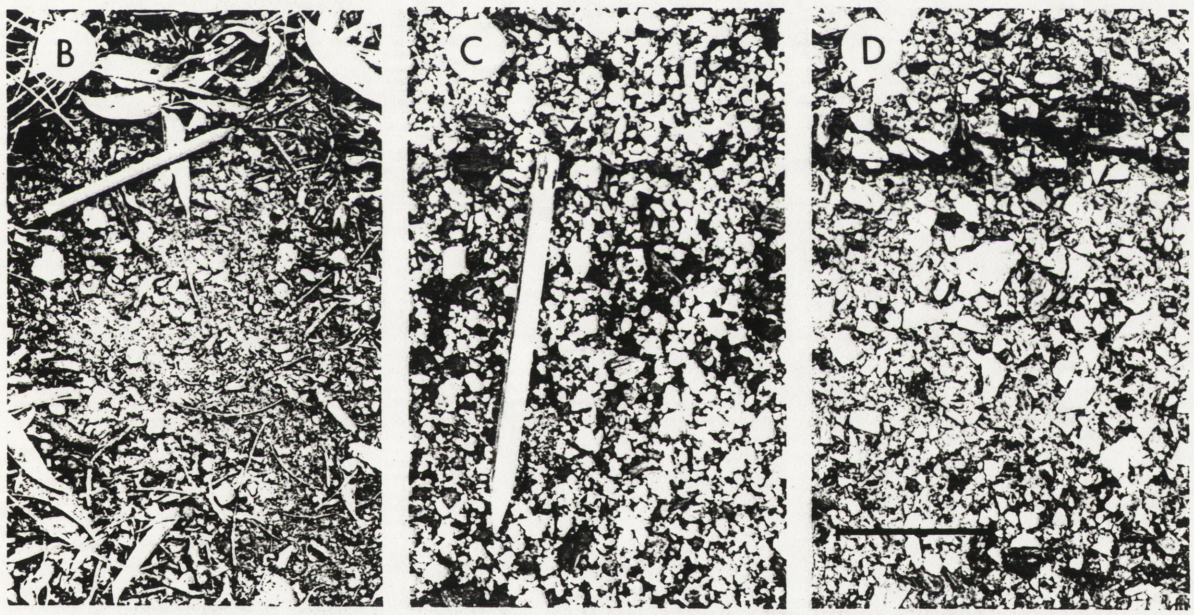

PLATE 4

A) An example of a weathering profile developed on metasediments as displayed in a road cutting. (Parent material: phyllite).

B,C,D) These plates show the occurrence of tablet shaped cleavage fragments at the regolith surface. Plate B is an undisturbed regolith surface, the litter layer has been cleared for the photo. Plates C and D are disturbed regolith surfaces. The bar in Plate D is 20cm long.
Location: Narrabarba 8823-II-N 491702.

CHAPTER 6

SURFICIAL MATERIALS DEVELOPED ON DEVONIAN SEDIMENTS

6.1 INTRODUCTION

Three profiles have been examined (profile descriptions are given in Appendix B, and sample depths in Table 6.1; various profiles are illustrated in Plate 5). Profiles SS1 and SS3 are developed on sandstone. Their particle-size, mineralogy and chemistry (Tables 6.2, 6.3 and 6.4 respectively) are considered in detail.

Profile SS2 is not examined in detail; discussion of its characteristics is considered to the extent that they contribute to the understanding of texturally differentiated profiles.

Parent Rock of Profiles SS1 and SS3

The rocks (SSR1, 2) sampled as representative of the parent rock were not vertically contiguous with the weathering profiles, as weathering profiles are usually truncated by changes in rock type. The rock samples occur stratigraphically within 2m of the material from which the profiles were derived and were deposited under fluvial condition which commonly produce individual beds <1m thick (Steiner, 1966).

The parent rock is a well sorted, medium grained and even textured sandstone. The framework grains consist of quartz and illite (codominant) and partially altered feldspar. The matrix/cement consists of illite and kaolinite. The mineralogy and chemistry of SSR1 and 2 is given in Tables 6.3 and 6.4 respectively. The parent rock varies from poorly to well cemented. The collection of data, to determine whether the variation in cementation is due to near-surface or diagenetic processes, is outside the scope of this thesis.

Rock fabric and structural features likely to affect weathering are: i) primary sedimentary features such as bedding and foreset planes; and ii) joint planes which are usually 20cm to 100cm apart, except in areas of localised fold development.

Table 6.1 Sample depths for profiles SS1, 2, 3.

Sample	Depth (cm)	Sample	Depth (cm)
Profile SS1		Profile SS3	
SS101	0-3	SS301	0-10
SS102	20-25	SS302	40-50
SS103	32-35	SS303	80-90
SS104	40-50		
Profile SS2			
SS201	0-15		
SS202	20-25		

Table 6.2 Particle-size distribution of profiles SS1, 2, 3.

Sample	Size ϕ														
	<9	8	7	6	5	4	3	2	1	0	-1	-2	-3	-4	>-4
SS101	7.2	1.7	1.9	2.2	2.9	4.5	5.3	9.8	29.5	31.3	3.7	0.0	0.0	0.0	0.0
SS102	8.1	1.7	2.1	2.5	2.9	3.5	4.8	9.7	29.5	32.1	3.1	0.0	0.0	0.0	0.0
SS103	7.7	1.0	0.8	1.1	2.0	3.3	4.6	9.2	27.0	37.1	5.4	0.8	0.0	0.0	0.0
SS104	9.3	2.5	1.9	2.6	2.8	3.9	5.5	9.4	25.9	31.4	3.9	0.8	0.0	0.0	0.0
SS201	7.7	2.2	3.0	4.5	6.6	6.6	11.6	22.9	18.3	13.8	2.8	0.0	0.0	0.0	0.0
SS202	31.1	3.6	2.9	2.9	3.4	3.5	6.5	11.4	10.7	17.9	6.1	0.0	0.0	0.0	0.0
SS301	3.8	1.2	2.3	2.8	3.6	4.0	3.5	10.2	33.9	28.6	5.8	0.3	0.0	0.0	0.0
SS302	4.0	1.2	1.8	2.5	3.8	4.6	4.8	11.0	29.3	25.9	8.1	3.0	0.0	0.0	0.0
SS303	4.6	1.1	2.3	2.9	4.2	4.9	4.1	10.1	26.5	25.4	9.9	4.0	0.0	0.0	0.0

Table 6.3 Mineralogy of profiles SS1 and 3 and rocks SSR1 and 2. '++' indicates a concentration of 20-40%.

Sample Number	Mineralogy % Bulk Sample				Clay Mineralogy % Clay Fraction			
					Å			
	Quartz	K-feldspar	Plagioclase	Illite	14	12	10	7
SS101	80	nd	nd	nd	nd	15	70	15
SS102	78	nd	nd	nd	nd	10	80	10
SS103	66	nd	nd	++	nd	nd	70	30
SS104	70	nd	nd	++	nd	nd	70	30
SS301	79	nd	nd	nd	nd	nd	60	40
SS302	90	nd	nd	nd	nd	nd	50	50
SS303	90	nd	nd	nd	nd	nd	85	15
*SSR1	66	tr	nd	++				
*SSR2	77	tr	nd	++				

* Kaolinite was the only clay mineral other than illite to be detected.

Sample#	SS101	SS102	SS103	SS104	SS301	SS302	SS303	SSR1	SSR2
SiO_2	90.67	93.38	75.25	83.64	83.06	95.31	96.16	81.87	92.46
TiO_2	0.13	0.14	0.16	0.10	0.20	0.18	0.33	0.12	0.05
Al_2O_3	1.39	1.64	7.64	8.96	1.08	0.33	0.60	10.82	3.99
Fe_2O_3	0.16	0.18	1.64	1.29	0.07	0.07	0.15	0.92	0.56
FeO	<0.01	<0.01	<0.01	0.07	<0.01	<0.01	<0.01	0.10	0.07
MnO	<0.01	<0.01	<0.01	0.01	<0.01	<0.01	<0.01	<0.01	<0.01
MgO	0.55	0.55	0.72	0.85	<0.05	<0.05	<0.05	0.58	0.20
CaO	0.03	0.02	0.04	0.01	0.05	<0.01	<0.01	0.01	0.02
Na_2O	0.02	0.01	0.02	0.03	0.02	0.01	0.01	0.04	0.03
K_2O	0.28	0.33	1.09	1.97	0.11	0.06	0.54	2.77	1.85
P_2O_5	0.01	<0.01	0.01	<0.01	<0.01	<0.01	0.01	0.03	0.05
S	<0.02	<0.02	0.03	0.02	0.02	<0.02	0.30	0.09	0.30
loss	7.10	3.48	13.65	3.35	15.27	3.80	2.06	3.06	1.10
H_2O-	0.45	0.30	2.29	0.42	1.20	0.27	0.20	0.56	0.16
C	3.50	1.47	3.00	0.26	8.57	2.12	1.01	0.19	0.05
rest	0.02	0.02	0.04	0.03	0.02	0.02	0.03	0.04	0.02
	100.36	99.76	100.28	100.32	99.92	99.82	100.06	100.41	100.55
Trace elements									
P	50	40	105	40	55	15	35	165	225
Rb	18	20	62	94	3	1	6	130	59
Sr	8	5	7	6	13	4	9	31	62
Pb	2	1	7	6	2	1	2	7	2
Zr	115	111	97	70	132	120	159	56	38
Y	10	10	11	13	9	8	10	13	10
V	6	7	48	22	3	3	10	16	7
Cr	10	12	25	19	9	7	12	22	9
Mn	11	9	16	23	9	5	7	29	13
Ni	<1	<1	2	4	<1	<1	<1	5	<1
Cu	1	<1	<1	<1	<1	<1	1	1	1
Zn	16	4	12	19	<1	<1	1	26	10

Table 6.4 Chemistry of profiles SS1,3 and rocks SSR1,2.

6.2 REGOLITH PARTICLE-SIZE

Particle-Size Distribution of Profiles SS1 and SS3

The particle-size distribution of profiles SS1 and SS3 is given in Table 6.2. The size distribution of selected samples is illustrated in Figure 6.1. Particles larger than those recorded in profiles SS1 and SS3 do not occur in the immediate landscape.

The characteristics of the samples and profiles are as follows:

1) The samples have a single well defined mode. This mode persists throughout the profile (Table 6.2) and corresponds to the size distribution of framework grains in the parent rock (Figure 6.1A).

2) The clay concentration is low (< 10%) and relatively uniform throughout both profiles.

3) A remarkable similarity exists between the cumulative frequency histograms (Figure 6.1B) and the size distribution of fluvial sands as would be predicted from the work of Visher (1969). It should be noted that the fluvial origin of the parent rock was established by Steiner (1966) using hierarchically more diagnostic sedimentary attributes (Allen, 1967) than particle-size frequency characteristics (e.g., Visher 'curves'). The similarity described above, suggests that diagenetic, deformational and weathering processes have not been of sufficient intensity to destroy the signature of the fluvial conditions under which the sandstone was deposited $\approx 360 \times 10^6$ years ago. This is consistent with:

i) optical observations. These showed that most of the quartz framework grains are released from the parent rock with their original shape intact, viz., fragmentation is preferentially intergranular.

ii) the quartz content of the parent rock. It is sufficiently high that even with destruction of the labile minerals the residual quartz grains still retain the fluvial signature of the parent rock.

Particle-Size Distribution of Profile SS2

The particle-size distribution of profile SS2 is given in Table 6.2 and plotted in Figure 6.1C. Samples 201 and 202 differ in:

1) Their clay content, 8% and 31% respectively. This results in a spatially rapid textural differentiation.

2) The size of the sand size modes, 2.5ø and 0.5ø respectively.

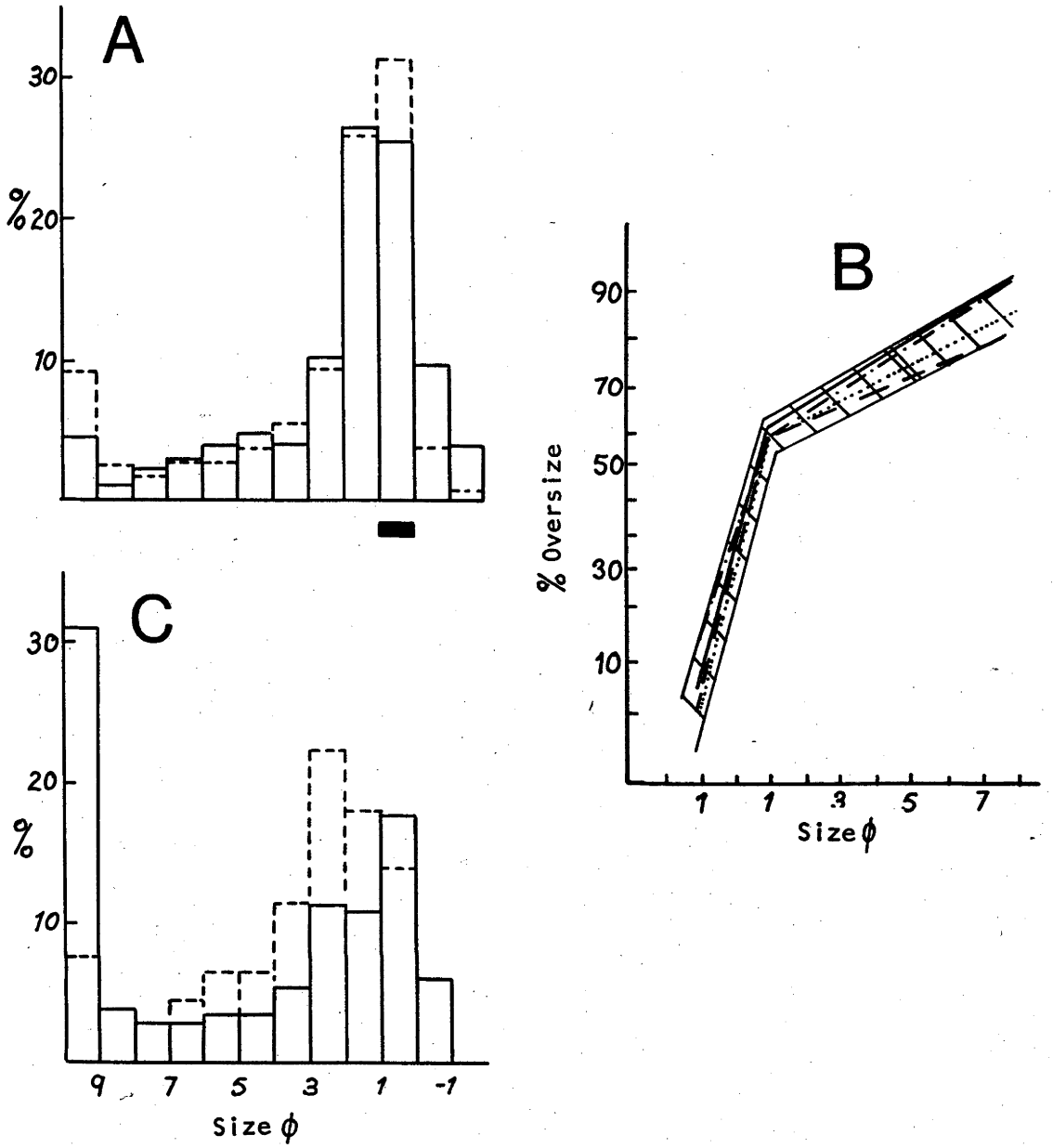

Figure 6.1 Particle-size distribution of profiles SS1, 2, 3.

A: Particle-size distribution of samples SS104 (dashed) and SS303 (solid). The bar graph represents the range in grain size of the parent rock.

B: Cummulative frequency distribution (log probability scale) of samples SS101 (·····), SS104 (- - -), SS301 (——) and SS303 (-·-·-). The hachured envelope represents the size distribution of fluvial sands which would be predicted from Visher (1969).

C: Particle-size distribution of samples SS201 (- - -) and SS202 (——).

The marked change in the sand size mode suggests that the two horizons were developed from different parent materials (cf. the uniform size of the sand size mode throughout profiles SS1 and SS3).

Field observations showed that samples 201 and 202 graded laterally to texturally similar, but less weathered, materials which were recognisable as different sedimentary rocks. The less weathered equivalent of sample 201 was a fine grained sandstone, whereas the equivalent of sample 202 was medium grained and had, compared with the overlying rock, a higher matrix content.

Thus the textural differentiation observed between samples 201 and 202 can be interpreted as resulting from the weathering of superposed sedimentary units of dissimilar texture, rather than from pedogenic or slope processes.

6.3 REGOLITH MINERALOGY

The mineralogy of profiles SS1 and SS3 is given in Table 6.3 and Figure 6.2. On a whole sample basis, quartz is dominant, exceeding 70% (organic free basis). Illite is the only other mineral present in significant quantities. The dominant clay minerals (clay fraction) are kaolinite and illite.

Except for the trace occurrence of K-feldspar in the parent rock and the minor occurrence of mixed layer clays in samples SS101 and SS102, the mineralogy of the regolith samples and their parent rocks are qualitatively identical. Consequently it is unneccessary to invoke extensive chemical weathering to explain the profile mineralogy. The minerals present in the profiles are probably inherited directly from the parent rock; the varying proportions of quartz and illite (the codominant minerals) being due to their separation on the basis of grain size. The removal of the illite-rich clay fraction leaves a residuum enriched in quartz.

6.4 REGOLITH CHEMISTRY

The high concentration of SiO_2 (>80%), the low concentration of the alkali and alkali earth elements and the generally low trace element concentration of the rock samples SSR1 and SSR2 (Table 6.4) reflect the dominance of quartz in the parent rock.

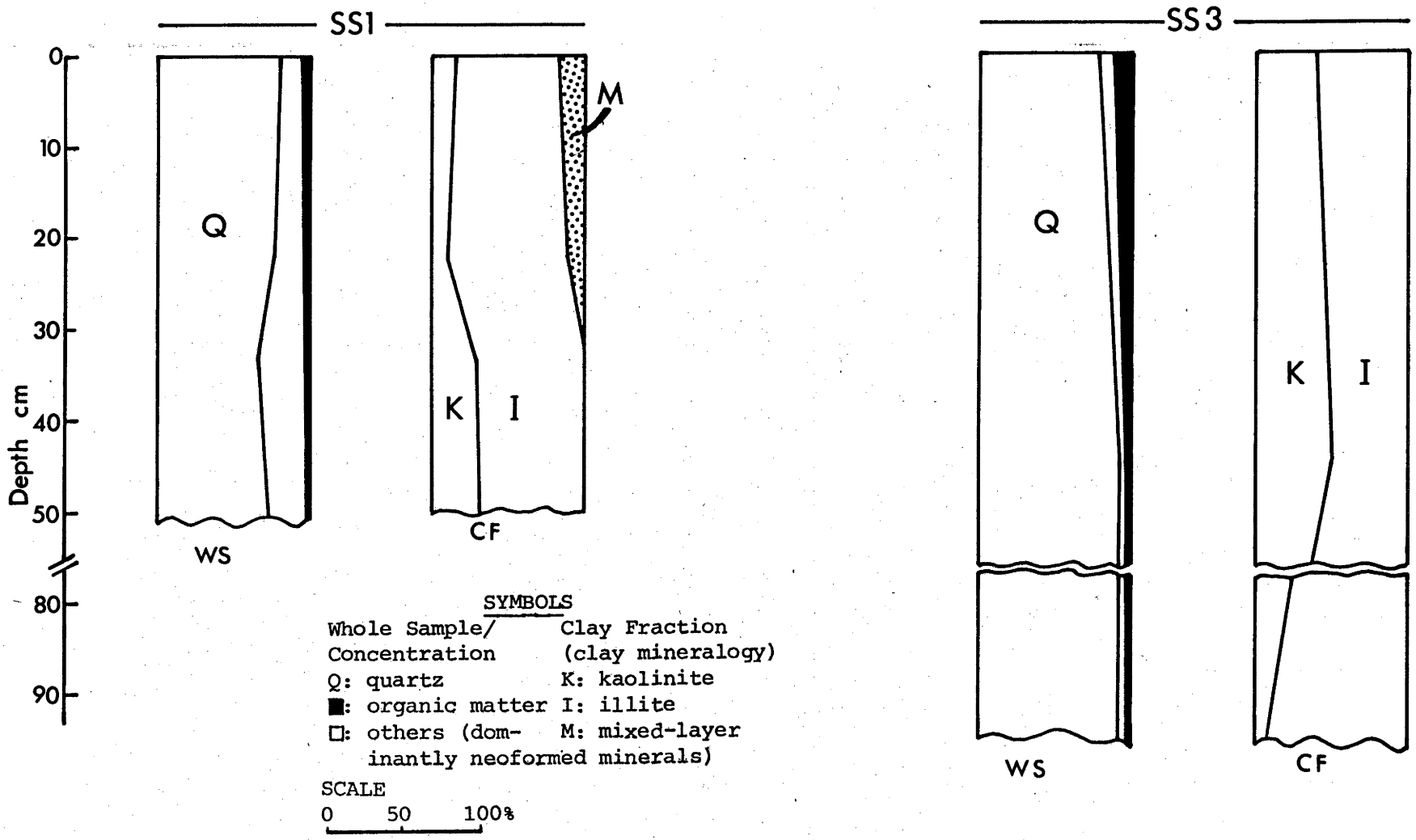

Figure 6.2 Depth dependent variation in mineralogy for profiles SS1 and SS3. Mineralogy is decribed for the whole sample (WS) and the clay fraction (CF, clay mineralogy).

The chemistry of the profile samples (Table 6.4) reflects the high initial SiO_2 concentration, with the concentration of SiO_2 usually exceeding 90% (volatile free basis) and with all other elements having a generally low to trace abundance.

The quantitatively small variation in regolith chemistry restricts the number of processes which can be unequivocally shown to occur. The high correlation (Table 6.5) between those elements concentrated in illite (Al_2O_3, K_2O and Rb) suggest that much of the inorganic changes in chemistry are a result of changes in the concentration of illite (the principal aluminous parent rock mineral) due to its physical removal from the profile. These high correlations would not occur if illite was transformed to kaolinite as this would require the loss of K_2O and Rb relative to Al_2O_3.

Thus the chemistry of the parent rock is such that the potential for change is minimal, given the weathering/soil formation processes operating in the area. Consequently the regolith chemistry strongly reflects the parent rock chemistry. The gross variation in inorganic chemistry is consistent with the physical removal of illite.

	TiO2	Al2O3	Fe2O3	FeO	MgO	CaO	Na2O	K2O	H2O+	C	P	Rb	Sr	Pb	Zr	Y	V	Cr	Mn	Zn	Qtz	Clay
SiO2	0.26	-0.75	-0.79	-0.29	-0.60	-0.56	-0.58	-0.46	-0.75	-0.25	-0.27	-0.61	0.03	-0.86	0.34	-0.62	-0.75	-0.81	-0.68	-0.55	0.65	-0.09
TiO2		-0.47	-0.36	-0.59	-0.52	-0.16	-0.63	-0.52	-0.24	0.28	-0.56	-0.55	-0.52	-0.24	0.88	-0.34	-0.07	-0.14	-0.48	-0.58	0.36	0.23
Al2O3			0.87	0.76	0.73	-0.02	0.82	0.89	0.72	-0.41	0.49	0.97	0.23	0.94	-0.71	0.92	0.65	0.82	0.96	0.86	-0.53	-0.18
Fe2O3				0.44	0.75	0.14	0.55	0.66	0.93	-0.31	0.36	0.76	0.06	0.92	0.54	0.76	0.91	0.91	0.72	0.63	-0.47	0.14
FeO					0.35	-0.30	0.90	0.95	0.17	-0.57	0.67	0.88	0.64	0.54	-0.86	0.72	0.07	0.38	0.83	0.74	-0.26	-0.64
MgO						0.13	0.45	0.50	0.72	-0.33	0.09	0.67	-0.17	0.70	-0.47	0.78	0.64	0.75	0.69	0.76	-0.39	0.42
CaO							0.08	-0.23	0.23	0.77	0.13	-0.13	-0.01	0.10	0.06	-0.09	0.25	0.11	-0.05	-0.05	-0.52	0.23
Na2O								0.90	0.33	-0.26	0.71	0.89	0.59	0.68	-0.82	0.75	0.23	0.50	0.89	0.84	-0.49	-0.56
K2O									0.45	-0.60	0.71	0.96	0.57	0.74	-0.83	0.84	0.36	0.63	0.91	0.81	-0.42	-0.51
H2O+										-0.23	0.28	0.57	-0.06	0.83	-0.35	0.59	0.98	0.89	0.54	0.51	-0.58	0.30
C											-0.32	-0.52	-0.31	-0.24	0.52	-0.46	-0.14	-0.27	-0.39	-0.44	-0.07	0.20
P												0.59	0.92	0.34	-0.79	0.33	0.18	0.25	0.48	0.46	-0.64	-0.70
Rb													0.39	0.85	-0.80	0.91	0.48	0.76	0.98	0.89	-0.51	-0.34
Sr														0.03	-0.71	0.12	-0.16	-0.09	0.26	0.25	-0.34	-0.81
Pb															-0.47	0.86	0.81	0.95	0.87	0.76	-0.54	-0.01
Zr																-0.57	-0.21	-0.35	-0.70	-0.70	0.43	0.49
Y																	0.54	0.82	0.94	0.87	-0.37	-0.04
V																		0.88	0.46	0.40	-0.50	0.36
Cr																			0.77	0.66	-0.59	0.17
Mn																				0.92	-0.50	-0.27
Zn																					-0.48	-0.18
Quartz																						0.20
Clay																						

$*P_{99.9}$ =0.95

$*P_{99}$ =0.87

$*P_{95}$ =0.75

*confidence limits cited ignore the constant sum effect in chemical analysis.

Table 6.5 Correlation matrix for profiles SS1,3 and rocks SSR1,2.

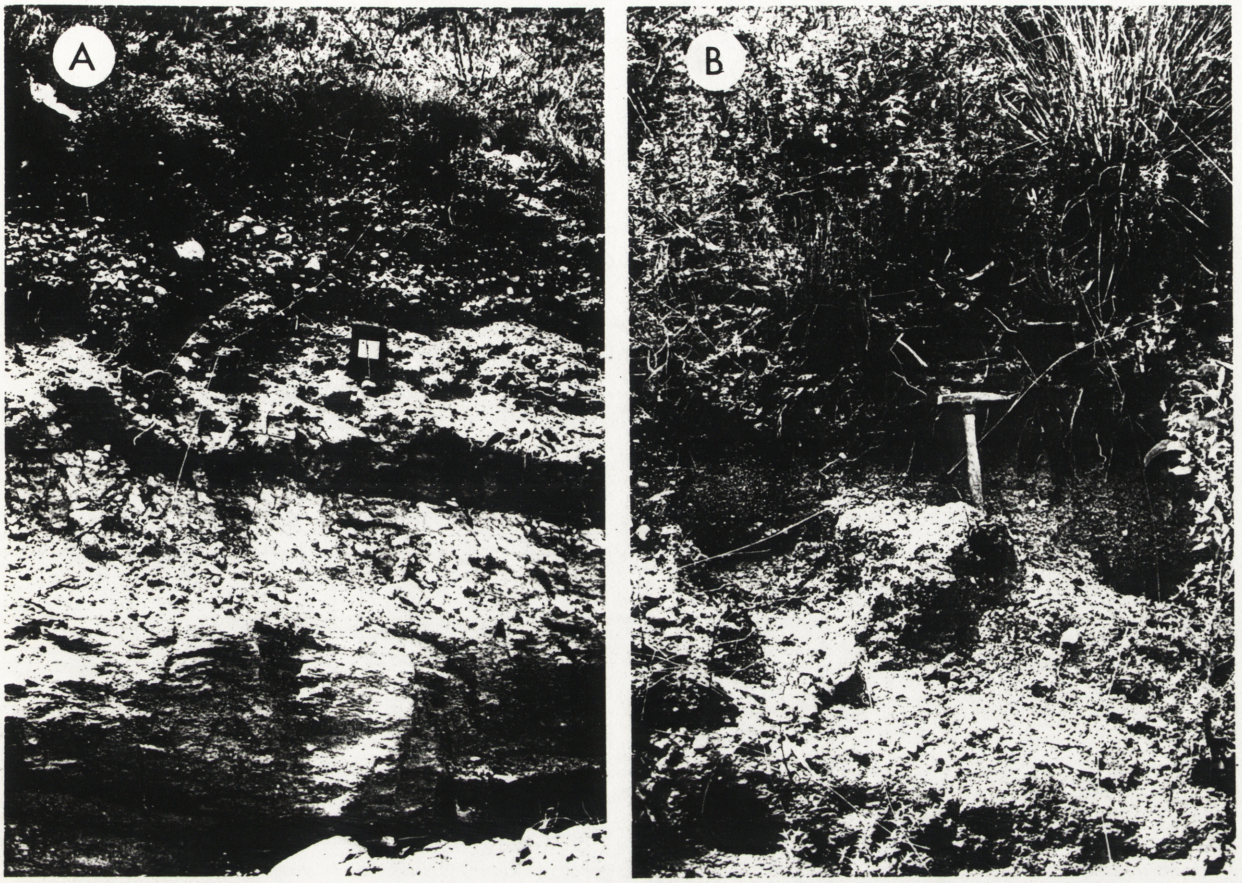

PLATE 5

A) A sedimentary sequence from the Twofold Bay Formation showing the variation in lithology which occurs. This profile varies with depth from coarse pebbly sandstone to sandstone to siltstone.
Location: Narrabarba 8823-II-N 539639.

B) Sandy regolith developed on the Twofold Bay Formation.
Location: Narrabarba 8823-II-N 539639.

CHAPTER 7

SURFICIAL MATERIALS DEVELOPED ON A BASALT DYKE

7.1 INTRODUCTION

The regolith profile examined is developed on a basalt dyke. The dyke is approximately 1.5m wide and intrudes metasediments. Metasediments and microgranite outcrop upslope of the profile. As a consequence, the profile (see Table 7.1 for sample depths, and Appendix B for description) is polygenetic in origin. The surface-sample, D101 consists of a mixture of weathered basalt and material derived from the weathering of the metasediments and microgranite. The depth of the weathering profile exceeds 3m.

Parent Rock

The basalt is fine grained (crystals <0.5mm) and consists of plagioclase, pyroxene, olivine and minor amounts of opaque oxides and sulphides. On the basis of less weathered basalt dykes, exposed elsewhere in the area, the structural features of the parent rock are restricted to a joint set developed parallel and orthogonal to the dyke margins.

7.2 REGOLITH PARTICLE-SIZE

The particle-size distribution of samples D101, 102 and 103 is given in Table 7.2.

During the weathering of the basalt, two dominant particle-size modes are generated, see Figure 7.1. The largest mode consists of unweathered core stones. These range in size from approximately 5cm to 40cm. The size of this mode is probably dependent on the spacing between joints as these are the largest scale feature present in the unweathered rock mass across which separation would most readily occur. Presumably, further size reduction of the joint free core stones would occur as a result of chemical weathering.

Table 7.1 Sample depths for profile D1.

*Profile D1	Sample	Depth (cm)
	D101	0-10
	D102	90-100
	D103	250-260

*Core stones, 5 to 40 cm in size occur throughout the profile.

Table 7.2 Particle-size distribution of profile D1.

	Size (Φ)										
Sample	<9	8	7	6	5	4	3	2	1	0	-1
D101	27.4	5.0	6.5	6.8	8.3	12.3	19.1	9.1	3.7	1.3	0.5
D102	52.8	5.0	6.6	7.7	7.0	5.1	5.1	5.1	4.5	1.1	0.0
D103	48.8	4.7	6.7	9.1	8.0	6.1	5.9	5.4	4.8	0.5	0.0

Table 7.3 Mineralogy of profile D1 and samples D201 and D301: nd, not detected.

	Mineralogy % (Bulk Sample)				Clay Mineralogy % (Clay Fraction)			
					Å			
Sample Number	Quartz	K-feldspar	Plagioclase	Illite	14	12	10	7
D101					25	nd	nd	75
D102	nd	nd	nd	nd	10	nd	nd	90
D103	nd	nd	nd	nd	5	5	nd	90
*D201					20	nd	nd	80
*D301					40	nd	nd	60

*Location: Timbillica; 1:25,000 sheet; Coords 315635.

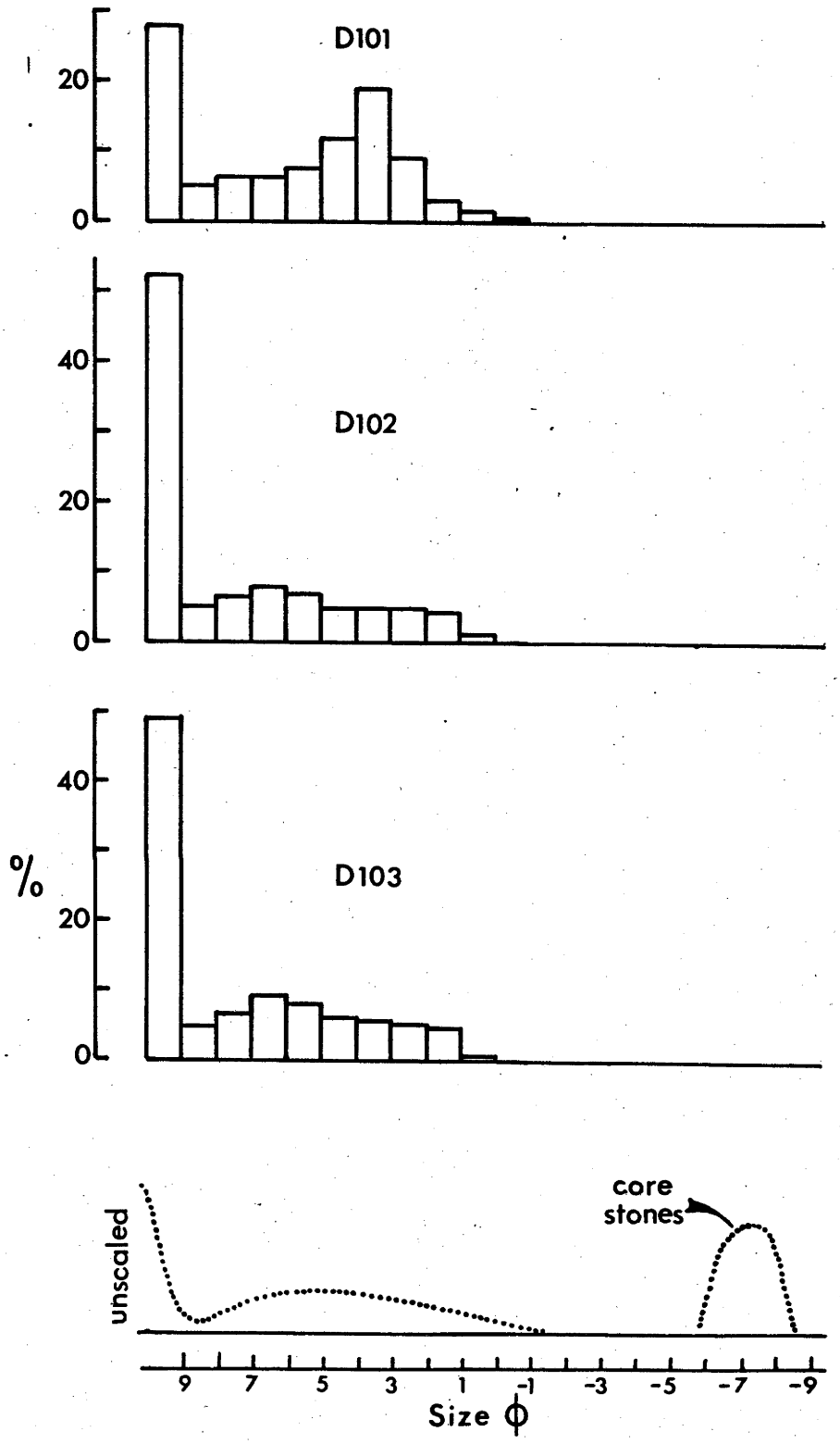

Figure 7.1 Particle-size distribution of samples D101, 102 and 103 (Table 7.2). The dotted distribution is schematic and represents the distribution of the dominant particle-size modes generated during the weathering of profile D1.

The second mode is clay size. This mode is attributed to the accumulation of the neoformed minerals in this size range.

The sand size mode present in sample D101 (Figure 7.1) consists dominantly of quartz and was generated by the addition of sand size material derived from the weathering of coarse grained (compared with basalt) quartzose rocks (metasediment and microgranite) occurring upslope of the profile. Consequently, the occurrence of the sand size mode is not genetically related to the weathering of the basalt.

7.3 REGOLITH MINERALOGY

None of the minerals present in the parent rock could be detected in the samples examined. The clay mineralogy (clay fraction) for profile D1 and samples D201 and D301 is given in Table 7.3 (samples D201 and D301 are samples of weathered basalt dykes, occurring elsewhere in the area). Table 7.3 shows that kaolinite is the dominant clay mineral with vermiculite present in minor proportions.

CHAPTER 8

PARTICLE-SIZE DISTRIBUTIONS

8.1 INTRODUCTION

Given the fundamental importance of particle-size distributions in determining regolith behaviour (Table 8.1), and more generally in controlling the extent and direction of processes within a landscape (Volobuyev, 1974; Moss and Walker, 1978), there is surprisingly little systematic description, particularly in Australia, of either particle-size variation within and among landscapes, or of the processes controlling this variation.

In this chapter, I propose to:

1) Demonstrate that for the samples examined, parent rock is a major determinant of regolith particle-size and that this effect is not restricted to the rock types examined or to the study area.

2) Examine those particle-size features (modes) which give rise to the parent rock effect and their origin.

3) Demonstrate that within a landscape a hierarchy of particle-size features can be recognised and to examine the role of parent rock in this hierarchy.

4) Formalise two principles evident from this work, which are likely to aid future studies. These are: i) the recognition that particles owe their origin to either comminutive or growth processes, and ii) the effect of the 'rate-limiting step'.

Before proceeding, it is appropriate to critically evaluate several aspects of particle-size studies, particularly as they apply to landscapes. The aspects to be reviewed are: 1) Particle definition and physical interpretation; 2) Particle-size scale and interval; and 3) Conventional approaches used to interpret particle-size distributions.

The reasons these aspects are reviewed are as follows:

1) Although to this point the implicit definition of a particle has been adequate, an explicit definition is necessary to prevent any confusion which may arise when different sorts of particles are compared.

Table 8.1 Regolith properties for which particle-size distribution is an important determinant.

1) Moisture characteristics: Salter and Williams, 1967; Thomasson, 1978; Lal, 1979.

2) Permeability: Talsma and Flint, 1958.

3) Pore size distribution: Leamer and Lutz, 1940.

4) Classification: Thompson, 1965; Northcote et al., 1975; Soil Survey Staff, 1975.

5) Structure and micromorphological classification: Paton, 1978; Stoops and Jongerius, 1975; Brewer, 1979.

6) Susceptibility to erosion: Wischmeier et al., 1971.

2) Particle-size data can influence the interpretation of the relationship between regolith particle-size and parent rock and landscape process, and therefore the nature of these data should be examined.

3) As an explanation of why conventional methods of interpreting particle-size data were not extensively used, a summary of the problems inherent in their use is given.

8.1.1 Particle Definition and Physical Interpretation

The variation in definitions of a particle (Table 8.2) exemplifies the complexity of what constitutes a particle. Where a large disparity exists in the nature of the bonds within the material being examined (e.g., in a mass of loose quartz grains the bond strength between individual quartz grains is considerably less than that within the grains) the conceptual idea of a particle is self evident. However, the conceptual definition of a particle is less clear when, for example, either the interactive effects of inorganic 'colloidal' and organic matter, or a partially weathered feldspar grain consisting of clay and feldspar, are considered.

For the purpose of this study a particle is defined as "an individual or compound element delimited by natural boundaries". This is straightforward enough in the case of 'free' particles occurring on the surface in a landscape. However, difficulties arise in the case of aggregates. For this case an empirical definition is adopted which approximates the 'natural' definition above, viz., 'a particle is a unit produced when many of the weaker electrostatic bonds within the aggregate have been ruptured by the technique outlined for particle-size distribution measurement in Appendix A.

The main problem in particle-size measurement is the physical separation of particles from each other. The amount of particle separation achieved is usually dependent on the technique used. Provided that the technique used is optimal in that it achieves both adequate dispersion and disaggregation without literally 'smashing' grains or chemically altering them, and provided

Table 8.2 Definitions of a particle.

1) 'A general term, used without restriction as to shape, composition, and internal structure, for a separable or distinct unit in a rock, e.g., a 'sediment particle', such as a fragment or a grain, usually consisting of a mineral.' Gary et al., 1972, p.518.

2) 'A particle is an individual or compound element delimited by natural boundaries (i.e. not resulting from sample preparation) which behaves or can behave as a unit with respect to internal or external forces.' Stoops and Jongerius, 1975, p. 190.

3) 'A particle consists of an aggregation of molecules without limit to the upper size.' Allen, 1968, p.16.

4) 'Soil particles or "ultimate soil particles" are the discrete units which comprise the solid phase of the soil. They generally cluster together as aggregates, but can be separated from one another by chemical and mechanical means.' Day, 1965, p.545.

5) A particle of a substance is that state of subdivision of matter whose shape depends on those processes by which it was formed and on the intramolecular cohesive forces present.' Irani and Callis, 1963, p.17.

6) The Glossary of Soil Science Terms (1971) although defining particle size and particle size analysis does not define a particle.

the technique is used systematically, then the data obtained are a measure of the sample to sample variation in particle distribution rather than a measure of the effect of the laboratory process. This is supported by the correlation which commonly exists between actual measurements and estimates of sample properties based on particle-size distributions. Under some conditions this approach breaks down, e.g., for subplastic clays. The measurement and interpretation of the size distribution of clay particles is often questioned. It appears (Walker and Hutka, 1979) that when the clay fraction is dominated by kaolinite and illite, then the size distribution attained is an intrinsic feature of the sample rather than an experimental artifact.

8.1.2 Particle-Size Scale and Scale Interval

The commonly used particle-size scales are logarithmic, e.g., ø scale, [$\phi = -\log_2$ (size mm)], and the International Scale. The advantages of the log scale and in particular the ø scale are outlined by Tanner (1969).

The choice of scale interval is ultimately constrained by the reproducibility of the data and the physical constraints involved in the actual measurement. The size frequency data when collected at the smallest practical interval are generally an approximation, albeit the best possible, of the actual distribution. As the scale interval increases in size the divergence between the actual distribution and that measured increases, and there is a consequent loss of information (Figure 8.1).

Figure 8.1 shows the divergence which exists between the actual size distribution of particles when measured at ø intervals and the distribution interpolated from measurements at International Scale intervals. The loss of data is forcefully illustrated when it is considered that nothing is known about the size distribution of particles which are arbitrarily grouped as either <2µm or > 2000µm when using the International Scale.

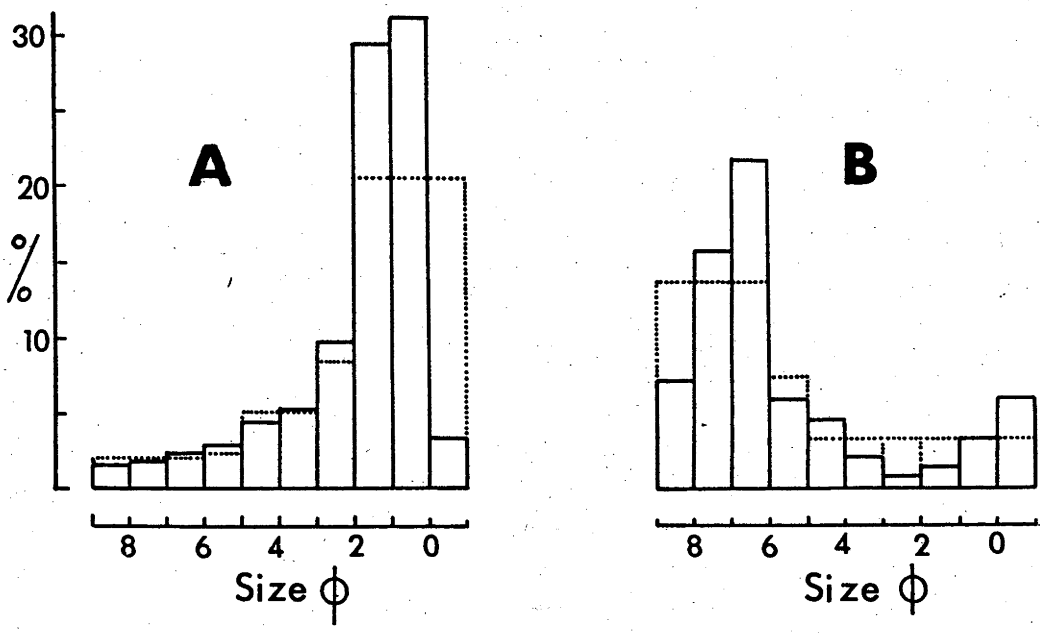

Figure 8.1 The variation in particle-size distribution with particle-size scale and scale interval for samples SS101 (A) and ER103 (B) in the size range 2μm to 2000μm.

Solid line. This distribution represents the actual distribution for measurements at 1ϕ intervals.

Dotted line. This represents the distribution interpolated from measurements made at International Scale intervals.

As much of the particle-size data in the soils literature (e.g., Stace et al.,1968) is given in intervals of the International Scale, an appraisal should be made of the constraints, the use of these intervals place on the interpretation of particle-size data.

The efficacy of the intervals of the International Scale is dependent on their coincidence with natural "breaks" in the particle-size distribution. To test this possible coincidence, a set of 132 samples for which data were available at 1ø intervals between 9 and -4ø was subjected to R-mode factor analysis. Although the sample set is numerically small, if persistent natural breaks in particle-size distribution occur, then they should be manifest in this group as they represent samples from 5 different parent materials. The results, in Figure 8.2 show that there is a remarkable coincidence between groupings in the data, as shown by the plot of the various factors, and the 2, 20, 200 and, 2000μm size class boundaries.

However, when random subsets of the 132 samples or samples derived from a single parent material are used, this coincidence, excepting for the 2μm boundary, is unstable. The stability of the 2μm boundary is a mechanical artefact resulting from assigning all material <2μm to one size class.

These data suggest that within the surficial environment, contrary to the opinion of Wentworth (1933), there are no well defined persistent breaks in the size distribution of particles.

Thus, much of the potential information about the size distribution of particles in a particular sample may not be recorded. This is especially so when large size class intervals are used, such as the International Scale. As a consequence of this loss of information, a greater similarity in particle-size distribution may appear between two samples than does in fact exist.

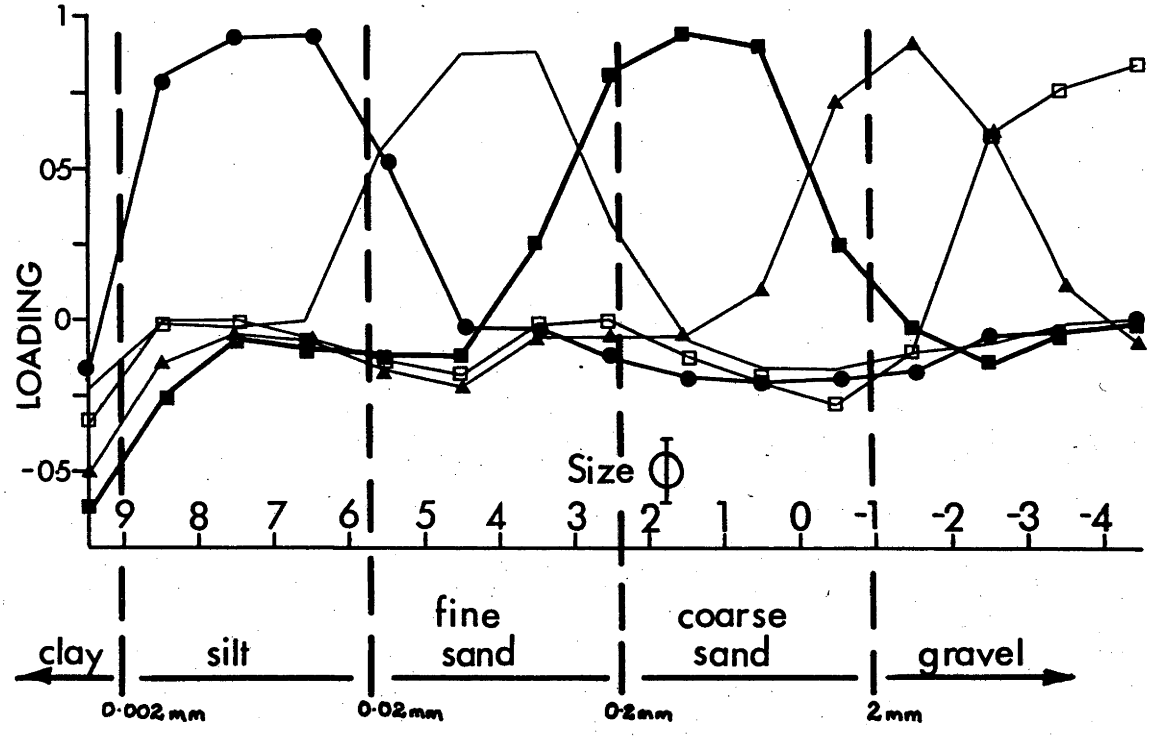

Figure 8.2 The relationship between size-class intervals of the International Scale (2,20,200,2000μm) and those predicted by R-mode factor analysis of 132 samples whose size distribution is known at 1ϕ intervals between 9 and -4ϕ. The first five factors account for 84% of the variance in the data set. The various factor loadings suggest that if the maximum amount of information is to be obtained with fewest measurements,then the optimum scale intervals are 0, 5.5, 3, 0 and -2.5ϕ.

Symbols: Factor I ■—; Factor II ⊖— ; Factor III ⊟— ; Factor IV ▲— ; Factor V ——.

Data: This thesis; profiles GR1 to 8, ER1 to 4, OR1 to 3, SS1 to 3 and D1. P.H.Walker; (written communication; profiles A1004, P116, P93, KC1, STP8). McConnell (1979; profiles 2A/1, 1A/6, 1/55).

8.1.3 Historical Approaches to the Interpretation of Particle-Size Data

The two approaches commonly used by landscape scientists are contrasted. For convenience the first has been termed the distribution approach, and the second the statistical approach.

Distribution Approach: In this approach, the particle-size distribution is compared directly with theoretically derived size probability distributions (e.g., Krumbein, 1964; Dapples, 1975; Russel, 1976). Under some circumstances high correlations between observed and theoretically derived distributions have occurred. Generally, however;

1) Deviations between observed and predicted distributions are common;

2) Various parts of the size distribution are ignored (e.g., Russel, 1976); and

3) The processes on which the theoretical distribution are based are empirically untenable.

For example:

1) In a study of the weathering of loess, Torrent and Nettleton (1979, p.337) proposed that particle-size reduction occurred as follows; "the primary mineral grain is peeled off under the attack of an advancing weathering front parallel to its surface. The primary mineral grain though reduced in size, retains its shape as it continues to weather". This model is comparable to the spheroidal weathering of granite or basalt tors. However, these particles are at least two orders of magnitude larger than the particles considered by Torrent and Nettleton. They are inappropriate analogues as their size reduction is dependent on mineral aggregate properties, whereas particles in loess are likely to be monomineralic. Their model is also inconsistent with the observed pattern of monomineralic particle comminution (Moss, 1966).

2) A distribution commonly used to describe particle-size distributions is the Weilbull distribution (also known as the Rosin distribution) and its variants. This distribution, which is based on the production of particles by failure along

randomly orientated planes (Dapples, 1975; Russel, 1976), is commonly used to describe partially fragmented granite (grus). In granite the major discontinuity within the rock is the grain interface. Grain interface distribution, particularly when the rock is even grained, is regular and systematic and can hardly be described as random.

Statistical Approach: Substantial effort has been made by sedimentologists (Friedman, 1979) to interpret particle-size distributions, through the use of statistical parameters (e.g., mean, standard deviation, etc), in terms of depositional environment (e.g., river, aeolian, beach environments).

There is mounting evidence that although specific features of particle-size distributions may, under some circumstances, be environmentally indicative, they are not universally applicable (Sedimentation Seminar, 1981). This is due to: i) a combination of different source populations; ii) the fact that within any broadly defined depositional environment a variety of processes is likely to operate, each with its own size signature; and iii) the samples which are commonly collected for size analysis often represent a large number of individual laminae which are assumed, without prior evidence, to have been deposited by a single process.

8.2 PARENT ROCK DEPENDENT PARTICLE-SIZE DISTRIBUTIONS

The previous chapters have shown that for regolith derived from a single parent rock, differences in particle-size within and between profiles are due principally to differences in the degree of weathering and soil formation. The question now arises: Does regolith from different rocks differ in particle-size?

The results of discriminant function analysis (Table 8.3) show that when the samples described in Chapters 3 to 7 of this thesis are grouped according to parent rock only 4 of the 76 samples are reallocated. Samples GR201 and GR202 are allocated to the sandstone group and samples ER404

Table 8.3 Prediction of group membership by discriminant function analysis. Samples are from profiles OR1, 2, 3; GR1, 2, 3, 4, 5, 6; ER1, 2, 3, 4; SS1, 2, 3; D1. Analyses are in 1ϕ intervals, see Chapters 3 to 7 for data.

Actual Group	Number of Samples	Predicted Group Membership				
		metasediment	granite	rhyolite	sandstone	basalt
metasediment	12	12	0	0	0	0
granite	34	0	32	0	2	0
rhyolite	18	1	1	16	0	0
sandstone	9	0	0	0	9	0
basalt	3	0	0	0	0	3

and ER405 are allocated to the metasediment and sandstone groups respectively. With these four exceptions, the results show that distinct parent rock dependent particle-size signatures are carried by this group of samples. To examine whether this conclusion is data set specific, the following two data sets were examined:-

1) All available regolith particle-size data from the study area (451 samples, International Scale* intervals).

2) Data from the literature and this thesis for regolith derived from granite, basalt, metasediments, coarse sand/sandstone, loess and rhyolite and formed under a variety of climates (826 samples, International Scale* intervals).

The results of discriminant function analysis and scatter diagrams for the two data sets are given in Table 8.4 and Figures 8.3 and 8.4 respectively. The apices of the scatter diagrams are those which give the greatest overall discrimination between groups in each data set. As such, the difference between any two groups may be reduced because of the plane of the projection, e.g., between the coarse sand/sandstone and rhyolite in Figure 8.4. The results indicate that despite the limits inherent in the use of the large size classes (2, 20, 200, 2000μm), systematic differences in particle-size exist between regolith derived from different rock types within and outside the study area. This suggests that differences in particle-size are likely to occur between regolith derived from a wide range of rock types and that the differences are due to attributes intrinsic to the parent rock.

---

* Large data sets, with which the parent rock effect could be tested, are only available in International Scale intervals. It should be noted that the lesser ability to discriminate between parent rock when using measurements at the International Scale, compared with measurements at 1ø intervals, will only be important if the parent rock effect can not be established.

Table 8.4 Prediction of group membership of 451 samples from the study area. Data were in the form gravel+ coarse sand+fine sand+silt+clay = 100. For the samples derived from unmetamorphosed sediments only those sites where the parent material had been identified as coarse grained sandstone were included in that group. All other samples i.e. samples supplied by the NSW Forestry Commission, for which only the stratigraphic division was known, were placed in the undifferentiated sediment group. Data are given in Chapters 3 to 7 and Hough (1982).

Actual Group / Soil Parent Material	Number of Samples	Predicted Group Membership % of total				
		metasediment	granite	rhyolite	coarse grained sandstone	undifferentiated sediments
metasediment	92	58 63%	1 1%	21 23%	0 0%	12 13%
granite	200	13 7%	129 65%	7 3.5%	29 15%	22 11%
rhyolite	45	9 20%	4 9%	25 56%	3 7%	4 9%
coarse grained sandstone	24	0 0%	2 8.3%	0 0%	18 75%	4 17%
undifferentiated sediments	90	9 10%	17 19%	2 2%	10 11%	52 58%

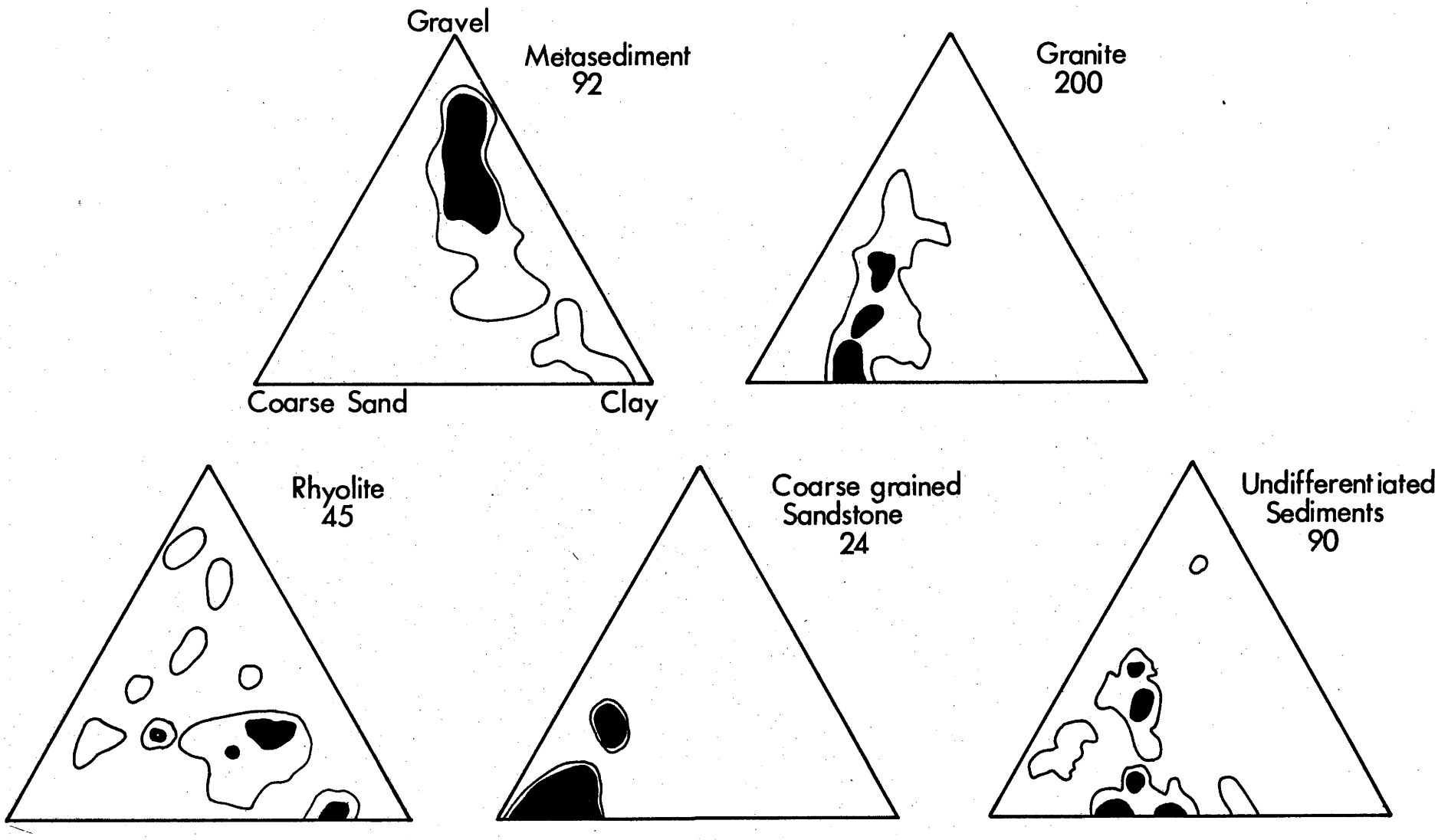

Figure 8.3 Variation in gravel, coarse sand and clay content of regolith samples from the study area. Contours are 2% and 5% per 1% area. Data are given in Chapters 3 to 7 and Hough (1982).

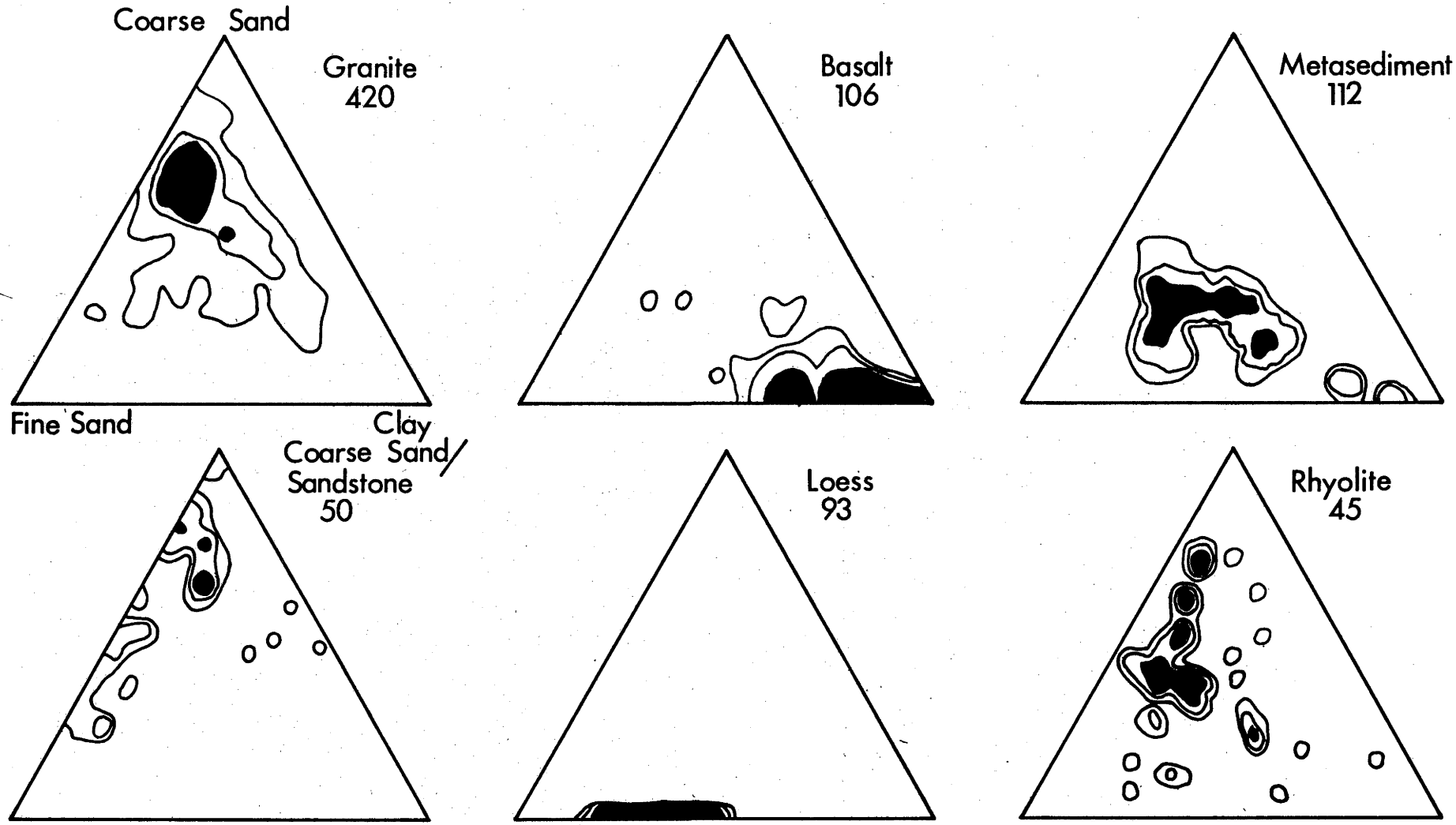

Figure 8.4 Variation in coarse sand, fine sand and clay content with parent rock. Contour intervals are 1,3,5% per 1% area. Data are from: Downes and Sleeman, 1955; Nicolls and Tucker, 1956; Loveday,1957; McArthur and Bettenay, 1960; Jessup, 1965; Blackburn et al., 1965; Stace et al., 1968; Bruce-Smith, 1972 and this thesis.

8.3 LANDSCAPE PARTICLE-SIZE MODES

Since it has been shown that differences in regolith particle-size distribution exist, those attributes and processes which give rise to size differences in particle modes will be examined.

The dominant particle-size modes produced as a consequence of weathering in the different landscapes described are given in Figure 8.5. Within these landscapes the following boundary conditions apply:

1) Evidence for the extensive development of transported slope mantles is absent.
2) Leaching conditions and the history of the surficial mantle is such that particle formation (for particles > 2μm) is by comminution.
3) Aggregation causing the formation of nodules is rare and usually absent.

The frequency graphs (Figure 8.5) have been plotted using the maximum concentration recorded for each ø fraction in all samples* derived from a particular rock type. For example, the concentration of particles in the 0 to -1ø fraction for the seven samples derived from sandstone (Table 6.2) is 3.7, 3.1, 5.4, 3.9, 5.8, 8.1, 9.9%; the maximum, 9.9% is used. The use of the maximum frequency ensures that all particle-size modes generated, will be recorded. The use of an average or minimum value would not. Size data for the clay fraction are available only for representative samples derived from metasediment, granite, rhyolite and basalt (Table 8.5).

The estimated size distribution of the mega particles has been described in Chapters 3 to 7. The relationship between the measured frequency distribution and that estimated for the mega particles is given in Table 8.6.

---

* As explained in Chapters 3 to 7, samples SS201-2 and D101 are atypical and thus are not included in this compilation.

Figure 8.5 Distribution of particle-size modes in landscapes derived from metasediment, granite, rhyolite, sandstone and basalt.

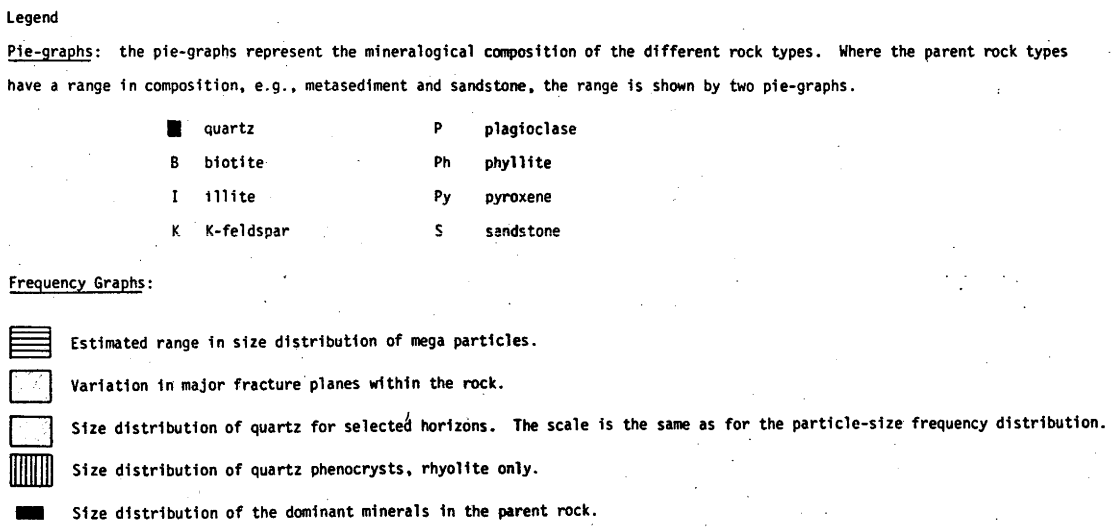

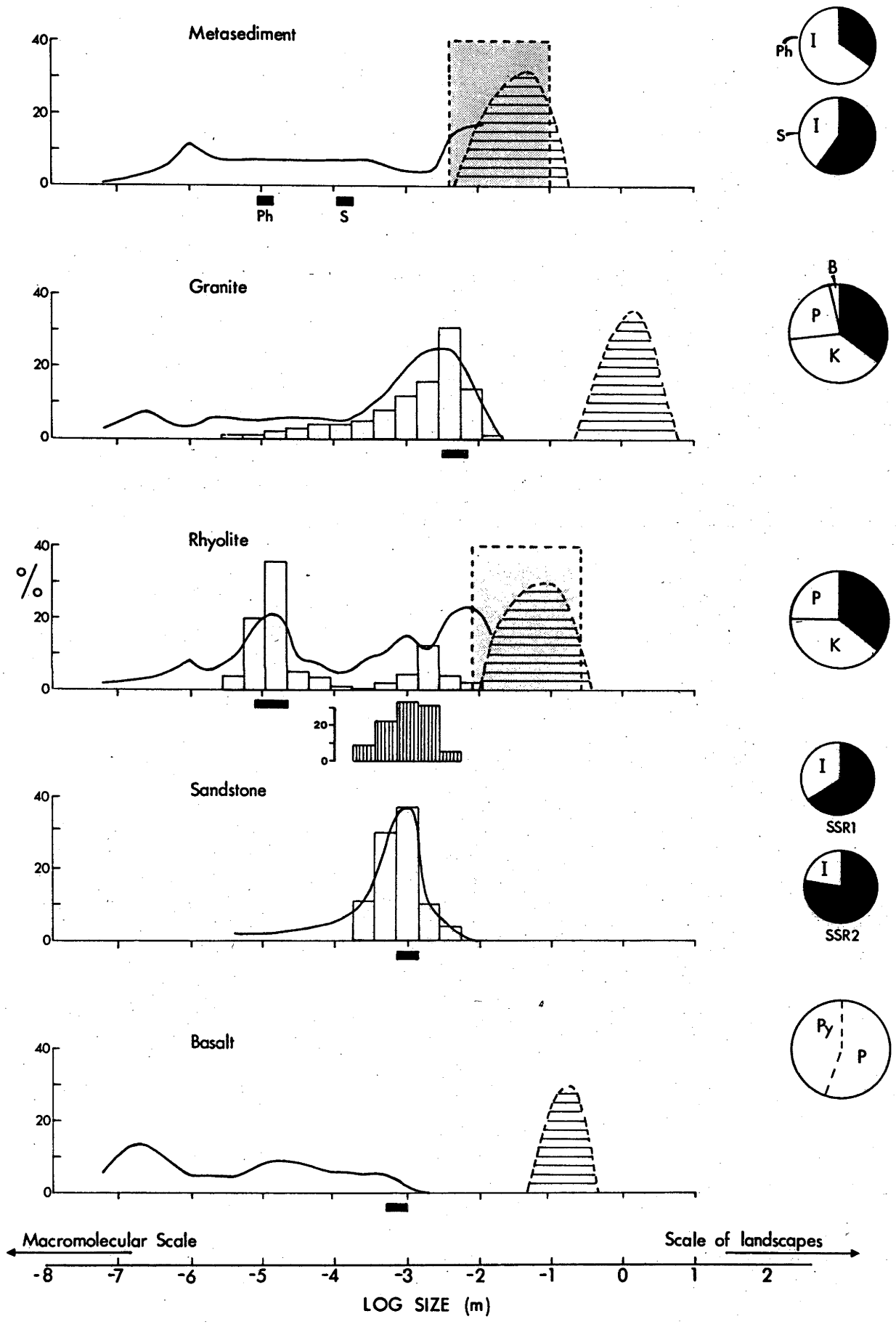
Metasediment
40
20
0
Ph
S
Ph
I
S
I
Granite
40
20
0
B
P
K
Rhyolite
%
40
20
0
20
0
P
K
Sandstone
40
20
0
I
SSR1
I
SSR2
Basalt
40
20
0
Py
P
Macromolecular Scale
Scale of landscapes
-8
-7
-6
-5
-4
-3
-2
-1
0
1
2
LOG SIZE (m)

Table 8.5 Particle-size distribution (cumulative weight %) of the <1μm fraction. Data supplied by P.H. Walker

	Size μm				
Sample Number	<0.06	<0.125	<0.25	<0.5	<1.0
OR103	1.38	2.79	5.90	12.31	23.93
OR104	1.88	2.31	5.40	10.64	19.98
GR103	1.02	1.76	3.95	7.10	10.60
GR203	2.12	3.14	5.79	7.00	9.14
GR206	2.88	8.76	16.69	20.76	23.93
ER202	2.50	5.14	8.57	13.33	17.90
ERU03	1.48	3.83	7.07	12.74	20.95
D103	5.95	18.31	30.71	39.07	43.74

Table 8.6 A summary of parent rock attributes relevant to particle formation, and the relationship between the measured frequency distribution and the estimated size of mega particles (Figure 8.5).

Texture	Structure	Quartz Distribution	Comments on the relationship between the measured data (solid line) and estimated size distribution (mega particles)
Metasediment Ranges from 10 to 20μm (phyllite) to 100 to 500μm (sandstone)	Spacing between cleavage or fracture planes is 0.5 to 30cm	Variation in quartz content with grain size was not determined. Optical observations of the sand and gravel size fractions suggest that mineralogical fractionation in this size range is minimal	The distribution is probably continuous.
Granite coarse even grained varieties, 3 to 5mm (Excludes particle size distribution associated with aplitic , pegmatitic and prophyritic phases)	Fractures commonly occur as zones in which they are closely spaced (< several centimetres) separated by apparently fracture free zones which can be up to several metres wide. Because of this variability their distribution is not shown	The distribution is the average of horizons GR103 and GR107 and was calculated for ease of presentation. It is not intended to represent the average distribution in the landscape	Separation of histograms is real
Rhyolite groundmass 5 to 20μm phenocrysts 0.3 to 4mm	Spacing between fracture cleavage is 1 to 30cm	The distribution of quartz is for horizon ER204, which is intensely weathered	The distribution is probably continuous
Sandstone average 1mm	Insufficient outcrop to determine spacing between fractures	The distribution of quartz was calculated by assuming that the concentration of quartz in the bulk samples is 80% and that the concentration in the individual 1φ intervals is 80%	Mega particles are not present in this landscape, although commonly present in other sandstone landscapes e.g. in areas in which the Hawkesbery Sandstone occurs
Basalt Range 0.5-1mm	Insufficient outcrop to determine spacing between fractures. Because of the tectonically undeformed nature of the dyke the spacing of joints will be determined by its cooling history.	Quartz concentration is less than the limit of detection for X-ray defraction techniques. Quartz has been recorded in other basalt landscapes although its origin has not always been unequivocally determined	Separation of histograms is real

A summary (from Chapters 3 to 7) of the parent rock attributes which determine the occurrence of some of the particle-size modes is given in Table 8.6.

From Figures 8.5 and 8.6, three types of mode can be recognised. Each mode need not necessarily be present in every landscape. They are:

Mode I: This mode is 2 to 5 orders of magnitude larger than the modal distribution of framework grains in the parent rock. It is 1 to 3 orders of magnitude smaller than components in which variations in the landscape, itself, are involved.

Mode II: This mode is approximately coincident with the modal distribution of framework grains in the parent rock.

Mode III: This mode is $<2\mu m$ in size and 2 to 5 orders of magnitude smaller than the modal distribution of framework grains in the parent rock.

The existence of a mode implies that some specific size particles are more common than others and its converse that some are less common. A dearth of particles of a specific size can be due to the following:

1) The particles are rarely formed; or
2) The particles are formed in abundance and are either physically or chemically unstable and thus have very short half lives. The comparative importance of either of these processes in particle comminution is not readily determined.

8.3.1 The Origin of Particle-Size Modes

Mode I

The size distribution of this mode is determined by the structural features of the parent rock. These are of either primary origin, e.g., bedding planes and cooling joints; or tectonic origin e.g., slaty and fracture cleavage and jointing

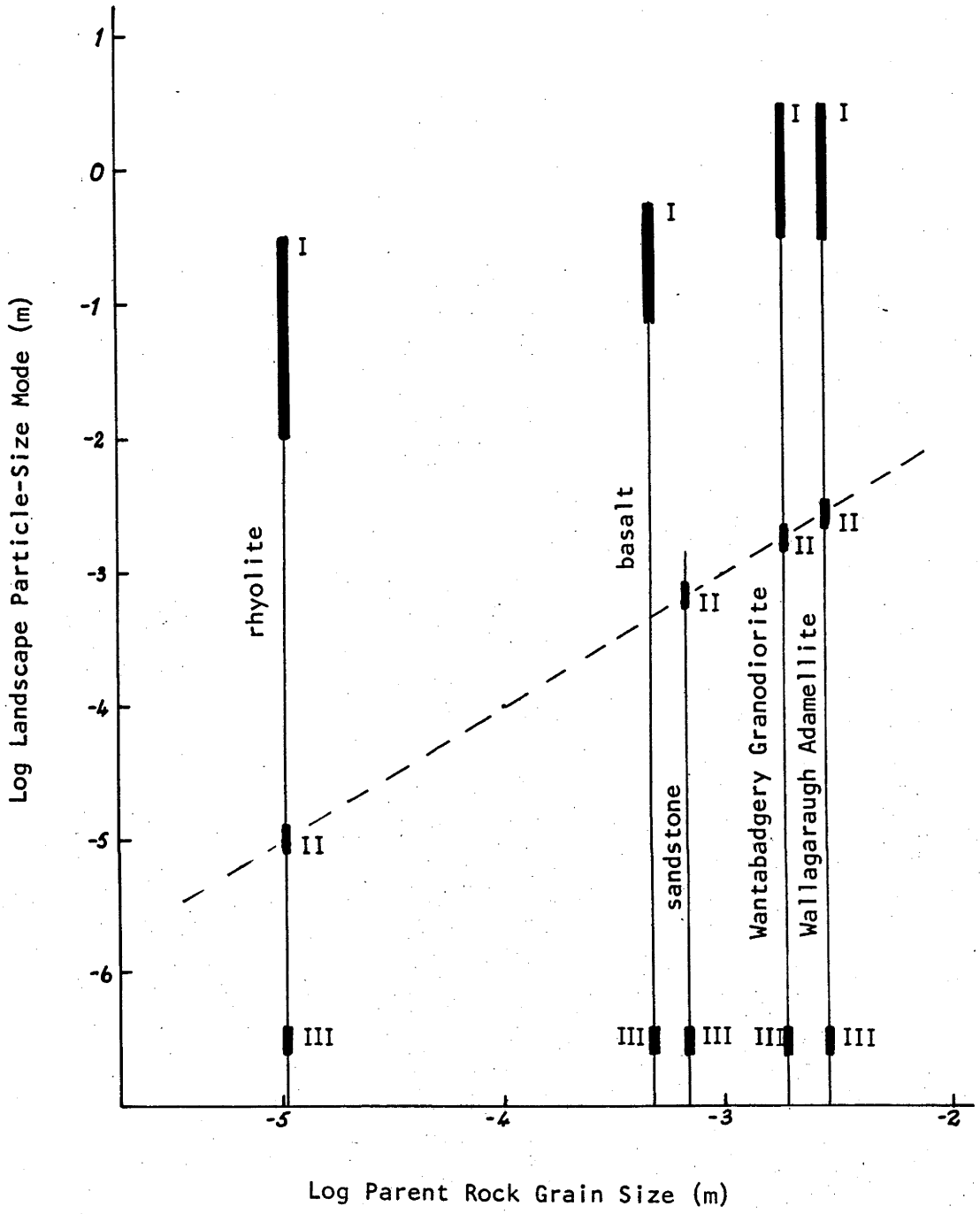

Figure 8.6 The size of landscape particle-size modes (Modes I, II and III) in relation to the size of the parent rock framework grains. Modes are represented as a bar graph. Mode III is shown as 10^{-7}m for schematic purposes. The dashed line has a slope of 1. Data are from this thesis and McConnell (1979, Wantabadgery Granodiorite).

(Table 8.6). The size of the particles is determined by the low cohesion across these structural discontinuities as they are the strength-limiting feature of the rock mass. The importance of structure is also reflected by the common occurrence of planar boundary faces on the particles. It is possible in some parent rocks that the rock mass itself is the strength-limiting feature rather than the structural discontinuities e.g., iron oxide infilled and cemented joints in soft porous sandstone.

In the sandstone landscape, this mode is absent in the environs of profiles SS1 and SS3. This is attributed to the comparatively more rapid rate of sandstone weathering compared with rate of erosion, which prevents the exhumation of coherent joint bounded blocks. However, at Mt. Imlay (approximately 30km southwest of Eden) the rate of erosion on the steep slopes ($>20^{\circ}$), compared with the rate of weathering is sufficient to allow the exposure of large (0.5 to 1m) joint bounded particles.

Once particles free of readily ruptured structural features are produced, further comminution occurs as a result of the effect of rock fatigue or chemical weathering.

Mode II

The size of this mode corresponds with the size distribution of framework grains of the parent rock, principally quartz (Figure 8.6). The dependence on quartz is due to its abundance and resistance to physiochemical weathering compared to other common rock forming minerals. Modes of this type can be associated with minerals other than quartz e.g., i) a mode is developed in regolith derived from the Wantabadgery Granodiorite, which corresponds to the size distribution of biotite (McConnell, 1979); ii) field observations of regolith derived from the Kameruka Granodiorite (Beams, 1980) indicate the development of a mode associated with the release of K-feldspar megacrysts during weathering.

The size of this mode also reflects the difference in behaviour of aggregates which consist of relatively few crystals and those which consist of numerous crystals. This behaviour has been described by Harrell and Blatt (1978) in terms of the Griffith 'Fracture Theory'. On the scale of individual crystals, maximum stress release occurs between or within crystals, as crack propagation across crystal boundaries rapidly dissipates energy due to the effect of changing crystal lattice structure and alignment. As a consequence:

1) When the size of a polycrystalline aggregate is constant, the aggregate with fewest crystals will be more susceptible to breakage than a comparatively more finely crystalline aggregate.

2) When crystal size remains constant, the smaller the aggregate, the lower the crystal interface area to aggregate volume ratio and the more susceptible it is to breakage.

In the landscapes examined, the paucity of particles, equivalent in size to an order of magnitude larger than the modal grain size of the parent rock, is consistent with the combined effects of the Griffith 'Fracture Theory' and chemical weathering.

Mode II is present in the granite, rhyolite and sandstone landscape and absent from the basalt (quartz is not present) and metasediment landscape. The possible reasons for the absence of this mode in the metasediment landscape have been described in Section 5.2.

Mode III

The size distribution of this mode (Figure 8.5) is based on the analysis of selected samples given in Table 8.5. Figure 8.5 shows that the clay size mode can be much smaller than 2μm. This is consistent with the work of Fordham and Norrish (1979a, b). The mode is determined principally by the distribution of clay minerals. As previously stated, when the clay minerals consist principally of illite and kaolinite or equivalents, the shape of the mode can be related to features intrinsic to the material (Walker and Hutka, 1979). Where montmorillonite

is the dominant clay, the resulting distribution will reflect its variably expanding lattice properties, hence it is unclear how the resulting mode should be interpreted.

The dominance of clay minerals in this mode is due to a combination of their mode of formation and physical properties. Where the lattice difference between a clay mineral and its precursor is small, clay minerals can form large pseudomorphs (1 to 2mm) in physically sheltered environments; e.g., the hedenbergite to nontronite transformation described by Eggleton (1975).

Normally however, there is a large disparity in lattice structure between a mineral and its eventual weathering products (e.g., plagioclase and kaolinite), requiring the formation of either a solutional or highly disordered lattice phase. If a solutional phase is involved, then because of the comparative insolubility of aluminous species, the clay minerals will tend to nucleate and grow immediate (both spatially and temporally) to the site of formation, preventing the formation of large clay mineral crystals. This is in contrast to the behaviour of comparatively soluble salts which will tend to form fewer and larger crystals (e.g., $CaSO_4$).

When a disordered lattice is the intermediate species between a clay and its precursor it will tend to break repeatedly in order to accommodate the stress induced during the transformation. These breaks occur at submicron intervals (related to unit cell dimensions) thus preventing the formation of extended crystals.

Clay minerals are also susceptible to comminution due to their well developed '001' cleavage and expansion on hydration. Thus in any regolith environment in which wetting and drying and shear stress are common (e.g., the regolith zone which is affected by the weight of a tree and its movement, hill creep, etc.), large ($> 2\mu m$) non-occluded clay minerals are unlikely to survive.

8.3.2 Discussion

The three genetic modes identified vary in size by seven orders of magnitude.

The size of two of the modes can be related directly to spatial features of the source rock; Mode I to structural features and Mode II to grain size. Modes I and II are comparatively robust parent rock indicators as, although their magnitude may vary with weathering, their size once manifest is comparatively insensitive to weathering.

Except where the clay size fraction is inherited directly from the parent rock, such as could occur with the weathering of clay stone, the size of Mode III is unrelated to any spatial feature of the parent rock. Despite this, the magnitude of Mode III can reflect the influence of parent rock mineralogy. Figure 8.4 shows that those samples derived from basalt generally have a higher clay concentration than those from other rock types. The magnitude of Mode III is however, highly sensitive to weathering. Its usefulness as a parent rock indicator will only be resolved by further work.

8.4 SYNTHESIS

To summarise the preceding discussion:

1) There is currently no universally accepted definition of a particle which provides a clear conceptual understanding of what it is.

2) The size intervals commonly used to measure the size distribution of surficial materials (e.g., the International Scale) have boundaries which often do not coincide with natural 'breaks' in the size distribution. Consequently a considerable amount of the actual variation in the particle-size distribution is not recorded.

3) Both the distribution and statistical approaches to the interpretation of particle-size distributions have deficiencies which restrict their interpretative power.

4) The size distribution of in situ weathered material is commonly polymodal. In a landscape where most of the processes result in particle comminution rather than growth:

i) The dearth of particles separating modes results from either:-

(a) the particles being rarely formed

(b) the particles being formed in abundance but are either physically or chemically unstable.

ii) Three genetic particle-size modes can be identified. These modes can vary in size by seven orders of magnitude.

Mode I reflects the structure of the parent rock.

Mode II reflects the size distribution of the physiochemically stable minerals in the parent rock.

Mode III reflects the physiochemical properties of the clay minerals.

5) Within a landscape the parent rock imparts distinctive features to the size distribution of in situ weathered material. The signature of the parent rock is reflected by the size distributions of Modes I and II and, because of the interactive nature of the parent rock and weathering, to a certain extent by the magnitude of Mode III.

Two points arise from this synthesis. Firstly, so far the particle-size distribution of isolated samples has been considered. Regolith samples rarely exist as isolated entities in the landscapes in which they occur, but often are related to contiguous samples. Consequently, a sample and a particular particle-size distribution can be considered to form part of a hierarchy of landscape elements (Dijkerman, 1974) and particle-size distributions. Secondly, given that the statistical and distribution approaches do not always lend themselves to providing an insight to particle formation, there is a need for an approach which will.

These two points are now discussed.

8.5 THE HIERARCHY OF PARTICLE-SIZE DISTRIBUTIONS: A LANDSCAPE CONTEXT

The hierarchical organisation of components within a landscape is described in Figure 8.7. With respect to particle-size distributions, a landscape can most simply be considered to consist of the following three components. In order of increasing scale they are:

1) Horizons: individual samples.
2) Profiles: a sequence of vertically contiguous samples.
3) Hillslopes - streams - estuaries (major depositional sites): a sequence of laterally contiguous samples.

Horizons

The expression of the effect of parent rock on the particle-size distribution of individual samples has been described. The effect of parent rock is most pronounced as the size fraction described in most detail, the non-clay fraction, strongly reflects the parent rock signature (i.e., the size distribution of quartz).

The clay fraction is normally dominated by the products of chemical weathering. The arbitrary grouping of those particles (clay minerals) whose size distribution is likely to be sensitive to weathering, in a single group, is likely to suppress any signature indicative of the weathering/soil environment. Walker and Hutka (1979) have shown that when the clay fraction is divided into its coarse and fine clay components, the silt/coarse clay/fine clay ratios can discriminate between the A and B horizons of profiles which have a marked textural differentiation.

Thus, it appears that under some circumstances, information diagnostic of the weathering environment is carried by the particle-size distribution. Whether the effect of weathering environment can be systematically identified for a large range of samples remains to be investigated.

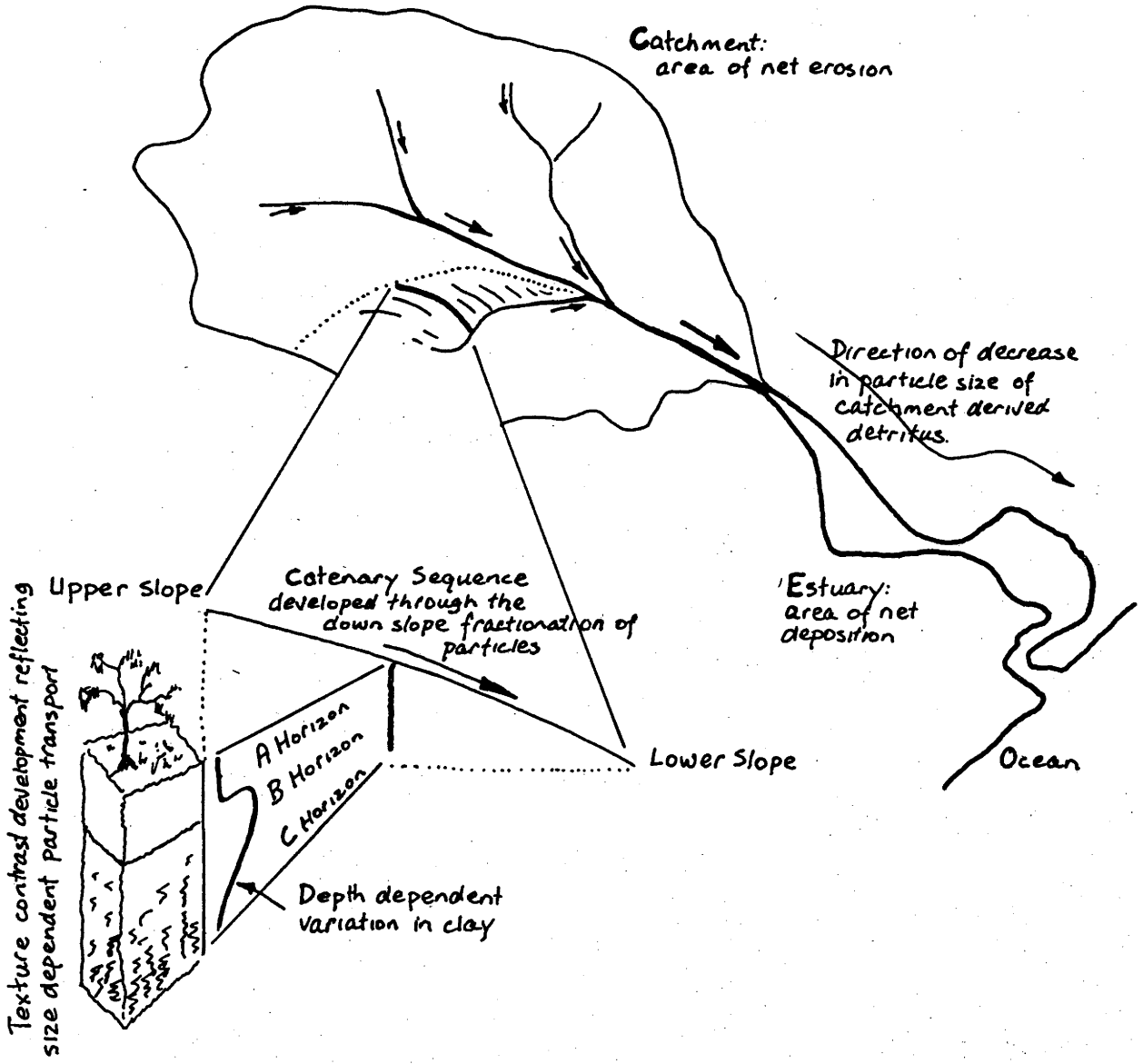

Figure 8.7 A schematic illustration of the hierarchical organisation of landscape elements in which distinct patterns of particle-size variation can be recognised.

Profiles

The most discussed profile particle-size attribute is its variation in clay content. The range in variation of clay content can be described by two end members. The first, a profile with little or no variation in clay content. The second, a profile having a marked variation in clay content, i.e., shows strong textural differentiation. As a profile having no variation in clay content can be considered analogous to a single sample, only the features of texturally differentiated profiles will be discussed.

Texturally differentiated profiles are expressed by the occurrence of two horizons,* the surface horizon having a clay content less than that of the horizon beneath it. This specific variation in particle-size distribution is common and readily recognised.

Historically, as Oertel (1968) and Brewer (1968) have shown, it was usual to consider that the two horizons were genetically related, with the variation in clay due to illuviation, viz., a specific spatial variation in particle-size distribution (in this case, clay content) was accepted as evidence for a specific process, clay illuviation.

In fact, a variety of processes can lead to the same textural differentiation. Processes which lead to a lower clay content of the A horizon compared with the B horizon are given in Figure 8.8 and described as follows. It should be noted that the following is not a discussion of the relative merits of any particular model.

Model 1: The low clay content of the A horizon is due to the selective loss of clay from the A horizon. As described for profile GR1 (Section 3.5.4) this loss can occur as a result of chemical or physical processes.

---

* It is appropriate for the reason given on page 6 to revert to the use of horizon nomenclature. It should be noted that no genetic relationship need necessarily exist between the A and B horizon.

Figure 8.8 Modes of formation of texture contrast profiles.

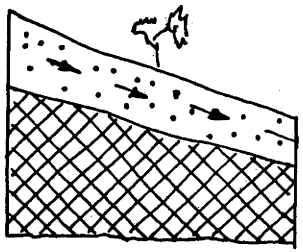

sandy layer ▨ clay rich layer ▨

lateral movement & removal of clay

Model

1. Selective removal of clay from the surface horizon, leading to the development of an horizon depleted in clay compared with that beneath it, e.g., profile GR1.

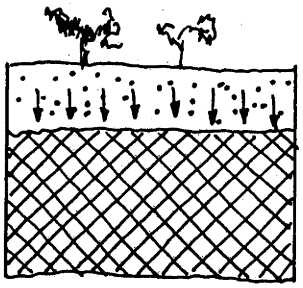

vertical clay movement

2. Vertical translocation of clay leading to the depletion of clay in the surface horizon and its enrichment in the underlying horizon. Profiles of this nature are commonly developed from Tertiary sediments occurring on flat lying erosion terraces to the west of Mallacoota (Hough and Beams, 1979; Little and Ward, 1981)

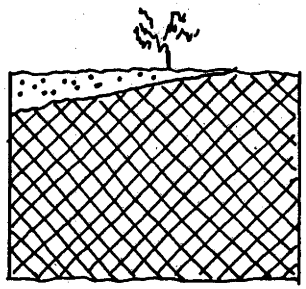

stratigraphic superposition of sedimentary horizons

3. Stratigraphic superposition of a sandy layer over a heavier textured layer. This involves no clay translocation and the separate layers are genetically unrelated e.g. profile SS2.

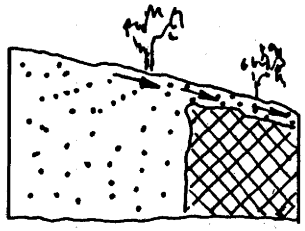

superposition of sandy detritus by its downslope movement over a heavy textured substrate

4. The upslope occurrence of a source producing sandy detritus which is then deposited on a heavier textured substrate (occurring at a topographically lower position) as a result of its down hill movement. This is demonstrated by profile D1

Model 2: The distribution of clay in the profile is a result of its removal from the A horizon and deposition in the B horizon. An example of the effects of this process have been described by Little and Ward (1981) for the area west of Mallacoota.

Model 3: The weathering of a heterogeneous sedimentary sequence in which sandstone overlies shale, can lead to the development of a texturally differentiated profile, with a sandy layer overlying a heavier textured layer (e.g., SS2). The processes leading to this textural differentiation are unrelated to those which operate within the landscape in which the profile occurs. No genetic relationship exists between the two weathering horizons.

Model 4: This occurs where a source of sandy detritus occurs upslope of a more heavily textured regolith (e.g., profile D1). Under the influence of gravity, the sandy detritus moves down slope. This results in the formation of a profile in which a sandy horizon overlies a more heavily textured horizon.

These four models demonstrate that although texturally differentiated profiles are common and represent a particular variation in particle-size distribution, it alone is not unequivocal evidence for the operation of a specific process.

There is evidence (e.g., Stace et al., 1968) to suggest, in general terms, that a rock which on weathering produces a sand/clay regolith (e.g., granite) is, compared with one that produces clay rich regolith (e.g., basalt), more likely to develop a profile with a greater degree of textural differentiation. However, the precise boundary conditions, viz., parent rock composition and weathering environment, under which this occurs have yet to be determined.

Hillslopes - Streams and Estuaries

The existence of persistent changes in particle-size down slope, i.e., catenary variation, was recognised by Milne (1936). These persistent changes are restricted to areas of net deposition as the areas of net erosion carry no signature of the transportational process.

Moss and Walker (1978) have described these changes in particle-size distribution in terms of the downslope change in transporting power of thin overland flow. They state (p.134) 'Depositional differentiation on hydraulic mantle slopes is characterised by a series of discrete physical environments, each with characteristic sediments as transporting power and turbulence wane downhill.
The sequence is:-

Rheologic bed stage with clogged contact population.

Rheologic bed stage without clogged contact population.

Coarse bare bed stage without clogged contact population.

Fine ripple bed stage.

Suspended bed load stage.

This represents the overland flow expression of what is probably a universal differentiation sequence, also occuring in rivers and probably in marine environments.'

Thus although stream bed and estuarine environments differ in scale to hillslopes, the processes controlling the particle-size populations are identical (Moss and Walker, 1978). The parent rock signature is only effective to the extent that it controls the size range of particles in the source population.

For example, Figure 8.9 shows that the source population of stream sediments derived from the Wantabadgery Granodiorite (McConnell, 1979) and the Wallagaraugh Adamellite are dissimilar. With transportation (indicated by the arrow) the particle-size distribution of the stream-bed sediment becomes truncated, compared with its source population, through the removal of clay, silt and fine sand. Consequently, initial differences between source populations (populations A and B, Figure 8.9) are diminished with fluvial transport.

Thus with increasing transportation, the sediment particle-size distribution tends to reflect to a greater extent the transportation processes which gave rise to it, and to a lesser extent the rock from which it was derived. Although the particle-size distribution of sediments may become independent of the source rock (particle-size range of the source not limiting), there is growing evidence that substantial information about the sediment source rock is

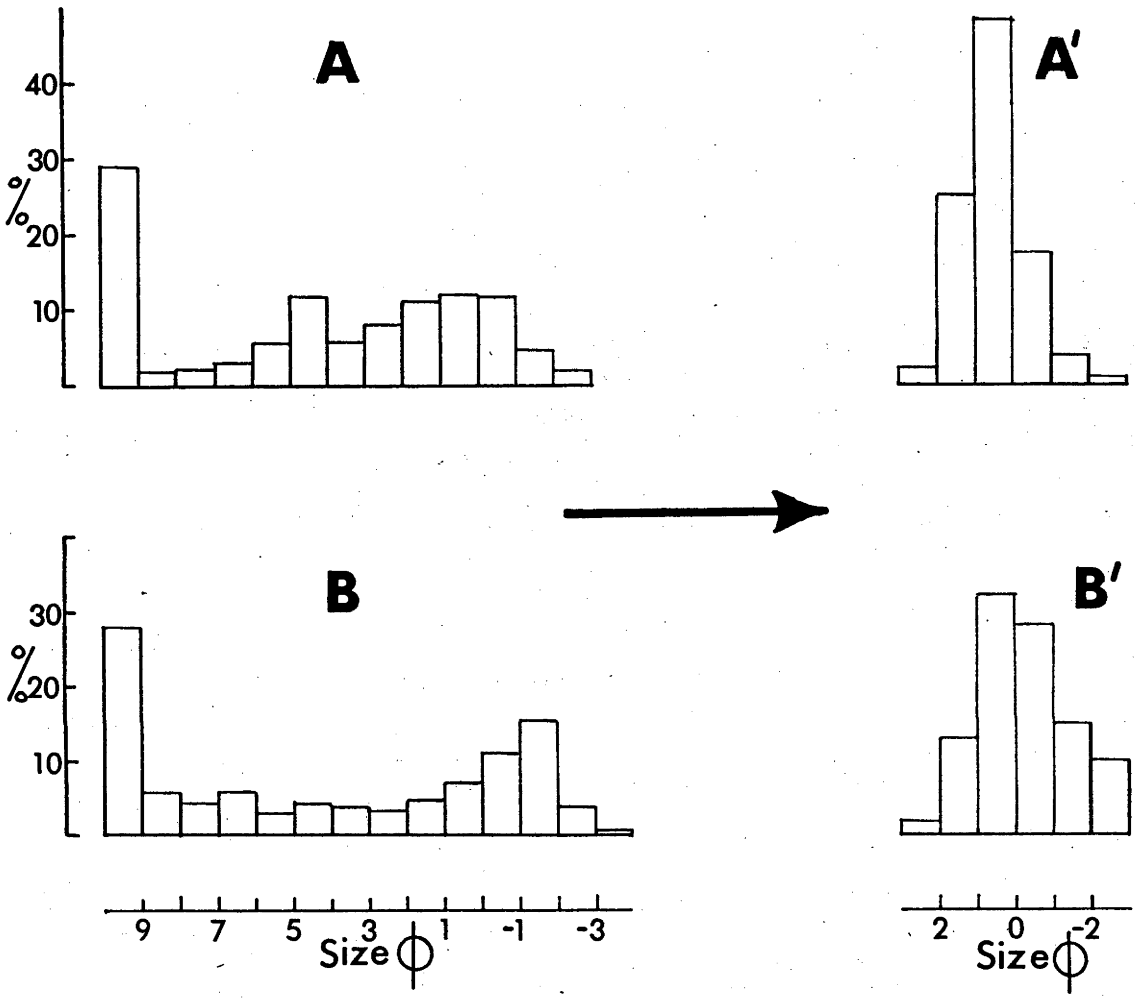

Figure 8.9 The reduction in initial differences between particle-size populations through the effects of fluvial transport.

A: 'Average' particle-size distribution of in situ weathered Wantabadgery Granodiorite (McConnell, 1979).

B: 'Average' stream-bed sediment size distribution for streams draining the Wantabadgery Granodiorite (McConnell, 1979).

C: Particle-size distribution of sample GR104, which is taken as indicative of the stream-bed sediment source population, for streams draining the Wallagaraugh Adamellite.

D: 'Average' stream-bed sediment size distribution for streams draining the Wallagaraugh Adamellite (see Figure 3.3).

carried by the size-shape characteristics of the individual particles (Ehrlich et al., 1980).

SUMMARY

It would appear that as the scale of the landscape components examined increase, the effect of:

1) Parent rock, although important in determining the range in size of particles available, becomes less conspicuous.
2) Environmental processes, principally those involving the size sorting of particles, becomes increasingly apparent.

Care is required in the interpretation of specific particle-size distributions as the distributions themselves may not be process specific.

8.6 AN EMPIRICAL APPROACH TO PARTICLE-SIZE INTERPRETATION

Two persistent features or principles can be recognised from the particle-size data collected. These principles, once described could be considered as self apparent. The question arises however, if these principles and their implications were self apparent, why has so little progress been made in the development of models for such an important landscape parameter as particle-size.

The first principle involves the recognition that particles are formed as a result of either growth or comminution. The effects of comminution are readily apparent in the landscapes examined. Initially coherent rock masses, on weathering, give rise to particles which can vary in size by many orders of magnitude. The effects of growth though not as readily apparent (e.g., nodules are rare), are as equally important. It is probable that many of the neoformed clay minerals are a result of growth.
The processes limiting the size of particles formed by growth (e.g., neoformed clay minerals) are likely to be a combination of the availability of material for continued growth and the equilibrium between the processes controlling growth and comminution.

Particle comminution is most likely to occur along those discontinuities requiring the least energy to cause failure. Consequently, daughter particles will be inherently stronger than their parent. Consequently, for a given set of boundary conditions, unless the daughter particles weaken through the effect of fatigue or chemical alteration, the rate of comminution will decrease as the bonds required to be ruptured become progressively stronger. The progressive increase in the amount of energy required for continued rupture of daughter particles has been described by Moss (1972).

The i) growth of clay minerals is limited by the inherent insolubility of aluminium; ii) cessation of comminution of daughter particles as they become stronger relative to their parent; and iii) the existence of coarse sandy stream-bed sediments in terrains which produce both sand and clay, all have one thing in common, they are the expression of the existence of a 'rate limiting step'.

The 'rate limiting step' is the basis of the second principle. Its importance in chemistry is well recognised; the rate of formation of a species involving a series of reactions is determined by the rate limiting step. The examples cited above show that in a landscape the effects of the rate limiting step can be manifest at all scales.

The value of these two principles is seen, not in their ability to provide an immediate alternative to the conventional approaches to particle-size distribution (Section 8.1.3), but as a means of focusing attention on specific processes. The focusing effect of these two principles is implicit in the discussion of particle-size modes (Section 8.3).

Two other examples are used to illustrate this focusing effect. Firstly, if the sizes of clay minerals in a landscape are to be considered, then those processes which give rise to their formation and growth and those which cause their comminution must both be considered. Secondly, if the rate of landscape lowering is considered, this rate will be determined by the rate at which the slowest particle is removed. If there is insufficient energy to remove these slowest particles, they will be retained and form a residual layer. This amouring effect will tend to prevent further lowering of the landscape.

The continued exploitation and development of these principles awaits additional work.

CHAPTER 9

MINERALOGICAL FEATURES OF SURFICIAL MATERIALS

9.1 INTRODUCTION

In this chapter, the following are discussed:

i) the relative persistence of various minerals in the weathering environment; and

ii) the effect of parent rock on the size distribution of quartz, clay mineralogy and the composition of first cycle sands derived from granite.

Where appropriate comments are made on the existing climate based interpretations of regolith properties.

9.2 MINERAL BEHAVIOUR

The minerals in the profiles examined are either inherited from the parent rock or formed by its weathering. From Chapters 3 to 7 it would appear that all the primary minerals examined are susceptible to alteration. This alteration can result in both the chemical change and physical comminution of the mineral. As a result of the variation in physiochemical properties of the primary and neoformed minerals, their separation readily occurs, the most notable example being the physical separation of the neoformed clay minerals from quartz.

For the granite and rhyolite, the persistence of the dominant rock forming minerals is (in order of increasing persistence) plagioclase << K-feldspar<quartz. This sequence is consistent with that proposed by Goldich (1938). The comparative persistence of quartz and illite the dominant minerals in the metasediment and sandstone, could not be equivocally determined.

Unlike the major minerals, such as quartz and feldspar, the persistence of the minor minerals (biotite, apatite and zircon) can not be readily directly determined due to their low abundance. It is possible to indirectly infer the persistence of these minerals from the behaviour of elements concentrated in them (Table 3.12). Based

on the behaviour of the following indicator elements: Fe^{2+}, Mn, Zn (biotite); P (apatite); and Zr (zircon) in the profiles examined: biotite is comparable in persistence to plagioclase; apatite lies between K-feldspar and plagioclase in persistence; and zircon is more persistent than quartz.

9.2.1 Quartz: Its Size Distribution

Pettijohn (1975, p.44) states: "The size distribution of quartz grains must be closely restricted by the size distribution of quartz in the phaneritic crystalline rocks. Grains larger than 1mm are rare. The blocks generated become pebbles whose abrasion produces silt or clay-sized material, not sand. Moreover, further breakage in general does not occur unless exceptional forces come into operation. The decomposition products are of clay size; and hence it would appear that there should be a deficiency in the silt [2 to 63μm] range. Silt, however is relatively common, and its production is a problem".

The Size of Quartz in Phaneritic Rocks

As phaneritic rocks are the dominant source of quartzose sediments, the size of quartz within them is of interest. Dake (1921), Feniak (1944) and Blatt (1967) measured the average size of quartz in some plutonic rocks and found it to be 0.46, 0.52 and 0.72mm respectively. The range in size of quartz framework grains in the Wallagaraugh Adamellite was shown to commonly be 2 to 7mm (Appendix C). The size of quartz in the Bega Batholith of which the Wallagaraugh Pluton forms a part, ranges from approximately 1mm to 10mm and is most commonly between 3mm to 6mm (Beams 1980). The Bega Batholith is similar in texture to batholiths throughout the world (B.W. Chappell, pers.comm.).

Thus, the size of quartz given by Dake (1921), Feniak (1944) and Blatt (1967) although carefully measured for the samples examined, are not representative of the average global distribution. Therefore, the use of Dake, Feniak and Blatt's measurements as a basis for calculating the global change in the size of quartz between phaneritic rocks and their derived sediments (e.g., Blatt, 1970) are likely to be in error. Furthermore, it would appear that Pettijohn (1975) is wrong in asserting that parent rock quartz grains larger than 1mm are rare.

The Parent Rock Effect

The effect of differences in parent rock origin and history on the size distribution of quartz grains is illustrated by the weathering of granite, sandstone and rhyolite. During the weathering of granite it was shown (Section 3.4) that quartz comminution was common. This is attributed to the release of internal strain produced as a result of their cooling history (Moss, 1966; Winkler, 1980). By contrast it was inferred that quartz grains in profiles SS1 and SS3 underwent comparatively little comminution during profile formation. This is consistent with the following:

1) The quartz grains in the sandstone consist initially of 'sound' grains, as those grains predisposed to breakage were removed within the fluvial environment prior to deposition (Moss, 1966).

2) Absence of features indicating the pervasive deformation of the sandstone which would have tended to 'reset' the quartz grains, making them prone to breakage during their release with weathering.

In contrast with the granite and sandstone, the rhyolite is fine grained, with much of the quartz being silt-sized. Section 4.3 showed that much of the quartz was released with weathering as silt-sized grains.

Silt-Sized (2-63μm) Quartz

Various proposals for the formation of silt-sized quartz are: 1) chipping of silt-sized particles from larger grains (Rogers *et al.*, 1963; Smalley and Vita-Finzi, 1968); 2) weathering of fine grained quartzose rocks (Kuenen, 1969); 3) glacial grinding (Vita-Finzi and Smalley, 1970); and 4) fragmentation of larger grains (Moss *et al.*, 1973; Krinsley and Smalley, 1973).

As argued in Section 3.4.1, the occurrence of quartz grains finer than 1ϕ in profile GR1 is dominantly a result of the *in situ* fragmentation of larger grains. Given that:

1) the proportion of quartz <63μm in sample GR103 is 20% and that material similar to GR103 is common throughout the catchment; and

2) severe comminution of granitic quartz occurs during fluvial

transport (Moss, 1972b), then it is likely that a substantial proportion of quartz (30 to 40%, as a first order estimate) will be silt-sized (<63μm) when removed from these small catchments.

Section 4.3 has shown that with weathering, much of the quartz in the rhyolite is concentrated in the silt fraction. Consequently, Rogers et al., (1963) are wrong in asserting that the separation of individual parent rock grains with rhyolite weathering and the consequent formation of silt sized quartz is unlikely.

Summary

1) Quartz grains larger than 1mm in phaneritic rocks (the pristine source of sediments) are not rare. Substantial fragmentation of pristine quartz can readily occur.
2) The size of quartz grains formed with weathering depends on the interaction of three factors; parent rock grain size; strain within the quartz grains of the parent rock; and the effectiveness of the weathering process in allowing strain release.
3) The weathering of granite and rhyolite under conditions of low to moderate relief and warm temperate and subhumid climate, shows that the production of silt-sized quartz is readily achieved.

9.2.2 Clay Mineralogy (clay fraction)

The clay mineralogy of the regolith in the study area is summarised in Figure 9.1. From Figure 9.1 and previous discussion, the following points can be made:
1) Figure 9.1A shows for the regolith derived from the metasediment that a systematic difference in illite content exists between the regolith occurring in the coastal forests and further to the west, on the Bondi Plateau (Figure 2.1). The lower gravel content of regolith from the Bondi Plateau (Hough, 1982) compared with the coastal forest suggests that the Bondi Plateau regolith is more strongly weathered. Consequently the difference in illite concentration between the two areas may reflect the progressive destruction of illite with weathering.
2) As the granite and rhyolite (Figure 9.1C and D respectively) have similar chemistry, bulk mineralogy and the profiles examined occupy similar topographic positions, it was thought that

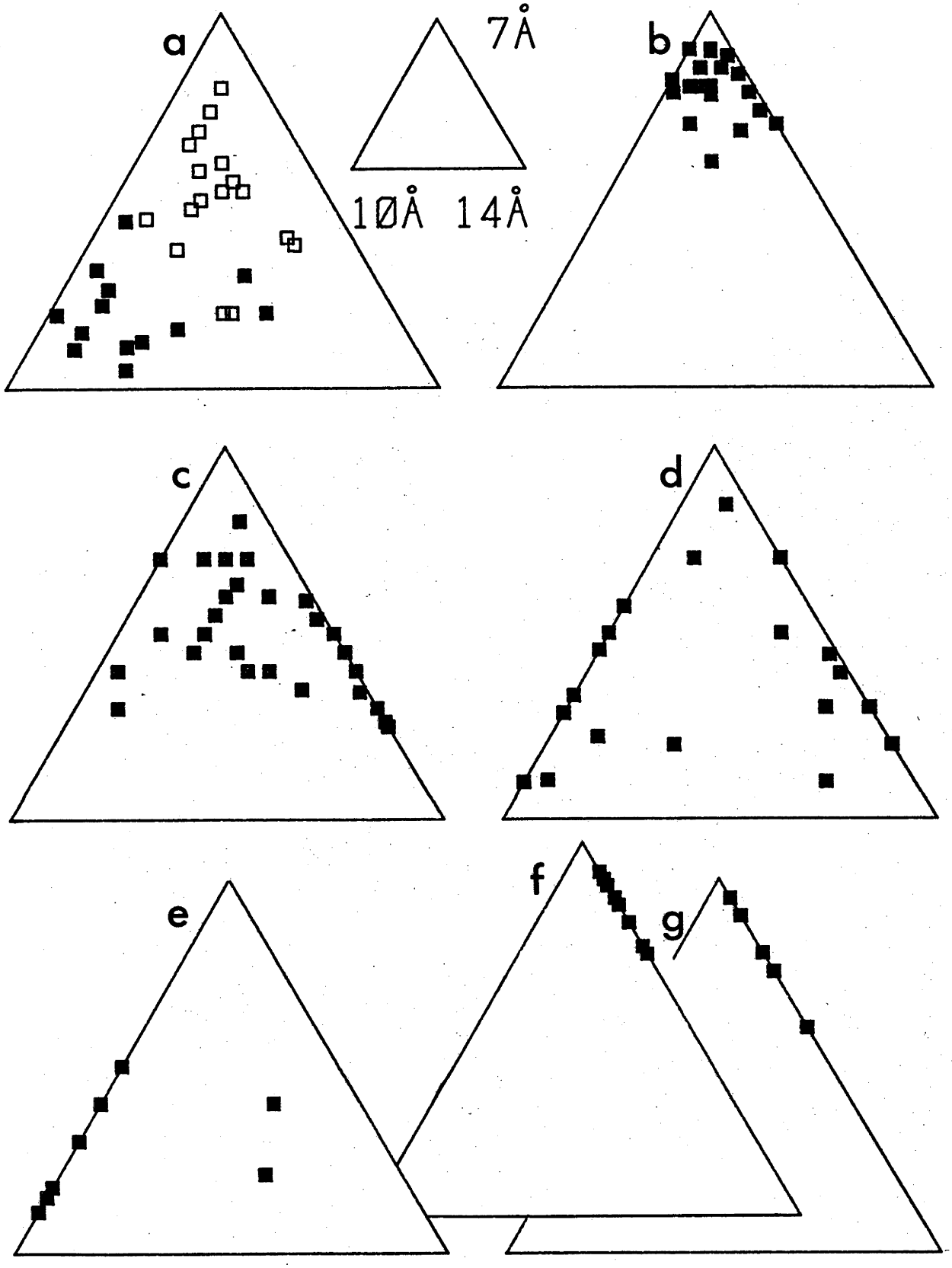

Figure 9.1 Parent rock dependent variation in regolith clay mineralogy (7, 10, 14Å clay minerals, clay fraction).

A: Metasediments (■ , coastal forests (Chapter 5); □, Bondi Plateau (Hough, 1982).
B: Granodiorite (Table 9.1).
C: Granite (Chapter 3).
D: Rhyolite (Chapter 4).
E: Devonian sediments (Chapter 6).
F: Tertiary sediments (Table 9.1).
G: Basalt (Chapter 7).

Table 9.1 Clay mineralogy (clay fraction) of regolith samples derived from Tertiary sediments (Hough and Beams, 1979) and granodiorite. The granodiorite samples are from Nalbaugh State Forest (east of Bombala). nd, not detected; tr, trace.

Sample Number	Depth cm.	Clay Mineralogy % A			
		14	12	10	7
Parent Rock: Tertiary sediments.					
5/2C		10	nd	nd	90
5/2A		15	nd	nd	85
10/8A		15	nd	nd	85
10/8D		30	nd	nd	70
11/12C		10	nd	nd	90
11/12D		10	nd	nd	90
12/12B		10	nd	nd	90
12/12C		30	nd	nd	70
12/8C		20	nd	nd	80
12/8D		15	nd	nd	85
Parent Rock: granodiorite. Sample numbers are those of the Forestry Commission of NSW.					
48A	0-25	10	nd	20	70
48B	25-115	5	nd	5	90
48C	115-200	nd	nd	tr	90
51A	0-30	20	nd	tr	80
51B	30-200	10	nd	tr	90
14A	0-30	30	nd	nd	70
14B	30-105	10	10	10	70
14C	105-200	tr	nd	20	80
22A	0-30	25	nd	tr	75
22B	30-90	10	tr	tr	90
22C	90-200	5	nd	10	85
7A	0-30	20	nd	20	60
7B	30-90	10	tr	10	80
7C	90-200	5	5	5	85
88A1	0-18	15	nd	tr	85
88A2	18-40	10	nd	tr	90
88B	40-90	10	nd	10	80
88C	90-200	5	nd	10	85
86A1	0-40	10	nd	10	80
86A2	40-90	10	nd	5	85
86B	90-200	nd	nd	10	90
90A1	0-25	25	nd	tr	75
90A2	25-60	15	nd	10	75
90B	60-100	5	nd	10	85
90C1	100-125	5	nd	15	80
90C2	125-200	10	nd	10	80

the regolith clay mineralogy would be similar. The difference in clay mineralogy may be an expression of the difference in the subsolidus alteration products of the two rocks. The testing of this hypothesis was outside the scope of this thesis.

3) Compared with the igneous rocks, a greater proportion of the clay minerals present in the regolith derived from sedimentary rocks are inherited (refer to Chapters 5 and 6).

4) Illite was not detected in the regolith derived from basalt (Figure 9.1G). This is due to the low parent rock concentration of K_2O which limits its formation (Barshad, 1966).

Thus, in the study area, regolith clay mineralogy depends on the interaction of two factors: i) the occurrence and composition of aluminosilicate minerals in the parent rock; and ii) weathering processes which determine the nature of the neoformation processes that occur. The effect of parent rock mineralogy is most pronounced when it either limits the formation of particular clay minerals, because of the low abundance of key elements, or results in the direct inheritance of clay minerals.

Further, this study shows that: i) a considerable variation in clay mineral concentration and mineralogy can occur in a relatively small geographic area; and ii) despite climate being considered the major determinant of clay mineralogy (Birkeland, 1974), this variation in clay mineralogy developed independently of climate.

9.3 MINERALOGY OF FIRST CYCLE SANDS DERIVED FROM GRANITE

The mineralogy of first cycle sands in granite landscapes has been described in detail by Basu (1976). Basu's work is important because its seminal nature is likely to influence later studies. Basu (1976) found that: i) there is systematic variation in the proportion of quartz, feldspar and rock fragments with grain size; and ii) when grain size is held constant, sands formed under differing climates can be distinguished from each other by their mineralogy.

Basu (1976) coined two terms to describe his data when plotted on a QFR diagram (Figure 9.2a). These terms are: 'tie lines', lines joining genetically related size separates; and 'trend lines', lines joining identical size separates derived from different sources. Basu (1976, p.705) states that "the trend lines signify trends of compositional variation with degree of weathering [and that] what has been termed 'degree of weathering' is really a measure of total energy expended[1] on the sands, and [hence] the concept of mineralogical maturity is therefore applicable (Lindsay, 1974). The position of a sand fraction on the trend line signifies its relative maturity [the greater the proportion of quartz, the more mature the sand]".

In respect to Basu's work, a comparison of the mineralogy of first cycle sands from the Wallagaraugh Adamellite and the portion of the Gabo Island Granite[2] occurring in the Watergums Creek area is instructive. These data (Figure 9.2c) are consistent with the size dependent trends described by Basu (1976). With decreasing grain-size, these trends are; the concentration of rock fragments decreases; the concentration of feldspar increases; and the concentration of quartz initially increases rapidly and then decreases slightly.

A QFR plot of these data (Figure 9.2b) shows that a difference in quartz enrichment, expressed as a separation along trend lines, exists between sands derived from the Wallagaraugh Adamellite and Gabo Island Granite. According to Basu (1976, p.705) this separation along trend lines is due to differences in the energy expended within, and climatic differences between the two sand source areas. If this argument is correct, then field evidence to this effect should be readily apparent.

The source areas for sands derived from the Wallagaraugh Adamellite and Gabo Island Granite are approximately 20km apart (Figure 2.2),

---

1 Basu provides no clear definition of the meaning of the term 'energy expended'. He cites Lindsay as a reference. Lindsay (1974, p.862) cites Pettijohn (1957). The inference from Pettijohn is that 'energy expended' is the product of the 'intensity of weathering' and time.

2 The location of the Gabo Island Granite is given in Figures 2.1 and 2.2. It is fine to medium grained, 1mm to 3mm and even textured (Appendix C). The mineralogy of first cycle sands derived from the Gabo Island Granite is given in Table 9.2.

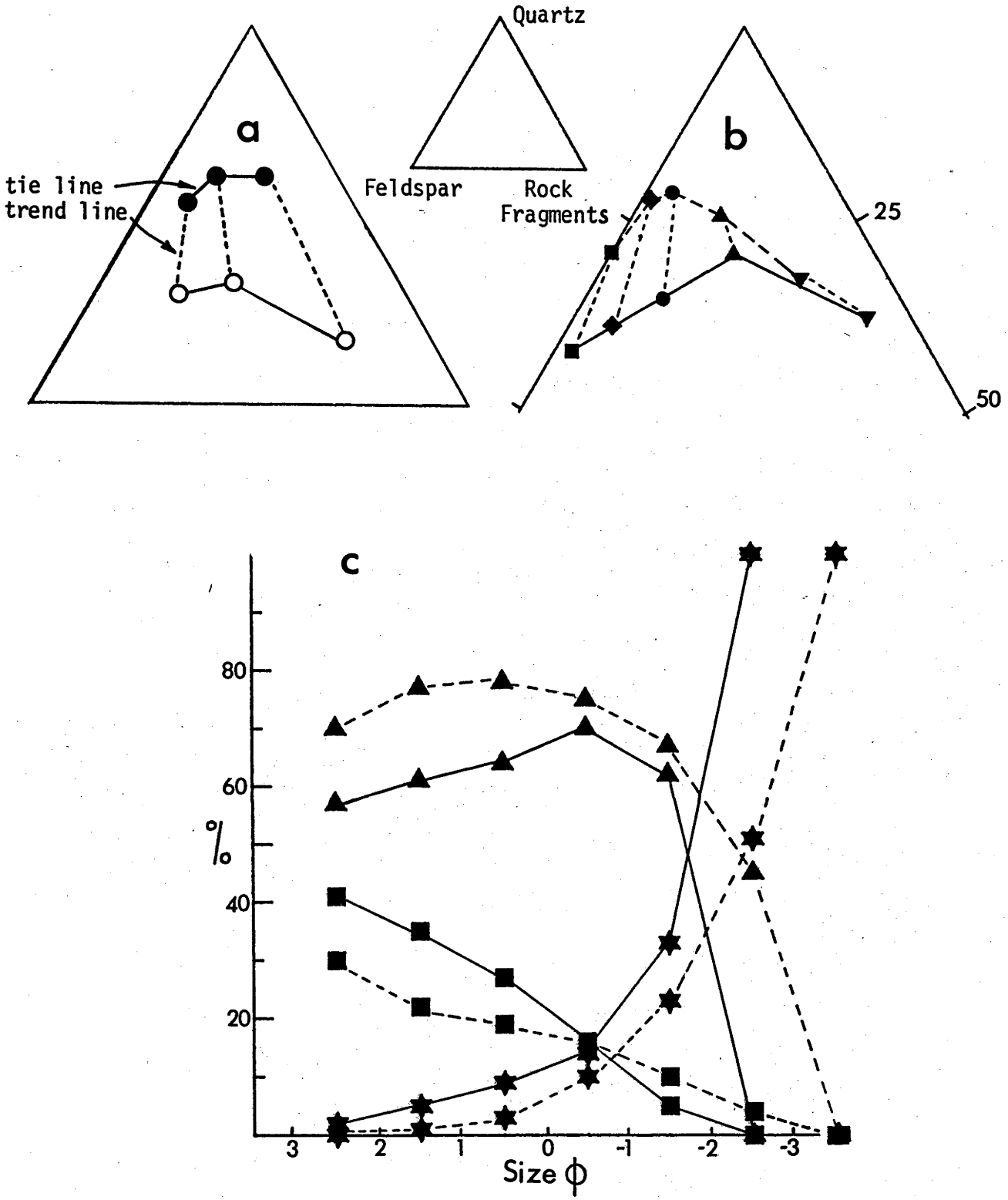

Figure 9.2 Mineralogy of first cycle sands derived from granite.

A: Mineralogy of the -1 to 1ϕ , 1 to 2ϕ, 2 to 4ϕ size fractions (corresponding to the decrease in rock fragments) of sands formed under humid (●) and arid (○) climates; showing tie and trend lines (data from Basu (1976)).

B; Size dependent variation in mineralogy of stream-bed sediments derived from the Wallagaraugh Adamellite (samples lying on the quartz-rich trend line) and the Gabo Island Granite. Data are given in Tables 3.20 and 9.2. Size fractions are; ■, 3 to 2ϕ; ◆, 2 to 1ϕ; ●, 1 to 0ϕ; ▲, 0 to -1ϕ; ▼, -1 to -2ϕ.

C: Size dependent variation in mineralogy of stream bed-sediments derived from the Wallagaraugh Adamellite (broken line) and Gabo Island Granite (solid line). Data are the same as B, above. Symbols: ★, rock fragments; ▲, quartz; ■, feldspar.

Table 9.2 Mineralogy of stream-bed sediment size separates derived from the Gabo Island Granite. The samples were collected from within the Watergums Creek area (Hough, 1982) and the mineralogy determined on the over-size fraction. Particles >-2ϕ in size consist of 100% rock fragment.

Sample Number	Quartz % Size ϕ					Feldspar % Size ϕ					Rock Fragment % Size ϕ				
	3	2	1	0	-1	3	2	1	0	-1	3	2	1	0	-1
1	58	70	83	87	74	40	27	12	7	3	2	3	5	6	23
2	57	52	58	65	45	39	42	26	8	2	4	6	16	27	53
3	57	61	57	68	54	36	28	32	17	7	7	11	11	15	49
4	68	76	73	79	72	30	24	18	11	3	2	0	9	10	25
5	45	58	67	75	60	55	36	22	12	3	0	6	11	13	37
6	70	60	63	68	63	30	34	29	23	8	0	6	8	9	29
7	56	55	58	65	66	44	42	38	24	6	0	3	4	11	28
8	49	59	72	77	65	51	36	16	9	2	0	5	12	14	33
9	67	71	56	73	68	31	25	40	23	7	2	4	4	4	25
10	66	62	61	81	79	34	35	35	12	5	0	3	4	7	16
11	52	61	58	59	62	47	34	29	6	4	1	5	13	35	34
12	63	67	63	72	63	36	29	22	16	7	1	4	10	12	30
13	49	53	60	73	61	48	37	30	11	4	3	10	10	16	35
14	65	52	60	54	47	34	43	28	23	5	1	5	12	23	48
15	48	57	62	64	52	51	46	30	19	4	3	7	8	17	44
16	61	64	64	72	63	39	32	24	14	8	0	4	12	4	29
17	47	62	68	66	63	51	36	26	26	12	2	2	6	8	25
18	48	61	60	66	60	52	35	31	17	5	0	4	9	17	35
$\bar{x}$	57	61	63	70	62	42	35	27	15	5	2	5	9	14	33
σ	8	7	7	8	9	8	6	7	6	3	2	3	3	8	10

have similar prevailing climate and relief. There is no field evidence to suggest that the residence time of grains in the weathering environment differs between the two source areas.

An alternative explanation for the enrichment of quartz in sands derived from the Wallagaraugh Adamellite is that it simply reflects differences in source rock texture. The Wallagaraugh Adamellite is coarse grained (2mm to 7mm), whereas the Gabo Island Granite is comparatively fine grained (1mm to 4mm) (Appendix C).

For the Gabo Island Granite, monomineralic particles can only commonly occur to 4mm in size. Particles larger than 4mm are likely to be coarser than the grain size of the parent rock and consequently will be polymineralic (rock fragments). By comparison, for detritus derived from the Wallagaraugh Adamellite, monomineralic grains (e.g., quartz) can commonly occur to 7mm in size. This initial difference in quartz/grain-size concentration between the detritus from the two rock types leads to a systematically higher quartz content (quartz is more persistent than feldspar) for sand size separates from the Wallagaraugh Adamellite.

To test the effect of climate on mineralogy, a compilation of the composition of first cycle sands derived from granite is given in Figure 9.3. If Basu's (1976) 'climate/mineralogy' hypothesis were universally applicable, then a simple and persistent relationship between mineralogy and climate should be observed. Figure 9.3 shows that this is not the case. Although there were differences in the techniques used to measure mineralogy (counts were done on either thin-section-resin-impregnated sand, or loose grains), these are not sufficient to account for the absence of a persistent trend in Figure 9.3.

The absence of a simple, persistent mineralogy/climate trend is attributed to:

1) Differences in texture of the source rocks.

2) Variation in the distance of fluvial transport of the sands examined. Basu (1976) assumed that fluvial transport for distances up to 19kms was not likely to cause mineralogical changes due to

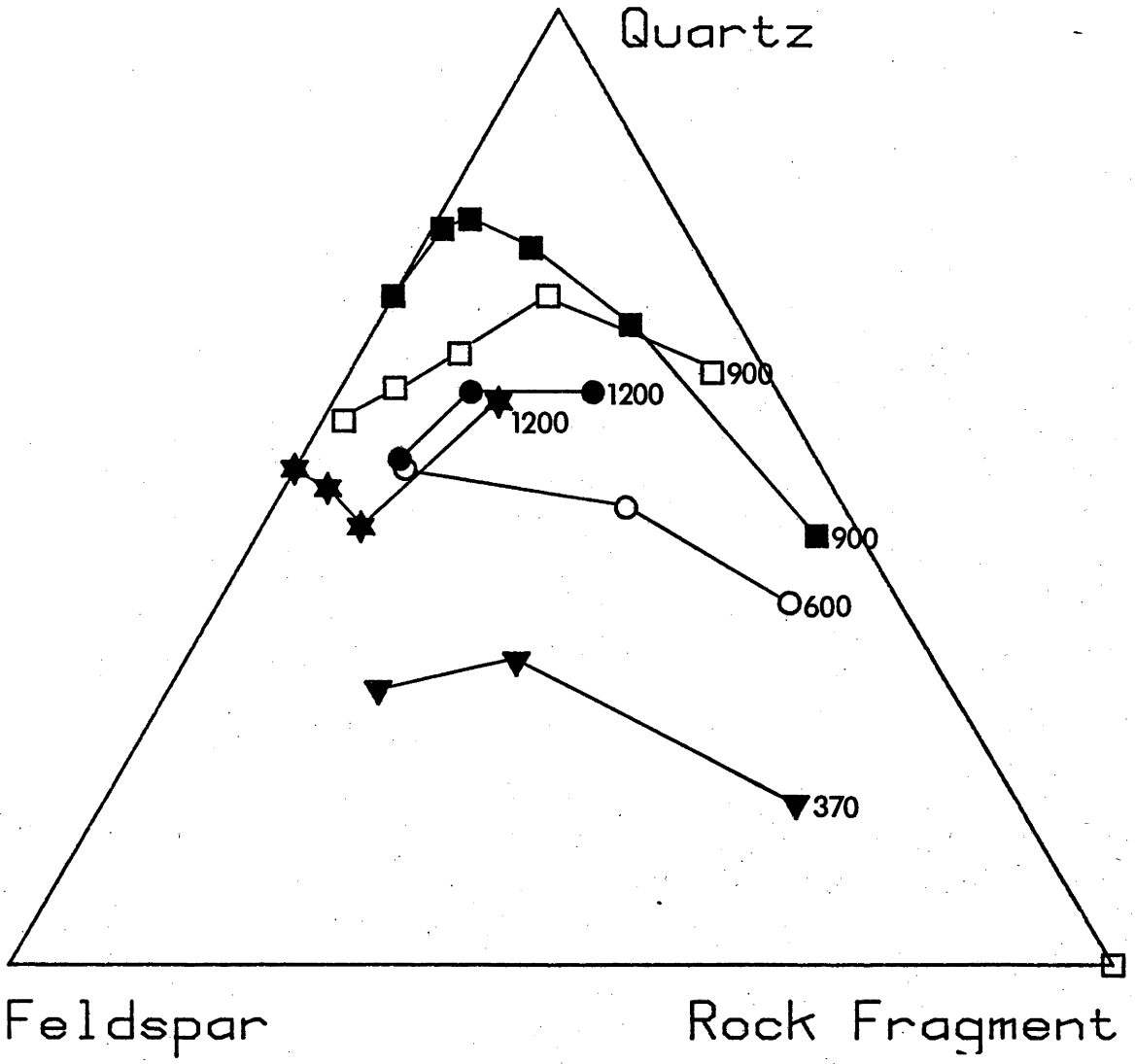

Figure 9.3 Composition of first cycle sands derived from granite in relation to climate. Genetically related size separates are joined by a tie line.

Data Source	Symbol	------ Present Climate ---- -------- Mean Annual ------ Rainfall mm	*Temperature °C	Relief
Mann and Cavaroc,1973	★	1200	15	low
Basu,1976	●	1200	18 (GW)	medium
Basu,1976	▼	370	7 (GW)	low
McConnell,1979	○	600	23(S),9(W)	low
This study				
Wallagaraugh/ Adamellite	■	900	19(S),8(W)	low
Gabo Island Granite	□	900	19(S),8(W)	low

* GW: ground water
S: summer
W: winter

grain breakage. This is contrary to the work of Moss (1972a) and McConnell (1979) which showed that substantial grain breakage, resulting in a change in mineralogy of size separates, would occur during transport over distances substantially shorter than 19km .

3) The mineralogy of first cycle sands derived from a particular catchment is likely to vary with time as the sediment source changes. For example, the mineralogy of sands will differ depending on the ratio of slope wash to gully erosion, and changes in the 'average weathering rate' to 'average erosion rate' ratio.

4) The variation in the lag time between weathering, consequent particle formation, and particle incorporation within the stream-bed sediments. This is likely to vary with relief and climate and could be in the order of tens of thousands of years. In this case, the climate which currently prevails in the sediment source area is likely to differ considerably from that which prevailed during the time in which the sediment characteristics were being determined by weathering.

The position of a size separate relative to the quartz apex on a QFR diagram is a measure of its mineralogical maturity. It is apparent however, that it is not a reliable indicator of the amount of energy expended during its formation. The position of a size separate reflects the complex interaction of those processes outlined above, consequently its use as a paleoclimatic indicator (Basu, 1976) should only be considered as tentative.

CHAPTER 10

CHEMISTRY OF SURFICIAL MATERIALS

10.1 INTRODUCTION

This chapter examines the effect of parent rock on regolith chemistry. This is done by examining: i) the effect of parent rock on the relative proportion of soluble products, hydrolyzates and relics in the regolith; ii) the nature of the parent rock signature in the profiles described; and iii) more generally, the nature of the difference between profiles derived from rocks of substantially different composition.

Before proceeding it is appropriate to discuss the following three important points: i) the division of major elements into the soluble products, hydrolyzate and relic groups; ii) the concept of chemical mobility; and iii) the concept of 'physical mobility' as an aid to understanding the separation of hydrolyzates and relics and variations in landscape chemistry.

10.2 ELEMENT BEHAVIOUR

10.2.1 Element Sources

The elements within a regolith are derived from either the source rock or the atmosphere. The principal atmospherically derived elements involved in weathering reactions are O, H and C.

Oxygen and hydrogen enter the profile dominantly as water in liquid form, whereas C enters the profile through either: i) the dissolution of CO_2 in water (particularly inthe soil atmosphere where the partial pressure of CO_2 is considerably higher than the atmosphere) to form the bicarbonate ion; and ii) plant uptake of CO_2 during photosynthesis and its subsequent inclusion in the regolith by biological cycling.

10.2.2 Element Fractionation: Soluble Products, Hydrolyzates and Relics

Because of marked differences in element behaviour with weathering, they can be divided into three broad groups. Although these groups can not be rigorously defined, the classification does provide a framework in which regolith chemistry can be examined. The three groups are; soluble products, hydrolyzates and relics. Soluble products are those elements present in unstable minerals which on weathering, form comparatively soluble species (e.g., CaO). Hydrolyzates are those elements in unstable minerals which, because of their inherent insolubility are precipitated on weathering, to form the neoformed minerals (e.g, Al_2O_3). Relics consist of those elements which occur in the resistant primary minerals (e.g., SiO_2 in quartz).
The classification of the major elements is summarised in Table 10.1.

It will be shown that it is the separation of these groups, as a result of their differing physiochemical properties which gives rise to the principal variations in regolith chemistry.

10.2.3 Chemical Mobility

The concept of chemical mobility has proved useful in understanding the gross features of the sedimentologic evolution of the earth's crust. Empirical estimates of chemical mobility are made either by comparing the concentration of an element in a rock with its concentration in the stream waters draining it; or by comparing the relative loss of an element during the rock to saprolite transition (Lelong et al., 1976).

Estimates of chemical mobility from the literature and saprolite samples GR108 and GR305 are given in Table 10.2. Table 10.2 shows that although there is a persistent difference in the estimated mobility between some groups of elements (e.g., Na_2O-CaO are more mobile than Al_2O_3- TiO_2- Fe_2O_3) other elements show marked variations in mobility.

Although the concept of chemical mobility has been used in weathering studies, it has not proved to be as successfull an approach as its use may suggest. To date, there has been little attempt to explain

Table 10.1 Partitioning of major elements with weathering. Where partitioning within a particular phase is important it is indicated 'x'.

	Phase		
	Soluble Products	Hydrolyzates	Relics
SiO_2	X		X
TiO_2		X	X
Al_2O_3		X	
Fe_2O_3		X	
MgO		X	
CaO	X		
K_2O	X		
Na_2O	X		

Table 10.2 Estimates of chemical mobility, listed in order of decreasing mobility.

$CaO > Na_2O > MgO > K_2O > SiO_2 > Al_2O_3 = Fe_2O_3$ (Smyth, 1913; Polynov, 1937)

$MgO > CaO > Na_2O > K_2O > SiO_2 > Al_2O_3 = Fe_2O_3$ (Anderson and Hawkes, 1958)

$CaO > Na_2O > MgO > SiO_2 > K_2O > Al_2O_2 > Fe_2O_3$ (Feth et al., 1964)

$CaO \simeq MgO \simeq Na_2O > K_2O > FeO > SiO_2 > TiO_2 > Fe_2O_3 > Al_2O_3$ (Loughnan, 1969)

Relative mobility of elements for selected samples from the granite regolith. Element mobility was calculated from its relative loss/gain compared with the average parent rock concentration. The mobility of Fe was calculated from the total Fe concentration expressed as Fe_2O_3.

Sample

GR108 $CaO > Na_2O > SiO_2 > K_2O > Al_2O_3 > TiO_2 > MgO > Fe_2O_3$

GR305 $Na_2O > CaO > K_2O > SiO_2 > Al_2O_3 > MgO > TiO_2 > Fe_2O_3$

this lack of success.

Two groups of reasons are advanced to explain this. They are:
i) the dependence of element behaviour on its host mineral; and
ii) the weathering environment.

Host Mineralogy

A particular element can occur in a number of different minerals in the same rock and in different minerals in different rocks.

In granite (Chapter 3) SiO_2 occurs in both quartz and feldspar (Table 3.11). The mobility of SiO_2 in quartz (a relic) is similar to the behaviour of other elements retained in the weathered residue in that it is low. During the weathering of feldspar, SiO_2 is both retained in the neoformed mineral, and removed in solution. The SiO_2 retained in the neoformed mineral has a low mobility similar to Al_2O_3 whereas the SiO_2 not retained has a high mobility, comparable with that of CaO and Na_2O which form soluble compounds and are leached from the regolith. Consequently, the intermediate mobility of SiO_2 (Table 10.2) represents the average of a high and low estimate of mobility and does not result from any specific process.

Consider the distribution of MgO in basalt and granite with weathering in an active leaching environment. In basalt much of the MgO is present in olivine and pyroxene. With the weathering of these host minerals, little MgO is retained in the neoformed minerals (Bain et al., 1980). Consequently, MgO has a high mobility. In granite (s.s.) biotite is the dominant MgO host mineral. If biotite is converted to oxybiotite then, because of the comparative stability of this neoformed mineral (Paton, 1978) much of the MgO will be retained in the weathering environment. Thus, MgO will have a low mobility.

The variation in host mineralogy is the dominant reason for the variation in MgO mobility in Table 10.2. For example, Loughnan (Table 10.2) lists MgO as being as equally mobile as CaO and Na_2O, whereas Nesbitt et al., (1980) and this thesis (Table 10.2) show that MgO is, considerably less mobile than CaO and Na_2O.

Weathering Environment

The localised variation in environmental factors can markedly alter the chemical mobility of an element. In water logged areas developed on the granite (e.g., the environment in which profile GR2 occurs) it is probable that the Eh suppression causes a reduction of Fe^{3+} to Fe^{2+} and a consequent increase in the mobility of iron. However, if when Fe^{2+} enters the stream environment, much of it would oxidise as a result of the oxic nature of the stream environment and be removed from solution. P is removed through leaching during incipient weathering of the granite and rhyolite. The rate of P loss decreases with weathering as the clay content (a measure of the surface active phase) increases as a result of P sorption and coprecipitation. Consequently, although solution loss is an important pathway for P in the rock/saprolite zone (and P is highly mobile within this environment), little P is likely to be removed from the landscape in solution. Thus, chemical mobility sequences are both parent rock dependent, despite assertions to the contrary (Anderson and Hawkes, 1958), and environment dependent.

Element mobility will only be adequately understood when tied to a specific group of weathering reactions in a specific environment.

10.2.4 Physical Mobility

This concept is introduced as an aid to understanding the changes in chemistry which occur as a result of the translocation of clay within a profile and size sorting of transported material. The physical mobility of an element depends on the size distribution of its host minerals, the more mobile elements are those which occur in the smaller sized minerals.

The variation in chemistry with particle-size for samples formed during the weathering of granite and rhyolite is given in Sections 3.5 and 4.4 respectively. They show that the most physically mobile elements are those concentrated in the clay fraction, the neoformed clay and oxide minerals (hydrolyzate group).

With the exception of those elements held in the relics (e.g., SiO_2 in quartz, Zr and Y in zircon), the clay fraction tends to act as a 'chemical sink', such that with increasing weathering, a greater proportion of some elements are concentrated within it. This is illustrated in Table 10.3.

Table 10.3 gives the proportion (as a percent) of the whole sample that occurs in the clay fraction (for any particular element). For example, Table 10.3 shows that the amount of Al_2O_3 contained in the clay fraction increases as a percent of the total concentration from 19% in GR107 to 51% in GR103; and yet the percentage of clay in the whole sample only increases from 11.0 to 13.7% respectively.

The degree of enrichment (expressed as percent loss or gain Table 10.3) of the clay fraction relative to the parent rock concentration is highly variable. The three major elements which show consistently high enrichment are those elements belonging to the hydrolyzate group; TiO_2, Al_2O_3 and Fe_2O_3. In sample GR103, for example, they show a percent gain of 320, 165 and 532 respectively.

Those trace elements which show persistently high gains are V, Cr, Mn and Ni, elements which tend to be sorbed on the clay and oxide minerals of the hydrolyzate group.

There are insufficient analyses of clay samples to equivocally demonstrate a relationship between the chemistry of the clay fraction and the parent rocks examined. It is likely, however, because of the sorptive capacity of the clay fraction, that differences in clay chemistry would exist for clays derived from rocks which differed chemically.

Thus, within a profile this difference in size distribution between the hydrolyzate and relic phase will, by the selective removal of micron and submicron sized hydrolyzates, lead to a change in chemistry. This variation in chemistry with particle-size becomes increasingly important with the removal of the entire profile by erosion and consequent transportation and deposition of particles which vary greatly in size. Within a landscape therefore, differences in transportation processes can lead to marked localised differences in particle-size and consequently chemistry (Reinson, 1973).

Table 10.3 Clay fraction composition calculated as either:

1) Percent loss or gain (%L,G) compared with the parent rock from which it was derived (GRRA, ERRA for samples derived from granite and rhyolite respectively). Loss is indicated as '-', and 'C' indicates the value should be multiplied by 100.

2) Percent of whole sample present in the clay fraction (% of WS).

		%clay	SiO_2	TiO_2	Al_2O_3	Fe_2O_3	MgO	CaO	Na_2O	K_2O	H_2O+
GR103	% of WS	13.7	8	15	51	45	22	5	14	19	58
	%L,G		-39	320	165	532	95	-96	-97	-38	12C
GR107	% of WS	11.0	6	15	19	27	12	3	10	7	37
	%L,G		-45	164	176	983	106	-98	-91	-33	13C
ER204	% of WS	43.8	28	47	72	86	22	53	44	34	82
	%L,G		-46	134	180	11C	-22	-86	-98	-83	13C

		P	Rb	Sr	Pb	Zr	Y	V	Cr	Mn	Ni	Cu	Zn
GR103	% of WS	35	48	19	21	3	11	44	28	39	55	41	50
	%L,G	-25	73	-59	-36	-37	-64	780	16C	-74	16C	215	38
GR107	% of WS	18	16	6	16	7	12	37	42	11	66	33	67
	%L,G	-38	36	-74	43	0	-64	11C	20C	-78	22C	216	116
ER204	% of WS	73	54	68	71	33	54	83	82	62	*100	*100	72
	%L,G	-36	-48	-31	99	1	7	10C	16C	-85	416	250	5

* the >100% recovery of Ni and Cu is attributed to sampling errors.

10.3 THE PROPORTION OF SOLUBLE PRODUCTS, HYDROLYZATE AND RELICS WITHIN THE REGOLITH

The variation in the proportion of soluble products, hydrolyzates and relics for samples derived from granite, rhyolite, metasediments and sandstone is given in Figure 10.1. This variation is illustrated where possible by the following samples; unweathered rock, the sample showing the maximum enrichment in hydrolyzates and the sample showing the maximum enrichment in relics. For ease of discussion, only the dominant major elements are considered.

Because of the uniformity of the granite and rhyolite parent rock, it was not necessary for the granite and rhyolite regolith samples chosen to be derived from the one profile. For example, samples ER203 and ER101 were chosen to represent the hydrolyzate and relic enriched rhyolite regolith samples respectively. As the metasediments and sandstone parent rocks vary in composition, only one profile from each, profile OR1 and SS1 respectively, is considered. Sample LW103 (Table 5.4) was assumed to be indicative of the composition of the parent rock for profile OR1. This assumption was based on immobility of Al_2O_3 during incipient weathering and the comparatively similar Al_2O_3 concentration of samples LW103 and OR105. Rock sample SSR1 was chosen for illustrative purposes as the parent rock for profile SS1. Compared with the parent rock there is little or no increase in concentration of the hydrolyzate fraction in profiles OR1 and SS1, consequently no hydrolyzate rich sample is plotted.

The arrows on the lines joining genetically related samples (Figure 10.1) indicate the direction of increasing intensity of weathering and soil forming processes.

Figure 10.1 shows that there is a progressive depletion in soluble products with weathering/soil formation. Concomitant with the initial loss of soluble products, the proportion of hydrolyzate may increase, as in the granite and rhyolite profiles, or decrease, as in the metasediment and sandstone profiles.

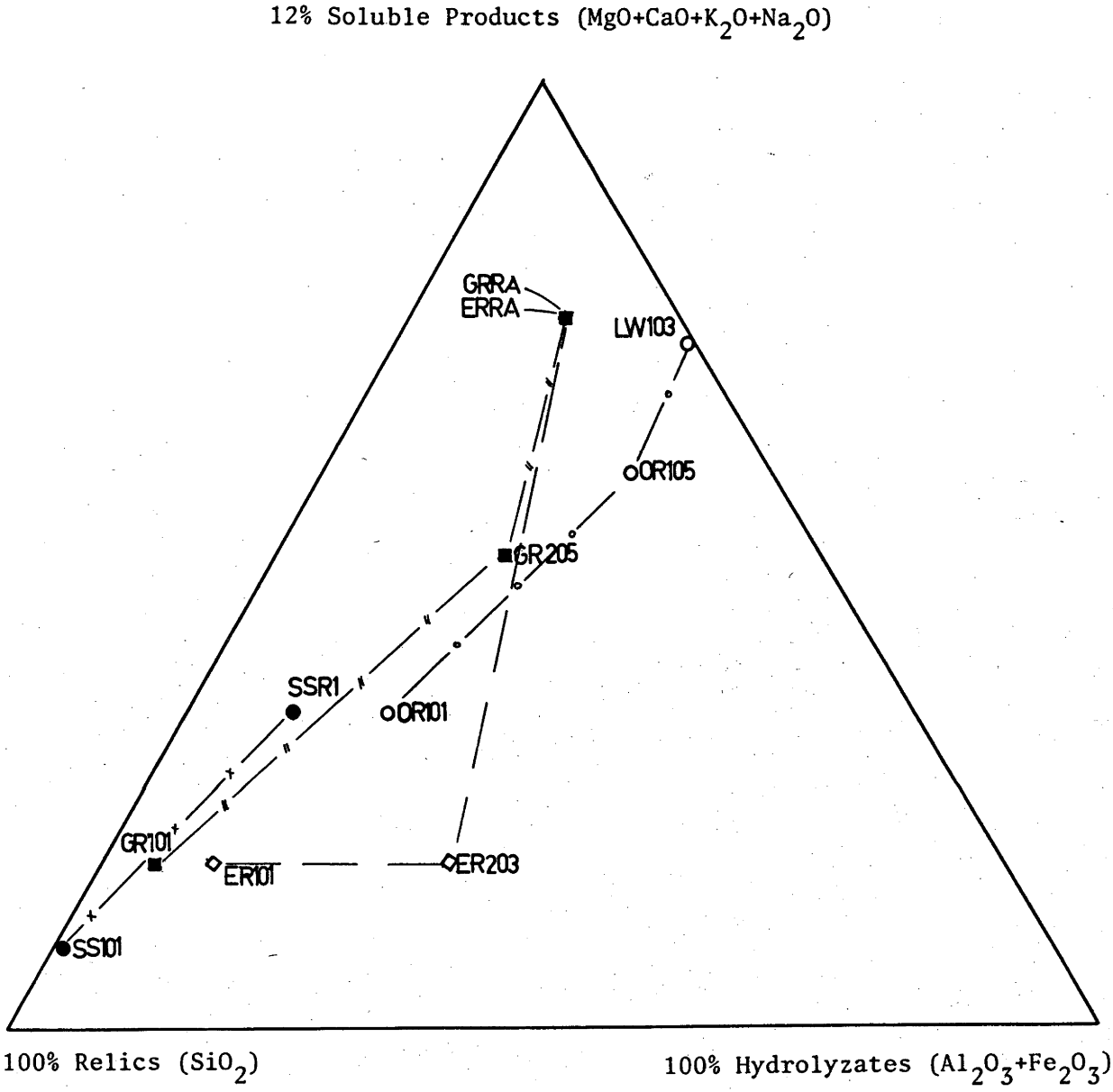

Figure 10.1 Soluble products, hydrolyzates and relics concentration. The composition of sample LW103 is given in Table 5.4. Note, this diagram forms part of a scalene triangle.

The difference between the granite/rhyolite profiles and the metasediment/sandstone profiles is a result of the sediments having been through a previous weathering cycle.

In the metasediment and sandstone, most of the soluble products, principally MgO and K_2O occur in the clay minerals (i.e., the clay mineral fraction is acting as a chemical sink). In addition, most of the hydrolyzate elements are already present in the relatively more stable clay and oxide minerals; in the sense that they represent the likely weathering end products of many silicate minerals. Consequently, the potential for chemical change of the regolith through the loss of soluble products for the metasediment and sandstone profiles is reduced compared with the granite and rhyolite profiles.

A striking feature of Figure 10.1 is the commonality of the separation of the three groups of elements for the profiles examined. This reflects the operation of the 'rate limiting step' principal described in Chapter 8. In a residual profile closed to particulate loss, it is the least soluble elements (hydrolyzates and relics) that remain. Whereas in a residual profile open to particulate loss, it is the least physically mobile elements (i.e., relics) which are retained.

Figure 10.1 shows that the parent rock composition is important in that it can effect the amount of change possible with weathering/soil formation. For example, because of the high initial concentration of relics the potential and actual change in chemistry of the sandstone profile is comparatively less than that of the other three rock types.

It would appear that with successive weathering and erosion cycles, and the concentration of relics in the resulting parent rock, that the potential for change in chemistry with weathering/soil formation is reduced. Consequently, under conditions similar to those which prevail in the Eden area, the chemistry of regolith developed from rocks rich in relics will vary little from the parent rock.

10.4 PARENT ROCK SIGNATURES IN THE REGOLITH

The extent to which the chemistry of the profiles in Chapters 3 to 6 reflect their parent rock was determined by discriminant function analysis. The results are summarised in Table 10.4 (detailed results are given in Hough, 1982). When using major and trace elements separately, 69 and 98% respectively of the samples could be correctly allocated. Those major and trace elements statistically significant in discriminating between parent rocks (listed in decreasing order of statistical significance) are respectively; Fe_2O_3, K_2O, Al_2O_3, TiO_2, H_2O+ and Y, Zr, Ni, Sr, Mn, P, Zn, Cu, Cr, V, Rb.

When both major and trace element data were combined, sample GR101 was the only sample which was not correctly grouped. Sample GR101 was most similar to the sandstone group. This similarity reflects the highly weathered and size fractionated nature of sample GR101; it consists dominantly of sand size quartz.

Because of the interaction which occurs between rocks and the weathering environment, it is important to demonstrate that the differences in regolith chemistry with parent rock are not a result of some parent rock related, fortuitous and systematic difference in the degree of weathering/soil formation. This is demonstrated using the granite/rhyolite pair.

The major element rock chemistry of the granite and rhyolite (Tables 3.3 and 4.3) is comparatively similar. The Al_2O_3/SiO_2 ratio is sensitive to both: i) weathering, in which Al_2O_3 tends to be conserved and SiO_2 lost; and ii) soil formation, in which Al_2O_3 is lost relative to SiO_2. Thus, if a systematic difference in weathering/soil formation were to exist between the granite and rhyolite regolith, it should be reflected in the Al_2O_3/SiO_2 ratio. Figure 10.2A shows that no systematic difference occurs.

A separation of the granite and rhyolite regolith samples does occur in the Y/TiO_2 plot* (Figure 10.2B). This separation of granite

---

* Two granite samples (GR207 and GR206) fall in the rhyolite field. This is a result of the anomalously high Y concentration in profile GR2 compared with profiles GR1 and GR3. Although samples GR207 and 206 can not be distinguished from the rhyolite regolith using Y/TiO_2 concentrations, they can be distinguished with the use of additional trace elements (Table 10.4).

Table 10.4 Prediction of group membership for samples from profiles OR1. 3; GR1, 2, 3; ER1, 2, 4; SS1, 3 using major elements and trace elements. The prediction of group membership for trace elements is shown in parenthesis.

Actual Group	Number of Samples	Predicted Group Membership			
		Metasediment	Granite	Rhyolite	Sandstone
Metasediment	10	7 (10)	3 (0)	0 (0)	0 (0)
Granite	20	0 (0)	12 (19)	4 (0)	4 (1)
Rhyolite	14	0 (0)	5 (0)	9 (14)	0 (0)
Sandstone	7	0 (0)	0 (0)	0 (0)	7 (7)

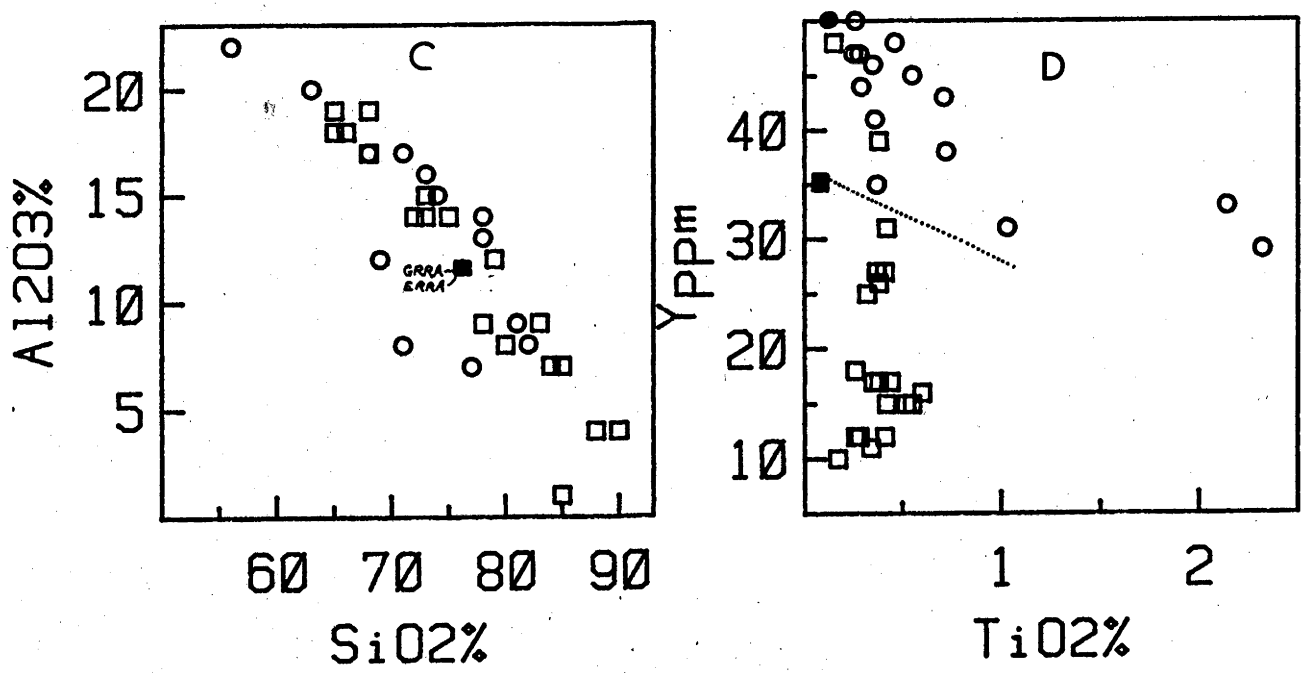

Figure 10.2 Parent rock dependent chemistry of regoliths derived from the Wallagaraugh Adamellite (profiles GR1, 2, 3; regolith □, rock ■) and the Eden Rhyolite (profiles ER1, 2, 4; regolith ○, rock ●).

A: SiO_2-Al_2O_3 plot. The initial SiO_2-Al_2O_3 concentration of the granite (76.39-12.22%) and rhyolite (75.61-12.10%) are essentially identical.

B: TiO_2-Y plot.

and rhyolite samples reflects the persistance of the initial difference in Y concentration, which is 36 and 54ppm respectively.

By inference, when the greater initial differences in chemistry (especially for the less mobile elements, e.g., Ti, Zr etc) are considered, between:

1) the granite/rhyolite pair and metasediment;

2) the granite/rhyolite pair and sandstone, and;

3) between metasediment and sandstone compared with that between granite and rhyolite, then it is likely that the variations in chemistry observed are not induced by parent rock dependent differences in the degree of weathering. Consequently, the differences in regolith chemistry of the profiles examined reflects differences in the parent rock composition. This results in the inheritence by the regolith of a distinctive parent rock chemical signature. This effect has been observed by others (e.g., Ure et al., 1979).

10.5 CHESWORTH'S RESIDUA SYSTEM AND THE PARENT ROCK EFFECT

Chesworth (1973) has argued that the chemical image of the parent rock will diminish with weathering. He states (p.223) 'as time progresses, the weathered products of rocks as dissimilar as granite and basalt should become more and more alike, to the extent of ultimately becoming indistinguishable'. Chesworth's principal evidence is the analysis of 17 and 19 clay fractions produced by the weathering of granitic and basaltic rocks respectively. He showed that in comparison to their parent rock, the clay fractions tended to a residua enriched in $SiO_2 + Al_2O_3 + Fe_2O_3$. Chesworth assumed that the existence of this residua was evidence for the destruction of the distinctive character of the parent rock. The formation of a $SiO_2+Al_2O_3+Fe_2O_3$ residua is consistent with the leaching of the soluble products and consequent reduction in the alkali (K_2O+Na_2O) and alkali earth (MgO+CaO) concentrations to the same low values (Figure 10.3).

However, when the relative proportions of SiO_2, Al_2O_3 and Fe_2O_3 are considered (Figure 10.3B) it can be seen that the weathered residues of basalt and granite are distinctly different. The granite residue

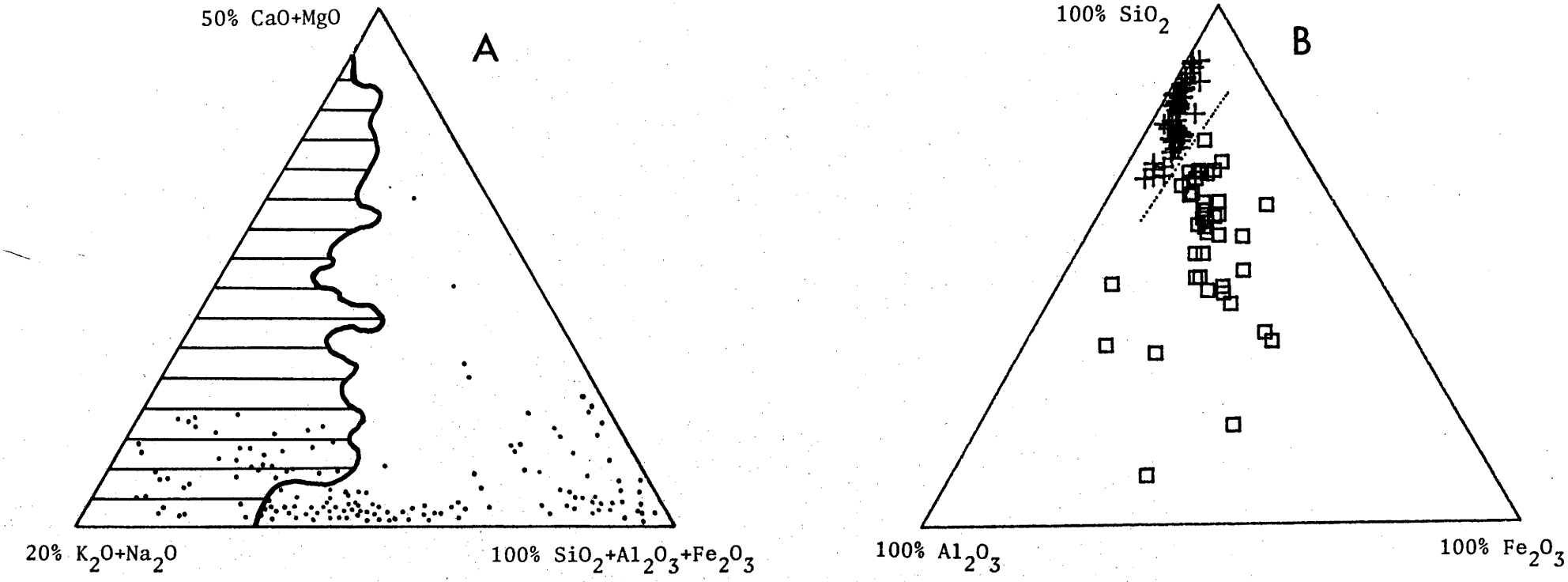

Figure 10.3 Chesworth's residua and the parent rock effect. Analysis of the weathered residues of 'acid' and 'basic' rocks are from Craig and Loughnan (1964), Short (1961), Hendricks and Wittig (1968), Clemency and Busenberg (1976), Plaster and Sherwood (1976), Bruce-Smith (1972) and this thesis.

A: $CaO+MgO-K_2O+Na_2O-SiO_2+Al_2O_3+Fe_2O_3$ plot for the weathered residua of 'acid' and 'basic' rocks (note the scalene triangle). The hatched area forms part of the zone containing 85% of 600 analyses of common 'acid' and 'basic' rocks (from Chesworth, 1973). Note, this diagram is part of a scalene triangle.

B: $SiO_2-Al_2O_3-Fe_2O_3$ plot of the weathered residua of 'acid' (+) and 'basic' (□) rocks plotted in 'A' above.

is enriched in SiO_2 due to the presence of quartz. Consequently, the existence of a $SiO_2 + Al_2O_3 + Fe_2O_3$ residuum cannot be construed as evidence for the destruction of the parent rock character. Furthermore, it is probable even if quartz was removed from the granite residue (e.g., in laterite formation) and the SiO_2-Al_2O_3-Fe_2O_3 concentration was no longer diagnostic of the difference in parent rock, that the variation in elements, such as Zr, Hf, Y, Ti and Cr (which occur in resistant accessory minerals) would be diagnostic of the parent rock.

Although the chemistry of laterites has been documented (e.g., Knight, 1975), there is insufficient trace element data to allow verification of this supposition. Nevertheless, it is thought likely that further work will show that the weathered residues of rocks as dissimilar as granite and basalt are unlikely to become indistinguishable (contrary to Chesworth's opinion) but will retain some chemical characteristics diagnostic of their source rocks.

CHAPTER 11

SUMMARY AND CONCLUSION

In the study area, an area of comparatively low relief and one in which acid leaching conditions prevail, the effect of parent rock on the resultant regolith is striking.

In gross terms, much of the variation between regolith samples derived from different rock types can be attributed to the effect of parent rock. The effect of parent rock can be either:

1) direct, e.g., the inheritence of clay minerals and particle-size distribution from the parent rock by the regolith developed on sandstone; or

2) indirect, e.g., compared with other rock types the high labile mineral content of basalt tends to give rise to a regolith with a higher clay content.

An additional striking feature of the surficial materials examined and the landscapes in which they occur is the constant expression of rate limiting reactions. For example, the particles which survive within the landscape are those which are the least susceptible to chemical alteration, comminution and removal.

Particle-Size Distributions

1) Size intervals commonly used to measure the size distribution of surficial materials (e.g., the International Scale), have boundaries which often do not coincide with natural 'breaks' in the size distribution. Consequently, a considerable amount of the actual variation within a particle-size distribution is not recorded.

2) In the Eden area, the size distribution of *in situ* weathered material is commonly polymodal. In a landscape where most of the processes result in particle comminution rather than growth, then:

i) The dearth of particles separating modes results from either:-

a) the particles being rarely formed.

b) the particles being formed in abundance but are either physically or chemically unstable.

ii) Three commonly occurring particle-size modes can be identified. These modes reflect properties of the parent rock and their weathering products.

Mode I reflects the structure of the parent rock.

Mode II reflects the size distribution of the physiochemically stable minerals in the parent rock.

Mode III reflects the physiochemical properties of the clay minerals.

3) Within a landscape the parent rock and degree of weathering impart distinctive features to the size distribution of in situ weathered material. The signature of the parent rock is reflected by the size distribution of modes I and II and, because of the interactive nature of the parent rock and weathering, to a certain extent by the abundance of mode III. The signature of the weathering environment is carried by mode III.

4) Models of regolith particle-size distribution are few in number, theoretical and of restricted application. Two empirical principles which are likely, through their explicit statement, to further the understanding of particle-size distributions are:-

i) Particles are formed as a result of either comminution or growth.

ii) Attributes which are rate limiting are important in determining the size distribution of particle modes.

5) Size dependent fractionation has been shown to occur through the effects of:

i) biological activity, e.g., termites.

ii) water movement. This can be expressed in terms of the development of texturally differentiated profiles or sandy lag deposits in stream beds.

6) With increasing particle-size fractionation, as a result of fluvial transport:

i) the signature of the parent rock is diminished, with the sediment source only controlling the size range and proportion of particles available; and

ii) the size range of transported particles tends; (a) to reflect the processes which led to its formation, and (b) to be reduced compared with the size range present in the source population.

7) Within any individual depositional environment a variety of processes can operate each with their own distinctive signature. As a consequence of this and variations in the nature of the source population, the size distribution of sediments need not discriminate between different environments.

8) Texturally differentiated profiles can develop as a result of a variety of processes. These processes are:-

i) The selective loss of clay from the surface horizon and its removal down slope.

ii) The selective loss of clay from the surface horizon and deposition in the horizon beneath.

iii) The primary superposition of two sedimentary layers - the upper layer having a lower clay content than that beneath.

iv) The superposition by slope processes of sandy detritus derived from a sand source occurring upslope, over a clay rich substrate.

9) Changes in particle-size characteristics can be recognised within a hierarchy of landscape elements. These elements vary in scale from individual samples/horizons to profiles to hillslopes to streams and estuaries.

Mineralogy

1) The relative persistence of the dominant rock forming minerals in the granite and rhyolite is, in order of increasing persistence; plagioclase >>K-feldspar > quartz. There is insufficient chemical weathering in the metasediment profiles examined to allow an equivocal determination of the comparative stability of quartz and illite. Of the accessory minerals, apatite and zircon, apatite has a stability intermediate to that of plagioclase and K-feldspar whereas zircon is more persistent than quartz.

2) With weathering the tendency is for the aluminosilicate minerals present in the parent rock to form cation depleted clay minerals (e.g., kaolinite). This is consistent with the acid reaction of the regolith samples.

3) The clay minerals present in the regolith can not be simply related to climate as:

i) They can be inherited from the parent rock.

ii) The nature of the clay minerals formed by weathering is dependent on its immediate physical environment. Two important determinants are the antecedent mineral and the localised leaching conditions. The external climatic factors may, and usually have little relationship to the variation in leaching conditions which can exist in a mass of weathering rock.

iii) The parent rock composition can be such to inhibit the formation of particular clay minerals. For example, the low K_2O concentration of basalt limits the formation of illite during its weathering. It is worth noting that some parent rock compositions are such that they inhibit the formation of clay minerals (e.g., quartzites).

4) Quartz grains are neither physically nor chemically immutable and depending on their size and pre-emergent history can undergo considerable comminution in the surficial environment. The occurrence of silt size quartz grains is neither uncommon nor difficult to achieve.

5) Basu's (1976) suggestion that size dependent trends in mineralogy of first cycle sands derived from granite are indicative of the amount of energy expended in their formation and are climatically sensitive, can not be supported by this study. It would seem that size dependent mineralogical trends are dependent on: i) parent rock texture; ii) relief (which in part, determines the rate of profile rejuvenation compared with the rate of weathering); iii) climate; iv) antecedent landscape conditions (e.g., whether the sand is derived from a deeply weathered or recently glaciated terrain); and v) the distance of transport between the point of origin of the sand and the point at which it is sampled.

Chemistry

1) None of the elements examined (including TiO_2, Al_2O_3, Fe_2O_3 and Zr) could be demonstrated to be chemically immobile.

2) The chemical mobility of an element is dependent on:

i) susceptibility of its host mineral to weathering.

ii) the extent to which the element, on release from its host mineral, remains in solution, or is precipitated due to its inherent insolubility or the presence of coprecipitating ions.

iii) variations in the local weathering environment. For example, it was proposed in Chapter 3 that the difference in the distribution of Fe_2O_3 between profile GR2 and profiles GR1 and GR3 was due to the localised effect of drainage.

3) The clay fraction acts as a chemical sink for the less soluble elements released during weathering. In the Eden area, major changes in profile chemistry occur through:

1) Removal of soluble phases in solution (chemical fractionation).

2) Selective translocation of the clay size particles from the

regolith surface horizons (physical fractionation). This results in the selective enrichment of elements present in the physiochemically resistant minerals (e.g., SiO_2 in quartz, TiO_2 in ilmenite and Zr in zircon) and the depletion in the elements which on their release with weathering are precipitated in clay size particles (e.g., Al_2O_3, Fe_2O_3, V, Cr etc.).

4) Because of the effect the properties of the host minerals (both primary and neoformed) have on an element's behaviour, an understanding of element partitioning is vital if variations in regolith chemistry are to be correctly interpreted.

5) Despite the comparative similarity of the rocks which were examined (metasediments, granite, rhyolite and sandstone all of which represent siliceous end members of their respective suites) initial differences in parent rock chemistry are reflected in their weathered derivatives.

6) It is likely, despite Chesworth's argument to the contrary, that the weathered residues of rocks as dissimilar as basalt and granite will never become identical.

The data and discussion of the effect of parent rock on regolith particle-size, mineralogy and chemistry presented here, represent a substantial advance on information previously available. In spite of this, the field is still barely explored. Much fruitful knowledge is still to be gained through the study of a greater range of rock types and weathering environments.

REFERENCES

Abrol, I. P., Khosla, B. K. & Bhumbla, D.R., 1968. Relationship of textures to some important soil moisture constants. Geoderma, 2 33-39.

Allen, J. R. L., 1967. Notes on some fundamentals of palaeocurrent analysis with reference to preservation potential and sources of variance. Sedimentology, 9, 75-83.

Allen, T., 1968. Particle Size Measurement. Chapman and Hall Ltd., London.

Anderson, D.H. & Hawkes, H.E., 1958. Relative mobility of the common elements in weathering of some schist and granite areas. Geochim. Cosmochim. Acta, 14, 204-210.

Andrews, R.H., Gibson, J.A. & Shaw, I.M., 1979, The quantitative determination of quartz in clay mixtures by infrared spectroscopy. In: Mortland, M.M. & Farmer, J.C. (Eds) Developments in sedimentology No 27. Elsevier, Amsterdam, pp.447-455.

Bain, D.C., Ritchie, P.F.S., Clark, D.R. & Duthie, D.M.L., 1980. Geochemistry and mineralogy of weathered basalt from Morvern, Scotland. Mineral. Mag., 43, 865-872.

Barshad, I., 1966. The effect of a variation in precipitation on the nature of clay mineral formation in soils from acid and basic igneous rocks. Proc. Int. Clay Conf. Jerusalem, 1, 167-173.

Barth, T.F.W., 1961. Abundance of the elements areal averages and geochemical cycles. Geochim. Cosmochim. Acta, 23, 1-8.

Basu, A., 1976. Petrology of Holocene fluvial sand derived from plutonic rocks: implications to palaeoclimatic interpretation. J. Sediment. Petrol., 46, 694-709.

Bates, R. L. & Jackson, J. A. (Eds) 1980. Glossary of Geology. American Geological Instute, Virgina.

Beams, S.D., 1980. Magmatic evolution of the south east Lachlan Fold Belt. Unpub. Ph.D. Thesis, LaTrobe University, Bundoora, Victoria.

Birkeland, P., 1974. Pedology, Weathering and Geomorphological Research. Oxford Univ. Press, Oxford.

Bishop, P.M., Mitchell, P.B. & Paton, T.R., 1980. The formation of duplex soils on hillslopes in the Sydney Basin, Australia. Geoderma, 23, 175-189.

Blackburn, G., Bond, R.D. & Clarke, A.R.P., 1965. Soil development associated with stranded beach ridges in south-east South Australia. CSIRO Aust. Soil Publ., No.22.

Blackwelder, E., 1927. Fire as an agent in rock weathering. J. Geol. 35, 134-140.

Blatt, H., 1967. Original characteristics of clastic quartz grains. J. Sediment. Petrol., 37, 401-424.

Blatt, H., 1970. Determination of mean sediment thickness in the crust: a sedimentologic model. Geol. Soc. Am. Bull., 81, 255-262.

Bockheim, J.G., 1980. Solution and use of chronofunctions in studying soil development. Geoderma, 24, 71-85.

Box, J.E., 1981. The effects of surface slaty fragments on soil erosion by water. Soil Sci. Soc. Am. Proc., 45, 111-116.

Brewer, R., 1955. Mineralogical examination of a yellow podzolic soil formed on a granodiorite. CSIRO Aust. Soil Publ. No.5.

Brewer, R., 1968. Clay illuviation as a factor in particle-size differentiation in soil profiles. Trans. 9th Inst. Congr. Soil Sci., Adelaide, Vol.4, 489-500.

Brewer, R., 1973. Micromorphology: A discipline of the chemistry mineralogy interface. Soil Sci., 115, 261-267.

Brewer, R., 1964. Fabric and Mineral Analysis of Soils. John Wiley & Sons, Inc., New York.

Brewer, R., 1979. Relationship between particle size, fabric and other factors in some Australian soils. Aust. J. Soil Res., 17, 29-41.

Brown, G., (Ed) 1961. The X-ray identification and crystal structure of clay minerals. Mineralogical Society, London.

Bruce-Smith, J.R., 1972. Soils and pedogenesis on the granitic rocks of Tenterfield, New South Wales. Unpub. Ph.D. Thesis, Univ. of New England, Armidale.

Burgess, J.S., Reiger, W.A. & Olive, L.J., 1981. Sediment yield change following logging and fire effects in dry schlerophyll forest in southern New South Wales. Int. Assoc. Sci. Hydrol., 132, 375-385.

Busenberg, E., 1978. The products of the interaction of feldspar with aqueous solutions at 25°C. Geochim. Cosmochim. Acta, 42, 1679-1686.

Bustin, R.M. & Mathews, W.H., 1979. Selective weathering of granitic clasts. Canadian J. Earth Sci., 16, 215-223.

Cas, R.A.F., Powell, C.M.A. & Crook, K.A.W., 1980. Ordovician paleogeography of the Lachland Fold Belt; a modern analagoue and tectonic constraints. J. Geol. Soc. Aust., 27, 19-31.

Chappell, B.W., 1966. Petrogenesis of the granites at Moonbi, New South Wales. Unpub. Ph.D., Thesis, Aust. Nat. Univ.

Chesworth, W., 1973. The parent rock effect in the genesis of soil. Geoderma, 10, 215-225.

Chesworth, W., 1975. Soil minerals in the system Al2O3-SiO2-H2O phase equilibrium model. Clays & Clay Minerals, 23, 55-60.

Chesworth, W., 1976. Conceptual models in pedogenesis: A rejoinder. Geoderma, 16, 257-260 & 265-266.

Clemency, C.V. & Busenberg, E., 1976. A comparison of the chemistry and mineralogy of weathering sequences from quartz-rich and quartz-free rocks from Brazil. In: Cadek, J. & Paces, T. (Eds). Proceedings Inter. Sym. Water-Rock Interaction, Czechoslavakia 1974, pp.54-63.

Collins, W.J., 1977. Geology and geochemistry of the Gabo Island Granite suite and associated rocks. Unpub. Hons Thesis, Aust. Nat. Univ.

Cooper, J.A., 1963. The flame photometric determination of potassium in geological materials used for potassium-argon dating. Geochim. Cosmochim. Acta, 27, 525-546.

Craig, D.C. & Loughnan, F.C., 1964. Chemical and mineralogical transformations accompanying the weathering of basic volcanic rocks from NSW. Aust. J. Soil Res., 2, 218-234.

Dake, C.L., 1921. The problem of the St. Peter Sandstone. Bull. Mines & Metall., Univ. Missouri No.6(1).

Dapples, E.C., 1975. Laws of distribution applied to sand sizes. Geol. Soc. Am. Memoir, 142, 37-61.

Day, P.R., 1965. Particle fractionation and particle-size analysis. In: Black, C.A. (Ed) Methods of soil analysis. Am. Soc. Agron., Madison, Wisc., pp.545-567.

Deer, W.A., Howie, R.A. & Zussman, J., 1963. Rock-forming minerals. Longmans, London.

Dijkerman, J.C., 1974. Pedology as a science: The role of data, models and theories in the study of natural soil systems. Geoderma, 11, 73-93.

Downes, R.G. & Sleeman, J.R., 1955. The soils of the Macquarie Region, N.S.W. CSIRO Aust. Soil Publ. No.4.

Edwards, K. & Charman, P.E.V., 1980. The future of soil loss prediction in Australia. J. Soil Cons. Service of N.S.W., 36, 211-218.

Eggleton, R.A., 1975. Nontronite topotaxial after hedenbergite. Am. Mineral., 60, 1063-1068.

Eggleton, R.A. & Buseck, P.R., 1980. High resolution electron microscopy of feldspar weathering. Clays & Clay Minerals, 28, 173-178.

Ehrlich, R., Brown, P.J., Yarus, J.M. & Przygocki, R.S., 1980. The origin of shape frequency distributions and relationship between size and shape. J. Sediment Petrol., 50, 475-484.

Eswarin, H.& Bin, W.C., 1978. A study of a deep weathering profile on granite in peninsular Malaya. Soil Sci. Soc. Am. Proc. 42, 149-153.

Feniak, M.W., 1944. Grain sizes and shapes of various minerals in igneous rocks. Am. Mineral., 29, 415-421.

Fernadoz-Marcos, M.L., Macías, F. & Guitián-Ojea, F., 1979. A contribution to the study of the stability of clay minerals from the soil solution composition at different pF values. Clay minerals, 14, 29-37.

Feth, J.H., Roberson, C.E. & Polzer, W.L., 1964. Sources of mineral constituents in water from granitc rocks, Sierra Nevada, California and Nevada. U.S. Geol. Surv. Water Supply Paper 1535-I.

Flinter, B.H., 1975. Quantitative mineral analysis by X-ray diffraction using the heavy absorber method. N. Jb. Minerl. Abh., 125, 243-277.

Fordham, A.W. & Norrish, K., 1979a. Electron microprobe and electron microscope studies of soil clay particles. Aust. J. Soil Res., 17, 283-306.

Fordham, A.W. & Norrish, K., 1979b. Asenate-73 uptake by components of several acidic soils and its implication for phosphate retention. Aust. J. Soil Res., 17, 307-316.

Forestry Commission of NSW (undated). Woodchips from Eden. Pamphlet.

Friedman, G.M., 1958. Determination of sieve-size distribution from thin-section data for sedimentary petrological studies. J. Geol., 66, 394-416.

Friedman, G.M., 1979. Differences in size distributions of populations of particles among sands of various origins. Sedimentology, 26, 3-32.

Fyfe, W.S., 1981. The environmental crisis: Quantifying Geosphere Interactions. Science, 213, 105-109.

Gardner, L.R., 1980. Mobilisation of Al and Ti during weathering-isovolumetric geochemical evidence. Chem. Geol., 30, 151-165.

Gardner, L.R., Kheoruenromme, I. & Chen, H.S., 1978. Isovolumetric geochemical investigation of a buried granite saprolite near Columbia, Sc., USA. Geochim. Cosmochim. Acta, 42, 417-424.

Garrels, R.M., 1967. Genesis of some ground waters from igneous rocks. In Abelson, P.H. (Ed) Researches in geochemistry. John Wiley and Sons Inc. N.Y. pp405-420.

Garrels, R.M. & Mackenzie, F.T., 1971. Evolution of sedimentary rocks. W.W. Norton & Co. Inc. N.Y.

Gary, M., Mcafee, R.I. & Wolf, C. (Eds), 1972. Glossary of Geology. Geological Inst. Washington, D.C.

Gilkes, R.J. & Little, I.P., 1972. Weathering of chlorite and some associations of trace elements in Permian phyllites in southeast Queensland. Geoderma, 7, 233-247.

Goldich, S.S., 1938. A study of rock weathering. J. Geology, 46, 17-58.

Grim, R.E., 1968. Clay mineralogy. McGraw-Hill, New York.

Harrell, J. and Blatt, H., 1978. Poly-crystallinity effect on the durability of detrital quartz. J. Sediment. Petrol., 48, 25-30.

Hembree, C.H. & Rainwater, F.H., 1961. Chemical degradation on the opposite flanks of the Wind River Range, Wyoming. U.S.G.S. Wat. Supp. Pap. 1535-E.

Hendricks, D.M. & Wittig, L.D., 1968. Andesite weathering. II. Geochemical changes from andesite to saprolite. J. Soil Sci., 19, 147-153.

Hlavay, J., Jonas, K., Elek, S. and Inczedy, J., 1978. Characterisation of the particle size and the crystallinity of certain minerals by IR spectrophotometry and other instrumental methods. II. Investigations on quartz and feldspar. Clays and Clay Minerals, 26, 139-143.

Hough, D.J., 1981. Long Corner Creek hydrologic project: Aspects of the geology, physiography and soils. Unpub. Report for the Soil Conservation Authority, Victoria.

Hough, D. J., 1982. Surficial materials and landscape feature of the Eden-East Gippsland region. Report to Harris-Daishowa Australia Pty Ltd.

Hough, D.J. & Beams, S.D., 1979. The relationship between soil characteristics and the occurrence of dieback in East Gippsland, Victoria. Unpub. report undertaken for the Forests Commission, Victoria.

Huggett, R.J., 1976. Conceptual models in pedogenesis - A discussion. Geoderma, 16, 261-262.

Hunt, C. B., 1972. Geology of soils. W. H. Freeman and Company, San Francisco.

Irani, R.R. & Callis, C.F., 1963. Particle size: measurement, interpretation and application. Wiley, N.Y.

Isherwood, D. & Street, A., 1976. Biotite-induced grussification of the Boulder Creek Granodiorite, Boulder County, Colorado. Geol. Soc. Am. Bull., 87, 366-370.

Jenny, H., 1941. Factors of soil formation - a system of quantitative pedology. McGraw Hill, N.Y.

Jessup, R.W., 1965. The soils of the central portion of the New England Region, N.S.W. CSIRO Aust. Soil Publ. No.21.

Joyce, A.S., 1970. Geochemistry of the Murrumbidgee Batholith. Unpub. Ph.D. Thesis, Aust. Nat. Univ.

Jurinak, J.J., Whitmore, J.C. & Wageret, R.J., 1977. Kinetics of salt release from a saline soil. Soil Sci. Soc. Am. Proc., 41, 721-724.

Karamanos, R.E. & Turner, R.C., 1977. Potassium supplying power of some Northern-Greece soils in relation to clay-mineral composition. Geoderma, 17, 209-218.

Kelly, J. & Turner, J., 1978. Soil nutrient-vegetation relationships in the Eden area, N.S.W.: 1. Soil nutrient survey. Aust. For., 41, 127-134.

Kesson, S.E., 1972. Basic Alkaline Rocks. Unpub. Ph.D. Thesis, Aust. Nat. Univ.

Khanna, P.K. & Ulrich, B., 1973. Ion exchange equilibria in an acid soil. Gottinger Bodenkundliche Berichte, 29, 211-230.

Kitagawa, R. & Kakitani, S., 1977. Alteration of plagioclase in granite during weathering. J. Sci. Hiroshima Univ., 7, 183-197.

Kittleman, L.R., 1964. Application of Rosin's distribution in size of frequency analysis of clastic rocks. J. Sediment. Petrol., 34, 485-502.

Knight, C.L., 1975. (Ed). Economic geology of Australia and Papua New Guinea. Monog. 5. Aust. Inst. Mining Metallurgy.

Koppi, A.J. & Williams, D.J., 1980. Weathering and development of two contrasting soils formed from granodiorite in southeast Queensland. Aust. J. Soil Res., 18, 257-272.

Krauskopf, K.B., 1967. Introduction to geochemistry. McGraw Hill, New York.

Krinsley, D.H. & Smalley, I.J., 1973. Shape and nature of small sedimentary quartz particles. Science, 180, 1277-1279.

Krumbein, W.C. & Tisdel, F.W., 1940. Size distribution of source rock of sediments. Am. J. Sci., 238, 296-305.

Kuenen, Ph.H., 1969. Origin of quartz silt. J. Sediment. Petrol., 39, 1631-1633.

Lal, R., 1979. Physical properties and moisture retention characteristics of some Nigerian soils. Geoderma, 21, 209-223.

Lambert, R. St. J. & Holland, J.G. 1974. Y ttrium geochemistry applied to petrogenesis utilizing calcium-yttrium relationships in minerals and rocks. Geochim. Cosmochim. Acta, 38, 1393-1414.

Larsen, D.J. von Doenhoff, L.J. & Crable, J.V., 1972. The quantitative determination of quartz in coal dust by infrared spectroscopy. J. Am. Ind. Hyg. Ass., 33, 367-372.

Leamer, R.W. & Lutz, J.F., 1940. Determination of pore-size distributions in soils. Soil Sci., 49, 347-360.

Lee, K.E., Warcup, J.H. & Hutson, B.R., 1981. The Soil biota. In: Turvey, N.D. (Chairman) Australian Forest Nutrition Workshop: Productivity in Perpetuity. CSIRO Aust. Div. For. Res., pp.65-78.

Lelong, F., Tardy, Y., Grandin, G., Trescases, J.J. & Boulange, B., 1976. Pedogenesis, chemical weathering and processes of formation of some supergene ore deposits. In: Wolf, K.H. (Ed.) Handbook of strata-bound and stratiform ore deposits, Vol.3. Supergene and surficial ore deposits; textures and fabrics. Part 1. Principles and general studies. p.93-166. Elsevier. Amsterdam.

Lindsay, J. F., 1974. A general model for the textural evolution of lunar soil. Proc. 5th Lunar Sci. Conf. Geochim Cosmochim Acta Suppl. 5, V1, 862-878.

Little, I.P. & Ward, W.T., 1981. Chemical and mineralogical trends in a chronosequence developed on alluvium in eastern Victoria, Australia. Geoderma, 25, 173-188.

Loughnan, F.C., 1969. Chemical weathering of the silicate minerals. Am. Elsevier Pub. Co., Inc., New York.

Loveday, J., 1957. The soils of the Sorell-Carlton-Copping area, South-East Tasmania, with special reference to soils formed on basalt. CSIRO Aust. Soil Publ., No.8.

Macias-Vazquez, F., 1981. Formation of gibbsite in soils and saprolites of temperate-humid zones. Clay Minerals, 16, 43-52.

Mann, W.R. & Cavaroc, V.V., 1973. Composition of sand released from three source areas under humid, low relief weathering in the North Carolina Piedmont. J. Sediment. Petrol., 42, 870-881.

Marel, van der, H.W. & Beutelspacher, H., 1976. Atlas of infrared spectroscopy of clay minerals and their admixtures. Elsevier, Amsterdam.

McArthur, W.M. & Bettenay, E., 1960. The development and distribution of soils of the Swan coastal plain, Western Australia. CSIRO, Aust. Soil Publ. No 16.

McConnell, A.D., 1979. A landscape history of the Wantabadgery area, New South Wales. Unpub. M.Sc. Thesis, Aust. Nat. Univ.

McEwan, M.C., Fesseden, E.W. & Rogers, J.J.W., 1959. Texture and composition of some weathered granites and slightly transported arkosic sands. J. Sediment. Petrol., 29, 477-492.

Meunier, A. & Velde, B., 1976. Mineral reactions of grain contacts in early stages of granite weathering. Clay minerals, 11, 235-240.

Meybeck, M., 1976. Total mineral dissolved transport by world major rivers. Hydro. Sci. Bull., 21, 265-284.

Mills, J.G. & Zwarich, M.A., 1972. Recognition of interstratified clays. Clays & Clay Minerals, 20, 169-174.

Milne, G., 1936. Normal erosion as a factor in soil profile development. Nature, 138, 548-549.

Moss, A.J., 1966. Origin, shaping and significance of quartz sand grains. J. Geol. Soc. Aust., 13, 97-136.

Moss, A.J., 1972. Bed-load sediments. Sedimentology, 18, 159-219.

Moss, A.J., 1972. Initial fluviatile fragmentation of granite quartz. J. Sediment. Petrol., 42, 905-916.

Moss, A.J. & Walker, P.H., 1978. Particle transport by continental water flows in relation to erosion, deposition, soils and human activities. Sediment. Geol., 20, 81-139.

Moss, A.J., Walker, P.H. & Hutka, J., 1973. Fragmentation of granitic quartz in water. Sedimentology, 20, 489-511.

Nesbitt, H.W., Markovics, G. & Price, R.C., 1980. Chemical processes affecting alkalis and alkaline earths during continental weathering. Geochim. Cosmochim. Acta, 44, 1659-1666.

Nie, N.H., Hull, C.H., Jenkins, J.G., Steinbrenner, K. & Bent, D.H., 1975. SPSS : Statistical package for the social sciences. McGraw-Hill Inc., New York.

Norrish, K. & Chappell, B.W., 1969. X-ray fluorescence spectrography. In: Zussman, J. (Ed.), Physical methods in determinative mineralogy. Academic Press, London, pp.161-214.

Norrish, K. & Hutton, J.T., 1969. An accurate X-ray spectrographic method for the analysis of a wide range of geological samples. Geochim. Cosmochim. Acta, 33, 431-453.

Northcote, K.H., 1979. A factual key for the recognition of Australian soils. Rellim Technical Publications, Glenside, South Australia.

Northcote, K.H., Hubble, G.D., Isbell, R.F., Thompson, C.H. & Bettenay, E., 1975. A description of Australian soils. CSIRO Australia.

Nicolls, K.D. & Tucker, B.M., 1956. Pedology and chemistry of the basaltic soils of the Lismore District, N.S.W. CSIRO Aust. Soil Publ., No.7.

Oertel, A.C., 1968. Some observations incompatible with clay illuviation. Trans. 9th Int. Congr. Soil Sci., Adelaide. Vol.4, pp.481-488.

Oertli, J.J., 1973. The use of chemical potentials to express nutrient availability. Geoderma, 9, 81-95.

Ollier, C.D., 1971. Causes of spheroidal weathering. Earth-Sci., Rev., 7, 127-141.

Peck, L.C., 1964. Systematic analysis of silicates. U.S. Geol. Surv. Bull. 1170.

Pettijohn, E.J., 1975. Sedimentary Rocks. Harper & Row, New York.

Piper, A.M. 1944. A graphic procedure in the geochemical interpretation of water analyses. Trans. Am. Geophys. Un., 25,914-923.

Pittman, E.D., 1969. Destruction of plagioclase twins by stream transport. J. Sediment. Petrol., 39, 1432-1437.

Plaster, R.W. & Sherwood, W.C., 1971. Bedrock weathering and residual soil formation in Central Virginia. Geol. Soc. Am. Bull., 82, 2813-2825.

Polynov, B.B., 1937. Cycle of Weathering. Murby, London.

Pritchard, D.W., 1967. What is an estuary: physical viewpoint. In: Lauff, G.H. (Ed.) Estuaries. A.A.A.S. Pub. 83, pp.3-5.

Reed, S.J.B. & Ware, N.G., 1975. Quantitative electron microprobe analysis of silicates using energy dispersive X-ray spectrometry. J. Petrol., 16, 499-519.

Reinson, G.E., 1973. Aspects of weathering and sedimentation in the Genoa River Basin and Estuary, New South Wales-Victoria. Unpub. Ph.D. Thesis, Aust. Nat. Univ.

Reinson, G.E., 1975. Geochemistry of muds from a shallow restricted estuary, Australia. Marine Geology, 19, 297-314.

Rhodes, J.M., 1969. The geochemistry of a Granite-Gabbro Association at Hartley, New South Wales. Unpub. Ph.D. Thesis Aust. Nat. Univ.

Rice, C.M., 1973. Chemical weathering on the Carnmenellis Granite. Mineral. Mag., 39, 429-447.

Rogers, J.J.W., Krueger, W.C. & Krog, M., 1963. Sizes of naturally abraded materials. J. Sediment. Petrol., 33, 628-632.

Ross, G. J., Wang, C., Ozkan, A. I. & Rees, H.W., 1982. Weathering of chlorite and mica in a New Brunswick podzol developed on till derived from chlorite-mica schist. Geoderma, 27, 255-267.

Rosseaux, J.M., 1978. Quantitative estimation of kaolinite in sediments by differential infrared spectroscopy. Clays & Clay Minerals, 26, 202-208.

Russel, D.A., 1976. Particle-size distribution characteristics for the coarse fraction of a granitic soil. Soil Sci. Soc. Am. Proc., 40, 409-421.

Ruxton, B.P., 1968. Measures of the degree of weathering of rocks. J. Geology, 76, 518-527.

Salter, P.J. & Williams, J.B., 1967. The influence of texture on the moisture characteristics of soils. IV. A method of estimating the available water capacities of profiles in the field. J. Soil Sci., 18, 174-181.

Sarazin, G., Fouillac, C. & Michard, G., 1976. Etude de l'acquisition d'éléments dissous par les eaux de lessivage des roches granitiques sous climate tempéré. Geochem. Cosmochim. Acta, 40, 1481-1486.

Scafe, D.W. & Kuzne, G.W., 1971. A clay mineral investigation of six cores from the Gulf of Mexico. Marine Geol., 10, 69-85.

Sedimentation Seminar, 1981. Comparison of methods of size analysis for sands of the Amazon-Solimoes Rivers, Brazil and Peru. Sedimentology, 28, 123-128.

Shaw, H.F., 1972. The preparation of orientated clay mineral specimens for X-ray diffraction analysis by a suction-onto-ceramic tile method. Clay Minerals, 9, 349-350.

Short, N.M., 1961. Geochemical variation in four residual soils. J. Geology, 69, 534-571.

Smalley, I.J. & Vita-Finzi, C., 1968. The formation of fine particles in sandy deserts and the nature of 'desert' loess. J. Sediment. Petrol., 38, 766-774.

Smith, J.V., 1974. Feldspar minerals. Springer-Velag, Berlin.

Smith, R. T. & Atkinson, K., 1975. Techniques in pedology. Elek Science, London.

Smyth, C.H. Jr., 1913. The relative solubilities of the chemical constituents of rocks. J. Geol., 21, 105-120.

Soil Survey Staff, 1975. Soil taxonomy. U.S. Dept. Agric. Handbk. No.436. U.S. Govt. Print. Office, Washington, D.C.

Spyridakis, D.E., 1967. Kaolinization of biotite as a result of coniferous and deciduous seedling growth. Soil Sci. Soc. Am. Proc., 31, 203-210.

Stace, H.C.T., Hubble, G.D., Brewer, R., Northcote, K.H., Sleeman, J.R., Mulchay, M.J. & Hallsworth, E.G., 1968. A handbook of Australian soils. Rellim Technical Publications: Glenside, South Australia.

Steele, J.G. & Bradfield, R., 1934, The significance of size distribution in the clay fraction. Am. Soil Surv. Ass. Bull., 15, 89-93.

Steiner, J., 1966. Depositional Environments of the Devonian Rocks of the Eden-Merrimbula Area, N.S.W. Unpub. Ph.D. Thesis, Aust. Nat. Univ.

Stevens, P.R. & Walker, T.W., 1970. The chronosequence concept and soil formation. Q. Rev. Biol., 45, 333-350.

Stoke, P.R. & Larsen, B., 1973. Variation in clay mineral XRD results with the quantity of sample mounted. J. Sediment. Petrol., 43, 957-964.

Stoops, G. & Jongeri us , A., 1975. Proposal for a micromorphological classification of soil materials. Geoderma, 13, 189-199.

Strahler, A.N., 1969. Physical geography. John Wiley and Sons, Inc., New York.

Streckeisen, A.L., 1973. Classification and nomenclature of plutonic rocks, recommendations. Geotimes, 18, 26-30.

Tabatabi, M.A. & Bremner, J.M., 1970. Use of the Leco Automatic 70 second Carbon Analyser for total analysis of soils. Soil Sci. Soc. Am. Proc., 34, 608-610.

Talsma, T. & Flint, S.A., 1958. Some factors determining the hydraulic conductivity of subsoils with special reference to tile drainage problems. Soil Sci., 85, 195-206.

Talsma, T. & Hallam, P.M., 1980. Hydraulic conductivity measurement of forest catchments. Aust. J. Soil Res., 18, 39-148.

Tan, K.H., 1978. Effects of humic and fluvic acids on release of fixed potassium. Geoderma, 21, 67-74.

Tanner, W.F., 1969. The particle size scale. J. Sediment. Petrol., 39, 809-812.

Tardy, Y., 1971. Characterization of the principal weathering types by the geochemistry of waters from some European and African crystalline massifs. Chem. Geol., 7, 253-271.

Tardy, Y., Bocquier, G., Paquet, H. & Millot, G., 1973. Formation of clay from granite and its distribution in relation to climate and topography. Geoderma, 10, 271-284.

Tassel, J.V. & Grant, W.H., 1980. Granite disintegration, Panola Mountain, Georgia. J. Geology, 88, 360-364.

Thomas, M.F., 1974. Granite landforms: a review of some recurrent problems in interpretation. In: Brown, E.H. & Waters, R.S. Progress in Geomorphology. Inst. Brit. Geog. Spec. Publ. No.7. London. pp.13-33.

Thomasson, A.J., 1978. Toward an objective classification of soil structure. J. Soil Sci., 29, 38-46.

Thompson, J.G., 1965. The soils of Rhodesia and their classification. Rhodesia Agric. J. Tech. Bull. No.6.

Tiller, K.G., 1958. The geochemistry of basaltic minerals and associated soils of south-eastern South Australia. J. Soil Sci., 9, 225-241.

Torrent, J. & Nettleton, W.D., 1979. A simple textured index for assessing chemical weathering in soils. Soil Sci. Soc. Am. Proc., 43, 373-377.

Turekian, K.K. & Kulp, J.L., 1956. The geochemistry of strontium. Geochim. Cosmochim. Acta, 10, 254-296.

Twidale, C.R. & Bourne, J.A., 1975. The subsurface initiation of some minor granite landforms. J. Geol. Soc. Aust., 22, 477-484.

Ure, A.M., Bacon, J.R., Berrow, M.L. & Watt, J.J., 1979. The total trace element content of some Scottish soils by spark source mass spectrometry. Geoderma, 22, 1-23.

U.S. Environmental Protection Agency, 1975. Logging roads and protection of water quality. Report No. EPA 910/9-75-007.

Visher, G.S., 1969. Grain size distribution and depositional processes. J. Sediment. Petrol., 39, 1074-1106.

Vita-Finzi, C. & Smalley, I.J., 1970. Origin of quartz silt: comments on a note by Ph.H. Kuenen. J. Sediment. Petrol., 40, 1367-1368.

Volobuyev, V.R., 1974. Main concepts of soil ecology. Geoderma, 12, 27-33.

Walker, P.H. & Coventry, R.J., 1976. Soil profile development in some alluvial deposits of eastern N.S.W. Aust. J. Soil Res., 14, 305-317.

Walker, P.H. & Hutka, J., 1979. Size characteristics of soils and sediments with special reference to clay fractions. Aust. J. Soil Res., 17, 383-404.

Watson, J.P., 1975. The composition of termite (Macrotermes spp.) mounds on soil derived from basic rock in three rainfall zones of Rhodesia. Geoderma, 14, 147-158.

Wedepohl, K.H., 1978. Strontium: 38-G. Behaviour during weathering and Rock Alteration. In: Wedepohl, K.H. (Ed.) Handbook of Geochemistry. Vol.II/4. Springer-Verlag, Berlin.

Wentworth, C.K., 1933. Fundamental limits to the size of clastic grains. Science, 77, 633-634.

Winkler, E.M., 1980. Selective weathering of granitic clasts: Discussion. Can. J. Earth Sci., 17, 956.

Wischmeier, W.H., Johnson, C.B. & Cross, B.V., 1971. A soil erodability nomograph for farmland and construction sites. J. Soil Wat. Conserv., 26, 189-195.

Wyborn, L.A.I. & Chappell, B.W., 1983. Chemistry of the Ordovician and Silurian greywackes of the Snowy Mountains, Southeastern Australia: An example of chemical evolution with time. Chemical Geology, 39, 81-92.

Yaalon, D.H., 1975. Conceptual models in pedogenesis: can soil forming functions be solved? Geoderma, 14, 189-205.

Yaalon, D.H., 1976. Conceptual models in pedogenesis - A reply. Geoderma, 16, 263-264.

APPENDIX A

SAMPLE PREPARATION

Rock Samples

Approximately 1 to 2 kg of fine grained rocks and 10 kg of coarse grained rocks were successively crushed and split using a WC swing mill to produce a 100 g aliquot with a grain size less than 20 mesh.

Soil Samples

Approximately 5 to 10 kg of sample was returned from the field in pieces 300 to 1000g in size and then dried at room temperature. These were then subsampled by picking individual pieces for:

A) Bulk sample chemistry and mineralogy. Approximately 2 to 3 kg of coarse textured soil and 1 kg of fine textured soil were crushed and split to produce 100 g aliquots with a grain size less than 20 mesh. These samples were not pretreated except for drying at room temperature and the removal of a grub from sample GR101.

B) Particle size analysis and exchange properties. Approximately 2 to 3 kg of coarse textured soil and 0.5 kg of fine textured soil were lightly ground by hand. All material passing through the 2mm sieve was retained and bagged. A 100g split of the fine earth was then ground to less than than 20 mesh in a WC mill for the analysis of C and P.

The material greater than 2mm was then sieved and the weight of the <-2, <-3, <-4, >-4 phi fractions recorded on an organic free basis, after removing as much organic matter as possible by hand picking.

C) Separation of size fractions from soil samples. Approximately 2 kg of soil was treated as follows:

(1) The soil was soaked overnight in a dispersant consisting of analytical grade 0.02N ammonia solution. (Tiller, 1968; Le Riche, 1972).

(2) The following morning the samples were sonified for 15 minutes in an ultrasonic bath. This was done by sonifying 50 to 100g splits in individual breakers.

(3) The soil splits were then mixed with 0.02N ammonia solution in a large polythene garbage bin and were allowed to settle and then decanted. The settling times used were calculated from Stokes equation, assuming spherical particles with a specific gravity of 2.61.

(4) With the exception of the <9 phi fraction, each fraction was decanted several times to remove larger and finer grained size fractions, and then the residue was oven dried. The size range of these fractions was verified by scanning electron microscopy.

(5) The <9 phi fraction was floculated by the addition of analytical grade HCl. Sufficient HCl was added so that floculation and settling occurred over a 2 day period, the clear supernatant was decanted and the clay suspension oven dried.

(6) The >5 phi fraction was oven dried and then sieved using brass analytical sieves to obtain samples at 1 phi intervals.

(7) Subsamples of all fractions >7 phi were ground in a WC swing mill to less than 20 mesh and retained for chemical and mineralogical analysis.

Stream Sediment Samples

Approximately 10 kg grab samples were collected from the stream beds immediately behind the stream gauging weir. These were then washed in distilled water to remove organic matter by flotation, oven dried and then sieved using brass analytical sieves. Grain size fractions were then crushed using a WC swing mill.

ANALYTIC TECHNIQUES

Major and Trace Elements

Major and trace element abundances were determined by X-ray fluorescence spectrometry. Major elements (except Na20, H20-, C, FeO)

were determined by using the method of Norrish and Hutton (1969). Sample DH1 to DH44 were determined in triplicate, whereas samples DH45 to DH78 were determined in duplicate.

Trace elements were measured in duplicate on pressed powder pellets as described by Norrish and Chappell (1967). Refer to Table A.1. Element concentrations (except for P) were calculated using direct measurement of mass absorption (for Sr Kα and Rb Kα) after corrections had been made for detector dead time, instrument drift and interelement interference. Mass absorption corrections for P were made using scattered background. All duplicates for P agreed to within 5, 10, 20 ppm of the stated value for concentrations in the range 0-250, 250-1000, and 1000-4000 ppm respectively.

C was determined on a Leco Induction Furnace. The principles of the technique are outlined by Tabatabi and Brenner (1970).

Na20 was determined in duplicate on a modified Baird Atomic double beam flame photometer using Li as an internal standard. The technique is similar to that described by Cooper (1963) for K.

FeO was determined in duplicate using the technique described by Peck (1964).

Loss is the percent loss in weight after heating the H_2O- free sample for 4 hours at 1050°C, under atmospheric conditions.

H_2O+ is the percent loss of H_2O on heating a H_2O- free sample at 1050°C for 4 hours. It can be calculated by subtracting the product of percent carbon and 1.72 (this converts percent carbon to percent organic matter) from the percent loss.

H_2O- is the percent loss in weight after heating a sample for one hour at 105°C.

Bulk Density

Bulk density was determined by the water displacement technique, using wax coated H_2O- free, 100 to 200g soil clods.

TABLE A.1 SUMMARY OF ANALYTICAL CONDITIONS FOR X-RAY SPECTROMETRY

Element	Analytical Line	X-Ray Tube	Analysing Crystal	Collimator	Machine	Detector	Absorption Coefficient	Background Position Peak (2θ)
Oxide %								
SiO_2	K_α	Cr	PE	C	2	F.C.		
TiO_2	K_α	Cr	LiF(200)	C	2	F.C.		
Al_2O_3	K_α	Cr	Pe	C	2	F.C.		
Fe_2O_3	K_α	W	LiF(200)	C	2	F.C.		
MnO	K_α	W	LiF(200)	C	2	F.C.		
MgO	K_α	Cr	TAP	C	2	F.C.		
CaO	K_α	Cr	LiF(200)	C	2	F.C.		
K_2O	K_α	Cr	LiF(200)	C	2	F.C.		
P_2O_5	K_α	Cr	Ge	C	2	F.C.		
S	K_α	Cr	Ge	C	2	F.C.		
ppm								
P	K_α	Cr	Ge	C	2	F.C.		
Rb	K_α	Mo	LiF(200)	F	1	S.C.	Rb	± .26
Sr	K_α	Mo	LiF(200)	C	1	S.C.	Sr	± .35
Pb	L_β	Mo	LiF(200)	F	1	S.C.	Rb	± .23
Zr	K_α	W	LiF(200)	C	1	S.C.	Sr	± .40
Y	K_α	Mo	LiF(200)	C	1	S.C.	Sr	± .40
V	K_α	W	LiF(220)	F	2	F.C.	Fe	±1.75
Cr	K_α	W	LiF(200)	F	2	F.C.	Fe	± .90
Ni	K_α	Au	LiF(200)	C	1	S.C.	Zn	± .40
Cu	K_α	Au	LiF(200)	C	1	S.C.	Zn	± .40
Zn	K_α	Au	LiF(200)	C	1	S.C.	Zn	± .40

C - coarse collimator = 480µm F.C. - flow counter S.C. - scintillation counter
F - fine collimator = 160µm 1 - PW 1220 2 - PW 1450.

MINERALOGY

Quartz Content by Infrared Spectroscopy

The theory for the recognition and quantitative analysis of minerals by infrared spectroscopy is given by van der Marel and Beutelspacher (1976). Techniques for the quantitative analysis of mixtures are outlined by Larsen et al. (1972), Hlavay et al. (1978) and Rosseaux (1978).

The technique used in this thesis for the determination of the proportion of quartz is as follows:

(1) Twenty milligram of powdered sample (average grain size 0.03mm) was ground with 8 drops of alcohol for 30 minutes in a vibrating agate ball mill.

(2) The ground sample was dried under a heat lamp. Two and half milligram of ground sample was then added to approximately 1.00g of oven dry reagent grade KBr. This mixture was blended using a vibrating shaker for two minutes.

(3) Approximately 500 mg and 200 mg of blended mix were then placed in a 13 mm vacuum die. The die was evacuated and the powder pressed at 7.5 Mpa for 10 mintues and then 150 Mpa for a further 2 minutes.

(4) The pressed pills were run on a Unicam SP1100 Infrared Spectrophotometer at the following settings: Scan speed, normal; Program, normal; Expansion, 1; Baseline, 0.

For the quantitative estimation of mineral proportions all weights were normalised for the following conditions: blend ratio, 1.00000g KBr and 2.50 mg of sample; pill weights 500 mg and 200 mg.

For the quantitative determination of quartz the 798 cm-1 absorption peak was compared with the background at 860 cm-1.

The calibration curve was established using acid washed quartz as a standard. The variation of peak height to background for quartz in a quartz KBr mixture is given in Figure A.1a and A.2. The limit of detection for quartz is 1-2%.

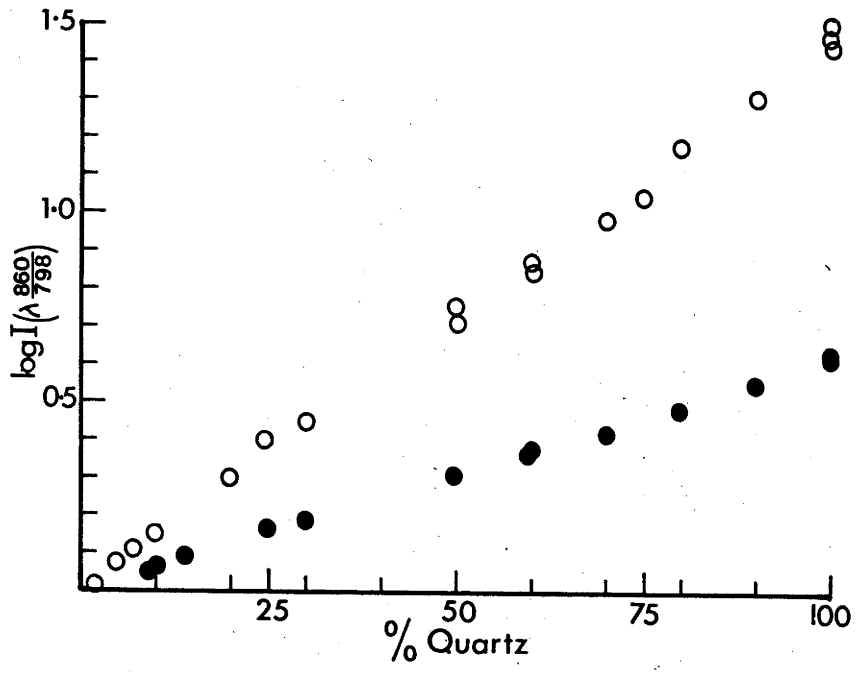

Figure A.1a Variation in the relative intensity of 798cm-1 quartz peak for a quartz, KBr mixture. o 500mg pill • 200mg pill

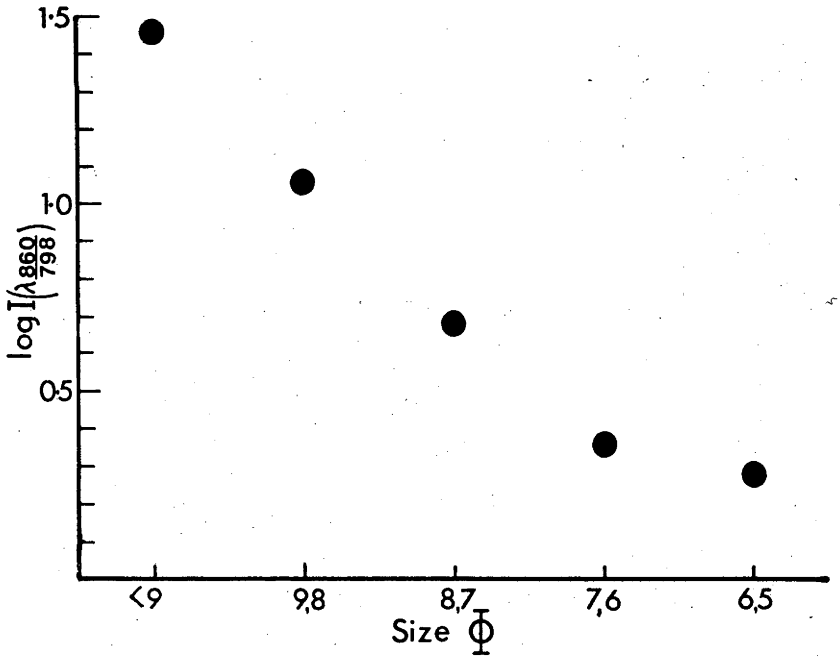

Figure A.1b Variation in the relative intensity of the 798cm-1 quartz peak with grainsize. Pills were standardised by using 2.5mg of quartz in 500mg pills.

Figure A.2 Variation in infrared signature with quartz content, using the <9 phi fraction.

Curve	Quartz content mg/g	Quartz content %	Pill weight mg
A	0	0	200
B	0.058	2.3	200
C	0.118	4.7	200
D	0.170	6.8	200
E	0.170	6.8	500
F	0.342	13.7	500
G	1.230	49.0	500

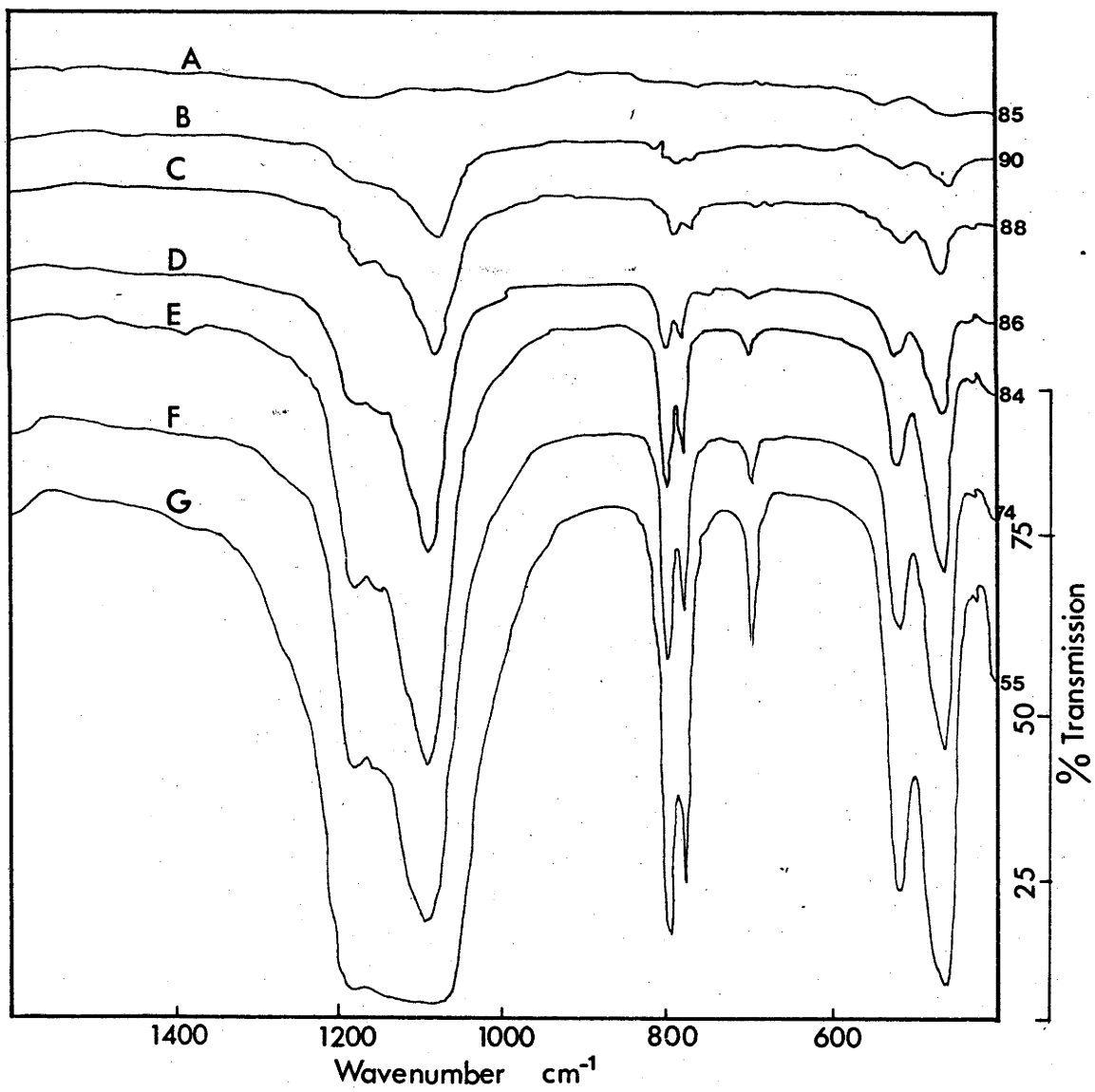

Figure A.3 Variation in the infrared signature of quartz with grainsize. Size fractions were obtained by sedimentation.

Curve	Grain size (phi)	Quartz content mg/g	Quartz content %	Pill weight mg
A	6,5	1.78	71	500
B	7,6	1.62	65	500
C	8,7	1.85	74	500
D	9,8	2.07	83	500
E	<9	1.25	50	500

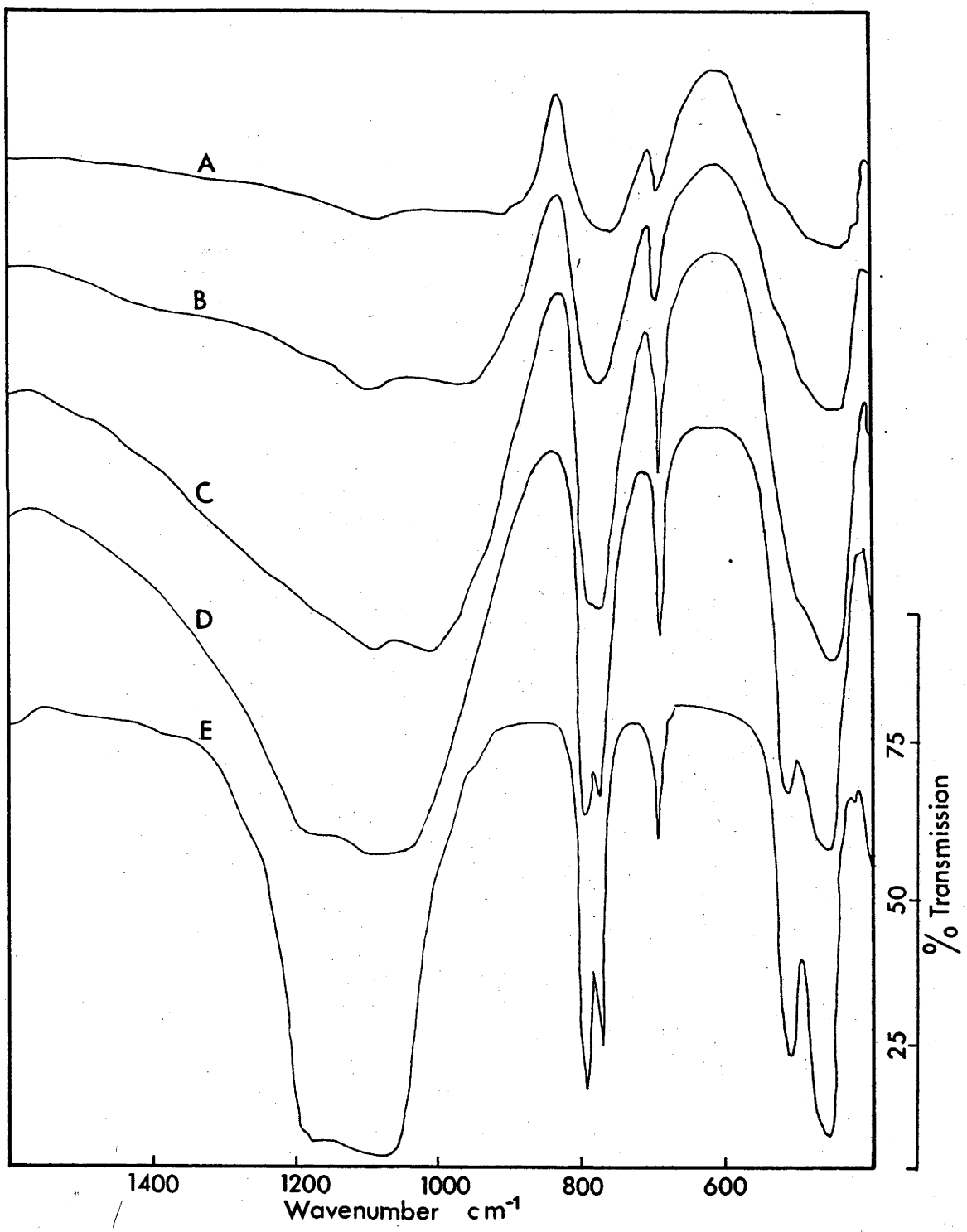

The effect of grainsize on the absorption spectra and the importance of using a grinding technique which ensures that all samples are ground to the same grain size, approximately 0.002 mm, is shown in Figure A.1b and A.3. These results supplement those of Hlavay et al. (1978, p. 143) who found the infrared intensities of quartz <0.002 mm to "depend on the average particle size of the primary particles, on the crystalline state of the particles and on their mechanochemical activation".

The possible interference by absorption peaks of other minerals with the 798 cm-1 quartz peak and the background at 860 cm-1, was checked by spiking representative samples with known amounts of quartz and examining data available from literature sources. The only source of interference found was due to changes in the opacity of the pill with varying proportions of organic matter and clay. This error is <3% (absolute) and is only apparent for samples with >50% quartz. Sample replicates agreed to better than 5%.

This technique is superior to that outlined by Andrews et al. (1979) who stated that the limit of detection of their technique was 5%.

Quantitative Mineralogy by X-Ray Diffraction

The K-feldspar and plagioclase content was determined by measuring the 27.5 and 28.0 2θ (Cu Kα radiation) peaks respectively.

The calibration curves for K-feldspar and plagioclase were established by mixing known proportions of quartz and kaolinite with crushed adamellite samples (samples collected from the catchment study area) for which the proportion of K-feldspar and plagioclase had been determined by point counting stained slabs. A linear relationship between feldspar content and peak height was assumed.

All samples were pelletised using a technique similar to that described by Flinter (1975) and 4 determinations were made of the peak height as the pellet was rotated through consecutive 90° intervals. Aberrant readings were rejected and the rest averaged.

Instrumental conditions were the same as those used for the XRD determination of quartz content and is described latter in this text.

The feldspar determinations are probably accurate to within 5% (absolute) of the stated value. The limit of detection was 1%.

Because of the time involved in determining quartz by infrared spectroscopy considerable effort could be saved if the same degree of accuracy and precision could be obtained by XRD techniques.

This would necessitate the use of powders which have been previously prepared for chemical analysis (saving time on duplicate sample preparation) and would preclude techniques involving: measurement of mass absorption; addition of heavy absorber; and spiking with an internal standard. As these techniques are as involved as those by infrared spectroscopy.

The efficacy of the use of X-ray diffraction was examined by:

(1) determining the degree of correlation between the proportion of quartz determined by infrared spectroscopy.

(2) determining variation in the relative X-ray intensity with varying grainsize and sample preparation.

Samples were run under the following instrumental conditions: Cu Kα radiation; 40kv/24ma; 1/4° entrance and exit slits; time constant, 4 seconds; chart speed 20mm per minute; scan speed 1/2° 2θ per minute; using a Seimens flat-bed goniometer. The results are summarised in Figures A.4 and A.5.

The results indicate that for samples with a relatively uniform matrix (quartz contents of 30 and 80%) the quartz content can usually be determined to within ±5% (absolute) of the stated value (with relatively little effort) for previously powdered samples once calibration conditions have been established.

The results (Figure A.4a) on the effect of grainsize confirms the work of Klug and Alexander (1954) who found that the optimum size range of particles with respect to the reproducibility of peak intensity and ease of sample preparation is from 0.02-0.03mm.

Semiquantitative Estimation of Clay Mineral Proportions

The procedure for the identification and estimation of the proportion of clay minerals in the <9 phi fraction is as follows.

Soil samples were sonified and dispersed in a solution containing NaOH and Na tripolyphosphate. Organic-rich samples were also treated with concentrated H_2O_2 (see notes on particle size analysis). The <9 phi fraction was separated by settling.

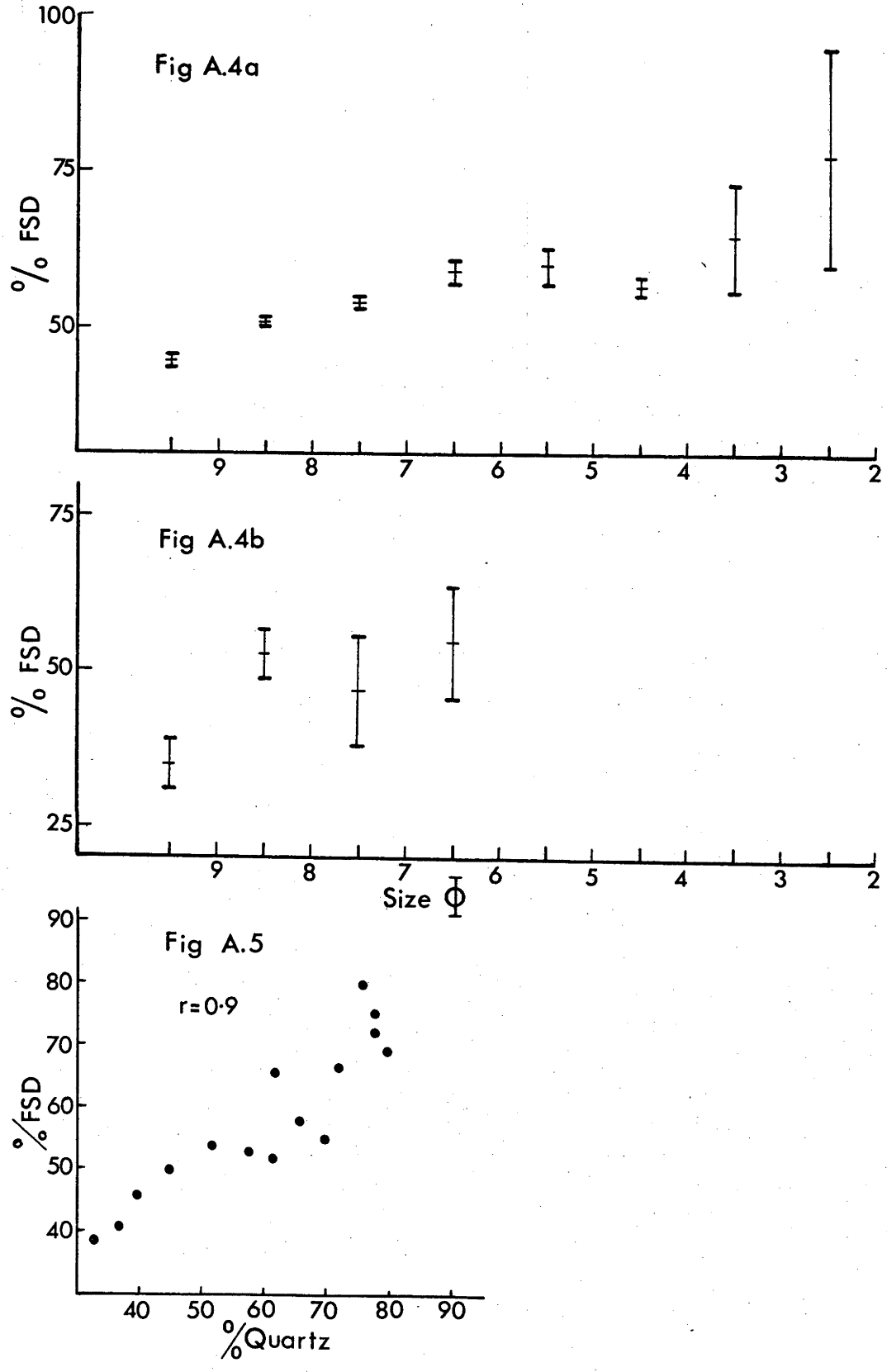

Figure A.4a,b Grainsize dependent variation in X-ray intensity of the 4.26Å quartz peak. The mean value is indicated by the central bar, while the bar is two standard deviations in length. In figure a , the grains were loose mounted in a rock-n-roll device, while in figure b the samples were pelletised. The greater precision achieved by the use of the rock-n-roll device is due to the increased proportion of grains which interact with the X-ray beam.

Figure A.5 Variation in the intensity of the 4.26Å quartz peak with quartz content. (%FSD: % full scale deflection) The proportion of quartz in the sample was determined by infrared spectroscopy.

Orientated mounts of the <9 phi fraction were prepared using the suction-onto-a-ceramic-tile method (Shaw 1972).

The following diffractograms were run on the orientated samples:

(1) air-dried
(2) ethylene glycol saturated
(3) heat treated at 450°C for 30 minutes
(4) heat treated at 600°C for 1 hour.

Approximately one third of the samples examined were heat treated.

The diffractograms were run using the following conditions: scan speed, 1°2θ per minute; chart speeds of 600 mm per hour; filtered Cu or Co Kα radiation; 1/4° entrance and exit slits and a graphite monochromator.

The criteria used for the identification of the clay mineral are those of Brown (1961), Grim (1968) and Carroll (1970) and are identical to those used by Reinson (1973). The following criteria are from Reinson (1973, pp. 77-81):

'Kaolinite: This mineral was identified by the presence of the diffraction maxima at 7Å and 3.5Å, which are unaffected by glycolation and heat treatment at 450°C. At 450°C the 7Å peak shows no decrease in intensity, but at 600°C it collapses completely. The 7Å and 3.5Å peaks of kaolinite correspond closely to those of three-layer clay minerals such as chlorite, vermiculite and montmorillonite. However, the loss of the 14Å basal reflection and retention of the 7Å reflection after treatment at 450°C is taken as confirming the presence of kaolinite.

Illite: In this study the term "illite" is used as originally defined by Grim et al. (1937), as a general term for clay minerals belonging to the mica group. This group is identified by diffraction maxima at 10, 5 and 3.3Å, which are not affected by glycolation or heat treatment. The 10Å peak where sharp and intense, is taken to indicate the presence of well crystalised mica: lack of peak resolution was taken to indicate the presence of micas with K deficiency between the unit layers.

Montmorillonite: Montmorillonite, as used here refers to the expanding dioctahedral mineral of the smectite group (Grim, 1968) which has a

basal spacing of 14Å in untreated samples, and which expands to 17Å on glycolation.

Vermiculite: The term "vermiculite" is used here for the mineral with a 14Å basal spacing, which does not expand on glycolation, but collapses to the 10 to 12Å range after thermal treatment at 450°C. It gives a strong intense peak at 14Å but contributes very little, if any to the 7Å peak. According to Walker (1961) and Grim (1968) this is indicative of vermiculite, which has a strong basal reflection relative to the higher order reflections. It is believed this mineral is a dioctohedral vermiculite, where interlayers between mica unit layers are occupied largely by hydroxy-Al and hydroxy-Fe complexes. The unit-layers are tightly bound to the hydroxyl interlayer, thus no expansion occurs. On thermal treatment the hydroxy-cations decompose and the structure collapses. Rich (1968, p.20) suggests that the collapse of the interlayer clay minerals of this type indicates that the interlayer spaces are only partially filled.

Vermiculite-Illite Mixed-Layer: This clay mineral phase is identified by deffraction maxima at 24, 12 and 6Å. It exhibits a variable tendency to expand on glycolation, but generally expansion is minimal. These regular reflections; 24, 12 and 6Å are interpreted as being due to regular interstratification of vermiculite and (or) montmorillonite with illite.'

The technique used to semiquantitatively determine the proportion of clay is as follows and is taken from Scafe and Kunze (1971).

The peak areas were measured and the following weightings used: the area of the 14Å peak was compared to 3 times the area of the 10Å peak, the area of the 17Å peak was compared to 4 times the 10Å peak, the area of the 7Å peak was compared to twice the area of the 10Å peak. Weighted percentages of each clay mineral were calculated from the sum of these four ratios.

Particle Size Analysis

All particle size analysis reported in this study was carried out at the Canberra Division of the CSIRO Soil Laboratories.

For soils whose particle size distribution was determined at one phi intervals, the following technique was used.

A 25g subsample of the <2 mm fraction was treated as follows:

(1) treated with peroxide to remove organic matter if necessary,

(2) disaggregated in water with an ultrasonic probe (20 kHz, 125 watt) for 15 minutes,

(3) dispersed with NaOH and sodium tripolyphosphate and then placed on an end-over-end shaker overnight which rotated at 12 rpm giving the sample a maximum travel per revolution of 20 cm,

(4) the particle size analysis for the material 2 to 31 μm was determined by the method of Day (1965). Settling times were calculated using Stokes' equation assuming spherical particles of density 2.61,

(5) particle size analysis in the range 0.06 to 2 μm were determined by the centrifugation method of Steele and Bradfield (1934),

(6) the <5 phi fraction was decanted 5 times and the residue dried to constant weight at 105°C,

(7) the size distribution of this residue was determined by sieving on an Endecott sieve shaker for 15 minutes.

Recoveries, excepting for samples with organic matter were generally between 98.5 and 100.5%.

For those samples for which only the clay, silt, fine and coarse sand and gravel fractions were measured using the International Scale, the following modifications were made:

(1) The fine earth fraction was separated by hand sieving samples dried at room temperature. The weight of the gravel component was recorded on an organic free basis after the removal of organic matter by hand picking.

(2) Disaggregation was effected by sonification in an ultrasonic bath for 15 minutes.

(3) All material <0.02 mm was removed by decanting and the >0.02 mm fraction was determined by sieving the dried residue for 3 minutes.

Statistical Techniques

All statistical manipulation of data was done on a Univac 1100/42 computer using programs described in the Statistical Package for the Social Sciences (SPSS) Manual (Nie et al. 1975).

The main programs used were:

(1) Principal component analysis: all factors were calculated using principal factoring without iteration (option PA1) and orthogonal rotation (option varimax).

(2) Discriminant function analysis using "Rao V" option.

APPENDIX B

PROFILE DESCRIPTIONS

Texture: Regolith texture was determined for the fine earth fraction, using laboratory particle-size analysis. These analyses are given in the relevant chapters. The particle-size distributions were then classified according to the textural classes described by the International Society of Soil Science (Smith and Atkinson, 1975).

pH: pH was determined at 20°C in a 1:5 soil (fine earth fraction):water solution after it had been shaken for 1 hour and allowed to stand for 30 minutes.

Colour: Colour was determined on dry (d) and moist (m) fine earth samples using the Revised Standard Soil Colour Charts (M. Oyama and H. Takehara, 1967; Research Council for Agriculture, Forestry and Fisheries, Ministry of Agriculture and Forestry, Japan).

Profile classification: Profiles have been classified according to criteria outlined in Stace et al. (1972).

PROFILE:GR1
CLASSIFICATION:Yellow podzolic
LOCATION:50m south of saddle,1m below the top of the spur.
MAP REFERENCE:Timbillica 8823-III-N 32276368

TOPOGRAPHY	ALTITUDE	ASPECT	SLOPE
Hilly	430m	East	5°

EXTERNAL DRAINAGE: free
REMARKS: Surface horizon contains many scattered chips of vein quartz, no vein quartz fragments are present in the lower part of the profile.

SAMPLE NUMBER	DEPTH cm	pH	PROFILE DESCRIPTION
GR101	0-2	5.1	Organic rich horizon contains abundant roots; charcoal fragments; dominant colour brownish grey; lighter grey colour is due to large fragments of vein quartz and granite derived quartz; loamy sand ; apedal; loose dry consistence; sharp irregular boundary; over 1cm to
GR102	3-8	5.0	dull yellow (2.5Y7/2(d), 2.5Y6/3(m)); loam ; some fragments of vein quartz; apedal; extremely hard dry consistence; no charcoal fragments; abundant voids to 1mm in diameter; grades to
GR103	15-20	5.2	dull yellow orange (10YR8/4(d), 10YR6/4(m)); loam ; no vein quartz fragments; apedal; extremely hard dry consistence; occasional fine roots; voids to 1mm common; grades over 5cm at 25cm to
GR104	30-35	5.4	light yellow orange (7.5YR8/4(d), 10YR7/4(m)); soil more whole coloured compared with overlying horizons; clay loam ; apedal; extremely hard dry consistence; contains voids to 2mm (commonly less than 1mm); grades to
GR105	50-55	5.4	light yellow orange (7.5YR8/4(d), 7.5YR7/4(m)); clay loam ; apedal; extremely hard dry consistence; contains some voids to 2mm, commonly <1mm; grades to
GR106	65-70	5.5	not whole coloured; colour varies from light yellow orange to yellow orange; clay loam ; contains voids to 1mm; feldspars visible; original rock fabric preserved; grades to
GR107	115-120	5.6	weathered rock; can be crumbled with difficulty in the hand when dry; sandy loam; readily crumbled when wet; orange colour: grades to
GR108	190-200	5.9	weathered rock; orange to redish brown colour; sand.

PROFILE:GR2
CLASSIFICATION:Gleyed Podzolic
LOCATION:Germans Creek Road - approximately 100m S.E. of the junction of Germans Creek and the main road entrance to catchment 3 and 4.
MAP REFERENCE: Timbillica 8823-III-N 33236493

TOPOGRAPHY	ALTITUDE	ASPECT	SLOPE
Hilly	350m	East	3°

EXTERNAL DRAINAGE: Impeded
REMARKS: Profile located in the upper end of a drainage line, water seeps from profile except in periods of severe drought.

SAMPLE NUMBER	DEPTH cm	pH	PROFILE DESCRIPTION
GR201	0-3	5.1	Organic rich; brownish grey (7.5YR6/1(d), 7.5YR4/1(m)); loamy sand; apedal; hard dry consistence; roots abundant; grades to
GR202	27-33	5.5	light brownish grey (7.5YR7/1(d), 7.5YR5/2(m)); loamy sand; apedal; hard/extremely hard dry consistence; contains many voids to 1mm; roots absent; grades to
GR203	39-44	5.7	irregularly shaped diffuse mottles to 1cm, with light grey (10YR7/1(d), 7/2(m)) dominant; bright yellowish orange areas (10YR7/1(d) 5/6(m)) are slightly more clay rich than the grey areas; loamy sand ; apedal; hard dry consistence; voids to 1mm are abundant; quartz grains are often in point contact with each other; sharp boundary with following horizon at 46cm
GR204	48-53	5.6	colour the same as overlying horizon; clay ; voids much less common than overlying horizon; apedal; hard dry consistence; grades to
GR205	80-85	5.7	mottled varying in colour from brownish grey (10YR6/1(d), 5/4(m)) to bright yellowish brown (10YR6/6(d),5/4(m)) clay ;weakly developed cutans which are brownish grey; weakly pedal coarse prismatic structure; earthy fabric; original rock fabric preserved between cutans; grades to
GR206	125-130	5.9	original rock texture preserved; light grey colour (10YR7/1(d),1/1(m)); with whitish flecks of feldspar to 1.5mm; clay loam ; apedal; some joint surfaces are yellow brown in colour; grades to
GR207	155-160	6.3	weathered rock; light grey colour; with white specks of feldspar; voids to 0.5mm very common; original rock fabric preserved; loamy sand.

PROFILE:GR3
CLASSIFICATION:Yellow Podzolic
LOCATION: Approximately 200m along main entrance track to S-W corner of catchment 5.
MAP REFERENCE: Timbillica 8823-III-N 32456450

TOPOGRAPHY	ALTITUDE	ASPECT	SLOPE
Hilly	400m	East	5-10°

EXTERNAL DRAINAGE: Free
REMARKS: Road cutting; very thin discontinuous litter layer.

SAMPLE NUMBER	DEPTH cm	pH	PROFILE DESCRIPTION
GR301	0-2	5.6	Light yellow orange(10YR8/3(d),7/4(m)); loamy sand ; apedal; hard dry consistence; organic matter only in top 0-0.5 cm and is discontinuously developed; grades to
GR302	10-15	6.0	light yellow orange (10YR8/3(d),7/4(m)); loam ; apedal; hard dry consistence; grades to
GR303	20-25	5.9	not whole coloured; light grey feldspar grains common; diffuse weak mottles from 1 to 5cm in size; varying in colour from orange (5YR6/8(d),5/3(m)) to light brownish grey (7.5YR/2(d)); clay loam ; apedal; hard dry consistence; contains abundant voids to 1mm in diameter; grades to
GR304	30-35	6.1	similar to above except lighter in colour, feldspar more obvious, clay loam, original rock fabric partially preserved; grades to
GR305	53-58	6.0	weathered rock, difficult to crumble in the hand when dry; clay loam ; not whole coloured, orange colour dominant.

PROFILE:GR4
CLASSIFICATION:Yellow Podzolic/Lithosol
LOCATION:Main access road to southern side of catchment 5.
MAP REFERENCE:Timbillica 8823-III-N 333643

TOPOGRAPHY	ALTITUDE	ASPECT	SLOPE
Hilly	330m	North	5-10°

EXTERNAL DRAINAGE:Free
REMARKS:Just north of pole 131, 5m down slope of a large rock outcrop.

SAMPLE NUMBER	DEPTH cm	pH	PROFILE DESCRIPTION
GR401	0-5	5.5	Organic rich,loamy sand ,brownish grey/brownish black colour; loose dry consistence,grades to
GR402	15-20	5.8	loamy sand ,colour varies from light yellow orange to dull orange,massive,loose dry consistence
GR403	25-30	5.8	as above.boundary grades from 30-35 cm to
GR404	35-40	5.7	sandy loamy ,colour varies as above,parent material texture is partially preserved,grey clay cutans(to 1mm in thickness) are weakly developed along joint planes,grades to
GR405	50-70	5.7	saprolite horizon, loam not whole coloured,generally yellow orange, irregular grey coloured zones surround joint faces (at the time of sampling this horizon was saturated with water)

PROFILE:GR5
CLASSIFICATION:Lithosol
LOCATION:Main access road to southern side of catchment 5
MAP REFERENCE:Timbillica 8823-III-N 333643

TOPOGRAPHY	ALTITUDE	ASPECT	SLOPE
Hilly	330m	North	5-10

EXTERNAL DRAINAGE:Free
REMARKS:Opposite main creek that is being checked for siltation; unweathered rock occurs at 60cm

SAMPLE NUMBER	DEPTH cm	pH	PROFILE DESCRIPTION
GR501	0-5	5.5	Organic rich, loamy sand ,brownish grey (7.5YR6/1(d),4/1(m)), massive,loose dry consistence,grades to
GR502	25-30	5.8	loamy sand ,light yellow orange (10YR8/4(d),(m)),massive, rock texture preserved
GR503	55-60	6.0	as above

PROFILE:GR6
CLASSIFICATION:Red Earth
LOCATION: Junction of Cooriwa and Bingera Road.
MAP REFERENCE: Timbillica 8823-III-N 31206420

TOPOGRAPHY	ALTITUDE	ASPECT	SLOPE
Undulating	370m	----	flat

EXTERNAL DRAINAGE: free
REMARKS: Discontinuous litter layer.

SAMPLE NUMBER	DEPTH cm	pH	PROFILE DESCRIPTION
GR601	0-5	5.9	Yellowish brown (10YR5/6(d),4/4(m)); loam ; massive; slightly hard dry consistence; abundant fine roots; grades to
GR602	10-15	5.7	yellowish brown (10YR5/6(d), 3/4(m)); loam ; massive; extremely hard dry consistence; grades to
GR603	20-25	5.7	orange (7.5YR6/8(d), 4/6(m); clay loam ; massive; hard dry consistence; grades to
GR604	50-55	5.9	bright reddish brown (5YR5/8(d), 4/8(m)); clay ; extremely hard dry consistence; grades to
GR605	100-105	5.8	as above except for very diffuse pale yellow mottling (see GR607), mottled areas less than 5mm in size; grades to
GR606	150-155	5.7	as above except mottles slightly more distinct (see GR607); grades to
GR607	195-200	5.7	reddish brown (2.5YR4/8(d), 3/6(m)); to yellowish brown (10YR5/8(d), 5/6(m)) equant mottles to 5mm in size; boundaries diffuse; clay ; slightly hard dry consistence.

PROFILE:ER1
CLASSIFICATION: Yellow Earth
LOCATION: Face of a small borrow pit 10m north of Link Road.
MAP REFERENCE:Narrabarba 8823-II-N 549698.

TOPOGRAPHY	ALTITUDE	ASPECT	SLOPE
Hilly	70m	South	5°

EXTERNAL DRAINAGE: Free
REMARKS: Surface organic horizon 5cm thick.

SAMPLE NUMBER	DEPTH cm	pH	PROFILE DESCRIPTION
ER101	5-10	5.6	Top 5cm organic rich horizon; sharp boundary between organic horizon and ER101; greyish yellow brown (2.5Y8/2(d), 10YR6/2(m) silty loam : slightly hard dry consistence; massive; many roots and fine voids to 1mm; grades to
ER102	12-17	5.8	pale reddish orange (2.5YR8/3(d),2.5YR7/3(m)); silty loam ; slightly hard dry consistence; massive; contains some roots; has a slightly greater number of voids than the overlying horizon; grades to the following except for stone fragments which cut out at 25cm.
ER103	55-65	6.1	bright yellowish brown (2.5Y8/3(d),10YR6/6(m)), silty clay loam ; hard dry consistence; massive; contains fine voids; grades to
ER104	90-100		weathered rock; light buff coloured with yellow brown clay film; developed along the joints; the rock can be crumbled with difficulty between the fingers; joint spacing varies from 2 to 5 cm.

PROFILE:ER2
CLASSIFICATION: Red Podzolic
LOCATION:Prominent outcrop of Eden Rhyolite that crosses Wonboyn Road, 20m east of borrow pit
MAP REFERENCE: Narrabarba 8823-II-N 552724

TOPOGRAPHY	ALTITUDE	ASPECT	SLOPE
Hilly	60m	East	5°

EXTERNAL DRAINAGE: Free
REMARKS:Profile is 50m from the hill crest, 50m further down the hill the slope changes to 10-15°

SAMPLE NUMBER	DEPTH cm	pH	PROFILE DESCRIPTION
ER201	0-10	5.7	Organic rich horizon, brownish black (7.5 YR4/3(d),7.5YR 3/2(m)) silty loam , massive,earthy fabric hard dry consistence, contains occasional charcoal fragments,many fine roots and voids to 1mm diameter,sample representative of top 20cm, grades over 5cm to
ER202	25-30	5.9	bright reddish brown (5YR6/3(d),5YR5/6 (m)), silty loam , medium nut structure; rough ped fabric; very hard dry consistence; contains numerous fine voids 0.5mm in diameter, grades to
ER203	57-62	5.9	dark reddish brown (5YR5/8(d),5YR3/6(m)), silty clay , readily breaks into a fine nut structure (5mm in size) with rough ped fabric, very hard dry consistence, contains many fine voids approximately 0.1 to 0.5 mm in size, grades to following sample over 5cm at 75cm
ER204	80-85	6.0	strongly weathered rock (5YR6/6(d),5YR5/6(m) dominant with occasional lighter coloured specks to 1mm in size; silty clay , massive,very hard dry consistence, some joint surfaces visible, grades to
ER205	95-105		weathered rock, rock is readily scratched by the finger nail reddish brown clay infilling common along joints, which are commonly 5cm apart

PROFILE:ER3
CLASSIFICATION: Yellow Earth
LOCATION: Approximately 80m east of hillcrest and log dump on Mountain Road
MAP REFERENCE: Narrabarba 8823-II-N 563682

TOPOGRAPHY	ALTITUDE	ASPECT	SLOPE
Hilly	100m	East	5°

EXTERNAL DRAINAGE: Free
REMARKS: Profile located near ridge crest, slope increase to 10-15° 50m further down hill from the site, profile dry at time of sampling, extensive thin organic mat.

SAMPLE NUMBER	DEPTH cm	pH	PROFILE DESCRIPTION
ER301	0-8	4.6	Organic rich,brownish black (10YR6/1(d), 10YR3/1(m)) massive, silty loam , soft dry consistence, abundant roots gradational to
ER302	20-30	5.1	brownish grey (2.5Y7/1(d), 10YR6/1(m)), silty loam massive, extremely hard dry consistence; occasional charcoal fragments and small voids to 1mm, sharp boundary to
ER303	32.5-40	5.4	pale reddish orange (2.5YR8/3(d),2.5YR7/3(m)); silty loam , massive; extremely hard dry consistence occasional large void to 0.8cm, occasional fine roots grades to
ER304	60-65	5.3	dull yellow orange (10YR8/1(d),10YR7/3(m)) silty loam ,joint planes with slightly heavier texture than surrounding soil, occasional fine pores to 1mm, hard dry consistence, grades to
ER305	110-120	5.6	same colour as ER304, silty loam , original rock jointing and fabric partially preserved, grades to
ER306	170-180	5.7	strongly weathered rock, "kaolinised" feldspars present, silty loam,can be readily crumbled in the hand.

PROFILE:ER4
CLASSIFICATION:Yellow Podzolic
LOCATION: Road cutting, Old Bridge Road
MAP REFERENCE: Narrabarba 8823-II-N 570698

TOPOGRAPHY	ALTITUDE	ASPECT	SLOPE
Hilly	100m	----	flat

EXTERNAL DRAINAGE: Poor
REMARKS: Organic rich surface mat, profile dry at time of sampling

SAMPLE NUMBER	DEPTH cm	pH	PROFILE DESCRIPTION
ER401	0-10	4.5	Organic rich, black, massive, silty loam , soft dry consistence, abundant fine roots and voids to 2mm, grades to following horizon over 8cm
ER402	22-29	5.0	Colour varies from brownish grey (7.5YR7/1(d),7.5YR5/1(m)) to light yellow orange (7.5YR8/3(d),(m)), the light yellow orange colour is due to weathered rock fragments, silty loam , extremely hard dry consistence many fine pores to 1mm in diameter occasional charcoal fragments,grades to
ER403	32-38	5.5	colour highly variable and consists of irregular diffuse patches, light yellow orange (10YR8/4(d), 10YR7/4(m)) which are associated with weathered rock fragments, the other colours are (10YR7/3(d), 10YR6/3(m)) and (10YR7/1(d), 10YR5/2(m)) loam ,extremely hard dry consistence, weakly developed medium nut structure, rough ped fabric, large irregular elongate voids to 3mm, occasional joint plane is visible,grades to
ER404	62-70	5.6	weathered rock, 1mm to 1cm clay cutans developed along joint planes, colour of weathered rock varies from yellow orange to reddish brown, readily excavated with a pick, loam, grades to
ER405	94-100	5.6	weathered rock dominantly greyish yellow in colour with reddish brown stain common along joint planes which are often 5cm apart, sandy loam .

PROFILE:OR1
CLASSIFICATION:Lithosol
LOCATION: Opposite abandoned stockyard,Ireland Timms Road
MAP REFERENCE: Narrabarba 8823-II-N 491702

TOPOGRAPHY	ALTITUDE	ASPECT	SLOPE
Hilly	50m	North	5-10°

EXTERNAL DRAINAGE: Free
REMARKS: Road cutting 20m West of the crest of the north-south spur, discontinous litter layer.

SAMPLE NUMBER	DEPTH cm	pH	PROFILE DESCRIPTION
OR101	0-2	5.5	Brownish black loose organic rich mat; contains numerous fine roots and occasional charcoal fragments; apedal; loose dry consistence; silty loam grades to
OR102	3-5	5.9	dull orange (5YR6/3(m),6/4(m)); silty loam ; weakly developed medium nut structure; rough ped fabric; hard dry consistence fine roots common; grades to
OR103	7-10	5.9	dull orange (7.5YR6/4(d),5YR6/4(m)); loam ; weakly developed medium nut; rough ped fabric; hard dry consistence, occasional fine roots; occasional voids to 1mm; grades to
OR104	25-30	6.0	weathered rock; structure of parent material poorly preserved; weathering takes place preferentially along bedding planes; weathered material is dull orange (5YR7/3(d),7/3(m)); occasional fine roots silty loam grades to
OR105	100-110		phyllite with a strongly developed cleavage producing tablet shaped fragments which are dull orange in colour.

PROFILE:OR2
CLASSIFICATION:Lithosol
LOCATION: 100m from Anteater Road along a north south logging track
MAP REFERENCE: Mount Imlay 8823-IV-S 418764

TOPOGRAPHY	ALTITUDE	ASPECT	SLOPE
Hilly	300m	East	20°

EXTERNAL DRAINAGE: Free
REMARKS: Samples taken from road cutting which is approximately 30m below the crest of the hill, discontinuous litter/organic layer

SAMPLE NUMBER	DEPTH cm	pH	PROFILE DESCRIPTION
OR201	0-10	5.7	Dull brown (7.5YR6/3(d),5/4(m)); silty loam ; moderately developed medium nut structure; rough ped fabric; hard /very hard dry consistence; abundant roots; occasional voids to 2mm; grades to
OR202	10-20	5.7	dull orange (5YR7/3(d),6/4 (m)); loam ; weakly developed medium nut structure; rough ped fabric; hard/very hard dry consistence; occasional fine root; occasional voids to 5mm; grades to
OR203	20-30	5.8	reddish brown (5YR6/6(d),4/8 (m)); loam .; weakly developed medium nut structure; rough ped fabric; extremely hard dry consistence; occasional voids to 2mm; grades to siltstone over 20cm.

PROFILE:OR3
CLASSIFICATION:Lithosol
LOCATION: 0.3km east of the junction of Maxwells and Stringy Roads
MAP REFERENCE: Nadgee 8823-II-S 483559

TOPOGRAPHY	ALTITUDE	ASPECT	SLOPE
Hilly	220m	West	5°

EXTERNAL DRAINAGE: Free
REMARKS: Samples taken from road cut, which is approximately 100m from the hill crest. Thin discontinuous litter/organic layer. Profile relatively dry at time of sampling.

SAMPLE NUMBER	DEPTH cm	PROFILE DESCRIPTION
OR301	0-7	Dull yellowish brown (10YR7/1(d),5/3(m)); silty loam ; medium nut structure; rough ped fabric; extremely hard dry consistence occasional charcoal fragments; abundant fine roots; voids to 5mm; grades to
OR302	7-12	diffuse, irregularly shaped patches of colour varying from dull yellow orange (10YR7/1(d),7/2(m)) to (75YR8/3(d),10YR7/3(m)) silty loam ; medium nut structure; well developed,rough ped fabric; extremely hard dry consistence; occasional fine roots; occasional voids to 3mm; sharp boundary with the following
OR303	12-18	light yellow (10YR8/1(d),2.5Y7/3(m)); silty loam ; medium/coarse nut structure; rough ped fabric; occasional fine roots, occasional voids to 2mm; extremely hard dry consistence; conspicuously bleached compared with over and underlying horizons, grades to
OR304	22-30	Colour varies from bright brown (7.5YR7/8(d),5/6(m)) at the centre of peds to light brownish grey (7.5YR8/3d,7/2(m))at the boundaries; silty loam ; coarse nut structure; rough ped fabric; extremely hard dry consistence; occasional fine roots; occasional fine voids to 2mm; grades to the following
OR305	80-90	disintegrating weathered light salmon pink/buff coloured siltstone/fine grained sandstone; weathering is dominantly along bedding planes; readily excavated with a pick.

PROFILE:SS1
CLASSIFICATION:Podzol/Siliceous Sand
LOCATION: Corner of Loop Road and Merrica River Road.
MAP REFERENCE: Narrabarba 8823-II-N 523606.

TOPOGRAPHY	ALTITUDE	ASPECT	SLOPE
Undulating	400m	----	Flat

EXTERNAL DRAINAGE: Impeded
REMARKS: Profile dry at time of sampling.

SAMPLE NUMBER	DEPTH cm	pH	PROFILE DESCRIPTION
SS101	0-3	4.4	Brownish black, (10YR4/1(d),3/1(m)); organic rich; loamy sand fine roots common; massive; loose dry consistence; grades to
SS102	20-25	4.3	brownish black,(10YR4/1(d),3/1(m)); organic rich; loamy sand massive; extremely hard dry consistence; occasional fine roots; boundary between this horizon and underlying one occurs at 32cm; the boundary is extremely irregular and a thin discontinuous 2cm bleached light grey layer is developed at the boundary,abrupt change to
SS103	32-35	5.2	indurated coffee rock extremely hard dry consistence; dark brown (7.5YR5/3(d),3/4(m)); massive; sand; represents an accumulation of organic matter; sharp boundary to following separated by a bedding plane.
SS104	40-50	5.3	yellow orange arenite; can be readily crumbled in the hand; loamy sand this bed probably represents the parent material for the overlying horizons.

PROFILE:SS2
CLASSIFICATION:Lithosol
LOCATION: Road cut on an E-W access road.
MAP REFERENCE: Narrabarba 8823-II-N 563643.

TOPOGRAPHY	ALTITUDE	ASPECT	SLOPE
Undulating	170m	North	8°

EXTERNAL DRAINAGE: Free
REMARKS:Texture contrast corresponds to different sedimentary layers

SAMPLE NUMBER	DEPTH cm	pH	PROFILE DESCRIPTION
SS201	0-15	5.4	surface organic layer absent; greyish yellow brown (10YR6/2(d),5/2(m); single grain structure, loose dry consistence; loamy sand ; some voids to 1mm; grades over 5cm to
SS202	20-25	5.5	bright yellowish brown (10YR8/4(d),6/6(m)) clay loam; massive; hard dry consistence; contains abundant voids to 1mm; grades into weathered arenite over the next 5cm

PROFILE:SS3
CLASSIFICATION:Siliceous Sand
LOCATION: Loop Road 1.4km east of Merrica Road junction
MAP REFERENCE: Narrabarba 8823-II-N 535607.

TOPOGRAPHY	ALTITUDE	ASPECT	SLOPE
Undulating	370m	East	5°

EXTERNAL DRAINAGE: Impeded
REMARKS: Profile dry at time of sampling.

SAMPLE NUMBER	DEPTH cm	PROFILE DESCRIPTION
SS301	0-10	Organic rich sand; loose dry consistence; abundant roots; brownish grey colour; grades to
SS302	40-50	as above, roots less common; slightly stronger dry consistence than above; grades to
SS303	80-90	as above, though with a slightly stronger dry consistence but still weakly coherent; abrupt change to weathered pebbly arenite over next 10cm.

PROFILE:D1
CLASSIFICATION: Krasnozem
LOCATION: Swamp Road west of prominent knob of microgranite.
MAP REFERENCE: Narrabarba 8823-II-N 513724

TOPOGRAPHY	ALTITUDE	ASPECT	SLOPE
Hilly	110m	West	5°

EXTERNAL DRAINAGE: Free
REMARKS: Profile dry at time of sampling, polygenetic profile,surface horizon formed by the addition of coarse microgranite derived slopewash and mixing by biological activity with clay rich subsoil derived from the dyke.

SAMPLE NUMBER	DEPTH cm	PROFILE DESCRIPTION
D101	0-10	Dark reddish brown (5YR5/4(d),5YR3/4(m)), organic rich loam ,well developed medium to fine nut structure, rough ped fabric,occasional fine roots, many fine voids to 0.5mm in diameter, extremely hard dry consistence,represents surface contaminated by addition of coarse slope wash material,texture changes around 15cm whilst the colour is transitional to
D102	90-100	dark reddish brown (5YR5/8(d),2.5YR3/6(m)), clay, medium developed coarse nut structure,rough ped fabric, occasional fine voids,extremely hard dry consistence occasional core stone of weathered basalt to 25cm in diameter;grades to
D103	250-260	Colour as above except for the presence of small (to 1mm) light orange coloured spots, clay , weakly pedal,coarse nut structure,occasional fine voids (0.5mm), core stones of fresh basalt to 35cm present.

C.1a

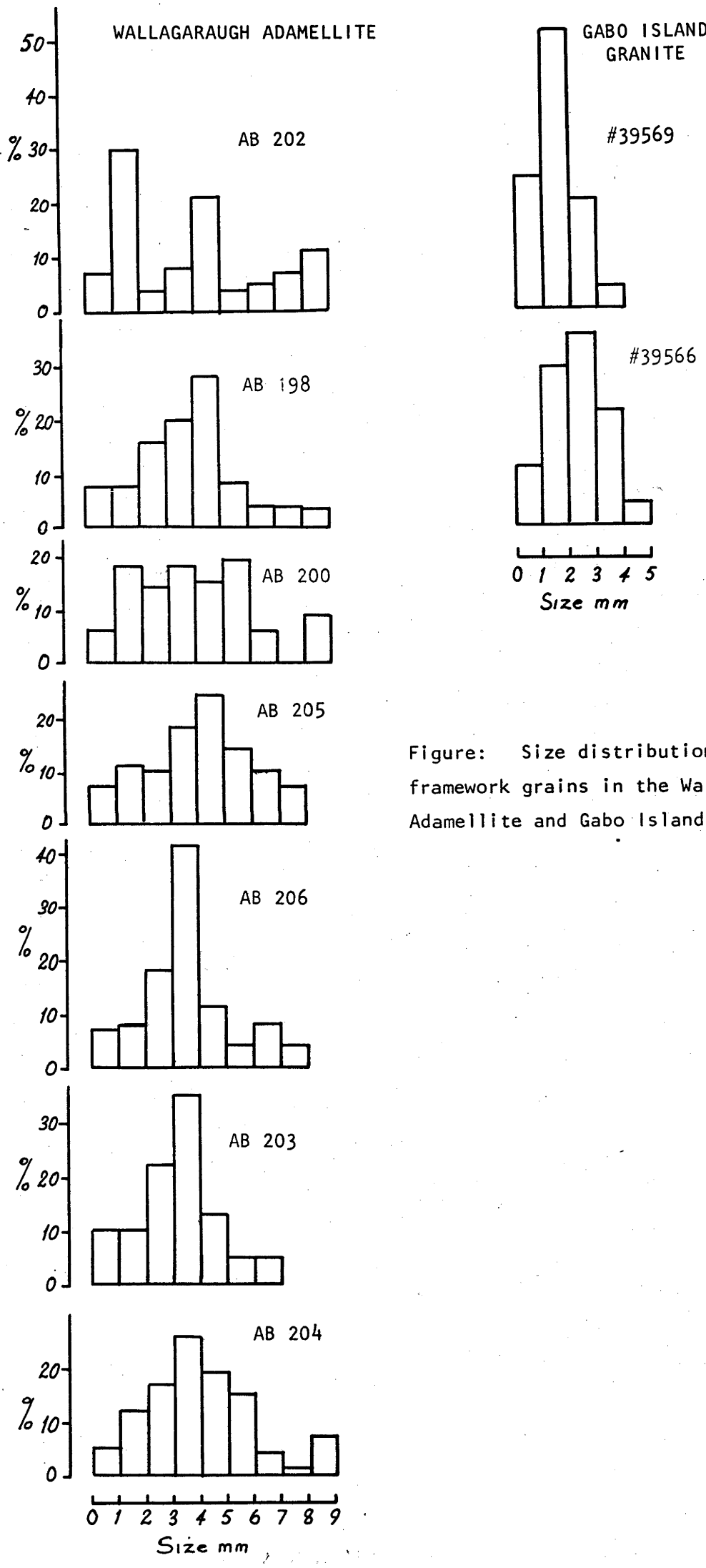

Figure: Size distribution of quartz framework grains in the Wallagaraugh Adamellite and Gabo Island Granite.

APPENDIX C

SIZE DISTRIBUTION OF FRAMEWORK GRAINS OF THE WALLAGARAUGH ADAMELLITE AND THE GABO ISLAND GRANITE.

The size of the framework grains was determined on stained rock slabs. These were overlaid by a transparent 1mm grid and the maximum diameter of quartz grains recorded with the aid of a binocular microscope. Depending on grain size, between 50 and 100 grains were measured. All available rock slabs were used.

Quartz was chosen partly for convenience. Its grain boundaries are readily distinguished, and it is one of the minerals whose size distribution is reflected in the regolith. As the framework grains are equidimensional, and the rocks examined are relatively even textured, the size of the quartz is indicative of the size of the feldspar framework grains.

The results are given in the following table and are illustrated on the opposite page.

Table: Quartz grain size distribution of the Wallagaraugh Adamellite and Gabo Island Granite.

Sample Number *	Size (mm) %							
	>1.0	>2.0	>3.0	>4.0	>5.0	>6.0	>7.0	>8.0
Wallagaraugh Adamellite								
AB 198	92	84	68	48	20	12	8	4
AB 200	94	76	62	44	29	15	9	9
AB 202	93	63	59	51	30	26	19	11
AB 203	90	80	58	23	10	5	0	0
AB 204	95	83	67	47	28	13	9	7
AB 205	93	83	73	55	31	17	7	0
AB 206	93	85	67	26	15	11	4	0
Gabo Island Granite								
39566	89	60	25	4	0			
39569	76	24	4	6	0			

* Sample numbers commencing with AB refer to samples collected by B.W. Chappell, Dept. Geology, A.N.U. Samples 39566,9 are A.N.U. Geology Dept., rock numbers.

The results show that the majority of framework grains of the Wallagaraugh Adamellite are between 2 and 7mm in size whereas those of the Gabo Island Granite are between 1 and 3mm in size. The grain size estimates are supported by field observations.

Because of the variability in grain size, particularly in the Wallagaraugh Adamellite in which any two samples can show markedly differing size distributions, statistically significant measures of grain size can not be readily determined.

APPENDIX D

List of thesis material catalogued at the department of Geology, ANU.
Grid references prefixed by the following letters refer to:
E: Eden (8823) 1:100,000 sheet.
K: Kiah (8823-I-S) 1:25,000 sheet.
N: Narrabarba (8823-II-N) 1:25,000 sheet.
Na: Nadgee (8823-II-S) 1:25,000 sheet.
T: Timbillica (8823-III-N) 1:25,000 sheet.

Thesis Number	ANU Number	Sample Description	Grid Reference
ER101	43559	Regolith	N 549698
ER102	60	"	"
ER103	61	"	"
ER104	62	"	"
ER201	63	"	N 552724
ER202	64	"	"
ER203	65	"	"
ER204	66	"	"
ER205	67	"	"
ER401	68	"	N 570698
ER402	69	"	"
ER403	70	"	"
ER404	71	"	"
ER405	72	"	"
ERR1	39555	Ash flow tuff	E 581113
ERR2	56	Rhyolite dyke	E 558238
ERR3	57	Ash flow tuff	E 575279
ERR4	59	"	E 591252
ERR5	60	"	E 566278
ERR6	61	"	E 566373
ERR7	62	"	E 550321
ERR8	63	"	E 529349
ER204 0,-1ϕ	43573	Regolith Size Separate	N 552724
ER204 7,6ϕ	74	"	"
ER204 8,7ϕ	75	"	"
ER204 <9ϕ	76	"	"

Thesis Number	ANU Number	Sample Description	Grid Reference
GR101	43577	Regolith	T 323637
GR102	78	"	"
GR103	79	"	"
GR104	80	"	"
GR105	81	"	"
GR106	82	"	"
GR107	83	"	"
GR108	84	"	"
GR201	85	"	T 332649
GR202	86	"	"
GR203	87	"	"
GR204	88	"	"
GR205	89	"	"
GR206	90	"	"
GR207	91	"	"
GR301	92	"	T 325645
GR302	93	"	"
GR303	94	"	"
GR304	95	"	"
GR305	96	"	"
GR103 -1,-2ϕ	97	Regolith Size Separate	T 323637
" 0,1ϕ	98	"	"
" 3,2ϕ	99	"	"
" 4,5ϕ	43600	"	"
" 7,8ϕ	01	"	"
" <9ϕ	02	"	"
GR107 -1,-2ϕ	03	"	"
" 0,1ϕ	04	"	"
" 2,3ϕ	05	"	"
" 4,5ϕ	06	"	"
" 7,8ϕ	07	"	"
" <9ϕ	08	"	"
GRS5 3,4ϕ	09	Stream-bed sediment size separate	T 344650
" 1,2ϕ	10	"	"
" -1,0ϕ	11	"	"
GRR1	38933	Adamellite	T 343675
GRR8	38930	"	T 335659
GRR15	38932	"	T 344640
GRR16	38931	"	T 333631

Thesis Number	ANU Number	Sample Description	Grid reference
GRR12	43648	Adamellite	T 332649
GRR13	12	"	T 340648
GRR17	13	"	T 340648
GRR21	14	Feldspar porphyry	T 333642
GRR22	15	Aplite	T 320631
GRR23	16	"	T 330649
OR101	17	Regolith	N 491702
OR102	18	"	"
OR103	19	"	"
OR104	20	"	"
OR105	21	"	"
OR301	22	"	Na 483559
OR302	23	"	"
OR303	24	"	"
OR304	25	"	"
OR305	26	"	"
SS101	27	"	N 523606
SS102	28	"	"
SS103	29	"	"
SS104	30	"	"
SS301	31	"	N 535607
SS302	32	"	"
SS303	33	"	"
SSR1	34	Sandstone	N 523606
SSR2	35	"	N 535607